

# **SYNTHESIS, CHARACTERIZATION AND MESOMORPHIC PROPERTIES OF NEW PYRIDINE DERIVATIVES**

Thesis

Submitted in partial fulfillment of the requirements for the degree of

DOCTOR OF PHILOSOPHY

by

AHIPA T.N.



DEPARTMENT OF CHEMISTRY

NATIONAL INSTITUTE OF TECHNOLOGY KARNATAKA

SURATHKAL, MANGALORE - 575 025

March, 2014

## DECLARATION

*By the Ph.D. Research Scholar*

I hereby declare that the Research Thesis entitled “**Synthesis, characterization and mesomorphic properties of new pyridine derivatives**” which is being submitted to the **National Institute of Technology Karnataka, Surathkal** in partial fulfillment of the requirements for the award of the degree of **Doctor of Philosophy in Chemistry** is a *bonafide report of the research work carried out by me*. The material contained in this Research Thesis has not been submitted to any University or Institution for the award of any degree.

Ahpa T.N.

Reg. No. CY10F06

Department of Chemistry

**Place:** NITK - Surathkal

**Date:**

## CERTIFICATE

This is to *certify* that the Research Thesis entitled “**Synthesis, characterization and mesomorphic properties of new pyridine derivatives**” submitted by **Mr. Ahipa T.N.** (Register Number: CY10F06) as the record of the research work carried out by him is *accepted as the Research Thesis submission* in partial fulfillment of the requirements for the award of degree of Doctor of Philosophy.

Prof. A. Vasudeva Adhikari

Research Guide

Date:

Chairman - DRPC

Date:

**DEDICATED TO MY**

**BELOVED PARENTS**

## ACKNOWLEDGEMENTS

I would like to express my deep sense of gratitude to my research supervisor Prof. A. Vasudeva Adhikari, Department Chemistry, NITK for his invaluable guidance and help rendered throughout the course of this investigation, without which I would not have completed this thesis successfully. The direction he gave and knowledge he shared in each and every single step of this work made it all possible. I am extremely thankful to him for all the help he provided during my research.

I sincerely thank Prof. Swapan Bhattacharya, Director, NITK and Prof. B.R. Bhat, Head, Chemistry Department for providing necessary facilities to carry out this research work. I am also thankful to Prof. A.N. Shetty, Prof. D.K. Bhat, Dr. A.M. Isloor, Dr. Udaya Kumar D., Dr. D.R. Trivedi and Dr. Sib Sankar Mal for their constant support and encouragement.

My special thanks are due to the RPAC members, Prof. A.C. Hegde, Chemistry Department and Prof. S.M. Kulkarni, Mechanical Engineering Department, NITK for spending their time to attend my research presentations and for giving valuable suggestions towards the improvement of research quality.

My special thanks to Dr. M.N. Sathyanarayan, Mr. Hidayath Ulla and Mr. M.R. Kiran, Optoelectronics Laboratory, Department of Physics, NITK for extending their lab facilities; NMR Research Centre, IISc Bangalore; IIT Madras; SAIF Punjab; SAIF Shilong; MIT Manipal and Sequent Scientific Limited, Mangalore for providing  $^1\text{H}$  NMR,  $^{13}\text{C}$  NMR and mass spectral analysis. I remain thankful to CSMR Bangalore; RRI Bangalore and SSCU, IISc Bangalore for providing their laboratories to carry out liquid crystalline studies.

I have to remember always and thank my friends Dr. Vishnumurthy K.A., Dr. Sunitha M.S., Dr. Shrikant, Mr. Dickson D. Babu, Mr. Naveenchandra and Mr. Praveen Naik for their regular help, suggestions and company. I extend my sincere

thanks to non-teaching staff of Chemistry Department, Mrs. Kasthuri Rohidas, Mr. Ashok, Mr. Santhosh, Mr. Prashanth, Mr. Pradeep, Mr. Harish, Mrs. Sharmila and Mrs. Deepa, who were timely enough to provide me a helping hand at times of need. Also, I would like to thank all the research scholar friends of Chemistry Department, NITK, for their constant help and support.

I do not have any words to express my gratitude to my father, Nagaraja Bhat T.S. and mother, Bhagya as well as my sister, Spoorthy T.N. for their constant support and encouragement. Finally, I thank all my family members and friends for their love and constant support.

**Ahipa T.N.**

## ABSTRACT

Luminescent liquid crystals (LC) are fascinating materials and have received significant, scientific and technological interest due to their wide range of applications. Among various LC materials, heterocyclic mesogens gain much interest. This is attributed to the ability of heterocycles to impart lateral and/or longitudinal dipoles combined with their favorable molecular shape. Also, their presence helps for exhibiting good photophysical properties. At present, there is a considerable attention among the researchers to develop new heterocyclic systems showing both liquid crystalline and luminescent properties. In this context, it was contemplated to design, synthesize and to investigate the liquid crystalline as well as optical properties of new pyridine derivatives.

Based on the literature survey, new pyridine derivatives (**LC<sub>1-48</sub>**) were designed as possible liquid crystalline materials. They were later successfully synthesized following the appropriate synthetic routes. Further, their synthetic methods as well as purification techniques were established and their yields were optimized. Further, their structures were confirmed by various spectral techniques such as FTIR, <sup>1</sup>H NMR, <sup>13</sup>CNMR spectral, single crystal followed by elemental analyses. Finally, the target compounds were characterized for their mesogenic, optical and optoelectronic properties. The liquid crystalline study on new pyridine derivatives indicated that the compounds **LC<sub>1</sub>**, **LC<sub>14</sub>** and **LC<sub>20-25</sub>** were shown to exhibit nematic phase at high temperature and **LC<sub>2-13</sub>**, **LC<sub>15-19</sub>**, **LC<sub>26-32</sub>** and **LC<sub>34-48</sub>** were shown to display columnar phase at ambient or higher temperature. Similarly, their optical study revealed that the compounds showed a strong absorption band in the range of 330-370 nm in solution state and a strong blue emission band in the range of 390-480 nm both in solution as well as in film state. The optoelectronic study of **LC<sub>38</sub>** evidenced its suitability in device applications. To sum up, suitably substituted new pyridine derivatives appeared as active templates for future development of new liquid crystalline materials.

**Keyword:** Liquid crystal; Cyanopyridine; Methoxypyridine; Cyanopyridone; Solvatochromism; Fluorescence.

## CONTENTS

<b>CHAPTER 1</b>	<b>Page No.</b>
<b>GENERAL INTRODUCTION TO LIQUID CRYSTALS</b>	
1.1 INTRODUCTION TO LIQUID CRYSTALS	1
1.2 CLASSIFICATION OF LIQUID CRYSTALS	2
1.3 LIQUID CRYSTAL PHASES	4
1.4 CHARACTERIZATION OF THE MESOPHASES	8
1.4.1 Polarized optical microscopy	8
1.4.2 Differential scanning calorimetry	12
1.4.3 X-ray diffractometry	14
1.5 APPLICATIONS OF LIQUID CRYSTALS	16
1.6 AN OVERVIEW OF THE PRESENT WORK	19
<b>CHAPTER 2</b>	
<b>LITERATURE REVIEW, SCOPE AND OBJECTIVES, DESIGN OF NEW PYRIDINES AS MEOSGENS</b>	
2.1 LIQUID CRYSTALLINE MATERIALS	21
2.1.1 Organic liquid crystals	21
2.1.2 Heterocyclic liquid crystals	23
2.2 PYRIDINE BASED LIQUID CRYSTALS	23
2.2.1 Chemistry of pyridine	23
2.2.2 Advantages of pyridine-based liquid crystals	27
2.3 LITERATURE REVIEW	32
2.4 SCOPE AND OBJECTIVES OF THE PRESENT RESEARCH WORK	44
2.5 DESIGN OF NEW PYRIDINE DERIVATIVES	46
2.5.1 Design of 4,6- dialkoxyaryl-2-methoxynicotinonitriles <b>(Series-I; LC<sub>1-13</sub>)</b>	47
2.5.2 Design of 6-alkoxyaryl/thiophenyl-4-substituted aryl-2-methoxy pyridines <b>(Series-II; LC<sub>14-33</sub>)</b>	49
2.5.3 Design of 2-(4,6-disubstituted aryl-3-cyanopyridyl)oxyaceto- hydrazones <b>(Series-III; LC<sub>34-38</sub>)</b>	50



2.5.4 Design of 4,6-disubstituted aryl-3-cyanopyridones (Series-IV; LC <sub>39-48</sub> )	51
<b>CHAPTER 3</b>	
<b>SYNTHESIS AND CHARACTERIZATION OF NEW PYRIDINE DERIVATIVES</b>	
3.1 INTRODUCTION	54
3.2 MATERIALS AND METHODS	54
3.3 SYNTHETIC METHODS	55
3.3.1 Synthesis of 4,6- dialkoxyaryl-2-methoxy nicotinonitriles (LC <sub>1-13</sub> )	55
3.3.1.1 Results and discussion	55
3.3.1.2 Experimental procedures	66
3.3.2 Synthesis of 6-alkoxyaryl/thiophenyl-4-substituted aryl-2- methoxy pyridines (LC <sub>14-33</sub> )	75
3.3.2.1 Results and discussion	75
3.3.2.2 Experimental procedures	88
3.3.3 Synthesis of 2-(4,6-disubstituted aryl-3-cyanopyridyl)- oxyacetohydrazones (LC <sub>34-38</sub> )	102
3.3.3.1 Results and discussion	102
3.3.3.2 Experimental procedures	104
3.3.4 Synthesis of 4,6-disubstituted aryl-3-cyanopyridones (LC <sub>39-48</sub> )	109
3.3.4.1 Results and discussion	110
3.3.4.2 Experimental procedures	113
3.4 CONCLUSIONS	130
<b>CHAPTER 4</b>	
<b>INVESTIGATION OF MESOGENIC, OPTICAL AND OPTOELECTRONIC PROPERTIES OF NEW PYRIDINE DERIVATIVES</b>	
4.1 INTRODUCTION	131
4.2 INVESTIGATION OF LIQUID CRYSTALLINE BEHAVIOR OF NEW PYRIDINE DERIVATIVES	131
4.2.1 Experimental procedures	131
4.2.2 Results and discussion	132

4.2.2.1 Mesomorphic behavior of 4,6-dialkoxyaryl-2-methoxy nicotinitriles ( <b>LC<sub>1-13</sub></b> )	132
4.2.2.2 Mesomorphic behavior of 6-alkoxyaryl/thiophenyl-4- substituted aryl-2-methoxy pyridines ( <b>LC<sub>14-33</sub></b> )	137
4.2.2.3 Mesomorphic behavior of 2-(4,6-disubstituted aryl-3-cyano- pyridyl)oxy acetohydrazones ( <b>LC<sub>34-38</sub></b> )	145
4.2.2.4 Mesomorphic behavior of 4,6-disubstituted aryl-3-cyano- pyridones ( <b>LC<sub>39-48</sub></b> )	150
<b>4.3 INVESTIGATION OF OPTICAL PROPERTIES OF NEW PYRIDINE DERIVATIVES</b>	<b>156</b>
4.3.1 Experimental procedures	157
4.3.2 Results and discussion	157
4.3.2.1 Optical properties of 4,6-dialkoxyaryl-2-methoxy- nicotinitriles ( <b>LC<sub>1-13</sub></b> )	157
4.3.2.2 Optical properties of 6-alkoxyaryl/thiophenyl-4-substituted aryl-2-methoxy pyridines ( <b>LC<sub>14-33</sub></b> )	161
4.3.2.3 Optical properties of 2-(4,6-disubstituted aryl-3-cyanopyridyl) oxy acetohydrazones ( <b>LC<sub>34-38</sub></b> )	164
4.3.2.4 Optical properties of 4,6-disubstituted aryl-3- cyanopyridones ( <b>LC<sub>39-48</sub></b> )	166
<b>4.4 INVESTIGATION OF OPTOELECTRONIC PROPERTIES OF LC<sub>38</sub></b>	<b>168</b>
4.4.1 Device fabrication and characterization	170
<b>4.5 CONCLUSIONS</b>	<b>173</b>
<b>CHAPTER 5</b>	
<b>SUMMARY AND CONCLUSIONS</b>	
<b>5.1 SUMMARY AND CONCLUSIONS</b>	<b>173</b>
<b>REFERENCES</b>	<b>176</b>
<b>LIST OF PUBLICATIONS</b>	<b>187</b>
<b>CURICULUM VITAE</b>	<b>189</b>

## LIST OF ABBREVIATIONS

LC	:	Liquid crystal
$T_m$	:	Melting temperature
$T_c$	:	Clearing temperature
n	:	Director
Cr	:	Crystal phase
D	:	Discotic phase
N	:	Nematic phase
$N_D$	:	Nematic discotic phase
$N_{col}$	:	Nematic columnar phase
SmC	:	Smectic C phase
SmA	:	Smectic A phase
SmB	:	Smectic B phase
SmI	:	Smectic I phase
G	:	3D analog of SmF
I	:	3D analog of SmI
S1, S2	:	Unidentified smectic phase
H, K	:	Tilted phase with chevron herringbone packing of the molecules
S	:	Order parameter
$Col_h$	:	Columnar hexagonal
$Col_r$	:	Columnar rectangular
$Col_o$	:	Columnar oblique
$Col_{ortho}$	:	Columnar orthorhombic
OLED	:	Organic light emitting diode
TFT	:	Thin film transistor
rt	:	Room temperature

## **CHAPTER 1**

### **GENERAL INTRODUCTION TO LIQUID CRYSTALS**

**Abstract**

Chapter 1 begins with a brief introduction to liquid crystals followed by classification of liquid crystals. Also, it covers description on various types of liquid crystalline phases and their physical properties. Further, it includes a concise account on characterization methods used for the identification of liquid crystal phases. Finally, the chapter highlights some of the interesting applications of liquid crystals.

**1.1 INTRODUCTION TO LIQUID CRYSTALS**

The field of liquid crystals is now well established not only in basic research but also in development of new applications and their commercial uses. As liquid crystals (LCs) represent a state in-between ordinary liquids and solids, the investigation of their physical properties is very complex and hence their study makes use of many different tools and techniques. At present, LCs play important role in material science and they are model materials for the organic chemist in order to investigate the relation between their chemical structure and physical properties. In fact, LC materials are unique in their properties and uses. As the research in this area continues, the new applications are developed; consequently its importance in modern technology is gaining much interest.

The study of liquid crystals began in 1888. An Austrian botanist Friedrich Reinitzer, while trying to melt a sample of cholesteryl benzoate (first liquid crystal), observed that the compound exhibited two melting points. At 145.5 °C, the compound melted to form a cloudy liquid and later it became completely clear at 178.5 °C. Soon after, this work was taken up by a German physicist Otto Lehmann who coined the term “liquid crystal” to describe this new state of matter. In the intervening century, since their discovery, considerable advances have been made in the study into the nature and properties of liquid crystals. Thus, the remarkable work by Friedrich Reinitzer and Otto Lehmann credited them to be called the grandfathers of liquid crystal science (Oswald and Pieranski 2005).

The liquid crystal state (known as a *mesophase*) represents a discrete state of matter which exists between the solid and liquid states as shown in **Figure 1.1**; like a

liquid it is fluid and yet like a solid, it has order. This combination of order and fluidity results in mesophases with anisotropic physical properties and hence LCs attracted widespread applications in many fields. In their solid phase, the molecules have a large amount of both positional and orientational order; in that the molecules maintain specific positions and orientations. In the liquid phase, there is no positional and orientational order, since the molecules diffuse about randomly, causing constant change in their positions as well as orientations. But, in the LC phase, the molecules can diffuse about as they do in liquids. So, they are orientationally ordered but positionally disordered in the LC phase.

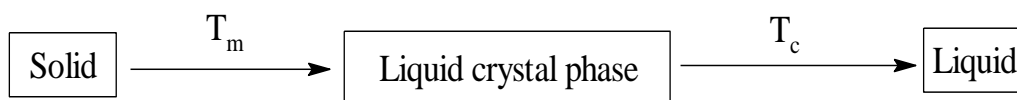


**Figure 1.1** Different states of matter

## 1.2 CLASSIFICATION OF LIQUID CRYSTALS

Liquid crystals are broadly classified as lyotropic and thermotropic based on the method used to destroy the order of the solid state. Further, thermotropic liquid crystals are classified into two main categories, *viz.* low molecular mass and high molecular mass liquid crystals.

### *Lyotropic:*

A liquid crystalline material is called lyotropic if the phases have long-ranged orientational order, which are induced by the addition of a solvent. Earlier, the term was used to describe materials composed of amphiphilic molecules. Such molecules comprise a water-loving 'hydrophilic' head-group (which may be ionic or non-ionic) attached to a water-hating 'hydrophobic' group. Typical hydrophobic groups include saturated or unsaturated hydrocarbon chains. Examples of lyotropic compounds are the salts of fatty acids, and phospholipids.

### *Thermotropic:*

In thermotropic liquid crystals, transitions from the solid to liquid crystal and liquid crystal to isotropic liquid state are affected by the action of temperature. From

the thermodynamic point of view, transitions between the solid state and mesophase are strongly first order, while transitions between a mesophase and the isotropic liquid state are weakly first order. But, transitions between mesophases are either weakly first order or, occasionally, second order. In fact, the most important criteria for the formation of mesophase is that the molecule should be structurally anisotropic, for which it is necessary to introduce additional anisotropic dispersion forces between the molecules that are strong enough to stabilize the mesophase. In general, thermodynamically stable mesophases which appear on heating and cooling are referred as enantiotropic, whereas mesophases that appear only on cooling are referred as monotropic. In the present research work, only thermotropic liquid crystal materials have been focused, but not lyotropic.

*Classification of thermotropic liquid crystals:*

Thermotropic LCs are generally classified into two main categories, low molecular mass and high molecular mass, which means non-polymeric and polymeric materials, respectively. Each class can then be represented by further sub-divisions. Thus, high-molar-mass systems include the side-chain and main-chain polymers, and dendritic molecules, while low-molar-mass systems consist of rod-like, disc-like and bent-core molecules. Nature of liquid crystal phases in them depends strongly on the shape of the molecules, and the stereochemistry. Generally, rod-like molecules are called calamitic, whereas, disc-like molecules are termed as discotic. Essentially, in liquid crystal molecules, the structural anisotropy is the determinant factor. In general, calamitic molecules have one long axis and two short axes, while discotic molecules have two long axes and one short axis.

In the simplest LC phase, all the molecules tend to arrange in one direction, usually along the main axis; this preferred direction is called the director and is denoted with the unit vector 'n'. It represents the average local direction and the optic axis of the system. **Figure 1.2** summarizes different classifications of LCs based on method used for inducing LC phase, molecular mass and shapes of molecules.

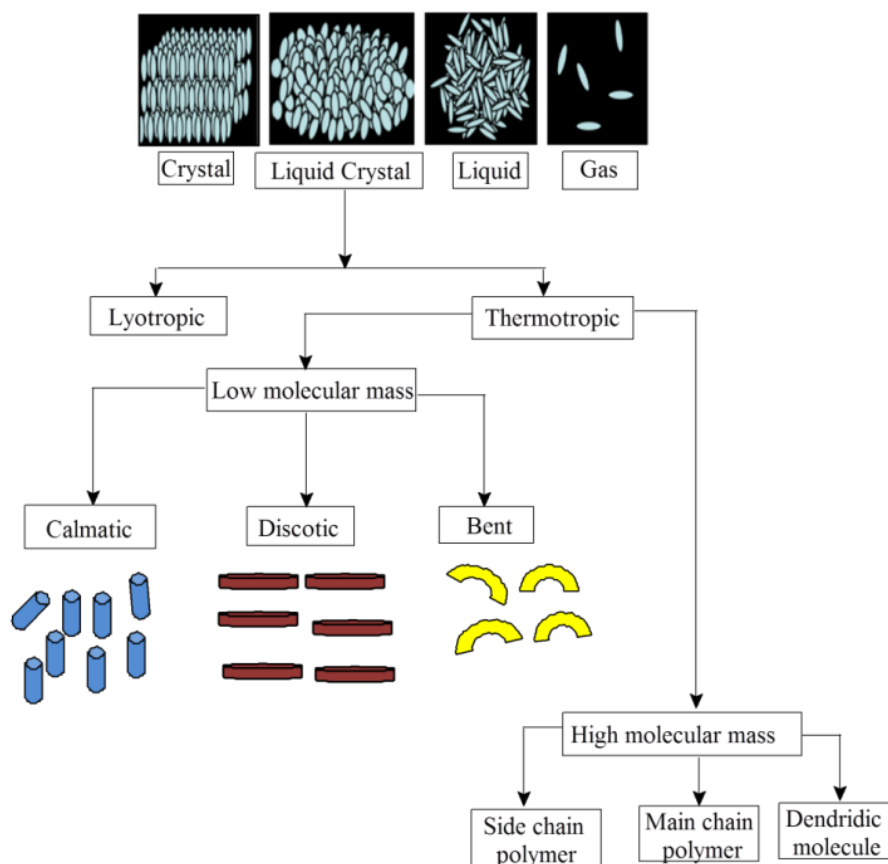


**Figure 1.2** Classification of LCs

### 1.3 LIQUID CRYSTAL PHASES

In 1922, a French scientist named George Friedel (Meyer et al. 1975) proposed a classification scheme based on the molecular arrangement of mesogens. Accordingly, liquid crystal phases are classified as nematic, smectic, cholesteric and columnar phases.

#### *Nematic phase:*

Nematic (N) is the most common and simplest liquid crystal phase. They form thread like textures when viewed under the polarized microscope. It is the most disordered type of liquid crystal mesophase. In case of thermotropic liquid crystals, three types of nematic phase are usually observed. They include one type derived from rod-like molecules and other two types derived from disc-like molecules. In the first type (**Figure 1.3a**), the mesophase comprises rod-like molecules which have long-range orientational order in one direction, without positional order. Here,



orientational order is defined by an average direction of molecules (director axis) and is denoted by a vector 'n'. In fact, the orientation of individual molecules differs significantly from that direction; thus the nematic phase can be characterized by an order parameter S. The orientational order parameter S is based on the average of the second order Legendre polynomial and it is defined as:

$$S = \frac{1}{2} \langle 3 \cos^2 \theta - 1 \rangle$$

In the above equation,  $\theta$  represents angle between the director and the long axis of each molecule,  $\langle 3 \cos^2 \theta - 1 \rangle$  denotes an average over-all molecules in the sample, and S shows the extent of order present in the liquid crystal. The order parameter S can be determined experimentally by a number of methods, including measurement of linear dichroism from UV and IR absorptions and by deuterium NMR spectroscopy. If the molecules are well aligned with the director, then S takes the value 1 and if the molecules are randomly oriented about n, then  $S = 0$ , *i.e.* isotropic.

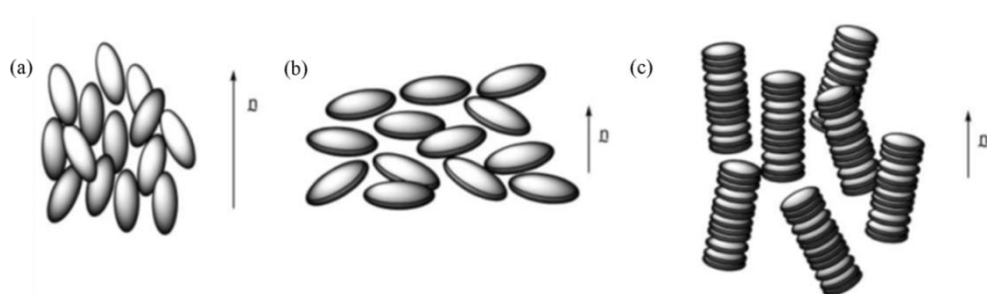


**Figure 1.3** (a) nematic phase of rod-like molecules, N (b) nematic phase of disc-like molecules,  $N_D$  (c) nematic phase of columnar-like molecules,  $N_{col}$

In most of the cases, the value of S lies in between 0.3 and 0.9. Generally, more the value of S, higher is the order of nematic phase. In fact, this phase appears in the majority of liquid crystal displays. **Figure 1.3b** shows a nematic phase of disc-like molecules and this phase is commonly known as nematic discotic phase ( $N_D$ ). Typically, these phases are characterized by their symmetry but not by the shape of the molecules of which they are comprised. **Figure 1.3c** displays characteristic  $N_{col}$  phase, which is termed as a columnar nematic phase. This phase is occasionally found in the mesogens of disc-like molecules.

*Smectic phase:*

Usually, smectic phases consist of layered arrangement of mesogens which possess both orientational order and translational order. Yet there are several such phases, only two of them, *viz.* smectic A (SmA) and smectic C (SmC) phases have been highlighted here. It is observed that, the SmA phase is the most disordered type and in it, the molecules are organized perpendicular to the direction of layer as indicated in **Figure 1.4a**. In SmC phase, as shown in **Figure 1.4b**, the organization of mesogens is similar to that of SmA, except that the molecules are now tilted at some angle,  $\theta$ , to the normal layer. Further, chiral versions of this phase have  $C_2$  symmetry in the layers and as such, are ferroelectric (a property which needs for display applications) in nature. It is important to note that in both SmA and SmC phases, the ‘layers’ as shown in the figure are not well-defined and in fact, the organization is best described as a sinusoidal molecular density wave. Also, these phases are highly fluidic and hence, there is a probability of molecules moving between the layers.

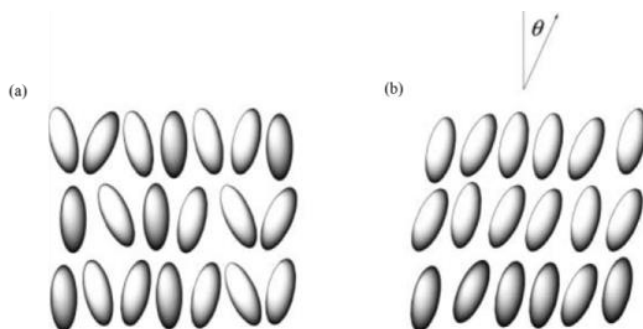


**Figure 1.4** Schematic representation of (a) SmA phase, (b) SmC phase

In addition to SmA and SmC phases, another kind of phase, called ‘chiral smectic’ is also observed in LCs. This phase (designated as  $C^*$ ) comprises chiral molecules which are optically active towards plane polarized light. Such chiral molecules are able to form mesophases with structures related to those of non-chiral molecules and they possess different optical properties. **Figure 1.5** shows the helical arrangement of chiral molecules in SmC\* phase. Here, in consistent with the smectic-C, the director makes a tilt angle with respect to the smectic layer. The main difference is that this angle rotates from layer to layer forming a helix as seen in **Figure 1.5**. In other words, the director of the SmC\* mesophase is not parallel or perpendicular to the layers, and it rotates from one layer to the next.

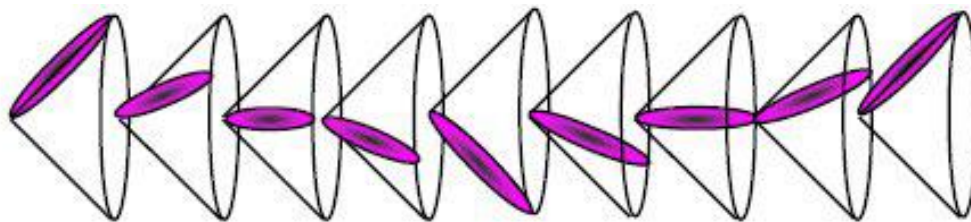


**Figure 1.5** Arrangement of molecules in SmC\* phase (helical)

*Cholesteric phase:*

When a nematic phase is incorporated with a chiral molecule, it leads to the formation of a structure as a stack of very thin 2-D nematic like layers with the director in each layer twisted with those above and below, as shown in **Figure 1.6**. In this structure, the directors actually form a continuous helical pattern about the normal layer. Interestingly, an important characteristic of the cholesteric mesophase is the pitch. It is defined as the distance it takes for the director to rotate one full turn in the helix. The necessary condition for the formation of cholesteric mesophase is that the molecules should be chiral. In general, this phase is also defined as chiral nematic phase and it is represented by N\*.

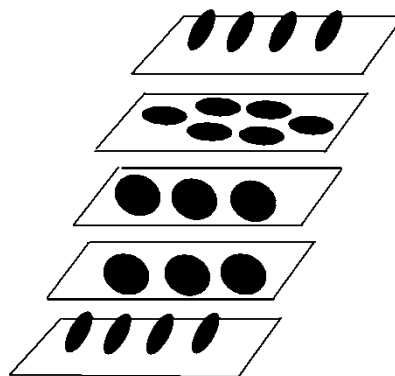


**Figure 1.6** An arrangement of molecules in cholesteric phase

*Columnar phase:*

As the name indicates, the basic building block for this type of mesophase is the column and in most of the cases, the columns are formed from disc-like molecules. However, the columns may be formed by a variety of different molecular types and the arrangement of these columns in two dimensions describes the complete structure of the mesophase. Amongst various types of columnar phases, hexagonal (Col<sub>h</sub>), rectangular (Col<sub>r</sub>) and oblique (Col<sub>o</sub>) phase are quite common. Based on

symmetry operations, columnar rectangular phase are further classified into different types *e.g.*  $P_{2gg}$  and  $C_{2mm}$ . **Figure 1.7** shows a side-on view of the columnar hexagonal phase (a-i) and then ‘aerial’ views of the hexagonal (a-ii), oblique (b) and rectangular (c and d) lattices. In **Figure 1.7**, circles represent discs which are orthogonal within the columns, whereas ellipses represent discs which are tilted.

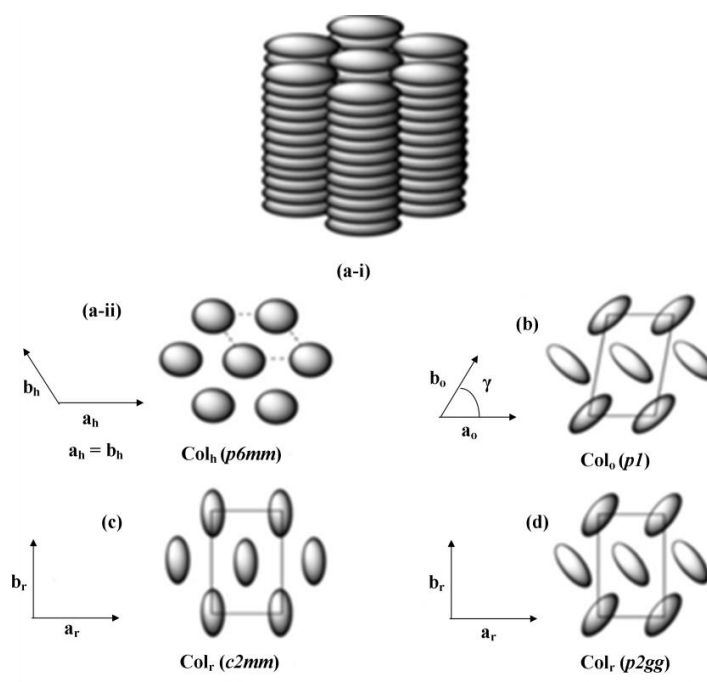


**Figure 1.7** Structure of the common columnar phases

## 1.4 CHARACTERIZATION OF MESOPHASES

Different methods are being used to characterize mesophases formed by liquid crystalline materials. Those methods reveal thermodynamic aspects of phase transition, phase identification, and mesophase type and other related textural information about mesogens. The frequently used methods include polarized optical microscopy (POM), differential scanning calorimetry (DSC) and X-ray diffractometry.

### 1.4.1 Polarized optical microscopy

The fastest and the simplest method used to recognize a LC phase is polarized optical microscopy, which makes use of the phenomenon of birefringence that is one of the physical properties commonly observed in a mesophase. This property is mainly due to the anisotropy of the phase. As mesophases possess at least two

different refractive indexes, when the light passes through the material, it will be refracted in two different directions with two different speeds. Among the two rays, one perpendicular to the director  $n$ , is usually called ordinary ray,  $n_o$  (or  $n_{\perp}$ ), and the other one that is parallel to  $n$  is called extraordinary ray,  $n_e$  (or  $n_{\parallel}$ ). They cause two different refractive indices and the maximum difference between these two refractive indices is called the birefringence ( $\Delta n = n_e - n_o$ ), which varies with temperature in an anisotropic medium. **Figure 1.8** shows a general trend in the variation of birefringence with temperature for a LC material.

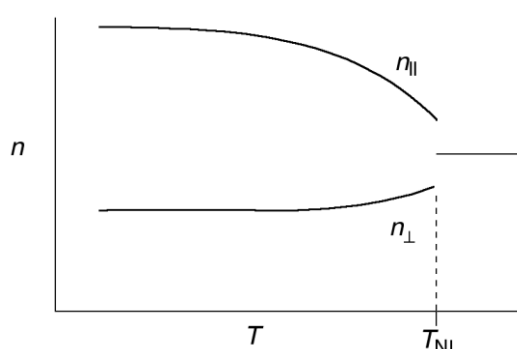


**Figure 1.8** Variation of birefringence ( $n$ ) with temperature ( $T$ ) for a particular wavelength in a LC

Normally, the instrument POM is equipped with two polarizers, one between the light and the sample, and the other between the sample and the observer, and they are oriented at  $90^\circ$  to each other. In the experiment, the sample under test is sandwiched between two glass cover slips and then placed on a hot-stage whose temperature can be controlled. The samples can be aligned in a homeotropic fashion (the main axes of the molecules are perpendicular to the plane of the cover glasses) or homogeneously (the main axes of the molecules lie in the same plane as the cover glasses). The light radiation, after plane polarized by the first filter passes through the sample and then comes out of the other filter. If the sample is in the isotropic phase or in the homeotropic state, it appears black because of the fact that no interference pattern is formed. This is because isotropic liquids are not birefringent, as it is possessing only one refractive index. In case of homeotropically aligned sample, there occurs no interference. This is because the polarized light passing through it is completely stopped by the analyzer. **Figure 1.9** shows the working principle of POM.

From the figure it is clear that if the LC sample is not aligned homeotropically, the polarized light passing through it will be split into two different beams that will bring about interference. This interference destroys the plane polarization and creates an interference pattern from which it is possible to recognize a mesophase.

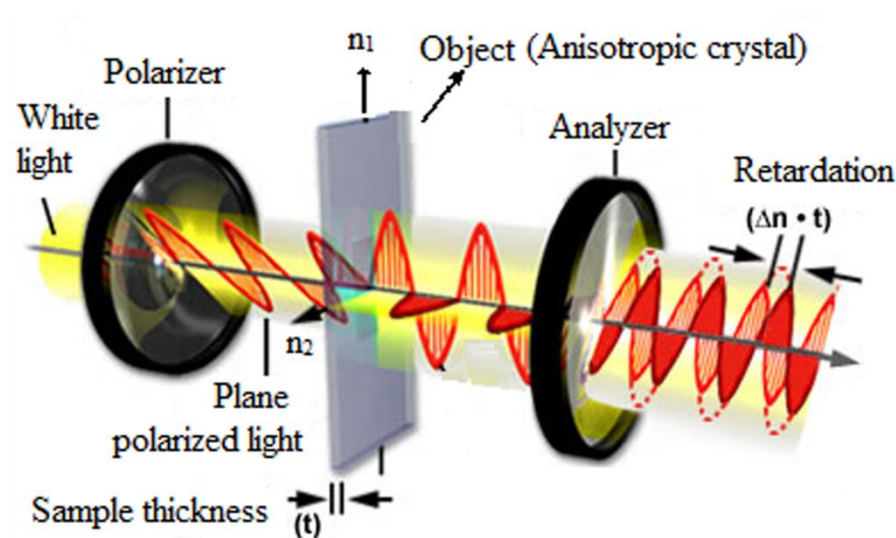


**Figure 1.9** Working principle of POM

In identification of phases with POM, not only the formed pictures are important, but also behavior of the sample in the liquid crystal phase as well as its behavior during the phase transitions has significance. For example, a nematic phase in full homeotropic alignment will result in a black spot, but a normal, unaligned sample will show characteristic textures. This is mainly due the fact that the director 'n' does not have points in the same direction in all the regions of the material. If the director changes through the whole sample, where the changes are drastic, no specific order can be defined and hence a defect is generated. These defects appear as black point (or point defect) or line defects in the texture. They are black because of the optical extinction caused by the cross polarizers. For occurring optical extinction, the molecules must be aligned homeotropically or in the direction of either of the two cross polarizers.

**Figure 1.10** shows molecular alignments of a LC phase in a typical way. In the first two cases where  $S=1$ , the defect results in the four-brush schlieren (red ring in **Figure 1.11c**), in the other two cases, where  $S=1/2$ , the defects result in the two-brush

schlieren (green ring in **Figure 1.11c**). The other phases display peculiar characteristic textures and their behavior in the phase transition is shown in **Figures 1.11a** and **b**. Normally, SmA phases of a LC material are characterized by the presence of black part due to the homotropical alignment and by the existence of clean and smooth focal conical fan texture.

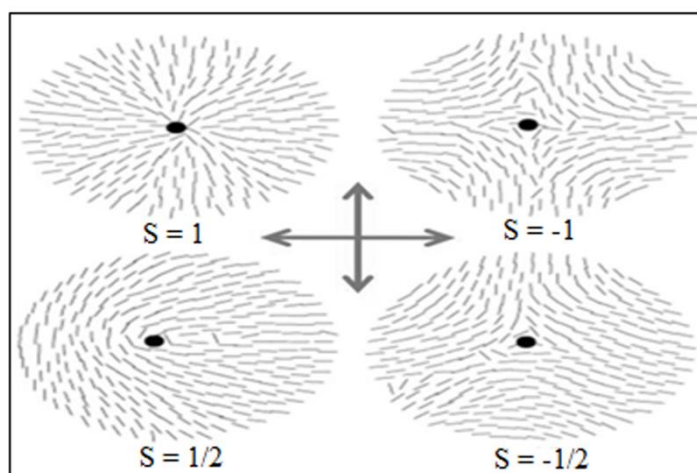


**Figure 1.10** Schlieren brush type molecular alignment. Black arrows indicate the direction of the cross polarizers

Further, the transition from crystalline to a SmC phase can be clearly visible by the appearance of a schlieren texture in the homotropic alignment (this is because SmC is a tilted phase) and by the observation of brushes on the focal conical fan texture.

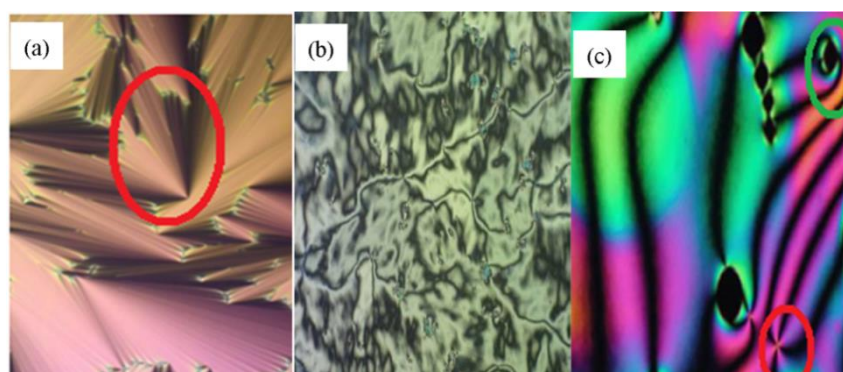


**Figure 1.11** POM images of: (a) SmA phase where the ring shows smooth focal conical fan texture, (b) brushed schlieren texture of SmI phase and (c) N phase with defect (encircled)

On the other hand, the presence of a SmI phase is characterized by the occurrence of even larger brushes on the focal conical texture and by a difficulty to focus on the phase. All these differences, mentioned herein, are not so easy to be detected and a lot of experience is required to recognize the different phases. Thus, although POM is a powerful tool for characterization of LC material, sometimes other analyses are essential to characterize a mesophase completely.

#### 1.4.2 Differential scanning calorimetry

Differential scanning calorimetry is normally used in parallel with optical microscopy, when a phase transition is not easily detected in the microscope, or an apparent textural change is not actually a real phase transition. Indeed, some times the defect textures may be very similar, for example during the SmA-SmB transition. Also, in some cases, the retention of the defect of the preceding phase in the new phase can contribute to the difficulty to identify clearly the liquid crystal phase. In such cases, DSC technique is quite useful to observe the occurrence of the transition. In some instances, a change in pattern detected by POM may or not be real and so DSC can be a preferred technique to confirm it. Yet, these two methods should be used in conjunction because they are complementary to each other. The principle of DSC technique involves the measurement of heat power that the instrument has to supply to the sample in order to maintain the same temperature against a reference during a phase transition. Usually, the sample (2-3 mg) is placed in an aluminium pan, covered with an aluminium slip and finally sealed. This is then inserted in the sample heater plate, while an empty pan is placed in the reference heater. The instrument contains two independent heaters that are controlled by platinum sensors and through these sensors, or using a thermocouple, the instrument checks the amount of heat power that has to be added (**Figure 1.12**).

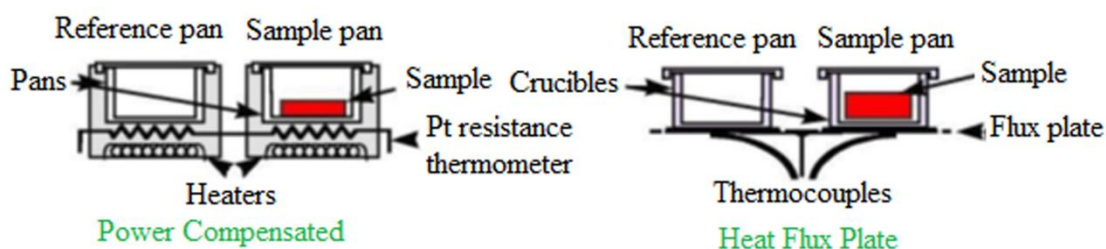


**Figure 1.12** Scheme of generic differential scanning calorimeters



During heating, when a phase transition occurs in the sample, the heat given is used up by the sample to change its phase, which is reflected in no change in temperature. Then, the calorimeter has to supply more heat power to the sample pan to maintain the same temperature as that of reference pan. This heat supply will then result in a peak on a plot of power against temperature. **Figure 1.13** depicts a typical DSC plot obtained with a small liquid crystal sample of 8OCB (octyloxycyanobiphenyl) at a rate of  $1^{\circ}\text{C}/\text{min}$ , for both heating and cooling cycles. In the thermogram, the lower curve corresponds to a heating process while the upper curve indicates a cooling process. Here, the lower heating curve indicates a crystal to liquid crystal (SmA) transition at  $55^{\circ}\text{C}$  followed by a barely detectable SmA to nematic transition at  $67^{\circ}\text{C}$  and finally the nematic (N) to isotropic (I) transition at about  $80^{\circ}\text{C}$ . Further, the upper cooling curve shows a slight displacement of the peak position of I to N transition. This is attributed to partially supercooling and partially instrumental hysteresis at scan rate temperature. Also, the displacement of peak position of SmA to crystal transition is depressed mainly due to supercooling of the SmA phase. Thus, the phase diagram for the cooling process would not be identical to that for heating.

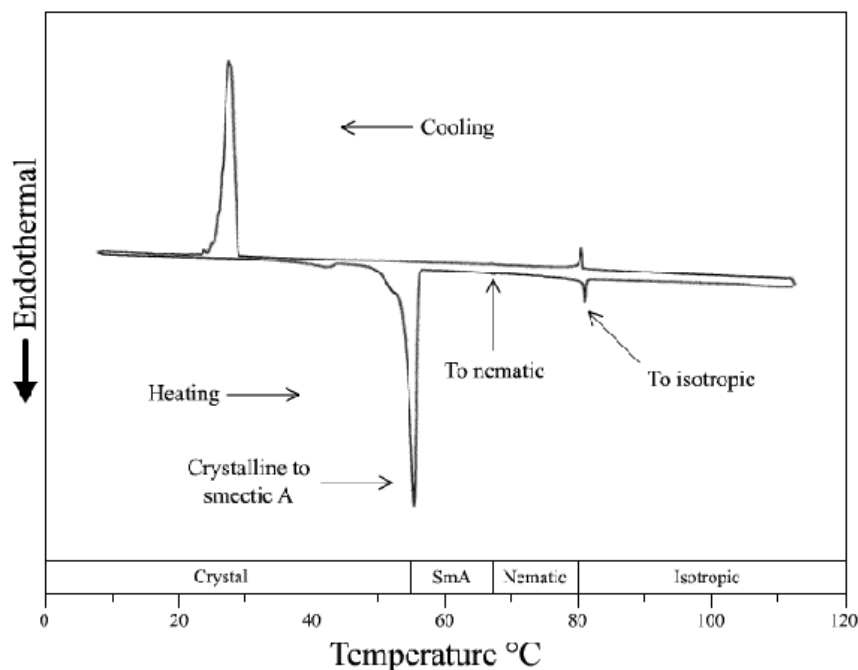


**Figure 1.13** DSC plot with phase diagram for the compound 8OCB

### 1.4.3 X-ray diffractometry

X-ray diffraction is a powerful technique to investigate the microscopic structure of liquid crystal phases (Binnemans 2009). X-ray diffractometer makes use of X-rays for getting characteristic diffraction pattern of the LC materials. Generally, in the mesophase, the molecules are partially ordered and form periodic structures. When the beam from an X-ray source passes through a sample of a mesogen, each molecule can be considered as a point in a net; each point can scatter the incident plane wave of X-rays in different directions. All these reflected rays will interfere with each other and the result of this interference is then detected on a film placed after the samples. The resulted picture is called a diffraction pattern. **Figure 1.14** indicates a schematic representation of X-ray diffractometer, where a thin film of LC sample could be aligned by a magnetic (B) or electric (E) field applied either perpendicular to the beam direction or parallel to it. It can also be aligned using a heating system in the instrument. The figure shows an incident beam with wavelength  $\lambda$  striking a structure with period 'd' in a direction perpendicular to the beam. Suppose the some of the X-rays are diffracted by an angle  $\theta$ , toward a detector; the path length difference for the scattered waves is  $2d \sin \theta$ . This is because the rays of the incident beam are always in phase and parallel up to the point at which the top beam strikes the top layer at particle Z (**Figure 1.15**). The second beam continues to the next layer where it is scattered by particle B. The second beam must travel the extra distance (AB + BC), if the two beams have to continue travelling adjacent and parallel. This extra distance has to be an integer (n) multiple of the wavelength  $\lambda$ . Therefore:

$$n\lambda = AB + BC, \text{ and } AB = d \sin \theta$$

$$n\lambda = 2AB \quad (\because AB = BC)$$

$$\therefore n\lambda = 2d \sin \theta, \text{ (mathematical form of Bragg's law)}$$

Thus, if the distance is equal to a multiple of the wavelength, then constructive interference occurs, and a peak is expected in the diffraction pattern. If the interference is not constructive, no signal is detected. Thus, only diffraction at certain angle,  $\theta$ , or its multiples will give constructive interference.

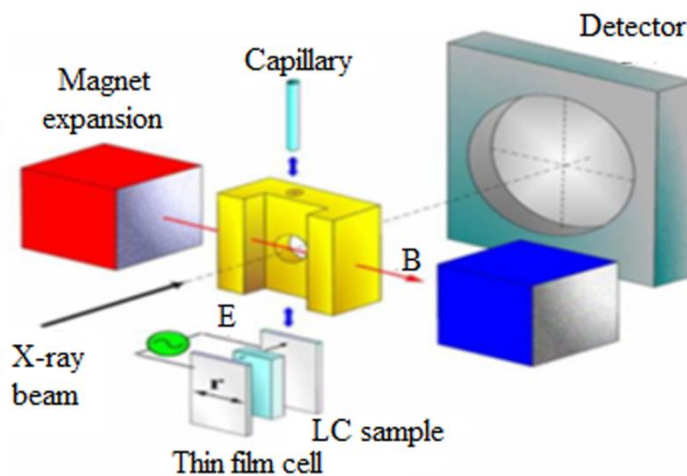


**Figure 1.14** Schematic representation of X-ray diffractometer

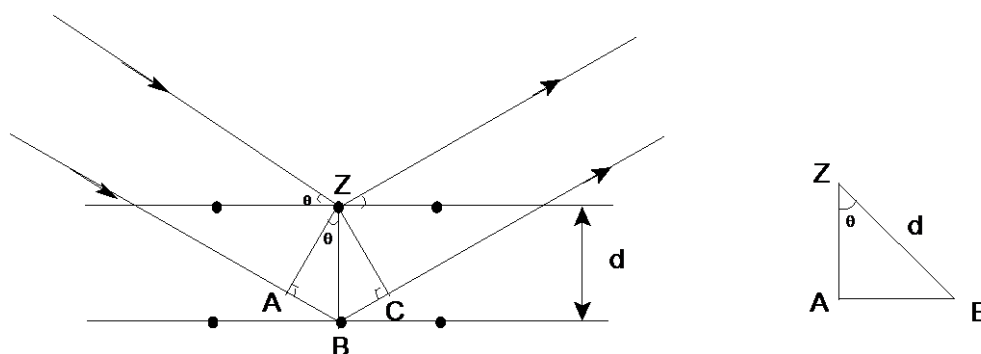


**Figure 1.15** Illustration of Bragg's Law

X-Ray diffraction from liquid crystals is almost similar to Bragg scattering from an ordered crystal. Presence of periodicities in the structure of the LC phase gives rise to constructive interference and therefore it leads to occurrence of peaks due to the scattering of X-rays. **Figure 1.16** depicts a typical X-ray diffraction pattern of  $\text{Col}_h$  obtained for an organic LC material carrying alkoxy chains. The assignment of the two-dimensional symmetry of the mesophase arises from the analysis of the  $d$ -spacings from the data obtained from the observed pattern. In the small-angle region ( $0 < 2\theta < 5^\circ$ ), three different reflection peaks are observed; these peaks correspond to the fundamental, harmonics, and higher orders of diffraction and are indicative of the two-dimensional lattice of the hexagonal phases. Further, in **Figure 1.16** at high angles ( $2\theta \sim 20^\circ$ ) a broad peak due to diffuse scattering is observed; this peak corresponds to the liquid-like order of the aliphatic chains.

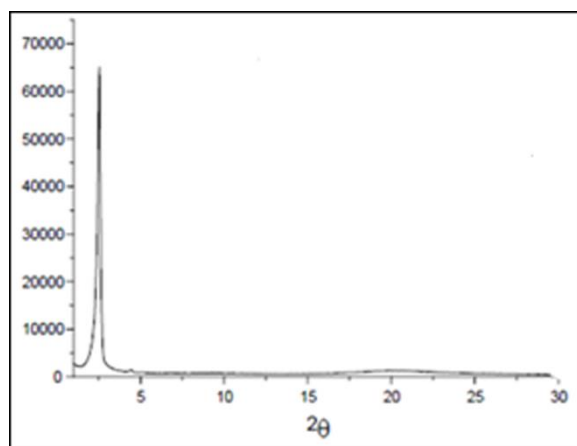


**Figure 1.16** X-ray diffraction pattern of a Col<sub>h</sub> liquid crystal material

### 1.5 APPLICATIONS OF LIQUID CRYSTALS

Liquid crystal technology has had a major effect in many areas of science and engineering, as well as device technology. Applications for this special kind of material are still being discovered and they continue to provide effective solutions to many different problems. Some of the major applications of LC materials are summarized in **Figure 1.17**.

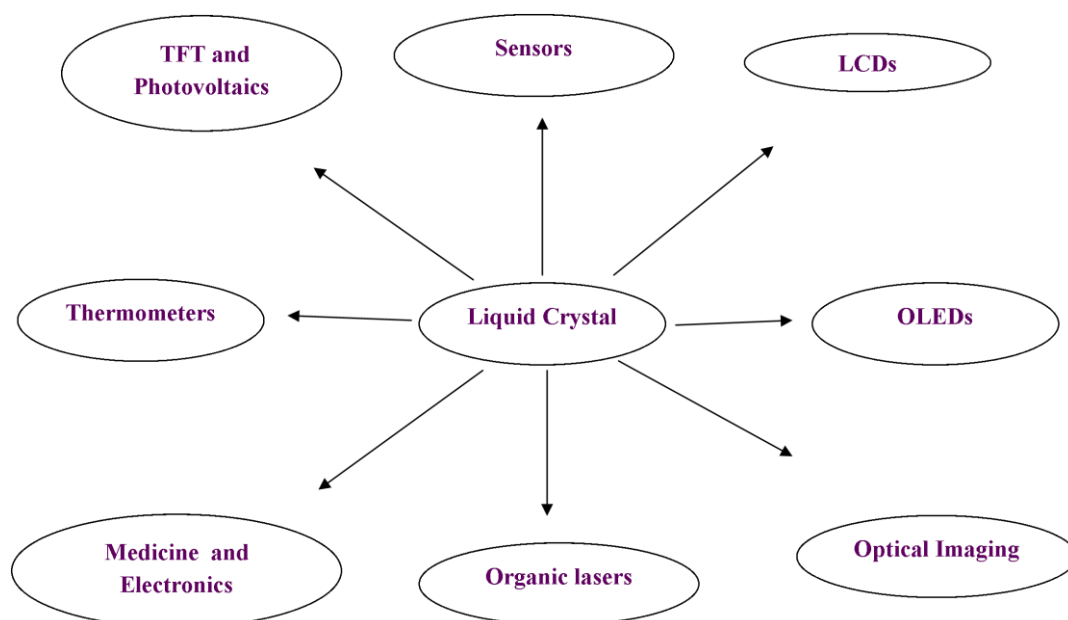


**Figure 1.17** Applications of LC material in various fields

The most common application of liquid crystal technology is in liquid crystal displays (LCDs.). Now, this field has grown into a multi-billion dollar industry. Many

significant discoveries have been made in this field and their technologies have been developed tremendously.

Liquid crystal materials exhibiting cholesteric phase can be used in liquid crystal thermometers, wherein, chiral nematic (cholesteric) liquid crystals reflect light with a wavelength equal to the pitch. Because the pitch is dependent upon temperature, the color reflected also depends upon temperature. Liquid crystals make it possible to accurately gauge temperature just by looking at the color of the thermometer. By mixing different LC compounds, a device for measuring any temperature range can be built.

The "mood ring", a popular novelty developed a few years ago, took advantage of the unique structural property of the chiral nematic liquid crystal. This device finds practical applications in the areas like medicine and electronics. Certain, special liquid crystal devices can be attached to the skin to show a "map" of temperatures. This is highly useful because often physical problems, such as tumors, have a different temperature from the surrounding tissues. Liquid crystal temperature sensors can also be used to find out the bad connections on a circuit board by detecting the abnormal high temperature region.

Another major application of liquid crystals that is now being largely explored is optical imaging and recording. In this technology, a liquid crystal cell is placed between two layers of photoconductor. Light is applied to the photoconductor, which increases the material's conductivity. This causes an electric field to develop in the liquid crystal corresponding to the intensity of the light. The arised electric pattern can be transmitted by an electrode, which enables the image to be recorded. This technology is still being developed and is one of the most promising areas of research in the field liquid crystals.

Liquid crystals have a multitude of many other uses. They are used for nondestructive mechanical testing of materials under stress. This technique is also used for the visualization of RF (radio frequency) waves in waveguides. They are used in medical applications where, for example, transient pressure transmitted by a walking foot on the ground can be measured. Particularly, low molecular mass

(LMM) liquid crystals have applications in erasable optical disks, full color "electronic slides" for computer-aided drawing (CAD), and light modulators for color electronic imaging. As novel properties and types of liquid crystals are investigated and researched, these materials are sure of gaining increasing importance in various applications.

Recently, there has been a great attention in the development of novel liquid crystalline materials for new areas such as thin-film transistors, solid organic lasers and photovoltaic devices; this is mainly due to their inherent self-assembling properties and the favorable supramolecular structures. There is no doubt that certain materials must possess organized structures to improve their performance, and consequently it is logical to think that the intrinsic ability of their molecules to self-organize into well-defined supramolecular structures could be one of the key advantages to impart the desired property in them.

A remarkable advantage of liquid crystals is that different phases can be used in order to obtain different physical effect. For example, some discotic liquid crystal oriented in columns can act as molecular wires and they are proved to have highly anisotropic charge mobility along the columns. Therefore with appropriate functionalization of disc-like molecules, it is possible to achieve a self-organized structure that forms specific channels for the transport of electrons or holes. Rod-like liquid crystals are not less important, indeed they can be used in all the devices that require application of a highly anisotropic material. Further, if luminescent molecules are used that can organize themselves in a nematic or smectic phase, it is possible to obtain polarized emission because all the molecules are capable of orienting in the same direction. This could be of great advantage for new generation of LCDs. A further interesting observation of luminescent liquid crystal materials is that the presence of certain aliphatic side-chain acts as spacer group in their structure, thereby reducing intermolecular forces of attraction due to steric effects; this can result in high solid-state luminescence efficiency (quantum yield).

## 1.6 AN OVERVIEW OF THE PRESENT WORK

In the past decade there has been a great deal of research in academia and industry involving the synthesis of new organic semiconductors along with the evaluation of their physical properties mainly for their applications in the fields of optoelectronics and electronics. At present, commercial organic light-emitting devices (OLEDs) make use of small aromatic molecules or main chain, conjugated polymers as charge transporters and emissive layers. However, their major drawbacks include the high processing costs of small molecules based OLEDs, poor multilayer capability of polymer based OLEDs, and low resolution pixelation techniques (shadow masking and printing respectively). These drawbacks can be overcome by using luminescent liquid crystalline materials because of their polarized emission behavior. They also exhibit efficient charge-transporting properties due to the presence of high degree of molecular order and ability for self-organization in the liquid crystalline state. This eventually leads to the quest of potential new luminescent LCs for OLED applications. These materials should satisfy a demanding set of criteria such as ability to show low temperature liquid crystal phases at ambient temperature processing, an essential range of molecular energies for electron and hole injection, moderately high charge transport for bright emission, good film forming ability from solution in organic solvents, chemical, photochemical and electrochemical stability, as well as tunable color and color purity for multicolor OLEDs.

In the literature, hole transporting luminescent LCs are much explored, but an attempt in development of electron transporting luminescent LCs are less reported. As literature reveals, one can achieve a good electron transport property by incorporating N-heterocyclic ring as a core in the molecular architecture. On the basis of thorough literature support, it is evident that the liquid crystalline materials based on various pyridine derivatives have been shown to be quite useful as electron transporting layers for various applications.

Against this background, as well as based on the literature reports, it has been thought of focusing the present research work on design and development of new pyridine based mesogens. Thus, taking into account of advantages of pyridine based LCs and their related literature reviews, precise objectives of the present work have

been evolved and accordingly four new series of pyridine based mesogens have been designed. Their details have been elaborated in **Chapter 2**. Newly designed four series, comprising forty eight target compounds have been synthesized successfully. Further, their synthesis and characterization details have been discussed in **Chapter 3**. Furthermore, the synthesized compounds have been subjected to their liquid crystalline, UV-visible and fluorescence studies using appropriate characterization tools. Experimentally obtained results have been discussed in **Chapter 4**. Finally, the summary and important conclusions of the entire research work along with the scope for future work have been outlined in **Chapter 5**.



## **CHAPTER 2**

### **LITERATURE REVIEW, SCOPE AND OBJECTIVES, DESIGN OF NEW PYRIDINES AS MESOGENS**

**Abstract**

*This chapter covers a brief account on various pyridine based mesogens. Also, it includes a review of reported literature on design and synthesis of various types of pyridine based liquid crystals consisting of different linking groups, terminal alkoxy chain lengths and polar groups. Further, it includes scope and objectives of the present research work, arrived at on the basis of detailed literature survey. Finally, it describes the design of four new series comprising forty eight pyridine derivatives as mesogens.*

**2.1 LIQUID CRYSTALLINE MATERIALS**

Liquid crystals materials are either organic or inorganic. Organic LC materials constitute only aromatic or heteroaromatic systems carrying different linking groups and terminal substituents. In the following sections a concise account of organic liquid crystalline materials has been discussed.

**2.1.1 Organic liquid crystals**

Functional organic materials are of great interest for a variety of LC applications. To obtain precise functional properties, well-defined hierarchically ordered supramolecular structures are crucial. Interestingly, the self-assembly of organic liquid crystals has proven to be an extremely useful tool in the development of well-defined nanostructured materials. Generally, these organic LCs can be constructed by employing various aromatic or heteroaromatic systems to fulfill the criteria for the desired applications. In this aspect, benzene (Jokisaari and Hiltunen 1983), biphenyl (Ghodbane et al. 1991), anthracenyl and phenanthrenyl moieties (Wang et al. 1992) have been most commonly explored as an aromatic core. Some of the heteroaromatic cores and their advantages over aromatic cores have been discussed under the section heterocyclic liquid crystals.

*Luminescent liquid crystals:*

There have been growing interests in luminescent liquid crystals in the past decades. The combination of intrinsic light-emitting ability and unique supramolecular organization and self-healing features within a liquid crystalline phase

is of fundamental interest for applications such as anisotropic light-emitting diodes, polarized organic lasers, information storage, sensors, and one-dimensional semiconductors. Particularly, their capability of emitting linear or circular polarized light when aligned can be utilized in the construction of bright as well as efficient emissive liquid crystal displays (LCDs). This would avoid the use of dichroic sheet polarizers and absorbing color filters in the LC cell and thus enhance the power efficiency of LCDs. Moreover, such approaches can simplify the device design and substantially increase the device brightness, contrast, efficiency, and viewing angle. In this aspect, various luminescent cores such as pyrene (Sagara and Kato 2008), tris(triazolyl)triazine (Beltrán et al. 2010), 1,3,4-oxadiazole (Tang et al. 2012) etc. have been successfully developed and employed for achieving luminescent LC properties.

#### *Liquid crystal semiconductors:*

In general, various molecular structures have been successfully utilized for the design of new liquid crystal semiconductors. Amongst them, flat shaped core containing flexible side chains and many other structural shapes such as cone-shaped, wedge-shaped or certain rod-shaped compounds are quite common in exhibiting LC aggregates. But, the majority of the reported mesogens are of p-type semiconducting materials derived from electron-rich heteroaromatic/aromatic cores such as porphyrin (Gregg et al. 1990), triphenylene (Iino et al. 2005), triphenylene-fused triazatruxenes (Zhao et al. 2010), and hexabenzocoronene (Liu et al. 2003) etc., which possess good hole transporting nature. On the other hand, n-type semiconducting LC materials are sparsely explored; however derivatives of certain electron deficient aromatic/heteroaromatic systems such as tris(N-salicylideneaniline) derivatives with peripheral branched alkyl chains (Yelamaggad and Achalkumar 2006), hexaazatriphenylene (Chang et al. 2005), and hexa-azatrinaphthylene (Kestemont et al. 2001) etc. were shown to be n-type LC materials possessing good electron transporting property. As these materials have several drawbacks such as lack of high performance, poor thermal stability, inability to form columnar mesophases at close to ambient temperature and lack of tendency to give oriented monodomains, a search for new defect-free n-type semiconducting LC materials has gathered momentum.

### 2.1.2 Heterocyclic liquid crystals

Heterocyclic liquid crystals include mainly heterocycle as a core moiety. Precisely, a heterocyclic compound is one that contains a ring made up of one or more than one kind of atoms such as nitrogen, oxygen or sulfur in addition to carbon. Generally, the design of novel thermotropic liquid crystals involves the suitable selection of a core fragment, linking group and terminal functionality. Over many years, a large number of liquid crystalline compounds containing heterocyclic units as core moieties have been synthesized. Modern synthesis techniques allow researchers to access tailor-made compounds with predictable properties, particularly in the field of LC materials. The incorporation of heterocyclic moieties as core units in thermotropic liquid crystals can result in large changes in their mesophases and physical properties, because they possess more polarizable heteroatoms, such as nitrogen, oxygen and sulfur atoms in their structure.

In the recent years, the development of new liquid crystalline materials bearing heterocyclic ring such as pyridine, pyrimidine, pyrazole, imidazole, oxadiazole and benzothiazole are of great interest, as they impart long range mesogenic stability to the resulting liquid crystals.

## 2.2 PYRIDINE BASED LIQUID CRYSTALS

Pyridine based LCs constitutes pyridine ring as a core moiety. Presence of pyridine moiety not only imparts rigid stable structure but also induces complex LC phases in the resulting molecules. Also, it adds wide range of photophysical properties. Keeping this in view, the present research work has been mainly focused on pyridine based LCs. In this context, a brief account on chemistry of pyridine and its role in liquid crystals have been discussed in the following sections.

### 2.2.1 Chemistry of pyridine

Pyridine **S-2.1** is an important six membered aromatic heterocyclic system which resembles very much to the structure of benzene except one atom where carbon is replaced by nitrogen atom. It is planar molecule, stable liquid with strong penetrating odour and is completely miscible with water. It plays multiple roles in organic reactions. It can act as a reagent, a solvent, or as a base in different reaction conditions. Pyridine is particularly used as a catalyst in reactions such as N- and O-

acylation. Structure of pyridine with delocalized  $\pi$  electron cloud (molecular orbital) is shown in **Figure 2.1**. The dipole moment of pyridine is 1.57 D. As the resonance contributors and the electrostatic potential map indicate, the electron-withdrawing nitrogen is the negative end of the dipole.

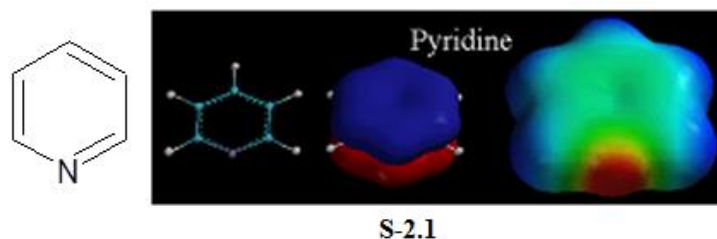
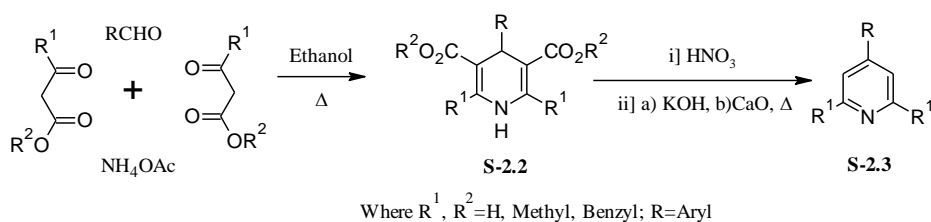


**Figure 2.1** Structure showing pi molecular orbital of pyridine ring

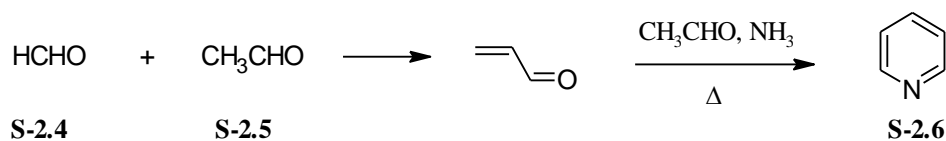
Pyridine was first isolated from bone pyrolysates. Pyridine and its simple alkyl derivatives were for a long time produced by isolation from coal tar, in which they occur in good quantity. Unlike benzene, pyridine is readily undergoing nucleophilic substitution reaction at positions -2 and -4. This is because of the presence of electron withdrawing nitrogen atom on the ring. Because of the same reason, electrophilic substitution reaction is bit difficult on the pyridine ring. However, under forceful conditions, it undergoes reaction at position -3. Pyridine and its derivatives can be conveniently obtained by synthetic processes. There are many ways of achieving the synthesis of pyridines; a few of them are mentioned below.

The well-known method, which is commonly used for the synthesis of pyridine is Hantzsch method (Hantzsch 1881). This reaction allows the preparation of dihydropyridine derivatives **S-2.2** by condensation of an aldehyde with two equivalents of  $\beta$ -dicarbonyls in presence of ammonia or ammonium acetate, as shown in **Scheme 2.1**. Subsequent oxidation (or dehydrogenation) of it gives pyridine-3,5-dicarbonyls, which can be decarboxylated to yield the corresponding pyridines **S-2.3**.



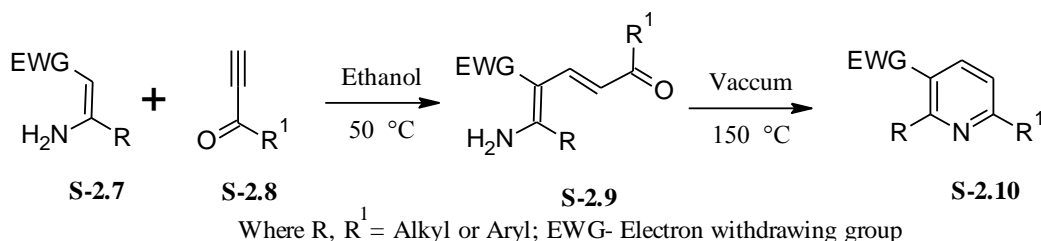
**Scheme 2.1** Hantzsch pyridine synthesis

The industrial production of pyridine is mainly achieved by Chichibabin method (Frank and Seven 1949). It involves condensation of aldehydes, ketones,  $\alpha$ ,  $\beta$ -unsaturated carbonyl compounds, or any combination of the above, with ammonia or its derivatives. In particular, unsubstituted pyridine **S-2.6** is synthesized from formaldehyde **S-2.4** and acetaldehyde **S-2.5** through Knoevenagel condensation. This reaction is depicted in **Scheme 2.2**.



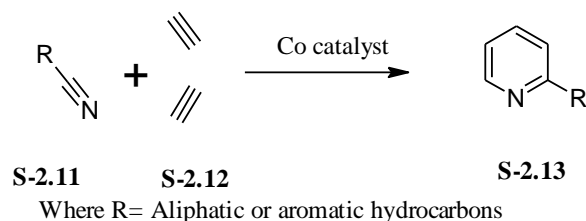
**Scheme 2.2** Chichibabin pyridine synthesis

Another method for the pyridine synthesis is Bohlmann-Rahtz route (Bohlmann and Rahtz 1957), which allows the generation of substituted pyridines in two steps. Condensation of enamines **S-2.7** with ethynylketones **S-2.8** leads to formation of an aminodiene intermediate **S-2.9** that upon heat-induced isomerization, undergoes a cyclodehydration to yield 2,3,6-trisubstituted pyridines **S-2.10**. The general synthetic route is shown in **Scheme 2.3**.



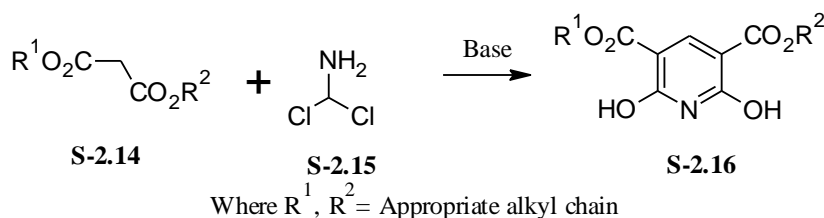
**Scheme 2.3** Bohlmann-Rahtz pyridine synthesis

The trimerization of one part of a nitrile molecule **S-2.11** and two parts of acetylene **S-2.12** to form pyridine **S-2.13** is called Bonnemann pyridine synthesis (Bönnemann 1985). It is shown in **Scheme 2.4**. The thermal activation requires high pressures and temperatures, the photo-induced cycloaddition proceeds at ambient conditions with  $\text{CoCp}_2(\text{cod})$  (Cp = cyclopentadienyl, cod = 1,5-cyclooctadiene) as a catalyst, and can be performed even in water.



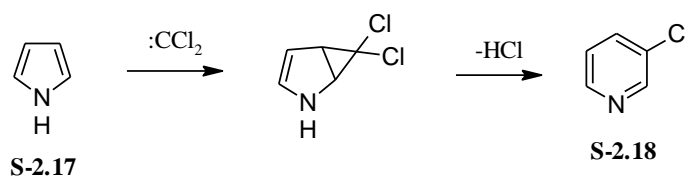
**Scheme 2.4** Bonnemann cyclization

Gattermann-Skita synthesis (Gattermann and Skita 1916) is an interesting method for the synthesis of pyridine ring **S-2.16**, which involves the reaction of dialkyl malonates **S-2.14** with dichloromethyl amines **S-2.15** under basic condition. The reaction is summarized in **Scheme 2.5**.



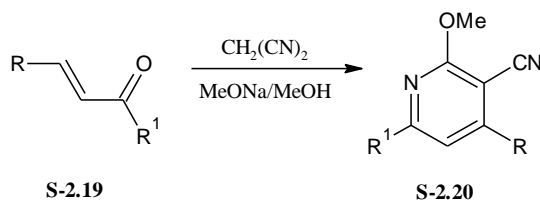
**Scheme 2.5** Gattermann-Skita synthesis

Ciamician-Dennstedt rearrangement (Jones and Rees 1969) is also an important route (**Scheme 2.6**) for the synthesis of pyridine **S-2.18**, which involves ring expansion of pyrrole **S-2.17** in presence of dichlorocarbene intermediate.



**Scheme 2.6** Synthesis of pyridine through Ciamician-Dennstedt rearrangement

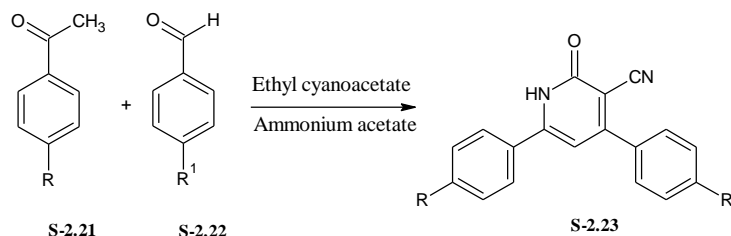
Pyridine derivatives **S-2.20** can be best synthesized in good yield via condensation of  $\alpha,\beta$ -unsaturated ketones **S-2.19** with malononitrile in sodium methoxide/methanol medium (Goda et al. 2004), as shown in **Scheme 2.7**.



Where, R and R<sup>1</sup> = Appropriate aromatic hydrocarbons

### Scheme 2.7 Synthesis of pyridine from $\alpha,\beta$ -unsaturated ketones

Cyano condensation reaction of compound **S-2.21** with the appropriate aromatic aldehydes **S-2.22** and ethyl cyanoacetate in presence of excess ammonium acetate in *n*-butyl alcohol medium gives the corresponding cyanopyridones **S-2.23** in one pot reaction (Hamdy and Gamal-Eldeen 2009), as indicated in **Scheme 2.8**.



Where R and R<sup>1</sup> = alkyl or aryl

### Scheme 2.8 Synthesis of pyridine from ketones and aldehydes

Amongst the various schemes described above, the method which makes use of condensation of  $\alpha,\beta$ -unsaturated ketones with malononitrile in sodium methoxide/methanol medium (**Scheme 2.7**) is quite convenient for the synthesis of pyridine carrying appropriate functional groups. Also, the method described in the **Scheme 2.8** is quite advantageous for the construction of cyanopyridone derivatives, as it is being a one-pot synthetic route. These methods give high yield and good purity for the products. So, in the present research work, it has been thought of synthesizing new pyridine derivatives as per the **Schemes 2.7** and **2.8**.

#### 2.2.2 Advantages of pyridine-based liquid crystals

Many pyridines based LCs were reported in the literature. Some of the references pertaining to the liquid crystalline behavior of the biphenyl **S-2.24** and phenylpyridine **S-2.25** based LCs are given in **Tables 2.1** and **2.2**, respectively. In comparison, it is clear that the introduction of a nitrogen atom into the benzene ring



results in a more complex mesomorphic behavior. In some cases higher ordered smectic phases (e.g. **G**, **H**) are observed at or near room temperature (**Table 2.2**, compounds **18-20**, **22**, **23**, **34**, **37**, **42**), which would be of much interest. Such materials possess useful charge mobilities and hence they will have good scope for device applications. It was also shown (Breemen van et al. 2006) that rich mesomorphic behavior in liquid crystalline phases facilitates the formation of highly ordered monodomains, which were obtained in the size up to 150 mm in diameter. It allowed the fabrication of the monodomain field-effect transistor with mobilities 10 times larger than in multi-domain based devices. These effects are also achieved in terphenyls by the introduction of fluorine groups in sites of the aromatic core.

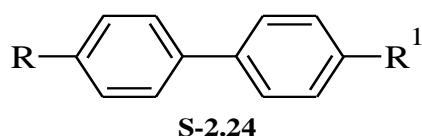


**Table 2.1** LC behavior of reported biphenyl derivatives

Comd.	R	R <sup>1</sup>	LC behavior	Ref.
1.	C <sub>5</sub> H <sub>11</sub>	C <sub>5</sub> H <sub>11</sub>	Cr 25.1 E 46.1 E' 47.1 B 52.3 Iso	Czupryński et al. 1995
2.	C <sub>6</sub> H <sub>13</sub>	C <sub>6</sub> H <sub>13</sub>	Cr 34.1 E 35 E' 40 B 53.4 Iso	
3.	C <sub>7</sub> H <sub>15</sub>	C <sub>7</sub> H <sub>15</sub>	Cr E 19.5 E' 35.1 B 61 Iso	
4.	C <sub>3</sub> H <sub>7</sub>	C <sub>5</sub> H <sub>11</sub>	Cr 18 S1 47.8 Iso	Osman 1985
5.	C <sub>6</sub> H <sub>13</sub>	OC <sub>6</sub> H <sub>13</sub>	Cr 9 S1 68 S2 84 Iso	Ashton et al. 1994
6.	C <sub>5</sub> H <sub>11</sub>	OC <sub>2</sub> H <sub>5</sub>	Cr 72 S Iso	Osman and Huynh- Ba 1983
7.	C <sub>5</sub> H <sub>11</sub>	OC <sub>4</sub> H <sub>9</sub>	Cr 37 S1 80.1 S2 88.1 Iso	
8.	OC <sub>6</sub> H <sub>13</sub>	OC <sub>6</sub> H <sub>13</sub>	Cr 124 N 130 Iso	Kubo et al. 2002

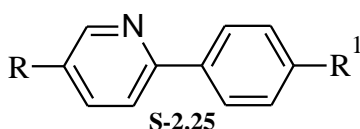


**Table 2.2** LC behavior of reported phenylpyridine derivatives

Comd.	R	R <sup>1</sup>	LC behavior	Ref.
1.	OC <sub>6</sub> H <sub>13</sub>	C <sub>8</sub> H <sub>17</sub>	Cr 57 SmI 37 SmC 58 SmA 79 Iso	Kelly and Fünfsch-
2.	O(CH <sub>2</sub> ) <sub>4</sub> C	C <sub>8</sub> H <sub>17</sub>	Cr 39 SmI 37 C 48 SmA 69 Iso	

	H=CH <sub>2</sub>			illing 1996	
3.	C <sub>7</sub> H <sub>15</sub>	OC <sub>11</sub> H <sub>23</sub>	Cr 48.8 SmF 63.7 SmC 81.4 Iso	Inoue et al. 1987	
4.	C <sub>7</sub> H <sub>5</sub>	OC <sub>10</sub> H <sub>21</sub>	Cr 39.5 SmF 62 SmC 82.1 Iso		
5.	C <sub>8</sub> H <sub>17</sub>	OC <sub>10</sub> H <sub>21</sub>	Cr 40.8 SmF 65.5 SmC 82.1 Iso		
6.	C <sub>9</sub> H <sub>19</sub>	OC <sub>10</sub> H <sub>21</sub>	Cr 38.6 B 69.2 SmC 86.3 Iso		
7.	C <sub>8</sub> H <sub>17</sub>	OC <sub>9</sub> H <sub>19</sub>	Cr 37.5 SmF 61.5 SmC 81.4 Iso		
8.	C <sub>9</sub> H <sub>19</sub>	OC <sub>9</sub> H <sub>19</sub>	Cr 37.4 B 69.6 SmC 84.9 Iso		
9.	C <sub>7</sub> H <sub>15</sub>	OC <sub>9</sub> H <sub>19</sub>	Cr 42.5 SmF 58.5 SmC 80.7 Iso		
10.	C <sub>7</sub> H <sub>15</sub>	O(CH <sub>2</sub> ) <sub>9</sub> CH=CH <sub>2</sub>	Cr 31 B 62 SmC 75 SmA 78 Iso		Kelly et al. 1993a
11.	C <sub>7</sub> H <sub>15</sub>	O(CH <sub>2</sub> ) <sub>8</sub> CH=CH <sub>2</sub>	Cr 37 SmI 55 SmC 74 SmA 76 Iso		
12.	C <sub>8</sub> H <sub>17</sub>	O(CH <sub>2</sub> ) <sub>8</sub> CH=CH <sub>2</sub>	Cr 32 SmI 60 SmC 77 Iso		
13.	C <sub>9</sub> H <sub>19</sub>	O(CH <sub>2</sub> ) <sub>8</sub> CH=CH <sub>2</sub>	Cr 37 B 67 SmC 80 Iso		
14.	C <sub>8</sub> H <sub>17</sub>	O(CH <sub>2</sub> ) <sub>7</sub> CH=CH <sub>2</sub>	Cr 33 SmI 61 SmC Iso		
15.	C <sub>9</sub> H <sub>19</sub>	O(CH <sub>2</sub> ) <sub>7</sub> CH=CH <sub>2</sub>	Cr 32 B 69 SmC 80 SmA 82 Iso		
16.	C <sub>7</sub> H <sub>15</sub>	O(CH <sub>2</sub> ) <sub>7</sub> CH=CH <sub>2</sub>	Cr 36 B 52 SmC 75 SmA 78 Iso		
17.	C <sub>8</sub> H <sub>17</sub>	O(CH <sub>2</sub> ) <sub>6</sub> CH=CH <sub>2</sub>	Cr 23 SmI 53 SmC 75 Iso		
18.	C <sub>7</sub> H <sub>15</sub>	O(CH <sub>2</sub> ) <sub>6</sub> CH=CH <sub>2</sub>	Cr 30 G 29 SmI 48 SmC 73 Iso		
19.	C <sub>7</sub> H <sub>15</sub>	O(CH <sub>2</sub> ) <sub>5</sub> CH=CH <sub>2</sub>	Cr 21 G 34 SmI 52 SmC 75 SmA Iso		
20.	C <sub>8</sub> H <sub>17</sub>	O(CH <sub>2</sub> ) <sub>5</sub> CH=CH <sub>2</sub>	Cr 26 G 53 SmI 59 SmC SmA 77 Iso		
21.	C <sub>9</sub> H <sub>19</sub>	O(CH <sub>2</sub> ) <sub>5</sub>	Cr 34 B 68 SmC 75 SmA 82 Iso		

		CH=CH <sub>2</sub>		
22.	C <sub>7</sub> H <sub>15</sub>	O(CH <sub>2</sub> ) <sub>4</sub> CH=CH <sub>2</sub>	Cr 23 G 32 SmI 49 SmC 66 Iso	
23.	C <sub>8</sub> H <sub>17</sub>	O(CH <sub>2</sub> ) <sub>4</sub> CH=CH <sub>2</sub>	Cr 31 G 44 SmI 54 SmC 68 Iso	
24.	C <sub>9</sub> H <sub>19</sub>	O(CH <sub>2</sub> ) <sub>4</sub> CH=CH <sub>2</sub>	Cr 41 B 64 SmC 70 SmA 73 Iso	
25.	C <sub>9</sub> H <sub>19</sub>	O(CH <sub>2</sub> ) <sub>3</sub> CH=CH <sub>2</sub>	Cr 46 B 72 SmA 78 Iso	
26.	C <sub>8</sub> H <sub>17</sub>	O(CH <sub>2</sub> ) <sub>3</sub> CH=CH <sub>2</sub>	Cr 43 B 65 SmC79A75 Iso	
27.	C <sub>8</sub> H <sub>17</sub>	O(CH <sub>2</sub> ) <sub>3</sub> CH=CH <sub>2</sub>	Cr 37 B 56 SmA 58 Iso	
28.	C <sub>6</sub> H <sub>13</sub>	O(CH <sub>2</sub> ) <sub>2</sub> CH=CH <sub>2</sub>	Cr 43.5 S 42.7 Iso	Buchecker et al. 1991
29.	C <sub>8</sub> H <sub>17</sub>	O(CH <sub>2</sub> ) <sub>4</sub> CH=CH <sub>2</sub>	Cr 31 SmI 54 SmC 68 Iso	Kelly 1996
30.	C <sub>9</sub> H <sub>19</sub>	OC <sub>8</sub> H <sub>17</sub>	Cr 37 S 66 SmI 69 SmC 85 Iso	Kelly and Fünfschilling 1993a
31.	C <sub>9</sub> H <sub>19</sub>	O(CH <sub>2</sub> ) <sub>6</sub> CH=CH <sub>2</sub>	Cr 33 B 62 SmC 77 SmA 78 Iso	Kelly 1993
32.	C <sub>8</sub> H <sub>17</sub>	OC <sub>8</sub> H <sub>17</sub>	Cr 38 SmI 62 SmC 82 Iso	Kelly and Fünfschilling 1993
33.	C <sub>7</sub> H <sub>15</sub>	OC <sub>8</sub> H <sub>17</sub>	Cr 45 G 45.5 SmF 56 SmC 80 Iso	Heinemann et al. 1996
34.	C <sub>7</sub> H <sub>15</sub>	OC <sub>7</sub> H <sub>15</sub>	Cr 24 H 31 G 40 SmF 53 SmC 77 Iso	Heinemann et al. 1996
35.	C <sub>8</sub> H <sub>17</sub>	OC <sub>7</sub> H <sub>15</sub>	Cr 27.3 F 57 SmC 77.5 Iso	Inoue et al. 1987

36.	C <sub>9</sub> H <sub>19</sub>	OC <sub>7</sub> H <sub>15</sub>	Cr 33 B 64 SmC 81.5 Iso	Inoue et al. 1987
37.	C <sub>7</sub> H <sub>15</sub>	C <sub>7</sub> H <sub>15</sub>	Cr 34 H 31.2 G 44.4 SmF 53 SmC 74.4 N 75.2 Iso	Inoue et al. 1987
38.	C <sub>8</sub> H <sub>17</sub>	OC <sub>6</sub> H <sub>13</sub>	Cr 30 G 23 SmI 58 SmC 77 Iso	Kelly and Fünfsch- illing 1996
39.	C <sub>9</sub> H <sub>19</sub>	OC <sub>5</sub> H <sub>11</sub>	Cr 42.5 B 65 SmC 72.4 SmA 74.5 Iso	Inoue et al. 1987
40.	C <sub>8</sub> H <sub>17</sub>	OC <sub>5</sub> H <sub>11</sub>	Cr 37.4 B 52 SmC 70.1 Iso	Inoue et al. 1987
41.	C <sub>6</sub> H <sub>13</sub>	OC <sub>4</sub> H <sub>9</sub>	Cr 50 S 54 N 61 Iso	Pavluchenko 1980
42.	C <sub>7</sub> H <sub>15</sub>	OC <sub>4</sub> H <sub>9</sub>	Cr 54 G 40 SmF 48 SmC 64 N 70 Iso	Heinemann 1996
43.	C <sub>8</sub> H <sub>17</sub>	OC <sub>4</sub> H <sub>9</sub>	Cr 33 B 57.3 SmC 66.8 SmA 69.4 N Iso	Murashiro 1995
44.	OC(O)(CH <sub>2</sub> ) <sub>3</sub> CH=CH <sub>2</sub>	C <sub>8</sub> H <sub>17</sub>	Cr 42 SmF 54 SmC 58 Iso	Kelly and Fünfsch- illing 1996

It is interesting to note that, introduction of a nitrogen atom into the aromatic benzene core (**S-2.26**) comprised of three conjugated 6-membered rings (**Table 2.3**) is accompanied by a decrease of clearing point in comparison with terphenyl liquid crystals and a tendency to form tilted phases.

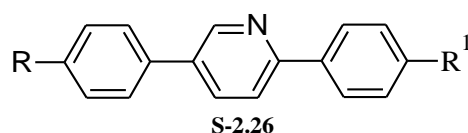


**Table 2.3** LC behavior of reported 2,5-bis-(phenyl)-pyridines

Comd.	R	R <sup>1</sup>	LC behavior	Ref.
1.	C <sub>2</sub> H <sub>5</sub>	C <sub>2</sub> H <sub>5</sub>	Cr 162 S2 164 S1 172 N	Pavluchenko

			183 Iso	et al. 1995
2.	C <sub>2</sub> H <sub>5</sub>	C <sub>3</sub> H <sub>7</sub>	Cr 125 S2 143 S1 168 N 192 Iso	
3.	C <sub>2</sub> H <sub>5</sub>	C <sub>4</sub> H <sub>9</sub>	Cr 110 S1 173 N 184 Iso	Schubert 1970
4.	CH <sub>3</sub>	OC <sub>10</sub> H <sub>21</sub>	Cr 111 H 93 G 133 F 151 C 156 A 188 N Iso	Asano et al. 1997
5.	C <sub>4</sub> H <sub>9</sub>	OCH <sub>2</sub> CH(OH)CH <sub>3</sub>	Cr 135.4 A 189.6 Ch 198.3 Iso	Kouji et al. 1989
6.	C <sub>4</sub> H <sub>9</sub>	OCH <sub>2</sub> CH(CH <sub>3</sub> )C <sub>2</sub> H <sub>5</sub>	Cr H 118.5 G 139.2 F 144.4 B 158.7 C 165.8 A 191.4	
7.	C <sub>4</sub> H <sub>9</sub>	O(CH <sub>2</sub> ) <sub>5</sub> CH(CH <sub>3</sub> )C <sub>2</sub> H <sub>5</sub>	Cr 61 S3 98.8 S2 102.5 S1 170 C 182.3 A 196.3 Iso	
8.	C <sub>4</sub> H <sub>9</sub>	OC(O)(CH <sub>2</sub> ) <sub>2</sub> CH(CH <sub>3</sub> )C <sub>2</sub> H <sub>5</sub>	Cr G 111.3 F 152.4 B 182.8 A 207 Iso	

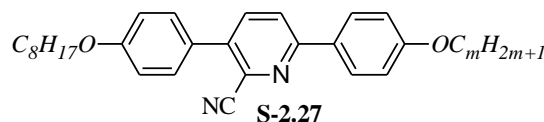
This propensity of the formation of higher ordered phases at or near room temperature with rather low clearing points (in most cases around 200 °C for mesogens with three aromatic rings in the core) and rich mesomorphic behavior makes these pyridine-containing liquid crystals attractive candidates for the examination of their charge transport.

### 2.3 LITERATURE REVIEW

In the past decades, design and successful synthesis of several thermotropic liquid crystals containing various substituted pyridines were reported. A brief account on literature reports on the synthesis of pyridine based liquid crystals, hydrogen bonded pyridine LCs, and effect of substituents, linking groups and alkyl chain lengths on their LC behavior has been discussed in the following section.

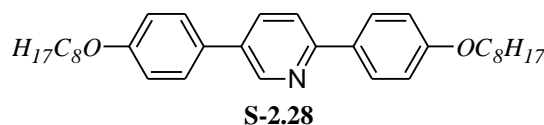
Kozhevnikov et al. (2008) designed and synthesized 2-cyanopyridine derivatives and evaluated their mesogenic properties. They prepared series of **S-2.27** compounds by varying alkyl chain from m=2 to m=12 and observed the formation of only a nematic phase for shortest chain homologues (*i.e.*, for m=2 and m=4). Further,

beyond this chain length, a SmC phase appeared on melting and quickly increased in stability with chain length. They also found that the nematic phase has disappeared with increase of chain length and presence of lateral cyano group destabilized both the melting and clearing points of the analogous.



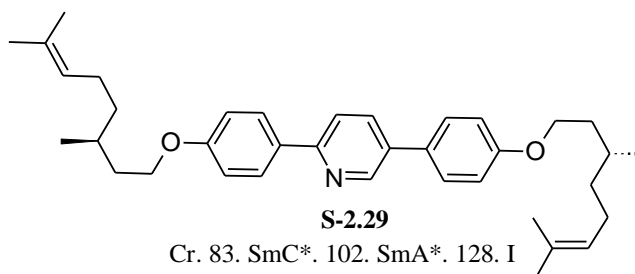
Cr. 43. SmC. 106. I (for  $m=12$ )

Further, they synthesized compound **S-2.28** containing no lateral cyano group and found SmC, SmI, and crystal J phases in it. Thus, it is evident that absence of cyano group increases the clearing point drastically. It was found that the presence of lateral cyano group on pyridine ring would increase the liquid crystalline property remarkably.



Cr. 107. J. 137. SmI. 187. SmC. 221. I

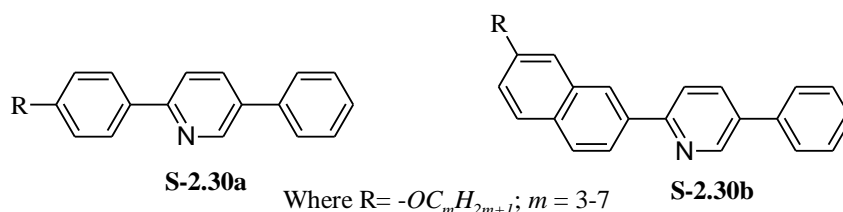
Aldred et al. (2005) reported the synthesis of a three ring aromatic compound containing pyridine as central core **S-2.29** and observed the formation of chiral smectic C (SmC\*) and SmA\* phase in it. They succeeded to get liquid crystal property by introduction of chiral alkoxy branched chains at the ends of three ring heterocyclic system.



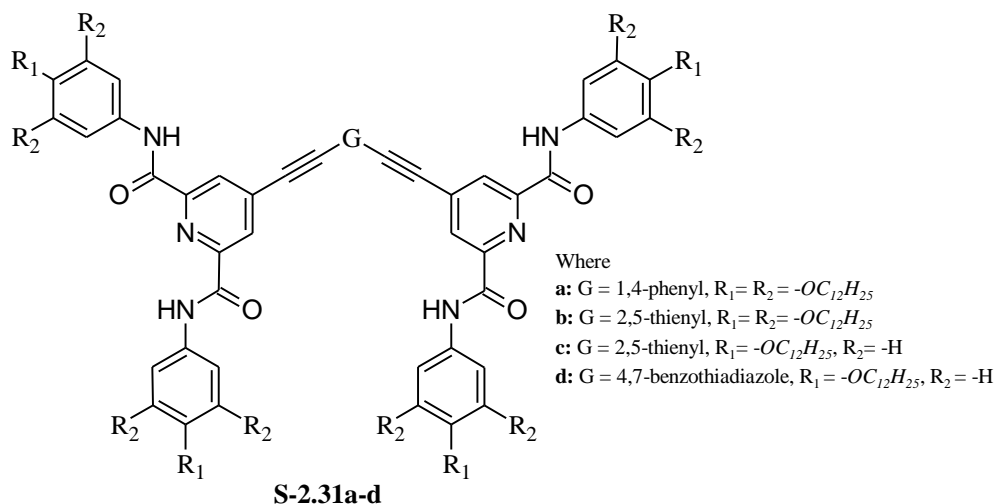
Cr. 83. SmC\*. 102. SmA\*. 128. I

In an attempt to investigate new pyridine based mesogens, Chia et al. (2009) synthesized two homologous series of pyridine containing liquid crystalline compounds (**S-2.30a** and **S-2.30b**), viz. 2-(4-alkoxyphenyl)-5-phenylpyridines and 2-(6-alkoxynaphthalen-2-yl)-5-phenylpyridines by varying alkyl chain length from  $m=3$

to 7. They found SmC, SmA and N phases in the compounds and it was further observed that pyridine moiety within the mesogen not only favors the appearance of smectic behavior, but also reduces the thermal stability of the crystal and simultaneously introduces an attractive force and causes the appearance of the nematic phase. Further, their experimental results showed that introduction of a slightly extended and tilted hard core, such as the 2,6-naphthalene moiety provides a much better nematogen than 1,4-phenylene.

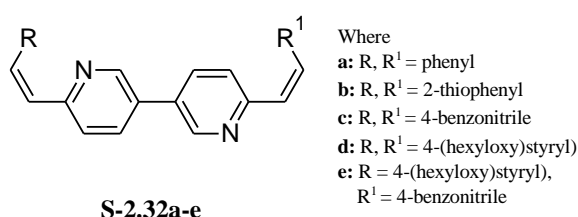


A series of new organogelators with  $\pi$ -conjugated phenylene-ethynylene **S-2.31a-d** framework featuring long-chain carboxamides was synthesized by Shen et al. (2009) and they studied their liquid crystalline, UV-visible and fluorescence properties. Almost all the compounds were shown to exhibit columnar mesophase and promising photophysical properties.

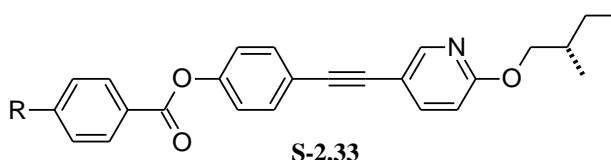


In another report, Attias et al. (1999) prepared six new liquid crystalline conjugated derivatives of 3, 3'-bipyridine **S-2.32a-e**, which are di-substituted with electron donor and acceptor groups, via Knoevenagel condensation reaction. Further, all the compounds were found to exhibit thermotropic liquid crystalline phases and

the presence of high degree of conjugation and the mesogenic character could lead to nonlinear applications. Furthermore, they explained the effects of terminal substituents on liquid crystalline properties; while the presence of terminal ring substituents, e.g. long *n*-alkyl chains favors smectic thermal stabilities as well cyano group markedly enhance nematic and diminishes smectic thermal stabilities. Compound **S-2.32d** is purely smectogen due to the presence of alkoxy terminal substituent's and the compound **S-2.32e**, obtained by the replacement of one alkoxy terminal substituent by cyano group exhibits the nematic phase.



Vasconcelos et al. (2005) successfully synthesized N-heterotolans **S-2.33** by introducing pyridine moiety into it using the Buchwald protocol and Sonogashira reaction. They studied the relation between structure and mesomorphic properties. In the synthetic strategy, they introduced different alkyl chain lengths ( $m=7$  to 10) at one end of the moiety and they observed that all the synthesized compounds possess a chiral nematic phase and smectic A phase. Further, they concluded that all the heterotolan derivatives display a broad, stable smectic A phase range and the temperature range of the smectic A increases as the alkyl tail changes from  $m=7$  to  $m=10$ . The thermal stability of the nematic phase decreased with an increased alkyl chain length.

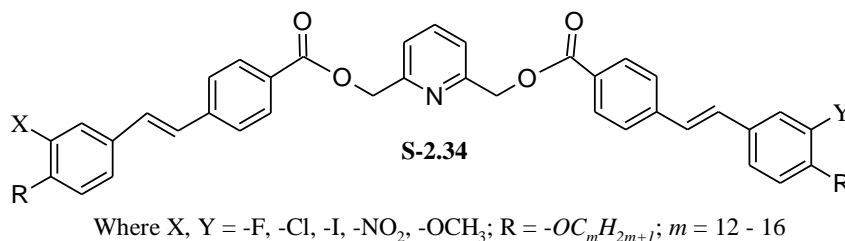


Cr. 85.6. SmA. 144. N. 144.7. I Where R =  $-OC_mH_{2m+1}$ ;  $m = 10$

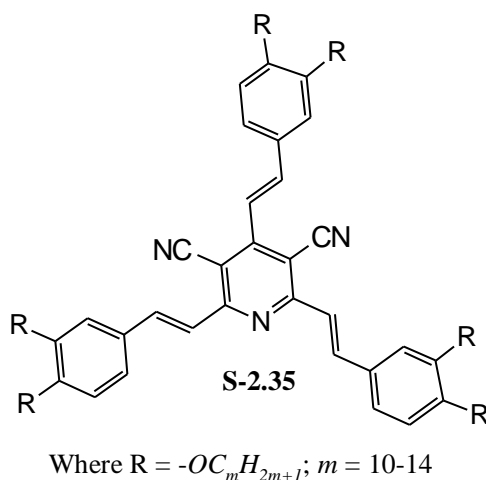
Mieczkowski and his coworkers, in an effort to develop new LC materials synthesized new asymmetric bent core compounds **S-2.34** with different branches and observed the typical rod-like or banana phases depending on the flexibility and the parity of the unit that joins the central ring with the alkyl branches (Mieczkowski et



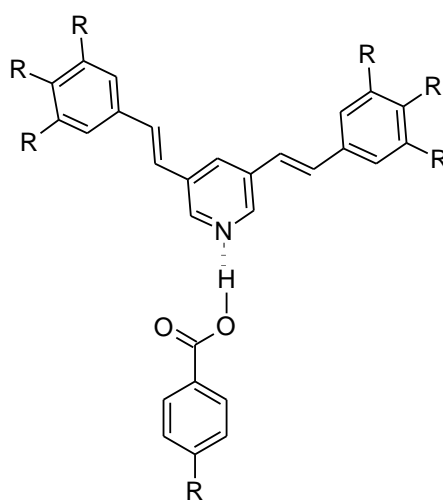
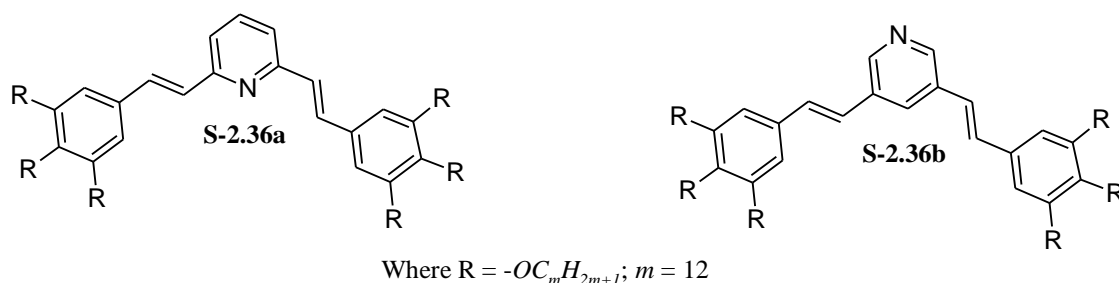
al. 2003). Further, their experimental results showed that the asymmetric materials usually have a broader mesophase range than their symmetric compounds and presence of ester linking group enhances the liquid crystalline property considerably.



Attias and his research associates reported the design and synthesis a new class of disc like LC materials **S-2.35** containing a permanent dipole (Attias et al. 2002). They investigated the mesomorphic properties of newly synthesized pyridine based molecules. The highly  $\pi$ -conjugated derivatives bearing 3,5-dicyano-2,4,6-tristyrylpyridine core, align in an antiparallel arrangement and form disc-shaped “dimeric” units that self-assemble over a broad temperature range (80-135 °C) into columns themselves packed together in a two-dimensional hexagonal lattice. They also investigated their electrochemical as well photophysical properties of the individual disc-like molecules in solution state. Further, the materials were found to possess high electron affinity and columnar self-organization behavior. These properties make them promising candidates for electron transport (n-type) and hence it opens the way to application in optoelectronics.



A bent-core type, polycatenar pyridines **S-2.36a** was reported by Torralba and his research team (Torralba et al. 2006). They synthesized several new pyridine derivatives carrying variable alkoxy chains via a Siegrist coupling of di- and tri-alkoxybenzylidene fragments with 2,6-dimethylpyridine. They found that none of these pyridines were liquid crystalline but their isomeric materials carrying a 3,5-disubstituted pyridine core **S-2.36b** and hydrogen bonded complex **S-2.36c** were mesomorphic in nature. Further, based on their work they concluded that suitable tuning of molecular structure leads to induce liquid crystallinity in a compound.

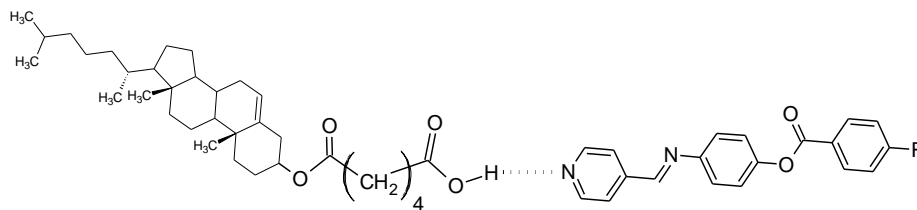


**S-2.36c**

Where R =  $-OC_mH_{2m+1}$ ;  $m = 12$

Hydrogen bonding is a powerful tool for assembling molecules and building new liquid crystalline structures. This was evidenced by Lee et al. (2003) through their reported work on synthesis and evaluation of mesogenic property of new pyridine based compounds. They synthesized non-symmetric dimesogens **S-2.37** which contain intermolecular hydrogen bonding between rationally designed a H-

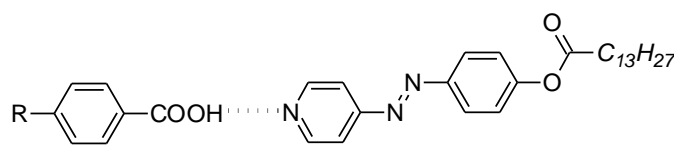
bond donor (3-cholesteryloxycarbonylpentanoic acid) and an acceptor (4-(pyridine-4-ylmethyleneimino)phenyl-4-alkoxybenzoate) moieties. Their liquid crystalline properties were investigated by differential scanning calorimeter, polarized optical microscopy and X-ray diffraction studies. Interestingly, cholesteric and smectic phases were observed in the new molecules.



S-2.37

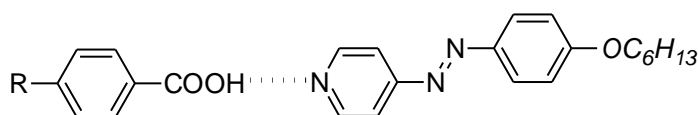
Where R =  $-OC_mH_{2m+1}$ ;  $m = 4$  to 8 and 10

New supramolecular liquid crystal (LC) materials based on azopyridines **S-2.38a,b**, were prepared by mixing 1:1 ratio of 4-substituted phenyl-4'-azopyridines and 4-*n*-alkoxybenzoic acids (Mallia et al. 2003). It was found that the supramolecular arrangement in them is due to the presence of hetero-intermolecular hydrogen bonding in them. These hydrogen bonded LC complexes exhibit well defined nematic, smectic A and smectic C phases over wide range of temperature depending upon the number of carbon atoms present in the alkyl chains. It was further confirmed that the presence of polar groups like  $-NO_2$ ,  $-Cl$ ,  $-CN$  etc. in the molecule leads to significant mesogenic property.



S-2.38a

Where R =  $-OC_mH_{2m+1}$ ;  $m = 4-12$

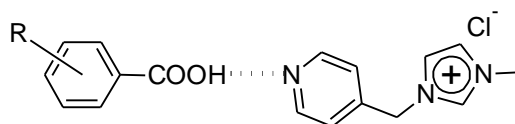


S-2.38b

Where R =  $-H$ ,  $-NO_2$ ,  $-Cl$ ,  $-CN$

Recently, Kohmoto et al. (2010) demonstrated a new methodology to create ionic liquid crystals in a supramolecular way. In their work, pyridinylmethylimidazolium halides **S-2.39** were developed as an ionic building

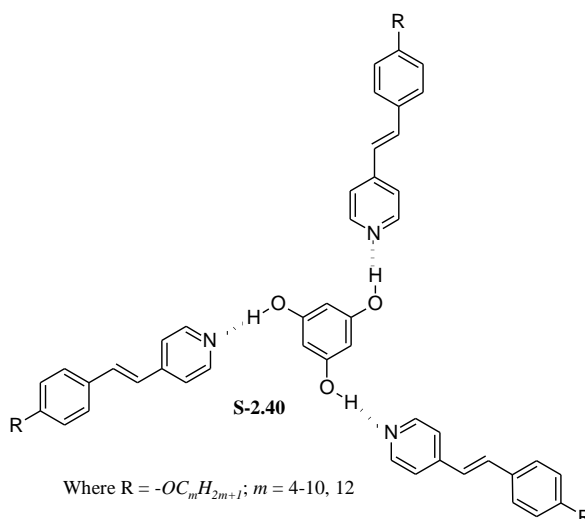
block. According to authors, hydrogen bonding between the pyridine moiety of the imidazolium and benzoic acids facilitated formation of stable liquid crystal phases and substitution patterns of benzoic acids diversify the way of self-assembly of the hydrogen-bonded complexes, which reflects to the morphology of mesophases generated.



S-2.39

Where R =  $-OC_mH_{2m+1}$ ;  $m = 8, 12, 16$

A series of discotic liquid crystals **S-2.40** was prepared through hydrogen bonding between a non-mesogenic phloroglucinol and alkoxy stilbazoles and their self-assembly behavior was investigated by Lee et al (2005). The C-10 and C-12 alkoxy complexes showed hexagonal columnar mesophase, while the other lower alkoxy complexes formed nematic columnar mesophase. These results indicated that the type of observed mesophase structure was strongly dependent on the alkyl chain length around the aromatic core. Further, the discotic H-bonded complexes with hexagonal columnar mesophases may serve as dynamic charge transport materials using reversibility of the hydrogen bonding.

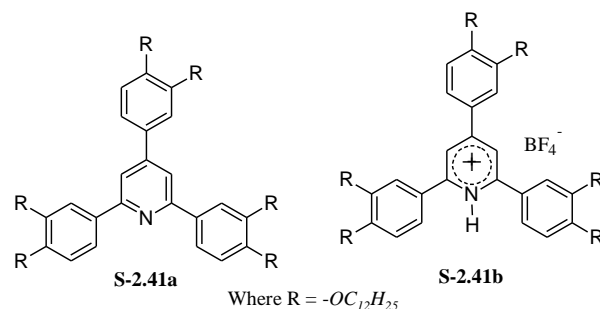


S-2.40

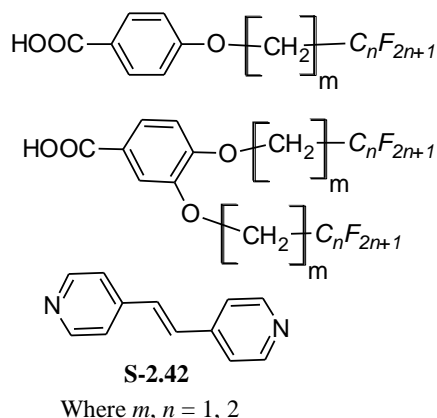
Where R =  $-OC_mH_{2m+1}$ ;  $m = 4-10, 12$

In an effort to develop a new LC material, Veber and Berruyer (2000) synthesized two new pyridine derivatives, *viz.* **S-2.41a** and its corresponding pyridinium salt **S-2.41b** as ionic liquid crystal. They observed that the newly

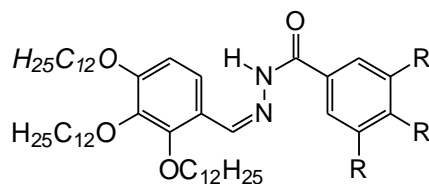
synthesized pyridine derivative **S-2.41a** is purely crystalline, but its pyridinium salt **S-2.41b** was found to possess a Col<sub>h</sub> columnar phase. But it limits its practical application because of the fact that pyridinium salt is highly unstable leading to the formation of starting pyridine via hydrolysis.



In an interesting report, thermal property of benzoic acid based mesogens carrying one or two semi-perfluorinated alkoxy tails linked to aromatic core **S-2.42** was investigated in binary mixtures with the non-liquid crystalline bidirectional *trans*-1,2-bis(4-pyridyl)ethylene (Kohlmeier and Janietz 2007). The hydrogen bonded complexes **S-2.42** built from the complimentary molecular species showed significantly enhanced mesophase stability compared with the fluorinated acids in their pure states. According to authors, the mesophase morphologies of the complexes are governed mainly by the number of the partially fluorinated chains grafted to the acid component. Mixed systems comprising the one-chain acids exhibit a smectic C phase followed by a smectic A phase at elevated temperatures. Incorporation of a second semi-perfluorinated chain into the acid leads to the formation of columnar mesophases. These columnar phases of the H-bonded complexes show ribbon phases resulting from the collapse of the smectic layers.

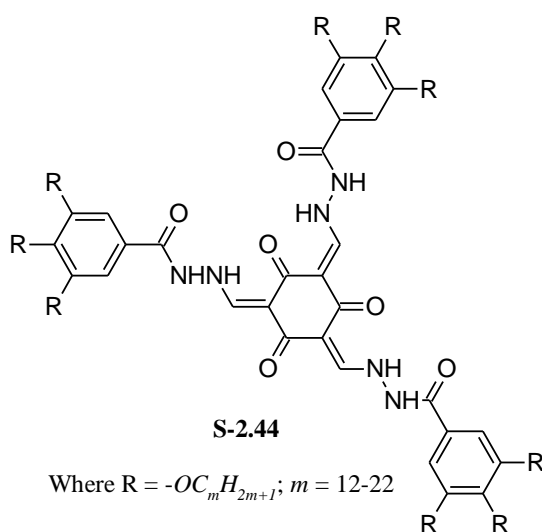


Recently, Shanker et al. (2011) reported the synthesis and self-assembly properties of new benzylidene hydrazine based compounds **S-2.43**, namely N-(2,3,4-tridodecyloxybenzylidene)-3,4,5-N'-trialkoxylbenzoylhydrazines. The newly synthesized molecules were confirmed to exhibit wide ranges of room temperature hexagonal columnar liquid crystalline phases ( $col_h$ ) as evidenced by optical polarizing microscopy, differential scanning calorimetry and X-ray diffraction studies. Further, the authors showed that the combination of 2,3,4- and 3,4,5-substitution patterns of aromatic cores linked via hydrazone group in a molecule provides a new way to form low melting columnar LC materials with wide mesophase range.

**S-2.43**

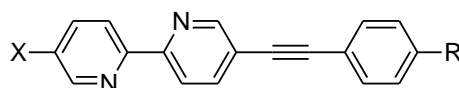
Where  $R = -OC_mH_{2m+1}$ ;  $m = 9-16$

New supramolecular liquid crystalline tri(N-salicylideneamine)s **S-2.44** featuring both inter- and intra- molecular hydrogen bonding were successfully synthesized by Yelamaggad et al. (2010). They reported that the compounds carrying hydrazone linkages exhibit self-assembly into supramolecular fluid hexagonal columnar phase over a wide thermal range. According to authors, the compounds act as n-type semiconductor because of their good electron transporting nature.

**S-2.44**

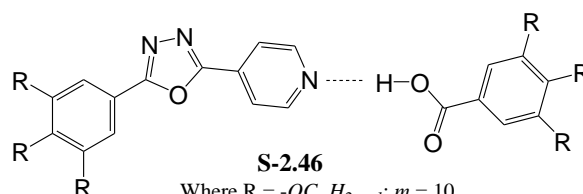
Where  $R = -OC_mH_{2m+1}$ ;  $m = 12-22$

Two series of unsymmetrical mesogenic compounds **S-2.45** involving the 2,2'-bipyridine frame work were synthesized using unsubstituted and bromo substituted pyridines by El-Ghayoury et al (2000). Compounds were shown to exhibit smectic B, Smectic A and nematic phases. Further, it was revealed that the molecules ending with a bromo substituent can be further derivatized for future functionalization leading to novel mesogenic compounds.

**S-2.45**

Where X = -H, -Br; R =  $-OC_mH_{2m+1}$ ;  $m = 6-16$

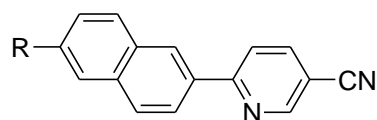
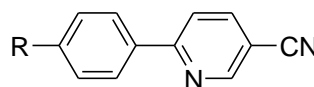
In a recent report by Han et al. (2012), a new supramolecular liquid crystal **S-2.46** was obtained by mixing a non-mesogenic benzoic acid derivative with 1,3,4-oxadiazole based pyridine to form intermolecular hydrogen bonding. According to authors, the compound containing terminal tri-decyloxy chain exhibited columnar hexagonal phase. Also, its UV-visible and fluorescence study in chloroform solution state reveals that the compound exhibits a strong absorption band at 303 nm and a blue emission band at 390 nm.

**S-2.46**

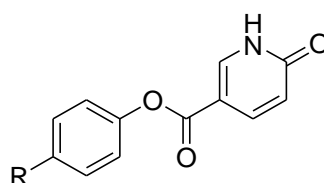
Where R =  $-OC_mH_{2m+1}$ ;  $m = 10$

Cr. 41.9. Col<sub>h</sub>, 46.1. I

A new series of liquid crystalline compounds, viz. 6-(6-alkoxynaphthalen-2-yl)nicotinonitrile (**S-2.47a**) and 6-(4-alkoxyphenyl)nicotinonitrile (**S-2.47b**) was synthesized via simple synthetic route by Chia and Lin (2013). They were shown to exhibit nematic and smectic phases. Based on the experimental results, authors concluded that 2,6-naphthalene moiety in the compound not only reduces its crystalline packing (low melting point), but also prohibits its lamellar packing (smectic phase). Thus, naphthalene moiety plays a key role in generating the nematic phase in the series.

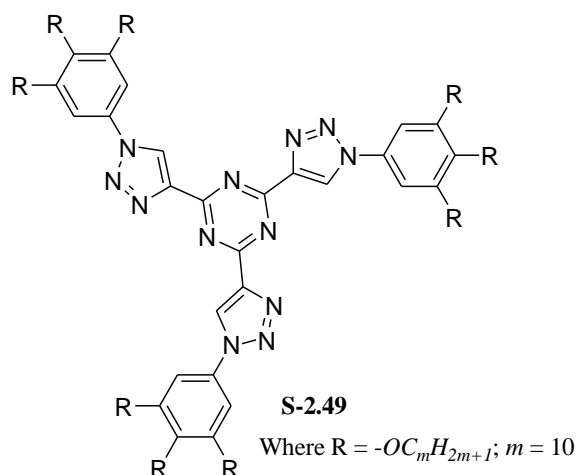
**S-2.47a**Where R =  $-OC_mH_{2m+1}$ ;  $m = 2-8$ **S-2.47b**Where R =  $-OC_mH_{2m+1}$ ;  $m = 3-7$ 

From the past few decades much work has been devoted to synthesize 2-pyridone derivatives for their applications in biomedical fields as biomesogens. In this context, Saravanan et al. (2010) reported the synthesis of 5-(4'-nonyloxyphenyloxy)-carbonyl-2-pyridone **S-2.48** as a well-organized columnar mesogen. The newly synthesized compound exhibited columnar mesophase at 139 °C. Further, the authors inferred that the observed mesophase in the compound is mainly due to the capability of 2-pyridone to form H-bond and presence of terminal nonyloxy chain in the structure.

**S-2.48**Where R =  $-OC_mH_{2m+1}$ ;  $m = 9$ 

Recently, Beltrán et al. (2010) designed and synthesized a highly electron-deficient tris(triazolyl)triazine **S-2.49** as a mesogenic core by adopting a one-pot procedure that combines a 3-fold deprotection of alkyne groups and “click chemistry” of the aromatic alkyne and azide precursors. The authors investigated the redox behavior as well as luminescent LC property of the compound. Their study revealed that the compound exhibit low reduction potential as well as room temperature columnar LC phase with luminescent behavior in the visible region. Further, authors revealed that the 1,2,3-triazole and triazine moieties contribute significantly to act **S-2.49** as highly electron deficient molecule.





Thus, the literature review clearly reveals that pyridine acts as a good mesogenic core and its proper functionalization with groups like cyano, nitro, halo, alkoxy, hydrazone etc. leads to different types of liquid crystalline behavior. Further, variation of length of alkoxy chain improves their mesogenic property considerably. Also, their photophysical properties can be tuned by introduction of these groups. By inserting certain electron deficient N-heterocyclic systems such as triazole, triazine, oxadiazole etc. into the cyanopyridine core it is possible to introduce desired level of n-type semiconducting property. All these factors have been kept in mind while designing four new series of pyridine derivatives in the present work.

From the foregoing account, it can be concluded that there is a good scope for design of new pyridine compounds carrying alkyl chains, polar substituents, hydrazone linking groups and other interesting heterocyclic moieties that leads to development of luminescent liquid crystalline materials with improved performance as well as electron transporting ability.

## 2.4 SCOPE AND OBJECTIVES OF THE PRESENT WORK

Thermotropic liquid crystals (TLC) have received great technological importance during the years due to their practical applications in many fields. Because of their applications, great efforts have been concentrated on design and synthesis of new mesogens with enhanced properties.

The present research work has been aimed at design and synthesis of new materials that possess the coexistence of liquid crystal and luminescent properties.

Based on the literature reports, pyridine moiety has been selected as a core owing to its peculiar properties in inducing liquid crystalline behavior. Further, it has been thought of designing new pyridine derivatives by incorporating proper groups like cyano, nitro, halo, alkoxy, hydrazone etc., with the hope that the new molecules would show significant LC properties. Also, it has been intended to achieve liquid crystal behavior for the new designs at ambient temperature by variation of linking groups and alkoxy chain lengths. Until now, only few materials are reported dealing with both properties, but the growing interest in this field is indicated by the review report from Binnemans (2009). Moreover, there are specific challenges in aiming to retain the luminescent properties of good chromophores, while imparting liquid crystallinity. Furthermore, there can be particular effects associated with the combination of the two properties, for example the way in which the liquid crystal properties can influence emission behavior (Kozhevnikov et al. 2008 and Sagara and Kato 2008). Also, it has been established that, liquid crystal phases with good charge carrier capability can be of great advantageous in several areas such as OLED, thin-film transistors (Sirringhaus et al. 1998), solid organic lasers (Hide et al. 1996) and photovoltaic devices (Halls et al. 1995).

Based on these facts and thorough literature reports, following main objectives have been intended in the present research work.

1. Design and synthesis of new pyridine derivatives with different alkoxy chain lengths, substituents like cyano, nitro, halo, and linking group at suitable positions, as mesogens
2. Characterization of intermediates and final compounds by FTIR,  $^1\text{H}$  NMR,  $^{13}\text{C}$  NMR and mass spectral techniques followed by elemental analysis
3. Investigation of 3-D crystal structure and identification of nature of contacts in selected compounds using single crystal X-ray diffraction study
4. Evaluation of their liquid crystalline properties using polarized optical microscopy (POM), differential scanning calorimetry (DSC) and phase confirmation by powder X-ray diffraction technique
5. Determination of UV-visible and photoluminescent properties of new pyridines
6. Study of structure-mesogenic property relationship of new pyridines

## 7. Preliminary optoelectronic study

In summary, a detailed literature survey clearly indicates that the compounds containing pyridine moiety as a core are useful candidates for LC materials. The incorporation of variable alkoxy chain and polar groups like -CN, -F, -Cl, -Br, -NO<sub>2</sub> would induce the liquid crystalline behavior in the resulting molecules. Further, presence of hydrazone functionality as a linking group would enhance the mesogenic property. Against this background, it has been planned to synthesize new pyridine derivatives with possible liquid crystal and desired photophysical properties. It is hoped that these molecules would be potential candidates for organo-electronic devices like OLED, TFT and photovoltaics.

### **2.5 DESIGN OF NEW PYRIDINE DERIVATIVES**

Pyridine based liquid crystalline compounds have been found to be thermally stable and miscible with other mesogenic partners. Besides, their structure leads to complex mesomorphic behaviour with higher order smectic phases at or near room temperature. Also, they possess good charge carrier mobilities which would be of much interest for their applications in optical, electrical and biomedical fields (Kelly et al. 1993; Moriya et al. 2000; Getmanenko et al. 2006). It has been further revealed that the lone pair of electrons on the nitrogen atom of the pyridine ring actively participate in enhancing inter molecular attractive forces (Bahadur 1990). Also, the literatures report that certain pyridines substituted with lower alkyl or alkoxy terminal groups are capable of exhibiting nematic phases because of their ability to show several other unusual properties like huge flexoelectricity and special rheological characteristics (Aziz et al. 2009).

In order to show pronounced mesogenic properties, the molecules are required to possess strong shape anisotropy and powerful inter molecular attractions, as a result of large polarizability, strong dipoles, hydrogen bonds, electron donor acceptor interactions. In compounds containing strong polar groups like -CN, -NO<sub>2</sub>, the interaction of permanent and induced electrical dipoles plays a remarkable role in enhancing mesogenic behavior (Demus and Hauser 1990; Longa and de Jeu 1982). Amongst polar groups, particularly the -CN group is an interesting substituent that contributes significantly in imparting liquid crystalline property in any molecule. Its

presence brings about partial dimerization of the molecule leading to increase in packing fraction, and hence the molecular density, which ultimately account for enhancement in its clearing temperature (Gray and Lacey 1983). Indeed, the dimerization may occur by interaction of the cyano group with neighboring aromatic ring or with adjacent cyano group, resulting in alteration in effective length-to-breadth ratio of the molecule, which explains the trend in their clearing temperatures.

At present, there is a considerable attention among the researchers to synthesize and develop new  $\pi$ -conjugated systems showing both liquid crystalline and luminescent properties (Attias et al. 2002; Ha et al. 2010). In this approach, many mesogens have been studied as good light emitters in their thin film form. In fact, thin films containing aligned luminescent liquid crystalline materials generally emit a linearly polarized light that could be conveniently used as a back light in flat panel displays and other device applications (Sung and Lin 2005; Misaki et al. 2004).

Thus, in the following section design of four new series of pyridine derivatives with different substituents as mesogens, has been discussed.

### 2.5.1 Design of 4,6-dialkoxyaryl-2-methoxynicotinonitriles (Series-I; LC<sub>1-13</sub>)

Rod shaped molecules carrying 2-cyanopyridine skeleton as core were found to possess good molecular organization ability through self-organization to form supramolecular networks. Kozhevnikov et al. (2008) observed that newly synthesized, 3,6-bis(4-(alkoxy)phenyl)picolinonitrile derivatives exhibited good LC property and compounds containing lower alkoxy (ethoxy and butoxy) group showed characteristic nematic phase while compounds carrying higher alkoxy chain displayed SmC phase. According to authors, absence of cyano group increases the clearing point by more than 100 °C. They concluded that presence of cyano group on pyridine ring would increase the liquid crystalline property remarkably.

Inspired from this, it has been thought of selecting 2-methoxy-3-cyanopyridine skeleton as a core in the present systematic study, keeping in view of its capability to form supramolecular networks through self-organization via a combination of non-covalent interactions and favorable molecular shape to induce columnar mesophase. However, no literature reports are available on synthesis and evaluation of LC

properties of rod-, bent-, disc-shaped mesogens based on 2-methoxy-3-cyanopyridines. Encouraged by this, it has been planned to derivatize 2-methoxy-3-cyanopyridine by introducing terminal alkoxy group with variable chain lengths in the proposed structure to achieve ambient temperature LC phase.

On the other hand, an extensive literature survey supports that cyanopyridine moiety carrying electron withdrawing cyano group attached to position-3 of electron deficient pyridine ring is an excellent luminescent core with good electron transporting property (Vishnumurthy et al. 2011; Bagley et al. 2009). Its various derivatives were reported to possess excellent thermal and photochemical stability as well as high luminescence efficiency (Matsui et al. 1992; Zhao and Mak 2004). Interestingly, their photophysical properties can readily be tailored through structural modification by introducing various donor-acceptor (D-A) moieties, which can lead to new D-A-D molecular frameworks with controlled electron properties. In view of their potential optoelectronic properties, it has been thought of selecting 2-methoxy-3-cyanopyridine moiety as a luminescent core in the present study leading to design and development of new blue light emitters with possible applications in OLEDs.

Motivated by the above background, it has been planned to design new 2-methoxy-3-cyanopyridine derivatives carrying a D-A-D architecture bearing electron rich alkoxyphenyl (donor) groups and electron deficient cyanopyridine (acceptor) unit placed in between them as possible luminescent mesogenic compounds. Accordingly, a new series of 4,6- dialkoxyaryl-2-methoxynicotinonitriles carrying variable alkoxy chains (**Series-I; LC<sub>1-13</sub>**) comprising thirteen derivatives has been designed as given in **Figure 2.2**.

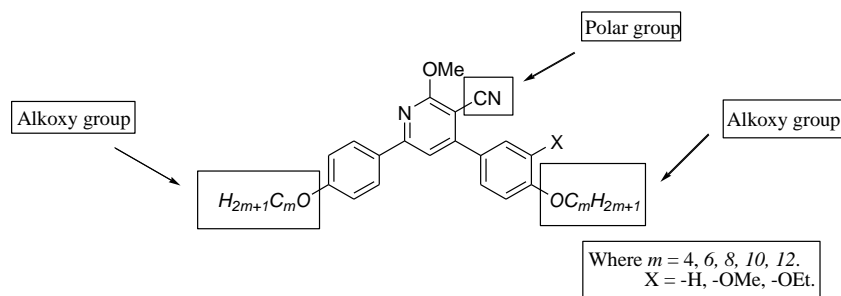


**Figure 2.2** Design of new 4,6- dialkoxyaryl-2-methoxynicotinonitriles carrying variable alkoxy chains (**LC<sub>1-13</sub>**)

### 2.5.2 Design of 6-alkoxyaryl/thiophenyl-4-substituted aryl-2-methoxy pyridines (Series-II; LC<sub>14-33</sub>)

A detailed literature reports on structure activity relationship study of pyridine derivatives suggests that terminal substituents like -CN, -NO<sub>2</sub>, -halo, 2-thiophenyl, 4-pyridyl, alkoxy etc. are capable of exhibiting a strong shape-anisotropy and powerful inter molecular attractions that lead to gain significant mesogenic property. Keeping this in view, it has been planned to incorporate such terminal substituents to methoxypyridine core in order to study the influence of these groups on their LC properties. Also, it has been intended to introduce cyano group to methoxypyridine core at position-3 to study its effect on the LC property. Against this background, it has been strategized to design new luminescent mesogens based on methoxypyridine as core carrying terminal alkoxy pendent and substituents like, -CN, -F, -Cl, -Br, -NO<sub>2</sub>, 2-thiophenyl, and 4-pyridinyl groups.

Accordingly, a new series of 6-alkoxyaryl/thiophenyl-4-substituted aryl-2-methoxy pyridines carrying variable terminal alkoxy chains and various substituents (Series-II; LC<sub>14-33</sub>) with twenty derivatives has been designed as shown in **Figure 2.3**.

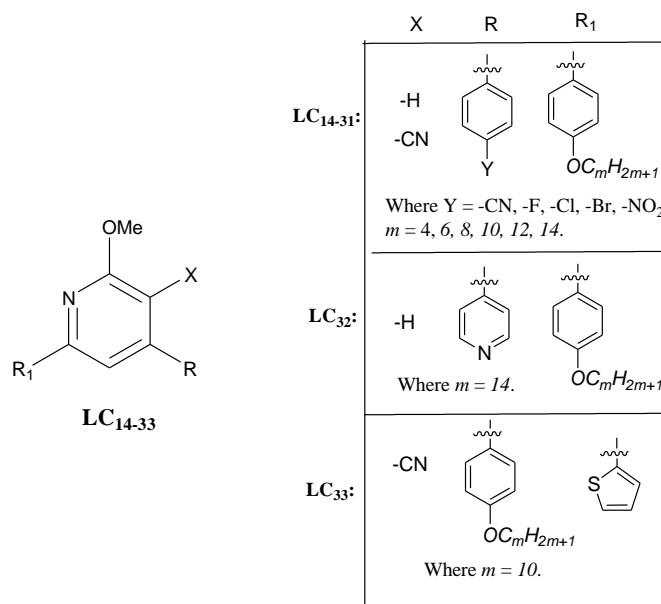


**Figure 2.3** Design of new 6-alkoxyaryl/thiophenyl-4-substituted aryl-2-methoxy pyridines with variable terminal alkoxy chains and various substituents (LC<sub>14-33</sub>)

In the new design, an electron donating methoxy group acts as a lateral substituent at position-6 of pyridine; alkoxy phenyl moiety at position-2 of pyridine acts as electron donating group; substituted aryl group at position-4 of pyridine behaves as electron withdrawing moiety. The ultimate design leads to form unsymmetrical bent shaped molecular structure. It is hoped that new molecules would show good luminescent as well as liquid crystalline behavior.

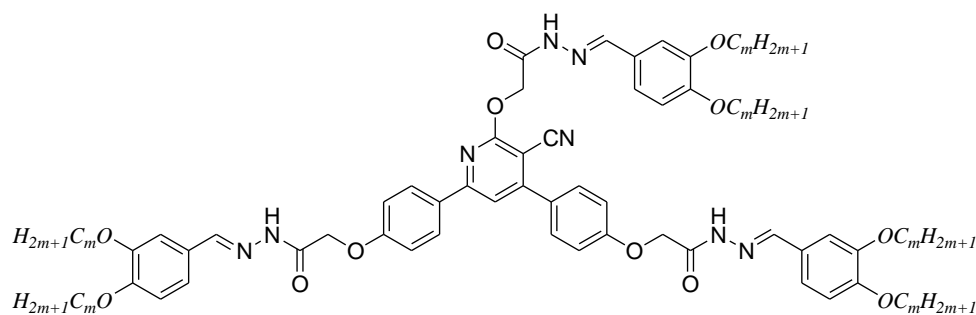
### 2.5.3 Design of 2-(4,6-disubstituted aryl-3-cyanopyridyl)oxyacetohydrazones (Series-III; LC<sub>34-38</sub>)

Since discovery, columnar liquid crystals have emerged as a promising class of materials because of their high charge carrier mobilities, defect-free grain boundaries, and their ability to form self-organized columnar nanostructures. In such columnar mesogens, the required properties are driven by the participation of  $\pi$ - $\pi$  interactions. Also, presence of a heteroaromatic/aromatic  $\pi$ -conjugated core plays a role in inducing non-covalent intermolecular interactions. Any factor which modifies the strength of  $\pi$ -stacking between neighboring molecules has an impact on their tendency to form columnar mesophases. In general, flat core, cone shaped, wedge-shaped or certain rod-shaped compounds bearing flexible side chain are quite common in exhibiting columnar aggregates (Kumar 2006).

Majority of the reported columnar mesogens are of p-type discotic materials derived from electron-rich heteroaromatic cores such as triphenylene-fused triazatruxenes (Zhao et al. 2010), which possess good hole transporting nature. On the other hand, n-type discotic mesogens are sparsely explored; however derivatives of certain electron deficient aromatic systems such as tris(N-salicylideneaniline) derivatives with peripheral branched alkyl chains (Yelamaggad and Achalkumar 2006), were shown to be n-type columnar materials possessing good electron transporting property. As these materials have several drawbacks, a search for new defect-free n-type discotic mesogens has gathered momentum.

In this context, it has been planned to design new disc shaped 3-cyanopyridine based molecules carrying 3,4-dialkoxyphenyl groups via hydrazone linkage. Accordingly, a new series of 2-(4,6-disubstituted aryl-3-cyanopyridyl)oxyaceto-

hydrazones (**Series-III; LC<sub>34-38</sub>**) comprising five derivatives has been designed as depicted in **Figure 2.4**. In the new design, the core 3-cyanopyridine contributes towards an excellent thermal and photochemical stability as well as high luminescence efficiency. In addition, it acts as a superior electron transporting n-type organic semiconducting moiety (You et al. 2012). It is anticipated that the new molecules would show luminescent liquid crystalline behavior with good electron transporting property.



Where  $m = 8, 10, 12, 14, 16$ .

**Figure 2.4** Design of new 2-(4,6-disubstituted aryl-3-cyanopyridyl)oxy acetohydrazones (**LC<sub>34-38</sub>**)

#### 2.5.4 Design of 4,6-disubstituted aryl-3-cyanopyridones (**Series-IV; LC<sub>39-48</sub>**)

2-Pyridone based liquid crystalline materials are well established in the literature. The advantage of 2-pyridones is that they are capable of forming columnar phase via hydrogen bonded dimer (Saravanan et al. 2010). Keeping this in view, it has been thought of selecting highly polarizable and luminescent 3-cyanopyridone moiety as a core for further functionalization. As well, the 1,2,3-triazole based heterocyclic materials were shown to exhibit good liquid crystalline behavior, wherein the 1,2,3-triazole ring plays a key role (Beltrán et al. 2010). Because of its planar structure and high chemical/thermal stability with molecular anisotropy, it contributes in enhancing LC property. In addition, it also possesses good electron affinity as well as electron-transporting property (Gallardo et al. 2008). Against this background, it has been intended to incorporate the 1,2,3-triazole unit at position-6 of 3-cyanopyridone through ether linkage.

In this context, it has been intended to design a new series of luminescent mesogens (**LC<sub>39-48</sub>**) by connecting 1, 4-disubstituted 1, 2, 3-triazole unit with



luminescent 3-cyanopyridone ring in order to get new molecular architecture. Also, it has been aimed to attach terminal substituents like  $-\text{CN}$  or  $-\text{NO}_2$  and variable alkoxy chain lengths ( $m=8-16$  (only even)) to create additional polarizability and flexibility to the resultant motifs. Accordingly, a new series of 4,6-disubstituted aryl-3-cyanopyridones (**Series-IV**; **LC<sub>39-48</sub>**) containing ten derivatives has been designed as shown in **Figure 2.5**. It is expected that the resulting motifs would show luminescent liquid crystalline behavior with good electron transporting property.

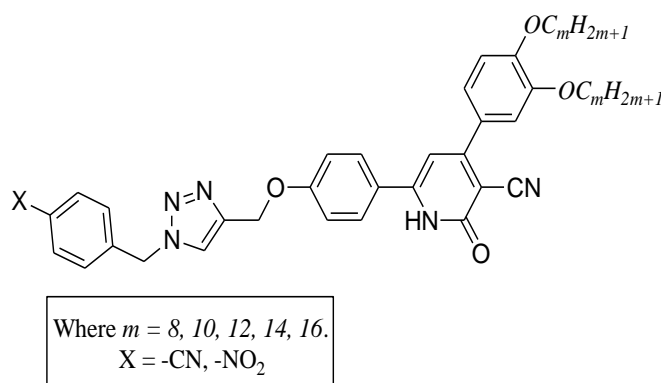


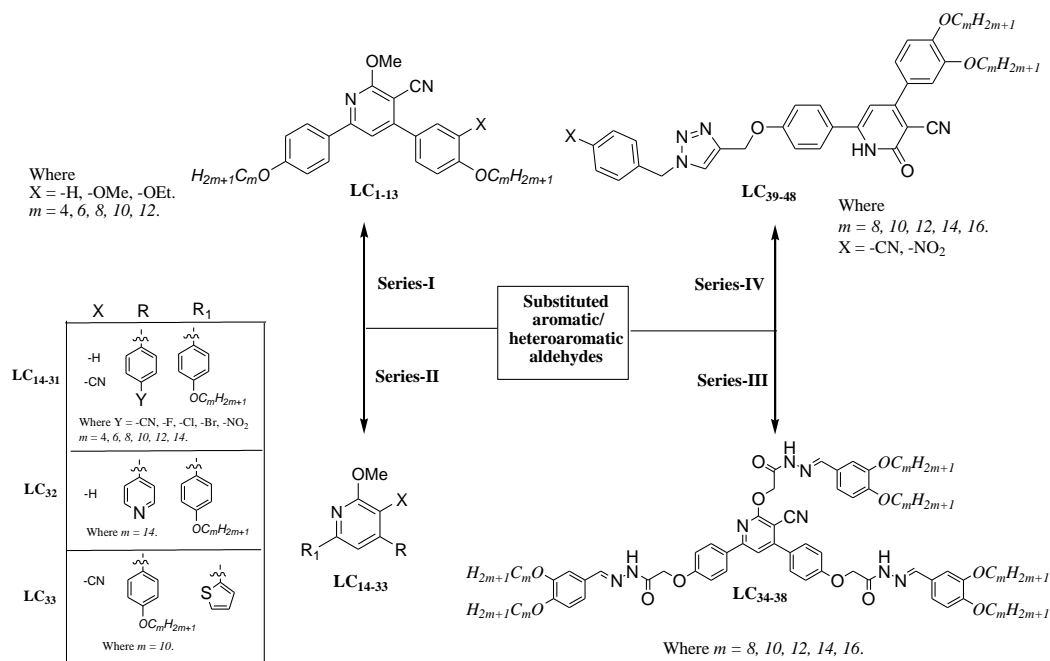
**Figure 2.5** Design of new 4,6-disubstituted aryl-3-cyanopyridones (**LC<sub>39-48</sub>**)

Further, the following four series of newly designed pyridine derivatives have been planned to synthesize:

- (i) 4,6- Dialkoxyaryl-2-methoxynicotinonitriles (**Series-I**; **LC<sub>1-13</sub>**)
- (ii) 6-Alkoxyaryl/thiophenyl-4-substituted aryl-2-methoxy pyridines (**Series-II**; **LC<sub>14-33</sub>**)
- (iii) 2-(4,6-Disubstituted aryl-3-cyanopyridyl)oxyacetohydrazones (**Series-III**; **LC<sub>34-38</sub>**)
- (iv) 4,6-Disubstituted aryl-3-cyanopyridones (**Series-IV**; **LC<sub>39-48</sub>**)

In the present work, above mentioned four new series of pyridine derivatives **LC<sub>1-48</sub>** have been synthesized adopting appropriate synthetic routes as outlined in **Scheme 2.9**. They have been prepared starting from simple organic compounds and their methods have been optimized to get high yield. Their purification methods have been established and accordingly they have been purified. The purified compounds are then characterized by various spectral techniques such as FTIR,  $^1\text{H}$  NMR,  $^{13}\text{C}$

NMR and mass spectrometry followed by elemental analysis. The structures of selected target compounds have been confirmed by their single crystal XRD studies.



**Scheme 2.9** New pyridine derivatives LC<sub>1-48</sub>

Further, the LC properties of the target compounds have been studied by DSC, POM, XRD analyses. Furthermore, their linear optical properties have been investigated by UV-visible and fluorescence spectrometry. The synthetic strategies and characterization data of new compounds have been discussed in **Chapter 3**, while, their mesogenic along with detailed optical properties have been described in **Chapter 4**. Finally, summary and important research outcomes have been highlighted in **Chapter 5**.

**CHAPTER 3**  
**SYNTHESIS AND CHARACTERIZATION OF NEW PYRIDINE**  
**DERIVATIVES**

### *Abstract*

*This chapter describes the synthetic protocols and spectral characterisation of newly designed four series of pyridine derivatives carrying various terminal substituents, alkoxy chain lengths and linking groups. Also, it deals with single crystal structural analysis of the selected intermediate and target compounds. Further it covers a detailed discussion on experimental results.*

## **3.1 INTRODUCTION**

In the previous chapter, design of four new series of pyridines has been discussed in detail. This chapter describes their synthesis and structural characterization in depth. Generally, the synthesis of any organic compound may be achieved by various possible reaction sequences. However, stabilization of an energy efficient, cheap and simple reaction path for the synthesis is a great challenge in organic chemistry. Reaction conditions such as solvent, temperature and purity of the precursors play an important role in various conversions. In the present study, the newly designed molecules were synthesized by stabilizing the appropriate synthetic routes for each series and the reaction conditions were optimized to get maximum yield. They were purified with appropriate techniques, for which required solvent systems were identified. The pure products were then characterized by various spectral techniques and elemental analysis. In the following sections, the synthetic strategy for the new compounds and their characterization data are discussed in detail.

## **3.2 MATERIALS AND METHODS**

All the chemicals used in the present work were procured from Sigma Aldrich and Spectrochem. All the solvents used were of analytical grade. They were purchased and used as such without any further purification. The progress of the reaction was monitored by thin layer chromatography, performed on a Silica gel 60 F254 coated aluminium sheet. Melting points were determined on open capillaries using a Stuart SMP3 (BIBBY STERLIN Ltd. UK) apparatus and were uncorrected. Infrared spectra were recorded on a Nicolet Avatar 5700 FTIR (Thermo Electron Corporation).  $^1\text{H}$  NMR and  $^{13}\text{C}$  NMR spectra were recorded on Bruker-400 MHz FT-

NMR spectrometer using TMS as internal reference and DMSO- $d_6$  or  $CDCl_3$  as solvent. Chemical shifts were reported in ppm ( $\delta$ ) and signals were described as singlet (s), doublet (d), triplet (t), quartet (q), doublet of doublet (dd) and multiplet (m). The coupling constant ( $J$ ) values were expressed in Hz. Elemental analyses were performed on a Flash EA1112 CHNS analyzer (Thermo Electron Corporation). Mass spectra (ESI) were recorded on Waters ZQ-4000 liquid chromatography-mass spectrometer. A crystal of suitable size was mounted using a Mitigen micromount and single crystal data collection was done on a Bruker Smart X2S bench top diffractometer equipped with a micro-focus MoK $\alpha$  radiation ( $\lambda = 0.71073$ ). The machine was operated at 50kV and 1mA. Data reduction was performed using SAINTPLUS. Scaling, absorption correction was done using SADABS, all embedded in the Apex2 software suite. The crystal structure was solved by direct methods using XS and the structure refinement was done using XL in the SHELXTL package. The position and thermal parameters of all the non-hydrogen atoms were refined. The hydrogen's were fixed in geometrically calculated positions and refined isotropically. The ORTEP diagrams and packing diagrams were created using Mercury 3.0 and POV ray.

### 3.3 SYNTHETIC METHODS

#### 3.3.1 Synthesis of 4,6- dialkoxyaryl-2-methoxy nicotinonitriles (Series-I; LC<sub>1-13</sub>)

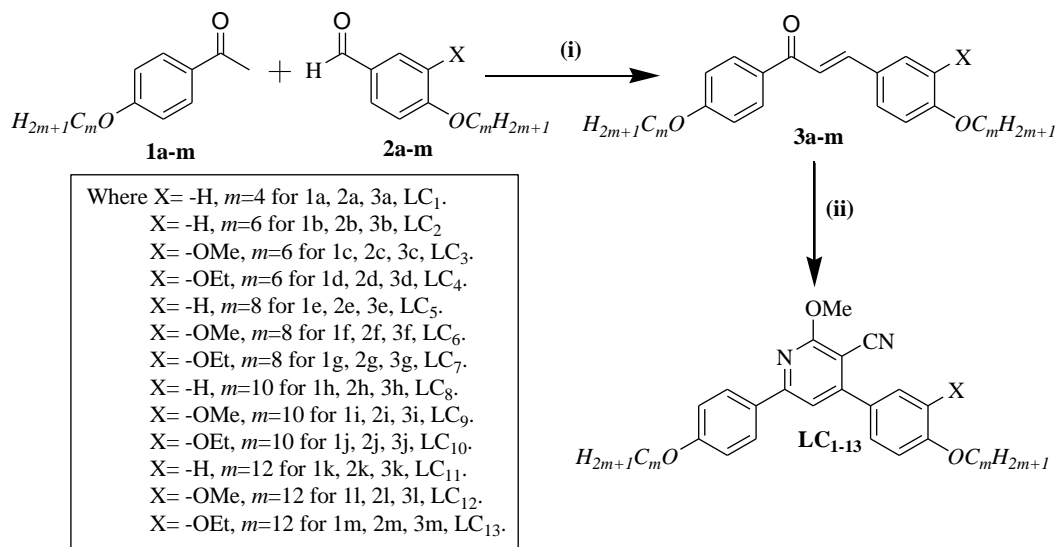
In this series, thirteen new pyridine derivatives were synthesized by reacting substituted dialkoxyarylprop-2-en-1-one with malononitrile. The synthetic route for the target 4,6- dialkoxyaryl-2-methoxy nicotinonitriles (LC<sub>1-13</sub>) is shown in **Scheme 3.1**.

##### 3.3.1.1 Results and discussion

###### *Synthesis:*

The starting materials alkoxyacetophenones **1a-m** and alkoxybenzaldehydes **2a-m** were prepared by the O-alkylation of 4-hydroxyacetophenone and 4-hydroxy benzaldehyde or meta substituted 4-hydroxybenzaldehyde by reacting with corresponding alkyl bromides in good yield as per the reported procedure (Tantrawong et al. 1993; Yelamaggad et al. 2007). The required dialkoxyarylprop-2-en-1-one **3a-m** were prepared from **1a-m** and **2a-m** using Claisen-Schmidt reaction.

It was then cyclized to obtain a 4,6- dialkoxyaryl-2-methoxy nicotinonitriles **LC**<sub>1-13</sub> by reacting them with malononitrile in presence of sodium methoxide as a catalyst.



**Scheme 3.1** Synthesis of 4,6- dialkoxyaryl-2-methoxy nicotinonitriles (**Series-I**; **LC**<sub>1-13</sub>). Reagents and conditions: (i) KOH / EtOH, rt; (ii) Malononitrile, NaOMe, MeOH, rt

The structures of newly synthesized compounds were confirmed by FTIR, <sup>1</sup>H NMR, <sup>13</sup>C NMR spectroscopy and elemental analysis. The compound **LC**<sub>2</sub>, in its FTIR spectrum showed two strong IR absorption bands at 2937 and 2857 cm<sup>-1</sup> that correspond to C-H stretching vibrations of hexyloxy group. Further, a strong IR absorption band at 2213 cm<sup>-1</sup> indicated the presence of cyano group in its molecular structure. Also, the absorption band at 1578 cm<sup>-1</sup> accounting for C=N stretching vibrations, confirmed the formation of pyridine ring.

In addition to FTIR data, its <sup>1</sup>H NMR spectrum showed unique resonances at  $\delta$  8.05, 7.61 and 7.02 ppm for the protons of aromatic moieties. Appearance of singlet at  $\delta$  7.36 ppm for one proton of aromatic pyridine ring confirmed its structure. Also, three protons of -OMe of pyridine resonated as a singlet at  $\delta$  4.16 ppm, which confirmed the successful construction of central pyridine ring via cyclization reaction as per **Scheme 3.1**. The appearance of primary and secondary protons signals in the range of  $\delta$  1.84-0.90 ppm in its <sup>1</sup>H NMR spectrum confirmed the presence of two hexyloxy chains. Its <sup>13</sup>C NMR spectrum showed the characteristic signals obtained at

higher frequency (downfield region). As expected, thirteen distinct signals appeared due to one pyridine ring and two aromatic ring carbon atoms. The carbon carrying methoxy group resonates at  $\delta$  165.12 ppm and carbon carrying cyano group of 2-methoxy-3-cyanopyridine resonates at  $\delta$  91.53 ppm confirming the formation of 2-methoxy-3-cyanopyridine ring. The two kinds of tertiary carbon atoms of 2-methoxy-3-cyanopyridine ring resonate in the region of  $\delta$  157.4-156.0 ppm and one kind of secondary carbon atom of 2-methoxy-3-cyanopyridine ring resonates at  $\delta$  112.2 ppm. The aromatic quaternary carbon atoms connected to oxygen resonate in the region of  $\delta$  161-160 ppm. The remaining signals appearing in the region of  $\delta$  129.7-128.4, 116.21-116.19 and 114.8-114.7 ppm are due to other aromatic carbons. Further, its mass spectrum showed the  $[M+H]^+$  peak at 487.3, which is in agreement with the calculated molecular weight for the formula of  $C_{31}H_{39}N_2O_3$ . **Figures 3.16-3.19** show FTIR,  $^1H$  NMR,  $^{13}C$  NMR and Mass spectra of compound **LC<sub>2</sub>**, respectively. Finally, the structure of compounds **LC<sub>1</sub>**, **LC<sub>2</sub>** and **LC<sub>3</sub>** were confirmed by single crystal X-ray diffraction analysis.

#### *Crystal structure analysis of LC<sub>1</sub>:*

Single crystal formation was achieved by dissolving the 4,6-bis(4-butoxyphenyl)-2-methoxynicotinonitrile in chloroform/methanol mixture at room temperature and allowing the resulting solution for slow evaporation of solvent through a plastic film containing pinholes. Superior quality crystals were used for single crystal X-ray analysis. Single crystal study reveals that 4,6-bis(4-butoxyphenyl)-2-methoxynicotinonitrile (**LC<sub>1</sub>**) crystallizes in monoclinic space group  $C2/c$  with cell parameters are  $a=25.181(4)$  Å,  $b=15.651(4)$  Å,  $c=12.7036(19)$  Å,  $V=4880.4(16)$  Å<sup>3</sup>,  $Z=8$  (**Table 3.1**). **Figure 3.1** shows the ORTEP diagram of the compound. From the X-ray analysis data, it is evident that the molecule is not planar and but distorted. Interestingly, 4-butoxyphenyl ring substituted at position-4 of central pyridine ring makes a torsion angle  $\chi[C(4), C(3), C(10), C(19)]$  of  $40.55^\circ$  with central pyridine ring. While the other 4-butoxyphenyl ring substituted at position-6, forms a torsion angle  $\chi[N(3), C(5), C(1), C(8)]$  of  $5.04^\circ$ , which is less than the previous one. Further, bond lengths and bond angles are all within the expected ranges, as shown in **Table 3.2**.

**Table 3.1** Crystallographic data and structure refinement parameters of **LC<sub>1</sub>**

Compound	LC <sub>1</sub>
Chemical formula	C <sub>27</sub> H <sub>30</sub> N <sub>2</sub> O <sub>3</sub>
Formula mass	430.53
Crystal system	Monoclinic
Space group	<i>C2/c</i>
<i>a</i> (Å)	25.181(4)
<i>b</i> (Å)	15.651(4)
<i>c</i> (Å)	12.7036(19)
$\beta$ (°)	102.890(8)
Unit cell volume (Å <sup>3</sup> )	4880.4(16)
<i>Z</i>	8
Temperature (K)	296(2)
$\rho_{\text{calc}}$ (g cm <sup>-3</sup> )	1.172
Absorption coefficient (mm <sup>-1</sup> )	0.076
<i>F</i> (000)	1840
Crystal size (mm <sup>3</sup> )	0.30 x 0.27 x 0.19
No. of reflections measured	4229
No. of independent reflections	2717
<i>R</i> <sub>int</sub>	0.0571
$\Delta\rho_{\text{min, max}}$ (e Å <sup>-3</sup> )	-0.32, 0.24
Final <i>R</i> <sub><i>I</i></sub> values ( <i>I</i> >2σ( <i>I</i> ))	0.054
Final <i>wR</i> ( <i>F</i> <sup>2</sup> ) values ( <i>I</i> >2σ( <i>I</i> ))	0.143
Final <i>R</i> <sub><i>I</i></sub> values (all data)	0.098
Final <i>wR</i> ( <i>F</i> <sup>2</sup> ) values (all data)	0.167
GOOF	1.012
CCDC	886565



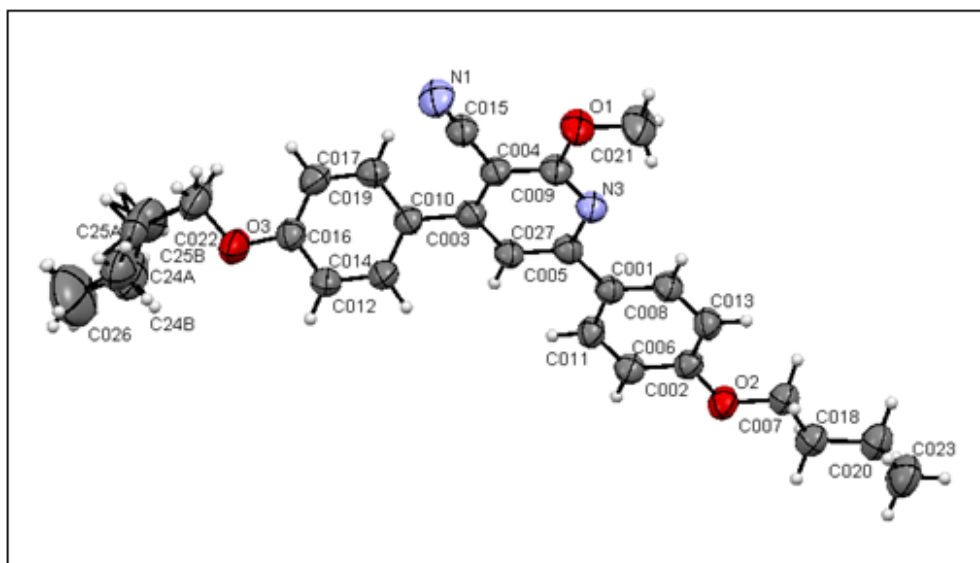


**Figure 3.1** ORTEP diagram of 4,6-bis(4-butoxyphenyl)-2-methoxynicotinonitrile ( $\text{LC}_1$ ) with labelling

**Table 3.2** Selected bond lengths ( $\text{\AA}$ ) and angles ( $^\circ$ ) for  $\text{LC}_1$

Bond Lengths ( $\text{\AA}$ )			
C1-C5	1.479 (2)	O1-C9	1.343 (2)
C1-C8	1.384 (2)	O1-C21	1.434 (3)
C4-C9	1.404 (3)	O2-C2	1.369 (2)
C7-HA	0.970 (2)	O3-C22	1.414 (3)
C8-H8	0.930 (2)	N1-C15	1.138 (3)
C10-C12	1.395 (3)	N3-C5	1.359 (2)
C10-C19	1.389 (3)	N3-C9	1.321 (2)
C11-H11	0.930 (2)	C25A-H25B	0.969 (9)
Bond Angles ( $^\circ$ )			
C9-O1-C021	117.3 (2)	C6-C2-C13	118.9 (2)
C2-O2-C7	118.4 (1)	C3-C4-C9	118.4 (2)
C16-O3-C22	119.8 (2)	N3-C5-C1	115.9 (2)
C5-N3-C9	117.7 (2)	N3-C5-C27	121.3(3)
C5-C1-C8	121.5 (2)	C11-C6-H6	119.6 (2)
C8-C1-C11	117.1 (2)	O2-C7-C18	107.3 (2)
O2-C2-C6	115.6 (2)	O2-C7-HA	110.3 (2)

O2-C2-C13	125.6 (2)	C1-C8-C13	122.1(2)
N3-C9-C4	124.5 (2)	C1-C11-H11	119.4 (2)
N1-C15-C4	178.2 (2)	O3-C16-C14	115.6 (2)
C18-C20-C23	112.6 (2)	C18-C20-H2B	109.1 (2)
O1-C21-H2C	109.5 (2)	O1-C21-H2E	109.5 (2)
H2C-C21-H2D	109.4 (2)	H2D-C21-H2E	109.5 (2)
H2F-C23-H2H	109.5 (3)	H2G-C23-H2H	109.5 (3)

Generally, crystal packing depends mainly upon intermolecular forces and molecular geometry. It is well-known that conventional hydrogen bonding ( $X-H\cdots Y$ ;  $X, Y = N$  or  $O$ ) has been extensively utilized to command supramolecular network formation in organic solids (Lehn 1995; Aoyama et al. 1996). However, the construction of networks through weak  $CH\cdots O$  hydrogen bonding interaction also plays an important role in crystallographic studies (Desiraju 1996). In addition to weak hydrogen bonding, Van der Waals interactions are important in the effective formation of crystal packing in the solid state as well as help to exhibit mesophase transitions by providing the proper molecular orientation in the liquid crystal state (Swanson and Sorensen 1995). The analysis of X-ray crystal structure of compound **LC<sub>1</sub>** reveals the presence of several intermolecular interactions in its crystal packing. These include the pair of non-covalent interactions Ar-H012 $\cdots$ C006 (Ar), (alkane) H24 $\cdots$ C009 (Ar) and (Ar) C027 $\cdots$ H02E (methoxy) having bond distance of 2.892, 2.885, and 2.869 Å, respectively. It is evident that here nitrogen atom of cyano group can form two kinds of nonconventional intermolecular hydrogen bonds N1 $\cdots$ H011 (Ar) and N1 $\cdots$ H027 (Ar) with bond length 2.546 and 2.698 Å, respectively.

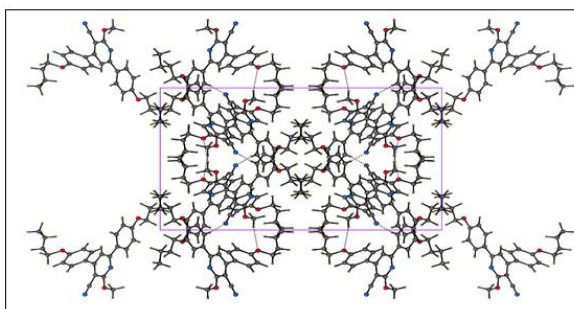


**Figure 3.2** Short intermolecular contacts in two dimensional arrangements when viewed down the b axis

From the observed crystal parameters, it has been proposed a new supramolecular network for compound **LC<sub>1</sub>**, as shown in **Figure 3.2**. The bond length of O1-C009 (*i.e.* methoxy group at position-2 of central cyanopyridine ring) is found to be 1.343 (2) Å. This shows that the lone pair of electrons on O1 has more delocalized to the  $\pi$  electron system of the pyridine ring. Further, the bond length of O2-C002 is shown to be 1.369 (2) Å (*i.e.* *para* butoxyphenyl group at position-6 of central cyanopyridine ring) and that of O3-C016 as 1.365 (2) Å (*i.e.* another *para* butoxyphenyl group at position-4 of central cyanopyridine ring). Appearance of shorter bond length of O3-C016 compared to that of O2-C002 indicates that the lone electron pairs in O3 contribute more for the delocalization of  $\pi$  electrons in the conjugated heteroaromatic system.

*Crystal structure analysis of LC<sub>2</sub> and LC<sub>3</sub>:*

Suitable crystals of **LC<sub>2</sub>** and **LC<sub>3</sub>** were grown at room temperature from 1:1 mixture of chloroform and methanol by slow evaporation of the solvent. Single crystal X-ray diffraction analysis was carried out for compounds **LC<sub>2</sub>** and **LC<sub>3</sub>** which clearly established their molecular structures (**Figure 3.3**). In both the compounds, two molecules crystallized together in the asymmetric unit; **LC<sub>2</sub>** in the monoclinic space group, *P2<sub>1</sub>/c* and compound **LC<sub>3</sub>** in the triclinic space group *P-1*. Presence of more than one symmetry-independent molecule in the crystal structures can be attributed to the high conformational flexibility of the terminal alkoxy chains along with the aromatic bent core (Dikundwar et al. 2011). A summary of the crystallographic data and structural refinement details of **LC<sub>2</sub>** and **LC<sub>3</sub>** are given in **Table 3.3**.

**Table 3.3** Crystallographic data and structure refinement parameters of **LC<sub>2</sub>** and **LC<sub>3</sub>**

Compound	LC <sub>2</sub>	LC <sub>3</sub>
Formula	C <sub>31</sub> H <sub>38</sub> N <sub>2</sub> O <sub>3</sub>	C <sub>32</sub> H <sub>40</sub> N <sub>2</sub> O <sub>4</sub>
Formula weight	486.63	516.66
CCDC number	916621	916818
Temperature (K)	100	120 (2)
Crystal form	Block	Block

Color	Colorless	Colorless
Crystal system	Monoclinic	Triclinic
Space group	<i>P21/c</i>	<i>P-1</i>
<i>a</i> (Å)	24.9425(17)	12.0411(5)
<i>b</i> (Å)	15.9287(10)	16.1624(5)
<i>c</i> (Å)	13.7042(9)	17.0125(4)
$\alpha$ (°)	90	69.175(2)
$\beta$ (°)	94.739(4)	73.371(3)
$\gamma$ (°)	90	69.132(3)
Volume (Å <sup>3</sup> )	5426.1(6)	2842.92(17)
<i>Z</i>	8	4
Density (gcm <sup>-3</sup> )	1.191	1.207
$\mu$ (mm <sup>-1</sup> )	0.076	0.079
F (000)	2096	1112
<i>h</i> <sub>min, max</sub>	-30, 30	-14, 14
<i>k</i> <sub>min, max</sub>	-19, 19	-19, 19
<i>l</i> <sub>min, max</sub>	-16, 16	-20, 20
Reflections collected	10581	11146
Independent reflections	6216	8686
<i>R</i> <sub>all</sub> , <i>R</i> <sub>obs</sub>	0.1194, 0.0546	0.0650, 0.0486
<i>wR</i> <sub>2_all</sub> , <i>wR</i> <sub>2_obs</sub>	0.1331, 0.1155	0.1978, 0.1720
$\Delta\rho_{\text{min,max}}$ (e Å <sup>-3</sup> )	-0.270, 0.251	-0.235, 0.344
GOOF	0.968	0.800

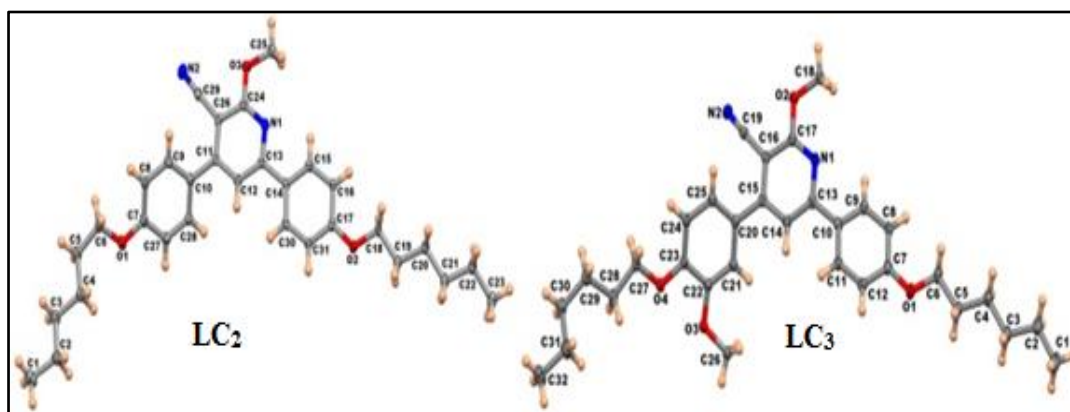


Figure 3.3 ORTEP diagram of LC<sub>2</sub> and LC<sub>3</sub>

It is observed that the intermolecular packing in **LC<sub>2</sub>** is mainly due to bifurcated C-H...N hydrogen bonded chains propagating along the 2<sub>1</sub> screw, whereas, **LC<sub>3</sub>** molecules pack as C-H...N hydrogen bonded dimers further interlinked through C-H...O interactions offered by the additional methoxy group (**Figure 3.4** and **Table 3.4**). In both the structures, the intermolecular packing is further supported by C-H... $\pi$  interactions (**Table 3.5**). It should be noted that short C-H...H-C intermolecular contacts in the range 2.27-2.31 Å have been observed between the terminal alkoxy chains in both **LC<sub>2</sub>** and **LC<sub>3</sub>**. The relevance of such interactions in the packing of hydrocarbon molecules was already established (Echeverría et al. 2011), and in the present structures these interactions could be the reason for the absence of any alkyl chain positional disorder.

An inspection of torsion angles in the crystal structures of compound **LC<sub>2</sub>** and **LC<sub>3</sub>** clearly shows that the molecules adopt non-planar geometry with respect to the central cyanopyridine core. Also, the extent of co-planarity of the three six membered rings in them differs significantly. Notably, compound **LC<sub>2</sub>** is considerably more planar than that of compound **LC<sub>3</sub>**, thus leading to better  $\pi$ ... $\pi$  (face to face) stacking interactions in **LC<sub>2</sub>** (**Figure 3.5** and **Table 3.6**). In addition to this, **LC<sub>2</sub>** and **LC<sub>3</sub>** differ in their conformations with respect to the orientation of alkoxy chains.

**Table 3.4** Intermolecular hydrogen bonds in the crystal structures of **LC<sub>2</sub>** and **LC<sub>3</sub>**

Compd	D-H...A	D-H/Å	H...A/Å	D...A/Å	$\angle$ D-H...A/°	Symmetry
<b>LC<sub>2</sub></b>	C30-H26...N2	1.08	2.260(1)	3.32	166	1-x,1/2+y,1/2-z
	C61-H69...N4	1.08	2.340(1)	3.38	161	-x,1/2+y,1/2-z
<b>LC<sub>3</sub></b>	C11-H11...N4	1.08	2.440(2)	3.51	170	1-x,1-y,1-z
	C51-H51...O8	1.08	2.470(1)	3.48	155	1-x,1-y,1-z
	C61-H61...O1	1.08	2.520(1)	2.90	100	1-x,1-y,1-z

**Table 3.5** C-H... $\pi$  interactions in crystal structure of **LC<sub>2</sub>** and **LC<sub>3</sub>**

Compd	D-H...A	D-H/Å	D...A/Å	H...A/Å	$\angle$ D-H...A/°	Symmetry
<b>LC<sub>2</sub></b>	C5-H16...Cg1	0.90	3.869(2)	2.79	167	1-x,-y,-z
	C20-H33...Cg3	0.89	3.683(1)	2.86	141	x,1/2-y,1/2+z
	C52-H44...Cg6	0.88	3.600(2)	2.79	140	x,3/2-y,1/2+z
	C35-H60...Cg4	0.86	3.652(1)	2.77	142	-x,1-y,-z

LC <sub>3</sub>	C3–H3B...Cg2	0.93	3.764(2)	2.87	154	-x,1-y,2-z
	C28–H28B...Cg3	0.85	3.563(1)	2.71	147	-x,-y,1-z
	C38–H38B...Cg2	0.91	3.793(1)	2.87	160	x,y,z

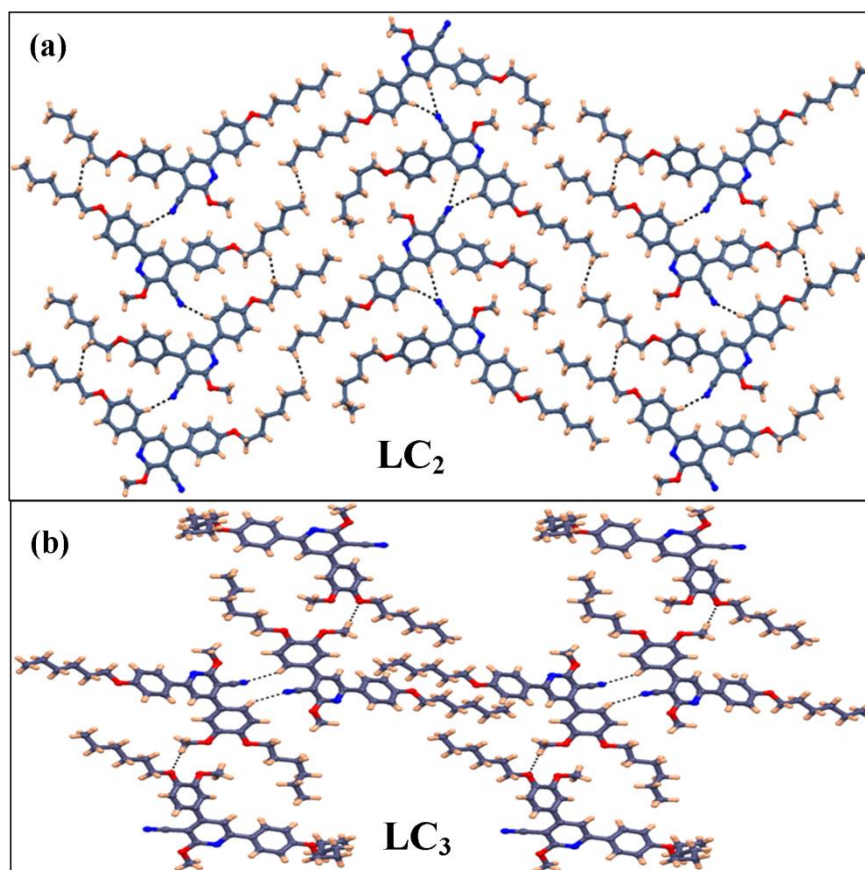


**Figure 3.4** Solid state packing; C-H...N interaction and H-H short contacts between the terminal alkoxy chains in LC<sub>2</sub>; C-H...N dimer and C-H...O hydrogen bonding in LC<sub>3</sub>

**Table 3.6**  $\pi$ ... $\pi$  interactions in crystal structures of LC<sub>2</sub> and LC<sub>3</sub>

Compd	Cg...Cg	d[Cg...Cg] (Å)	Symmetry
LC <sub>2</sub>	Cg(6) ...Cg(4)	3.649(2)	-x,1-y,1-z
	Cg(2) ...Cg(2)	3.631(1)	1-x,-y,-z
	Cg(3) ...Cg(1)	4.079(4)	1-x,-y,1-z
LC <sub>3</sub>	Cg(1)Cg(5)	3.707(2)	x, y, z
	Cg(3)Cg(4)	3.519(1)	x, y, z

**Table 3.7** Selected torsion angles of **LC<sub>2</sub>** and **LC<sub>3</sub>**

Torsion Angles (°)					
<b>LC<sub>2</sub></b> ( <i>Z'</i> =2)	C9–C10–C11–C26	-40.00	C15- C14-C13- N1	1.18	
	C40-C41-C42-C57	-39.04	C46-C45-C44- N3	-0.89	
<b>LC<sub>3</sub></b> ( <i>Z'</i> =2)	C25-C20-C15-C16	-35.69	C9-C10-C13-N1	-17.45	
	C41-C45-C46-C50	40.15	C57-C53-C48-N3	-22.41	

Note: *Z'* = number of molecules in asymmetric unit.

The relevant torsion angles measured for **LC<sub>2</sub>** and **LC<sub>3</sub>** (for both symmetry independent molecules) are given in **Table 3.7**. In compound **LC<sub>2</sub>**, 4-hexyloxyphenyl ring substituted at position -4 of central pyridine ring makes a torsion angle C(9)-C(10)-C(11)-C(26) of 40.0° with central pyridine ring. While the other 4-hexyloxyphenyl ring substituted at position -6, makes a torsion angle N(1)-C(13)-C(14)-C(15) of 1.18°, which is less than the previous one. Thus, the two ring systems having least torsion angle create near planarity. Similarly in compound **LC<sub>3</sub>**, 4-(hexyloxy)-3-methoxyphenyl ring substituted at position -4 of central pyridine ring makes a torsion angle C(25)-C(20)-C(15)-C(16) of 35.69° with central pyridine ring. Whereas, the other 4-hexyloxyphenyl ring substituted at position-6, forms a torsion angle N(1)-C(13)-C(10)-C(9) of -17.45° with central pyridine suggesting the non-planar geometry.

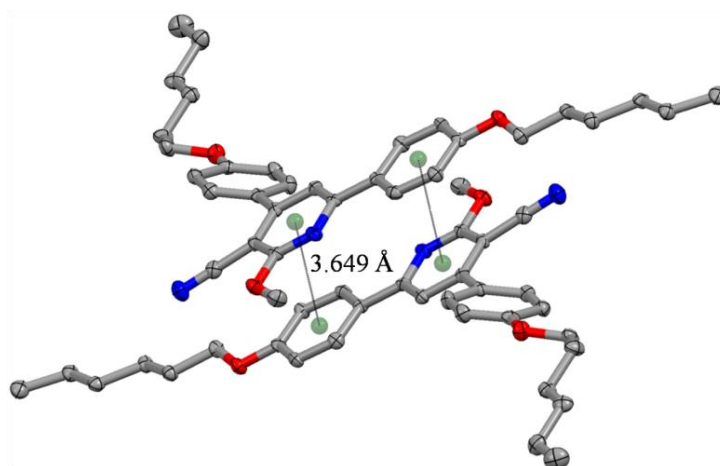


**Figure 3.5**  $\pi \cdots \pi$  (face to face) stacking in crystal structure of **LC<sub>2</sub>** (hydrogen atoms were omitted for clarity)

In addition, the measured bond length values were found to be in-between the single and double bond lengths (**LC**<sub>2</sub>: C<sub>13</sub>-C<sub>14</sub>=1.480 Å; **LC**<sub>3</sub>: C<sub>10</sub>-C<sub>13</sub>=1.484 Å) indicating the delocalization of  $\pi$ -electrons from the donating site (*i.e.* alkoxyphenyl) to the acceptor site (*i.e.* central pyridine). This observation is supportive of donor-acceptor-donor (D-A-D) nature in cyanopyridine mesogens.

### 3.3.1.2 Experimental procedures

In the following section, the appropriate synthetic protocol followed for the synthesis of various intermediates and target compounds of **LC**<sub>1-13</sub> were given. Further, their characterization data are also included.

*General procedure for the synthesis of alkoxyacetophenones 1a-m and alkoxy benzaldehydes 2a-m.*

The 4-alkoxyacetophenones **1a-m** were prepared from 4-hydroxy acetophenone by reaction with the corresponding alkyl bromide following standard procedures (Tantrawong et al. 1993).

The 4-alkoxybenzaldehydes and meta substituted 4-alkoxybenzaldehydes **2a-m** were prepared from 4-hydroxybenzaldehyde, vaniline and ethyl vaniline by reacting with the corresponding alkyl bromide according to reported procedure (Yelamaggad et al. 2007). All the obtained analytical data were in agreement with the reported data.

*General procedure for the synthesis of dialkoxyarylprop-2-en-1-ones (3a-m).*

An equimolar mixture of 4-alkoxyacetophenone **1a-m** and 4-alkoxy benzaldehyde or meta substituted 4-alkoxybenzaldehyde **2a-m** was taken in ethanol (5 ml). To this an aqueous solution of potassium hydroxide (1.2 equivalents) was added slowly with stirring and stirring was continued at room temperature for 4 h. The precipitated product was filtered. The crude product was purified by recrystallization from chloroform and methanol mixture. The characterization data of **3a-m** are given below.

*1,3-Bis(4-butoxyphenyl)prop-2-en-1-one (3a).* Yield 83 %, m.p. 73-74 °C. FTIR (cm<sup>-1</sup>): 2918, 2853, 1648, 1604, 1579, 1245, 1019, 824. <sup>1</sup>H NMR (400 M Hz, DMSO-



$d_6$ )  $\delta$  (ppm) 7.90 (d,  $J=15.4$  Hz, 1H, Olefinic-H), 7.70 (d,  $J=8.6$  Hz, 2H, Ar-H), 7.56 (d,  $J=15.6$  Hz, 1H, Olefinic-H), 7.19 (d,  $J=8.6$  Hz, 2H, Ar-H), 6.96 (d,  $J=8.4$  Hz, 2H, Ar-H), 6.72 (d,  $J=8.6$  Hz, 2H, Ar-H), 3.94 (t,  $J=6.6$  Hz, 4H, Ar-OCH<sub>2</sub>-), 1.74-1.71 (q, 4H, Ar-OCH<sub>2</sub>-CH<sub>2</sub>-), 1.50-1.26 (m, 4H, -CH<sub>2</sub>-), 0.96 (t,  $J=6.8$  Hz, 6H, -CH<sub>3</sub>). MS (m/z): 353.2 (M+H)<sup>+</sup>. Anal. Calcd. For. C<sub>23</sub>H<sub>28</sub>O<sub>3</sub>: C. 78.38; H. 8.01; Found: C. 78.46; H. 8.05.

*1,3-Bis(4-(hexyloxy)phenyl)prop-2-en-1-one (3b)*. Yield 78 %, m.p. 76-77 °C. FTIR (cm<sup>-1</sup>): 2918, 2853, 1648, 1604, 1579, 1245, 1019, 824. <sup>1</sup>H NMR (400 M Hz, DMSO- $d_6$ )  $\delta$  (ppm) 7.90 (d,  $J=15.4$  Hz, 1H, Olefinic-H), 7.70 (d,  $J=8.6$  Hz, 2H, Ar-H), 7.56 (d,  $J=15.6$  Hz, 1H, Olefinic-H), 7.19 (d,  $J=8.6$  Hz, 2H, Ar-H), 6.96 (d,  $J=8.4$  Hz, 2H, Ar-H), 6.72 (d,  $J=8.6$  Hz, 2H, Ar-H), 3.94 (t,  $J=6.6$  Hz, 4H, Ar-OCH<sub>2</sub>-), 1.74-1.71 (q, 4H, Ar-OCH<sub>2</sub>-CH<sub>2</sub>-), 1.50-1.26 (m, 12H, -CH<sub>2</sub>-), 0.96 (t,  $J=6.8$  Hz, 6H, -CH<sub>3</sub>). MS (m/z): 409.2 (M+H)<sup>+</sup>. Anal. Calcd. For. C<sub>27</sub>H<sub>36</sub>O<sub>3</sub>: C. 79.37; H. 8.88; Found: C. 79.41; H. 8.85.

*3-(4-(Hexyloxy)-3-methoxyphenyl)-1-(4-(hexyloxy)phenyl)prop-2-en-1-one (3c)*. Yield 71 %, m.p. 82-83 °C. FTIR (cm<sup>-1</sup>): 2926, 2847, 1651, 1603, 1584, 1242, 821. <sup>1</sup>H NMR (400 M Hz, DMSO- $d_6$ )  $\delta$  (ppm) 7.88 (d,  $J=15.6$  Hz, 1H, Olefinic-H), 7.70 (d,  $J=8.6$  Hz, 2H, Ar-H), 7.56 (d,  $J=15.4$  Hz, 1H, Olefinic-H), 6.96 (d,  $J=8.6$  Hz, 2H, Ar-H), 6.75 (d,  $J=8.4$  Hz, 1H, Ar-H), 6.70 (s, 1H, Ar-H), 6.61 (d,  $J=8.6$  Hz, 1H, Ar-H), 3.94 (t,  $J=6.8$  Hz, 4H, Ar-OCH<sub>2</sub>-), 3.73 (s, 3H, Ar-OCH<sub>3</sub>), 1.74-1.71 (q, 4H, Ar-OCH<sub>2</sub>-CH<sub>2</sub>-), 1.54-1.26 (m, 12H, -CH<sub>2</sub>-), 0.96 (t,  $J=6.8$  Hz, 6H, -CH<sub>3</sub>). MS (m/z): 439.3 (M+H)<sup>+</sup>. Anal. Calcd. For. C<sub>28</sub>H<sub>38</sub>O<sub>4</sub>: C. 76.68; H. 8.73; Found: C. 76.75; H. 8.71.

*3-(3-Ethoxy-4-(hexyloxy)phenyl)-1-(4-(hexyloxy)phenyl)prop-2-en-1-one (3d)*. Yield 68 %, m.p. 80-81 °C. FTIR (cm<sup>-1</sup>): 2923, 2849, 1646, 1600, 1573, 1244, 825. <sup>1</sup>H NMR (400 M Hz, DMSO- $d_6$ )  $\delta$  (ppm) 8.15 (d,  $J=8.6$  Hz, 2H, Ar-H), 7.79 (d,  $J=15.4$  Hz, 1H, Olefinic-H), 7.63 (d,  $J=15.6$  Hz, 1H, Olefinic-H), 7.5 (s, 1H, Ar-H), 7.34 (d,  $J=8.6$  Hz, 1H, Ar-H), 7.05 (d,  $J=8.4$  Hz, 2H, Ar-H), 6.99 (d,  $J=8.6$  Hz, 1H, Ar-H), 4.10 - 4.00 (m, 6H, Ar-OCH<sub>2</sub>-), 1.77 - 1.69 (m, 4H, Ar-OCH<sub>2</sub>-CH<sub>2</sub>-), 1.46 - 1.26 (m, 15H, -

$\text{CH}_2$ -), 0.88 (t,  $J=6.8$  Hz, 6H,  $-\text{CH}_3$ ). MS (m/z): 453.3 (M+H)<sup>+</sup>. Anal. Calcd. For.  $\text{C}_{29}\text{H}_{40}\text{O}_4$ : C. 76.95; H. 8.91; Found: C. 76.98; H. 8.85.

*1,3-Bis(4-(octyloxy)phenyl)prop-2-en-1-one (3e)*. Yield 79 %, m.p. 77-78 °C. FTIR ( $\text{cm}^{-1}$ ): 2931, 2851, 1648, 1598, 1577, 1241, 824.  $^1\text{H}$  NMR (400 M Hz, DMSO- $d_6$ )  $\delta$  (ppm) 8.12 (d,  $J=8.8$  Hz, 2H, Ar-H), 7.78 (d,  $J=15.6$  Hz, 1H, Olefinic-H), 7.64 (d,  $J=15.4$  Hz, 1H, Olefinic-H), 7.19 (d,  $J=8.6$  Hz, 2H, Ar-H), 6.96 (d,  $J=8.8$  Hz, 2H, Ar-H), 6.99 (d,  $J=8.4$  Hz, 2H, Ar-H), 4.08-3.98 (m, 4H, Ar-OCH $_2$ -), 1.72- 16.9 (m, 4H, Ar-OCH $_2$ -CH $_2$ -), 1.52-1.29 (m, 20H,  $-\text{CH}_2$ -), 0.89-0.87 (t,  $J=6.8$  Hz, 6H,  $-\text{CH}_3$ ). MS (m/z): 465.3 (M+H)<sup>+</sup>. Anal. Calcd. For.  $\text{C}_{31}\text{H}_{44}\text{O}_3$ : C. 80.13; H. 9.54; Found: C. 80.16; H. 9.52.

*3-(3-Methoxy-4-(octyloxy)phenyl)-1-(4-(octyloxy)phenyl)prop-2-en-1-one (3f)*. Yield 79 %, m.p. 87-88 °C. FTIR ( $\text{cm}^{-1}$ ): 2928, 2852, 1646, 1600, 1579, 822.  $^1\text{H}$  NMR (400 M Hz, DMSO- $d_6$ )  $\delta$  (ppm) 8.12 (d,  $J=8.8$  Hz, 2H, Ar-H), 7.78 (d,  $J=15.2$  Hz, 1H, Olefinic-H), 7.64 (d,  $J=15.2$  Hz, 1H, Olefinic-H), 7.50 (s, 1H, Ar-H), 7.33 (d,  $J=8.8$  Hz, 1H, Ar-H), 7.04 (d,  $J=8.4$  Hz, 2H, Ar-H), 6.99 (d,  $J=8$  Hz, 1H, Ar-H), 4.08- 3.98 (m, 4H, Ar-OCH $_2$ -), 3.85 (s, 3H, Ar-OCH $_3$ ), 1.76-1.63 (m, 4H, Ar-OCH $_2$ -CH $_2$ -), 1.45-1.28 (m, 20H,  $-\text{CH}_2$ -), 0.89-0.83 (t,  $J=6.8$  Hz, 6H,  $-\text{CH}_3$ ). MS (m/z): 495.3 (M+H)<sup>+</sup>. Anal. Calcd. For.  $\text{C}_{32}\text{H}_{46}\text{O}_4$ : C. 77.69; H. 9.37; Found: C. 77.64; H. 9.40.

*3-(3-Ethoxy-4-(octyloxy)phenyl)-1-(4-(octyloxy)phenyl)prop-2-en-1-one (3g)*. Yield 74 %, m.p. 85-86.1 °C. FTIR ( $\text{cm}^{-1}$ ): 2933, 2855, 1644, 1602, 1577, 824.  $^1\text{H}$  NMR (400 M Hz, DMSO- $d_6$ )  $\delta$  (ppm) 8.12 (d,  $J=8.8$  Hz, 2H, Ar-H), 7.77 (d,  $J=15.2$  Hz, 1H, Olefinic-H), 7.63 (d,  $J=15.6$  Hz, 1H, Olefinic-H), 7.50 (s, 1H, Ar-H), 7.33 (d,  $J=8.4$  Hz, 1H, Ar-H), 7.05 (d,  $J=8.2$  Hz, 2H, Ar-H), 6.99 (d,  $J=8$  Hz, 1H, Ar-H), 4.13-3.99 (m, 6H, Ar-OCH $_2$ -), 1.74-1.69 (m, 4H, Ar-OCH $_2$ -CH $_2$ -), 1.41-1.26 (m, 23H,  $-\text{CH}_2$ -), 0.85-0.83 (t,  $J=6.4$  Hz, 6H,  $-\text{CH}_3$ ). MS (m/z): 509.3 (M+H)<sup>+</sup>. Anal. Calcd. For.  $\text{C}_{33}\text{H}_{48}\text{O}_4$ : C. 77.91; H. 9.51; Found: C. 77.95; H. 9.46.

*1,3-Bis(4-(decyloxy)phenyl)prop-2-en-1-one (3h)*. Yield 82 %, m.p. 77-78 °C. FTIR ( $\text{cm}^{-1}$ ): 2931, 2851, 1648, 1598, 1577, 1241, 824.  $^1\text{H}$  NMR (400 M Hz, DMSO- $d_6$ )  $\delta$  (ppm) 8.12 (d,  $J=8.8$  Hz, 2H, Ar-H), 7.78 (d,  $J=15.6$  Hz, 1H, Olefinic-H), 7.64 (d,

$J=15.4$  Hz, 1H, Olefinic-H), 7.19 (d,  $J=8.6$  Hz, 2H, Ar-H), 6.96 (d,  $J=8.8$  Hz, 2H, Ar-H), 6.99 (d,  $J=8.4$  Hz, 2H, Ar-H), 4.08-3.98 (m, 4H, Ar-OCH<sub>2</sub>-), 1.72- 16.9 (m, 4H, Ar-OCH<sub>2</sub>-CH<sub>2</sub>-), 1.52-1.29 (m, 28H, -CH<sub>2</sub>-), 0.89-0.87 (t,  $J=6.8$  Hz, 6H, -CH<sub>3</sub>). MS (m/z): 521.4 (M+H)<sup>+</sup>. Anal. Calcd. For. C<sub>35</sub>H<sub>52</sub>O<sub>3</sub>: C. 80.72; H. 10.06; Found: C. 80.76; H. 10.09.

*3-(4-(Decyloxy)-3-methoxyphenyl)-1-(4-(decyloxy)phenyl)prop-2-en-1-one (3i)*. Yield 74 %, m.p. 86-87 °C. FTIR (cm<sup>-1</sup>): 2928, 2852, 1646, 1600, 1579, 822. <sup>1</sup>H NMR (400 M Hz, DMSO-*d*<sub>6</sub>) δ (ppm) 8.12 (d,  $J=8.8$  Hz, 2H, Ar-H), 7.78 (d,  $J=15.2$  Hz, 1H, Olefinic-H), 7.64 (d,  $J=15.2$  Hz, 1H, Olefinic-H), 7.50 (s, 1H, Ar-H), 7.33 (d,  $J=8.8$  Hz, 1H, Ar-H), 7.04 (d,  $J=8.4$ Hz, 2H, Ar-H), 6.99 (d,  $J=8$  Hz, 1H, Ar-H), 4.08- 3.98 (m, 4H, Ar-OCH<sub>2</sub>-), 3.85 (s, 3H, Ar-OCH<sub>3</sub>), 1.76-1.63 (m, 4H, Ar-OCH<sub>2</sub>-CH<sub>2</sub>-), 1.45-1.28 (m, 28H, -CH<sub>2</sub>-), 0.89-0.83 (t,  $J=6.8$  Hz, 6H, -CH<sub>3</sub>). MS (m/z): 551.4 (M+H)<sup>+</sup>. Anal. Calcd. For. C<sub>36</sub>H<sub>54</sub>O<sub>4</sub>: C. 78.50; H. 9.88; Found: C. 78.55; H. 9.92.

*3-(4-(Decyloxy)-3-ethoxyphenyl)-1-(4-(decyloxy)phenyl)prop-2-en-1-one (3j)*. Yield 77 %, m.p. 85-86.1 °C. FTIR (cm<sup>-1</sup>): 2933, 2855, 1644, 1602, 1577, 824. <sup>1</sup>H NMR (400 M Hz, DMSO-*d*<sub>6</sub>) δ (ppm) 8.13 (d,  $J=8.8$  Hz, 2H, Ar-H), 7.78 (d,  $J=15.2$  Hz, 1H, Olefinic-H), 7.62 (d,  $J=15.2$  Hz, 1H, Olefinic-H), 7.50 (s, 1H, Ar-H), 7.33 (d,  $J=8.4$  Hz, 1H, Ar-H), 7.05 (d,  $J=8.2$  Hz, 2H, Ar-H), 6.99 (d,  $J=8$  Hz, 1H, Ar-H), 4.13-3.99 (m, 6H, Ar-OCH<sub>2</sub>-), 1.74-1.69 (m, 4H, Ar-OCH<sub>2</sub>-CH<sub>2</sub>-), 1.41-1.26 (m, 31H, -CH<sub>2</sub>-), 0.85-0.83 (t,  $J=6.4$  Hz, 6H, -CH<sub>3</sub>). MS (m/z): 565.4 (M+H)<sup>+</sup>. Anal. Calcd. For. C<sub>37</sub>H<sub>56</sub>O<sub>4</sub>: C. 78.68; H. 9.99; Found: C. 78.74; H. 10.06.

*1,3-Bis(4-(dodecyloxy)phenyl)prop-2-en-1-one (3k)*. Yield 76 %, m.p. 84-85 °C. FTIR (cm<sup>-1</sup>): 2931, 2851, 1648, 1598, 1577, 1241, 824. <sup>1</sup>H NMR (400 M Hz, DMSO-*d*<sub>6</sub>) δ (ppm) 8.12 (d,  $J=8.8$  Hz, 2H, Ar-H), 7.78 (d,  $J=15.4$  Hz, 1H, Olefinic-H), 7.64 (d,  $J=15.4$  Hz, 1H, Olefinic-H), 7.19 (d,  $J=8.6$  Hz, 2H, Ar-H), 6.96 (d,  $J=8.8$  Hz, 2H, Ar-H), 7.00- 6.98 (d,  $J=8.4$  Hz, 2H, Ar-H), 4.08-3.98 (m, 4H, Ar-OCH<sub>2</sub>-), 1.72- 16.9 (m, 4H, Ar-OCH<sub>2</sub>-CH<sub>2</sub>-), 1.52-1.29 (m, 36H, -CH<sub>2</sub>-), 0.89-0.87 (t,  $J=6.8$  Hz, 6H, -CH<sub>3</sub>). MS (m/z): 577.4 (M+H)<sup>+</sup>. Anal. Calcd. For. C<sub>39</sub>H<sub>60</sub>O<sub>3</sub>: C. 81.20; H. 10.48; Found: C. 81.26; H. 10.52.

*3-(4-(Dodecyloxy)-3-methoxyphenyl)-1-(4-(dodecyloxy)phenyl)prop-2-en-1-one (3l)*. Yield 83 %, m.p. 81-82 °C. FTIR (cm<sup>-1</sup>): 2928, 2852, 1646, 1600, 1579, 822. <sup>1</sup>H NMR (400 M Hz, DMSO-*d*<sub>6</sub>) δ (ppm) 8.12 (d, *J*=8.8 Hz, 2H, Ar-H), 7.78 (d, *J*=15.2 Hz, 1H, Olefinic-H), 7.64 (d, *J*=15.2 Hz, 1H, Olefinic-H), 7.50 (s, 1H, Ar-H), 7.33 (d, *J*=8.8 Hz, 1H, Ar-H), 7.04 (d, *J*=8.4 Hz, 2H, Ar-H), 6.99 (d, *J*=8 Hz, 1H, Ar-H), 4.08-3.98 (m, 4H, Ar-OCH<sub>2</sub>-), 3.85 (s, 3H, Ar-OCH<sub>3</sub>), 1.76-1.63 (m, 4H, Ar-OCH<sub>2</sub>-CH<sub>2</sub>-), 1.45-1.28 (m, 36H, -CH<sub>2</sub>-), 0.89-0.83 (t, *J*=6.8 Hz, 6H, -CH<sub>3</sub>). MS (m/z): 607.5 (M+H)<sup>+</sup>. Anal. Calcd. For. C<sub>40</sub>H<sub>62</sub>O<sub>4</sub>: C. 79.16; H. 10.30; Found: C. 79.21; H. 10.35.

*3-(4-(Dodecyloxy)-3-ethoxyphenyl)-1-(4-(dodecyloxy)phenyl)prop-2-en-1-one (3m)*. Yield 74 %, m.p. 78-79 °C. FTIR (cm<sup>-1</sup>): 2933, 2855, 1644, 1602, 1577, 824. <sup>1</sup>H NMR (400 M Hz, DMSO-*d*<sub>6</sub>) δ (ppm) 8.12 (d, *J*=8.8 Hz, 2H, Ar-H), 7.78 (d, *J*=15.2 Hz, 1H, Olefinic-H), 7.62 (d, *J*=15.6 Hz, 1H, Olefinic-H), 7.50 (s, 1H, Ar-H), 7.33 (d, *J*=8.4 Hz, 1H, Ar-H), 7.05 (d, *J*= 8.2 Hz, 2H, Ar-H), 6.99 (d, *J*=8 Hz, 1H, Ar-H), 4.13-3.99 (m, 6H, Ar-OCH<sub>2</sub>-), 1.74-1.69 (m, 4H, Ar-OCH<sub>2</sub>-CH<sub>2</sub>-), 1.41-1.26 (m, 39H, -CH<sub>2</sub>-), 0.85-0.83 (t, *J*=6.4 Hz, 6H, -CH<sub>3</sub>). MS (m/z): 621.5 (M+H)<sup>+</sup>. Anal. Calcd. For. C<sub>41</sub>H<sub>64</sub>O<sub>4</sub>: C. 79.30; H. 10.39; Found: C. 79.35; H. 10.43.

*General procedure for the synthesis of 4,6-dialkoxyaryl-2-methoxy nicotinonitriles (LC<sub>1-13</sub>)*.

1,3-Bis(4-butoxyphenyl)prop-2-en-1-one (**3a**) (1 g, 1.9 mmol) was added slowly to a freshly prepared solution of sodium methoxide (20 mmol of sodium in 10 ml of methanol) while stirring. Malononitrile (0.12 g, 1.9 mmol) was then added with continuous stirring at room temperature until the precipitate separates out. The solid separated was collected by filtration, washed with methanol and finally recrystallized from chloroform and methanol mixture. Similarly remaining compounds were synthesized and their characterization data are as follows.

*4,6-Bis(4-butoxyphenyl)-2-methoxynicotinonitrile (LC<sub>1</sub>)*. Yield 65 %. FTIR (cm<sup>-1</sup>): 2937, 2857, 2213, 1578, 1544, 1453, 1235, 1171, 1017, 828. <sup>1</sup>H NMR (400 MHz, CDCl<sub>3</sub>) δ (ppm) 8.04 (d, *J*=8.8 Hz, 2H, Ar-H), 7.60 (d, *J*=8.8 Hz, 2H, Ar-H), 7.36 (s, 1H, Ar-H (pyridine)), 7.02-6.97 (m, 4H, Ar-H), 4.16 (s, 3H, -OMe of pyridine), 4.03-4.00 (m, 4H, -OCH<sub>2</sub>-), 1.84-1.79 (m, 4H, -OCH<sub>2</sub>CH<sub>2</sub>-), 1.51-1.35 (m, 4H, -CH<sub>2</sub>-),

0.93-0.90 (t,  $J=7$  Hz, 6H,  $-\underline{\text{CH}}_3$ ).  $^{13}\text{C}$  NMR (100MHz,  $\text{CDCl}_3$ )  $\delta$  (ppm); 165.12, 161.20, 160.64, 157.49, 156.04, 129.77, 129.52, 128.76, 128.48, 116.19, 114.86, 114.72, 112.23, 91.53, 77.00, 68.19, 54.37, 31.55, 22.58, 14.00. MS (m/z): 431.2 (M+H)<sup>+</sup>. Anal. Calcd. For  $\text{C}_{27}\text{H}_{30}\text{N}_2\text{O}_3$ : C.75.32; H.7.02; N.6.51; O.11.15; Found: C.75.41; H.7.05; N.6.43; O.11.11.

*4,6-Bis(4-(hexyloxy)phenyl)-2-methoxynicotinonitrile (LC<sub>2</sub>)*. Yield 72 %. FTIR ( $\text{cm}^{-1}$ ): 2921, 2860, 2215, 1579, 1454, 1251, 1032, 811.  $^1\text{H}$  NMR (400 MHz,  $\text{CDCl}_3$ )  $\delta$  (ppm) 8.04 (d,  $J=8.8$  Hz, 2H, Ar-H), 7.60 (d,  $J=8.8$  Hz, 2H, Ar-H), 7.36 (s, 1H, Ar-H(pyridine)), 7.02-6.97 (m, 4H, Ar-H), 4.16 (s, 3H, -OMe of pyridine), 4.03-4.00 (m, 4H,  $-\text{OCH}_2-$ ), 1.84-1.79 (m, 4H,  $-\text{OCH}_2\text{CH}_2-$ ), 1.51-1.35 (m, 12H,  $-\text{CH}_2-$ ), 0.93-0.90 (t,  $J=7$  Hz, 6H,  $-\underline{\text{CH}}_3$ ).  $^{13}\text{C}$  NMR (100MHz,  $\text{CDCl}_3$ )  $\delta$  (ppm); 165.12, 161.20, 160.64, 157.49, 156.04, 129.77, 129.52, 128.76, 128.48, 116.19, 114.86, 114.72, 112.23, 91.53, 68.19, 54.37, 31.55, 29.14, 25.68, 22.58, 14.00. MS (m/z): 487.3 (M+H)<sup>+</sup>. Anal. Calcd. For  $\text{C}_{31}\text{H}_{38}\text{N}_2\text{O}_3$ : C. 76. 51; H. 7.87; N. 5.76; Found: C. 76.58; H. 7.89; N. 5.69.

*4-(4-(Hexyloxy)-3-methoxyphenyl)-6-(4-(hexyloxy)phenyl)-2-methoxynicotinonitrile (LC<sub>3</sub>)*. Yield 68 %. FTIR ( $\text{cm}^{-1}$ ): 2929, 2859, 2206, 1579, 1251, 1014, 830.  $^1\text{H}$  NMR (400 MHz,  $\text{CDCl}_3$ )  $\delta$  (ppm) 8.05 (d,  $J=8.8$  Hz, 2H, Ar-H), 7.39 (s, 1H, Ar-H (pyridine)), 7.21 (d,  $J=10.2$  Hz, 2H, Ar-H), 6.99 (d,  $J=8.8$  Hz, 3H, Ar-H), 4.17 (s, 3H, -OMe of pyridine), 4.08- 4.01 (m, 4H,  $-\text{OCH}_2-$ ), 3.94 (s, 3H, -OMe of Aromatic), 1.89-1.79 (m, 4H,  $-\text{OCH}_2\text{CH}_2-$ ), 1.54-1.36 (m, 12H,  $-\text{CH}_2-$ ), 0.93-0.89(t,  $J=7.2$  Hz, 6H,  $-\underline{\text{CH}}_3$ ).  $^{13}\text{C}$  NMR (100MHz,  $\text{CDCl}_3$ )  $\delta$  (ppm); 165.15, 161.24, 157.54, 156.15, 150.24, 149.47, 129.73, 121.33, 116.20, 114.75, 112.73, 112.25, 112.03, 91.60, 69.13, 68.22, 56.28, 54.41, 31.56, 29.15, 29.05, 25.69, 25.63, 22.58, 14.01. MS (m/z): 517.3 (M+H)<sup>+</sup>. Anal. Calcd. For  $\text{C}_{32}\text{H}_{40}\text{N}_2\text{O}_4$ : C. 74.39; H. 7.80; N. 5.42; Found: C. 74.42; H. 7.83; N. 5.34.

*4-(3-Ethoxy-4-(hexyloxy)phenyl)-6-(4-(hexyloxy)phenyl)-2-methoxynicotinonitrile (LC<sub>4</sub>)*. Yield 75 %. FTIR ( $\text{cm}^{-1}$ ): 2921, 2860, 2215, 1579, 1251, 1032, 840.  $^1\text{H}$  NMR (400 MHz,  $\text{CDCl}_3$ )  $\delta$  (ppm) 8.05 (d,  $J=8.8$  Hz, 2H, Ar-H), 7.38 (s, 1H, Ar-H(pyridine)), 7.21 (d,  $J=10.2$  Hz, 2H, Ar-H), 7.00 (d,  $J=8.8$  Hz, 3H, Ar-H), 4.19 (m, 5H, -OMe of pyridine,  $-\text{OCH}_2-\text{CH}_3$ ), 4.09-4.01 (m, 4H,  $-\text{OCH}_2-$ ), 1.89-1.79 (m, 4H,-

OCH<sub>2</sub>CH<sub>2</sub>-), 1.54- 1.33 (m, 15H, -CH<sub>2</sub>-), 0.93-0.90 (t, *J*=6.8 Hz, 6H, -CH<sub>3</sub>). <sup>13</sup>C NMR (100MHz, CDCl<sub>3</sub>) δ (ppm); 165.15, 161.23, 157.50, 156.18, 150.74, 148.89, 129.76, 128.88, 128.78, 121.46, 116.21, 114.75, 114.01, 113.37, 112.29, 91.59, 69.26, 68.22, 65.05, 54.40, 31.56, 29.16, 29.08, 25.69, 25.65, 22.59, 14.86, 14.00. MS (m/z): 531.3 (M+H)<sup>+</sup>. Anal. Calcd. For. C<sub>33</sub>H<sub>42</sub>N<sub>2</sub>O<sub>4</sub>: C. 74.69; H. 7.98; N. 5.28; Found; C. 74.76; H. 7.93; N. 5.32.

*2-Methoxy-4,6-bis(4-(octyloxy)phenyl)nicotinonitrile (LC<sub>5</sub>)*. Yield 65 %. FTIR (cm<sup>-1</sup>): 2916, 2848, 2207, 1590, 1243, 1034, 836. <sup>1</sup>H NMR (400 MHz, CDCl<sub>3</sub>) δ (ppm) 8.04 (d, *J*=8.8 Hz, 2H, Ar-H), 7.60 (d, *J*=8.8 Hz, 2H, Ar-H), 7.36 (s, 1H, Ar-H(pyridine)), 7.02-6.97 (m, 4H, Ar-H), 4.16 (s, 3H, -OMe of pyridine), 4.03-4.00 (m, 4H, -OCH<sub>2</sub>-), 1.84-1.79 (m, 4H, -OCH<sub>2</sub>CH<sub>2</sub>-), 1.51-1.35 (m, 20 H, -CH<sub>2</sub>-), 0.93-0.90 (t, *J*=7 Hz, 6H, -CH<sub>3</sub>). <sup>13</sup>C NMR (100MHz, CDCl<sub>3</sub>) δ (ppm); 164.92, 157.15, 156.37, 156.14, 129.68, 128.03, 117.05, 114.96, 108.69, 93.32, 55.45, 31.96, 29.72, 26.01, 22.83, 14.17. MS (m/z): 543.3 (M+H)<sup>+</sup>. Anal. Calcd. For. C<sub>35</sub>H<sub>46</sub>N<sub>2</sub>O<sub>3</sub>: C. 77.45; H. 8.54; N. 5.16; Found: C. 77.53; H. 8.49; N. 5.19.

*2-Methoxy-4-(3-methoxy-4-(octyloxy)phenyl)-6-(4-(octyloxy)phenyl)nicotinonitrile (LC<sub>6</sub>)*. Yield 62 %. FTIR (cm<sup>-1</sup>): 2923, 2855, 2212, 1580, 1252, 1022, 826. <sup>1</sup>H NMR (400 MHz, CDCl<sub>3</sub>) δ (ppm) 8.06 (d, *J*=8.8 Hz, 2H, Ar-H), 7.39 (s, 1H, Ar-H(pyridine)), 7.21 (d, *J*=10.2 Hz, 2H, Ar-H), 7.00 (d, *J*=8.8 Hz, 3H, Ar-H), 4.17 (s, 3H, -OMe of pyridine), 4.09-4.01 (m, 4H, -OCH<sub>2</sub>-), 3.94 (s, 3H, -OMe of Aromatic), 1.89-1.79 (m, 4H, -OCH<sub>2</sub>CH<sub>2</sub>-), 1.54-1.35 (m, 20 H, -CH<sub>2</sub>-), 0.89 (t, *J*=6.8 Hz, 6H, -CH<sub>3</sub>). <sup>13</sup>C NMR (100MHz, CDCl<sub>3</sub>) δ (ppm); 165.15, 161.24, 157.54, 156.15, 150.24, 149.46, 129.73, 128.79, 121.33, 116.20, 114.75, 112.72, 112.25, 112.01, 91.60, 69.13, 68.22, 56.28, 54.41, 31.80, 29.33, 29.21, 29.08, 26.02, 25.95, 22.64, 14.07. MS (m/z): 573.3 (M+H)<sup>+</sup>. Anal. Calcd. For. C<sub>36</sub>H<sub>48</sub>N<sub>2</sub>O<sub>4</sub>: C.75.49; H.8.45; N. 4.89; Found: C. 75.51; H. 8.48; N. 4.85.

*4-(3-Ethoxy-4-(octyloxy)phenyl)-2-methoxy-6-(4-(octyloxy)phenyl)nicotinonitrile (LC<sub>7</sub>)*. Yield 69 %. FTIR (cm<sup>-1</sup>): 2918, 2854, 2218, 1579, 1248, 1031,824. <sup>1</sup>H NMR (400 MHz, CDCl<sub>3</sub>) δ (ppm) 8.05 (d, *J*=8.8 Hz, 2H, Ar-H), 7.38 (s, 1H, Ar-H(pyridine)), 7.21 (d, *J*=10.2 Hz, 2H, Ar-H), 6.98 (d, *J*=8.8 Hz, 3H, Ar-H), 4.19 (m,

5H, -OMe of pyridine, -OCH<sub>2</sub>-CH<sub>3</sub>), 4.09-4.01 (m, 4H, -OCH<sub>2</sub>-), 1.89-1.79 (m, 4H, -OCH<sub>2</sub>CH<sub>2</sub>-), 1.54- 1.33 (m, 23 H, -CH<sub>2</sub>-, -OCH<sub>2</sub>-CH<sub>3</sub>), 0.92(t, *J*=6.8 Hz, 6H, -CH<sub>3</sub>). <sup>13</sup>C NMR (100MHz, CDCl<sub>3</sub>) δ (ppm); 165.15, 161.22, 157.50, 156.17, 150.73, 148.88, 129.75, 128.87, 128.78, 121.45, 116.21, 114.75, 114.00, 113.37, 112.28, 91.58, 69.26, 68.22, 65.05, 54.40, 31.80, 29.33, 29.22, 29.12, 26.02, 25.97, 22.65, 14.86, 14.08. MS (m/z): 587.4 (M+H)<sup>+</sup>. Anal. Calcd. For. C<sub>37</sub>H<sub>50</sub>N<sub>2</sub>O<sub>4</sub>: C. 75.73; H. 8.59; N. 4.77; Found: C. 75.79; H. 8.56; N.4.73.

*4,6-Bis(4-(decyloxy)phenyl)-2-methoxynicotinonitrile (LC<sub>8</sub>)*. Yield 74 %. FTIR (cm<sup>-1</sup>): 2915, 2209, 1587, 1240, 1028, 831. <sup>1</sup>H NMR (400 MHz, CDCl<sub>3</sub>) δ (ppm) 8.00 (d, *J*=8.8 Hz, 2H, Ar-H), 7.60 (d, *J*=8.8 Hz, 2H, Ar-H), 7.40 (s, 1H, Ar-H(pyridine)), 7.00-6.95 (m, 4H, Ar-H), 4.17 (s, 3H, -OMe of pyridine), 4.04-4.00 (m, 4H, -OCH<sub>2</sub>-), 1.83-1.77 (m, 4H, -OCH<sub>2</sub>CH<sub>2</sub>-), 1.47-1.28 (m, 28H, -CH<sub>2</sub>-), 0.88 (t, *J*=6.8 Hz, 6H, -CH<sub>3</sub>). <sup>13</sup>C NMR (100MHz, CDCl<sub>3</sub>) δ (ppm); 164.84, 157.10, 156.38, 156.11, 129.65, 128.22, 128.05, 117.08, 114.93, 108.61, 93.33, 68.95, 55.40, 31.92, 29.71, 29.47, 26.06, 22.81, 14.18. MS (m/z): 599.4 (M+H)<sup>+</sup>. Anal. Calcd. For. C<sub>39</sub>H<sub>54</sub>N<sub>2</sub>O<sub>3</sub>: C.78.22; H.9.09; N.4.68; O.8.01; Found: C.78.21; H.9.11; N.4.71; O.8.05.

*4-(4-(Decyloxy)-3-methoxyphenyl)-6-(4-(decyloxy)phenyl)-2-methoxynicotinonitrile (LC<sub>9</sub>)*. Yield 82 %. FTIR (cm<sup>-1</sup>): 2920, 2851, 2212, 1586, 1258, 1020, 836. <sup>1</sup>H NMR (400 MHz, CDCl<sub>3</sub>) δ(ppm) 8.05 (d, *J*=8.8 Hz, 2H, Ar-H), 7.4 (s, 1H, Ar-H(pyridine)), 7.21(d, *J*=8.8 Hz, 2H, Ar-H), 7.00 (d, *J*=9.2 Hz, 3H, Ar-H), 4.18 (s, 3H, -OMe of pyridine), 4.09-4.01 (m, 4H, -OCH<sub>2</sub>-), 3.94 (s, 3H, -OMe of Aromatic), 1.89-1.78 (m, 4H, -OCH<sub>2</sub>CH<sub>2</sub>-), 1.32-1.21 (b, 28H, -CH<sub>2</sub>-), 0.88 (t, *J*=6.8 Hz, 6H, -CH<sub>3</sub>). <sup>13</sup>C NMR (100MHz, CDCl<sub>3</sub>) δ (ppm); 165.10, 157.50, 156.14, 156.10, 150.40, 148.88, 130.60, 128.87, 127.78, 120.45, 117.07, 116.21, 114.75, 112.28, 108.62, 91.58, 68.22, 56.25, 54.40, 31.90, 29.33, 29.22, 29.12, 26.02, 22.65, 14.86. MS (m/z): 629.4 (M+H)<sup>+</sup>. Anal. Calcd. For. C<sub>40</sub>H<sub>56</sub>N<sub>2</sub>O<sub>4</sub>: C.76.39; H.8.98; N.4.45; O.10.18; Found: C.76.42; H.8.95; N.4.49; O.10.21.

*4-(4-(Decyloxy)-3-ethoxyphenyl)-6-(4-(decyloxy)phenyl)-2-methoxynicotinonitrile (LC<sub>10</sub>)*. Yield 69 %. FTIR (cm<sup>-1</sup>): 2915, 2849, 2220, 1576, 1250, 1028, 828. <sup>1</sup>H NMR (400MHz, CDCl<sub>3</sub>) δ (ppm) 8.05 (d, *J*=9.2Hz, 2H, Ar-H), 7.4 (s, 1H, Ar-H(pyridine)),

7.20 (m, 2H, Ar-H), 6.99 (d,  $J=9.2$  Hz, 3H, Ar-H), 4.18 (s, 3H, -OMe of pyridine), 4.09-4.01 (m, 4H, -OCH<sub>2</sub>-), 1.88-1.78 (m, 4H, -OCH<sub>2</sub>CH<sub>2</sub>-), 1.47 (t, 8H, -CH<sub>2</sub>-), 1.28 (s, 26H, -CH<sub>2</sub>-), 0.88 (t,  $J=6.8$  Hz, 6H, -CH<sub>3</sub>). <sup>13</sup>C NMR (100MHz, CDCl<sub>3</sub>)  $\delta$  (ppm); 164.90, 157.30, 156.34, 156.10, 147.11, 130.60, 128.20, 127.78, 120.45, 117.09, 116.21, 114.75, 112.80, 108.62, 93.33, 68.92, 65.02, 55.40, 31.90, 29.89, 29.42, 29.12, 26.02, 22.65, 14.86. MS (m/z): 643.4 (M+H)<sup>+</sup>. Anal. Calcd. For. C<sub>41</sub>H<sub>58</sub>N<sub>2</sub>O<sub>4</sub>: C.76.60; H.9.09; N.4.36; O.9.95; Found: C.76.65; H.9.13; N.4.32; O.9.98.

*4,6-Bis(4-(dodecyloxy)phenyl)-2-methoxynicotinonitrile (LC<sub>11</sub>)*. Yield 76 %. FTIR (cm<sup>-1</sup>): 2913, 2848, 2209, 1602, 1241, 1032, 830. <sup>1</sup>H NMR (400 MHz, CDCl<sub>3</sub>)  $\delta$  (ppm) 7.88 (m, 2H, Ar-H), 7.62-7.57 (m, 2H, Ar-H), 7.37 (s, 1H, Ar-H(pyridine)), 7.00-6.92 (m, 4H, Ar-H), 4.20 (s, 3H, -OMe of pyridine), 4.04-3.90 (m, 4H, -OCH<sub>2</sub>-), 1.83-1.1.77 (m, 4H, -OCH<sub>2</sub>CH<sub>2</sub>-), 1.49-1.26 (m, 36H, -CH<sub>2</sub>-), 0.88 (t,  $J=6.8$  Hz, 6H, -CH<sub>3</sub>). <sup>13</sup>C NMR (100MHz, CDCl<sub>3</sub>)  $\delta$  (ppm); 165.12, 157.14, 156.38, 156.11, 129.68, 128.32, 128.05, 117.08, 114.93, 108.64, 93.35, 68.92, 55.40, 31.95, 29.76, 29.49, 26.16, 22.79, 14.21. MS (m/z): 655.5 (M+H)<sup>+</sup>. Anal. Calcd. For. C<sub>43</sub>H<sub>62</sub>N<sub>2</sub>O<sub>3</sub>: C.78.85; H.9.54; N.4.28; O.7.33; Found: C.78.87; H.9.58; N.4.25; O.7.36.

*4-(4-(Dodecyloxy)-3-methoxyphenyl)-6-(4-(dodecyloxy)phenyl)-2-methoxynicotinonitrile (LC<sub>12</sub>)*. Yield 71 %. FTIR (cm<sup>-1</sup>): 2919, 2852, 2212, 1584, 1251, 1021, 827. <sup>1</sup>H NMR (400 MHz, CDCl<sub>3</sub>)  $\delta$  (ppm) 8.05 (d,  $J=8.8$  Hz, 2H, Ar-H), 7.40 (s, 1H, Ar-H(pyridine)), 7.20-7.11 (m, 2H, Ar-H), 7.00 (d,  $J=9.2$  Hz, 3H, Ar-H), 4.18 (s, 3H, -OMe of Pyridine), 4.09-4.01 (m, 4H, -OCH<sub>2</sub>-), 3.94 (s, 3H, -OMe of Ar-H), 1.89-1.78 (m, 4H, -OCH<sub>2</sub>CH<sub>2</sub>-), 1.51-1.26 (m, 36H, -CH<sub>2</sub>-), 0.88 (t,  $J=6.8$  Hz, 6H, -CH<sub>3</sub>). <sup>13</sup>C NMR (100MHz, CDCl<sub>3</sub>)  $\delta$  (ppm); 165.10, 157.28, 156.12, 156.10, 150.40, 147.88, 130.20, 128.87, 127.90, 120.45, 117.07, 115.91, 114.94, 112.28, 108.62, 91.58, 68.22, 56.28, 54.45, 31.90, 29.37, 29.22, 29.12, 26.07, 22.65, 14.86. MS (m/z): 685.5 (M+H)<sup>+</sup>. Anal. Calcd. For. C<sub>44</sub>H<sub>64</sub>N<sub>2</sub>O<sub>4</sub>: C.77.15; H.9.42; N.4.09; O.9.34; Found: C.77.20; H.9.37; N.4.13; O.9.38.

*4-(4-(Dodecyloxy)-3-ethoxyphenyl)-6-(4-(dodecyloxy)phenyl)-2-methoxynicotinonitrile (LC<sub>13</sub>)*. Yield 78 %. FTIR (cm<sup>-1</sup>): 2953, 2849, 2220, 1583, 1243, 1034, 828. <sup>1</sup>H NMR(400 MHz, CDCl<sub>3</sub>)  $\delta$  (ppm) 8.04 (d,  $J=14.4$  Hz, 2H, Ar-H), 7.4 (s, 1H,



Ar-H (pyridine)), 7.20-7.09 (m, 2H, Ar-H), 6.95 (d,  $J=14.4$  Hz, 3H, Ar-H), 4.18 (s, 3H, -OMe of pyridine), 4.09-4.01 (m, 4H, -OCH<sub>2</sub>-), 1.88-1.78 (m, 4H, -OCH<sub>2</sub>CH<sub>2</sub>-), 1.47 (t, 8H, -CH<sub>2</sub>-) 1.28 (s, 39H, -CH<sub>2</sub>-), 0.88 (t,  $J=6.8$  Hz, 6H, -CH<sub>3</sub>). <sup>13</sup>C NMR (100MHz, CDCl<sub>3</sub>)  $\delta$  (ppm); 164.90, 157.26, 156.33, 156.10, 147.11, 130.20, 128.20, 127.80, 120.35, 117.09, 116.21, 114.75, 111.80, 108.62, 93.33, 68.92, 65.08, 55.43, 31.90, 29.49, 29.42, 29.12, 26.02, 22.65, 14.86. MS (m/z): 699.5 (M+H)<sup>+</sup>. Anal. Calcd. For. C<sub>45</sub>H<sub>66</sub>N<sub>2</sub>O<sub>4</sub>: C.77.32; H.9.52; N.4.01; O.9.16; Found: C.77.38; H.9.56; N.4.07; O.9.14.

### 3.3.2 Synthesis of 6-alkoxyaryl/thiophenyl-4-substituted aryl-2-methoxy pyridines (Series-II; LC<sub>14-33</sub>)

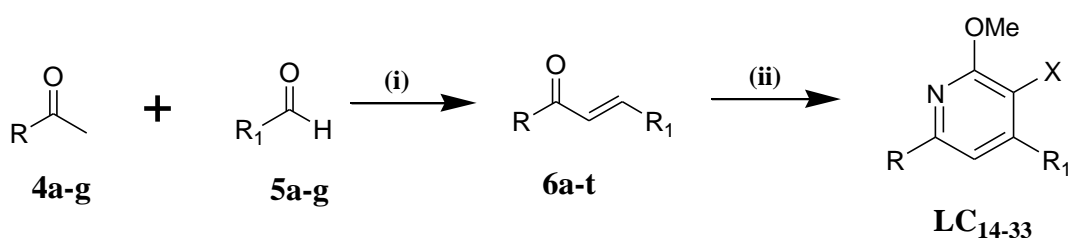
Twenty new 6-alkoxyaryl/thiophenyl-4-substituted aryl-2-methoxy pyridine derivatives (LC<sub>14-33</sub>) have been synthesized as per **Scheme 3.2**. In the following section, synthetic protocols for the preparation of new 2-methoxypyridine derivatives (LC<sub>14-33</sub>) carrying different electron withdrawing substituents, *viz.* -CN, -F, -Cl, -Br, -NO<sub>2</sub> and electron deficient pyridyl moiety as one of the terminal substituents and variable alkoxy chains as another terminal substituents, have been given.

#### 3.3.2.1 Results and discussion

##### *Synthesis:*

The synthetic route for the preparation of the target compounds is shown in **Scheme 3.2** and details of their derivatives are given in **Tables 3.8-3.10**. The starting materials (**4a-g**) were prepared in good yield by reacting various alkyl bromides [m=4-14 (only even)] with 4-hydroxyacetophenone according to the reported procedure (Tantrawong et al. 1993). The required prop-2-en-1-one (**6a-t**) was prepared from aryl or heteroaryl ketones (**4a-g**) and aryl or heteroaryl aldehydes (**5a-g**) using Claisen-Schmidt reaction. Further, it was cyclized to obtain 6-alkoxyaryl/thiophenyl-4-substituted aryl-2-methoxy pyridines derivatives (LC<sub>14-33</sub>) by reacting it with malononitrile in presence of sodium methoxide at room temperature. It has been well-established that the prop-2-en-1-one upon reacting with malononitrile in basic medium (*i.e.* sodium methoxide) cyclizes to 2-methoxy-3-cyanopyridine via dehydrogenation (Goda et al. 2004; Al-Arab 1989).

But, it is interesting to note that, prop-2-en-1-ones (**6a-f, m-s**), upon reacting with malononitrile in basic medium readily cyclizes to methoxypyridine (**LC<sub>14-19, 26-32</sub>**) via dehydrocyanation, but not to expected 2-methoxy-3-cyanopyridine via dehydrogenation. This unique observation is mainly due to presence of strong electron withdrawing substituents like 4-cyanophenyl, 4-nitrophenyl, 4-bromophenyl, 4-pyridinyl units attached to prop-2-en-1-one at position-3, which favors dehydrocyanation in alcoholic basic medium. This proposed hypothesis is well supported by the crystal structure analysis of **LC<sub>14</sub>**, **LC<sub>16</sub>** and **LC<sub>32</sub>**.



**Scheme 3.2** Synthesis of new 6-alkoxyaryl/thiophenyl-4-substituted aryl-2-methoxy pyridines. Reagents and conditions: (i) KOH / EtOH, rt; (ii) Malononitrile, NaOMe, MeOH, rt

**Table 3.8** Derivatives of **4a-g**

<b>4a-g</b>	<b>4a</b>	<b>4b</b>	<b>4c</b>	<b>4d</b>	<b>4e</b>	<b>4f</b>	<b>4g</b>
<i>m</i>	4	6	8	10	12	14	---
<b>R</b>							

**Table 3.9** Derivatives of **5a-g**

<b>5a-g</b>	<b>5a</b>	<b>5b</b>	<b>5c</b>	<b>5d</b>	<b>5e</b>	<b>5f</b>	<b>5g</b>
<b>R<sub>1</sub></b>							
<i>m</i>	---	---	---	---	---	---	10

**Table 3.10** Derivatives of **LC<sub>14-33</sub>** and intermediates **6a-t**

<b>6a-t</b>	<b>LC<sub>14-33</sub></b>	<i>m</i>	<b>X</b>	<b>R</b>	<b>R<sub>1</sub></b>
<b>6a</b>	<b>LC<sub>14</sub></b>	4	-H		
<b>6b</b>	<b>LC<sub>15</sub></b>	6			
<b>6c</b>	<b>LC<sub>16</sub></b>	8			

<b>6d</b>	<b>LC<sub>17</sub></b>	10			
<b>6e</b>	<b>LC<sub>18</sub></b>	12			
<b>6f</b>	<b>LC<sub>19</sub></b>	14			
<b>6g</b>	<b>LC<sub>20</sub></b>	10	-CN		
<b>6h</b>	<b>LC<sub>21</sub></b>	12			
<b>6i</b>	<b>LC<sub>22</sub></b>	14			
<b>6j</b>	<b>LC<sub>23</sub></b>	10	-CN		
<b>6k</b>	<b>LC<sub>24</sub></b>	12			
<b>6l</b>	<b>LC<sub>25</sub></b>	14			
<b>6m</b>	<b>LC<sub>26</sub></b>	10	-H		
<b>6n</b>	<b>LC<sub>27</sub></b>	12			
<b>6o</b>	<b>LC<sub>28</sub></b>	14			
<b>6p</b>	<b>LC<sub>29</sub></b>	10	-H		
<b>6q</b>	<b>LC<sub>30</sub></b>	12			
<b>6r</b>	<b>LC<sub>31</sub></b>	14			
<b>6s</b>	<b>LC<sub>32</sub></b>	14	-H		
<b>6t</b>	<b>LC<sub>33</sub></b>	10	-CN		

Structures of newly synthesized compounds were confirmed by  $^1\text{H}$  NMR,  $^{13}\text{C}$  NMR, Mass and FTIR spectroscopy. Further, their analytical purity was checked by elemental analysis. The compound **LC<sub>14</sub>**, in its FTIR spectrum showed two strong absorption bands at 2944 and 2859  $\text{cm}^{-1}$  that correspond to asymmetric and symmetrical C-H stretching vibrations of methylene. Further, the appearance of strong band at 2219  $\text{cm}^{-1}$  indicated the presence of cyano group in its molecular structure. Also, appearance of one more strong peak at 1577  $\text{cm}^{-1}$  that accounts for C=N stretching vibrations, confirmed the effective formation of central methoxypyridine via cyclization reaction. Further, its  $^1\text{H}$  NMR spectrum showed sharp peaks at  $\delta$  8.05, 7.84, 7.77 and 7.01 ppm accounting for the protons of aromatic moieties. Also, appearance of two singlets at  $\delta$  7.46 and 6.82 ppm for the presence of single protons at positions-3 and -5 of pyridine ring confirmed its structure. In addition, three protons of methoxy substituent at position-6 of pyridine ring resonated at  $\delta$  4.22 ppm as singlet, which further confirmed the construction of central pyridine ring. Furthermore, the appearance of primary and secondary proton signals in the range of  $\delta$  1.86-1.00 ppm in its  $^1\text{H}$  NMR spectrum confirmed the presence of terminal butoxy

chain in **LC**<sub>14</sub>. In its <sup>13</sup>C NMR spectrum, twelve distinct signals were observed at downfield due to one pyridine ring and two aromatic ring carbon atoms. The carbon carrying methoxy group and cyano group, and carbon of cyano group attached to aromatic resonate at  $\delta$  164.47, 115.19 and 112.05 ppm, respectively. This observation has confirmed the effective formation of methoxypyridine ring. The two kinds of quaternary carbon atom of pyridine ring resonate at  $\delta$  155.57 and 149.90 ppm, while two kinds of tertiary carbon atom resonate at  $\delta$  110.57 and 106.31 ppm. The quaternary carbon atoms connected to oxygen resonate in the region of  $\delta$  164.47-160.31 ppm. The primary and secondary carbon peaks of aliphatic chains appeared in the region of  $\delta$  68.25-14.08 ppm. Finally, its mass spectrum showed the  $[M+H]^+$  peak at 359.1, which matches with the calculated molecular weight for the formula of C<sub>23</sub>H<sub>23</sub>N<sub>2</sub>O<sub>2</sub>. **Figures 3.20-3.23** show the FTIR, <sup>1</sup>H NMR, <sup>13</sup>C NMR and Mass spectra of the representative compound **LC**<sub>18</sub>, respectively.

In addition, the FTIR spectra of compounds (**LC**<sub>20-25</sub> and **LC**<sub>33</sub>) showed two strong IR bands at about 2913 and 2850 cm<sup>-1</sup> that correspond to asymmetric and symmetrical C-H stretching vibrations of methylene group. Further, appearance of a strong IR band at around 2219 cm<sup>-1</sup> indicated the presence of cyano group in their molecular structure. Also, presence of a sharp peak at about 1577 cm<sup>-1</sup> that accounts for C=N stretching vibrations, confirmed the effective formation of central 2-methoxy-3-cyanopyridine from prop-2-en-1-one.

In FTIR spectrum of compounds **LC**<sub>26-32</sub>, stretching vibrations of C-H and C=N groups appeared as strong peaks at about 2913-2850 cm<sup>-1</sup> and 1577-1570 cm<sup>-1</sup>, respectively and the absence of a peak due to C $\equiv$ N at around 2220 cm<sup>-1</sup> clearly indicated the formation of methoxypyridine derivatives. In <sup>1</sup>H NMR spectrum of compounds (**LC**<sub>20-25</sub> and **LC**<sub>33</sub>), aromatic protons displayed unique resonances in the range of  $\delta$  8.07-7.03 ppm and protons of position-4 of pyridine ring appeared as singlet at about  $\delta$  7.38 ppm. Also, three protons of methoxy substituent at position-2 of pyridine ring resonated at around  $\delta$  4.22 ppm as singlet, which confirmed the effective construction of 2-methoxy-3-cyanopyridine from prop-2-en-1-one. In addition, the appearance of primary and secondary protons signals in the range of  $\delta$  1.86-1.00 ppm established the presence of terminal alkoxy chain in the compounds.

On the other hand, the  $^1\text{H}$  NMR spectra of the compounds (**LC**<sub>14-19</sub>, <sub>26-32</sub>) displayed one additional singlet at about  $\delta$  6.80 ppm when compared to  $^1\text{H}$  NMR spectra of compounds (**LC**<sub>20-25</sub> and **LC**<sub>33</sub>), that evidenced the dehydrocyanation reaction in them. This additional singlet is due to the presence of adjacent aromatic proton to methoxy group of pyridine ring. Further, mass spectral analysis of compounds **LC**<sub>20</sub> and **LC**<sub>32</sub> showed that the mass  $[\text{M}+\text{H}]^+$  peaks at 461.2 and 475.4 are in agreement with the calculated molecular weight for the formula of **LC**<sub>20</sub> ( $\text{C}_{29}\text{H}_{34}\text{FN}_2\text{O}_2$ ) and **LC**<sub>32</sub> ( $\text{C}_{31}\text{H}_{43}\text{N}_2\text{O}_2$ ), respectively. The crystal structure analysis of compounds **LC**<sub>14</sub>, **LC**<sub>16</sub>, **LC**<sub>32</sub>, and **LC**<sub>33</sub> further confirmed the formation of two types of cyclized products. **Figures 3.24-3.27** depict the FTIR,  $^1\text{H}$  NMR,  $^{13}\text{C}$  NMR and Mass spectra of **LC**<sub>20</sub> while **Figures 3.28-3.30** show the  $^1\text{H}$  NMR,  $^{13}\text{C}$  NMR and Mass spectra of **LC**<sub>32</sub>, respectively.

#### *Crystal structure analysis of **LC**<sub>14</sub> and **LC**<sub>16</sub>:*

It is not so easy to grow superior quality crystals of mesogenic compounds carrying flexible alkoxy chains. In spite, by repeated efforts high-quality colorless block-shaped crystals of compound **LC**<sub>14</sub> were obtained by slow evaporation of solution (chloroform and methanol in 1:1 ratio). Its crystal structure was determined using single crystal X-ray diffractometer and the procured crystal data are presented in **Table 3.11**. The compound crystallizes in triclinic centrosymmetric space group *P*-1 and cell parameters are  $a=8.978(3)$  Å,  $b=10.677(3)$  Å,  $c=10.877(3)$  Å,  $V=991.50(5)$  Å<sup>3</sup> with  $Z=2$ . Its molecular structure with atom labeling is shown in **Figure 3.6**. The structure was found to be non-planar as evidenced by the observed large torsion angle of  $29.4(3)^\circ$  (C9-C8-C5-C4) made by 4-cyanophenyl ring with the central pyridine ring and an angle of  $8.1(3)^\circ$  (C14-C13-C11-N1) made by 4-(butoxy)phenyl ring with the central pyridine ring. The butoxy chain was found to be completely staggered and almost planar with respect to the benzene ring.

As depicted in **Figure 3.7**, the structure involves in various kinds of intra- and inter-molecular interactions, *viz.* C-H...N, C-H... $\pi$ , C-H...O with the four neighboring molecules. Here, a C-H...N inter-molecular hydrogen bond (*i.e.*, between nitrogen atom of terminal cyano group and the nearby aromatic protons) and a

C-H...N intra-molecular hydrogen bond (*i.e.*, between the central pyridine ring and the neighboring aromatic protons) were observed (**Table 3.12**). Further, C-H... $\pi$  and C-H...O short contacts with the bond distance of 2.771 and 2.609 Å, respectively were noticed. Though, the compound possesses slightly distorted structure, the observed values of bond lengths in the three ring system are restraining partial double bond character, suggesting the presence of delocalized  $\pi$ -electrons.

**Table 3.11** Crystal data and structure refinement for **LC<sub>14</sub>** and **LC<sub>16</sub>**

Compound	LC <sub>14</sub>	LC <sub>16</sub>
Formula	C <sub>23</sub> H <sub>22</sub> N <sub>2</sub> O <sub>2</sub>	C <sub>27</sub> H <sub>30</sub> N <sub>2</sub> O <sub>2</sub>
Formula weight	358.43	414.53
CCDC number	958625	909202
Temperature (K)	296(2)	120(2)
Crystal form	Block	Block
Color	Colorless	Colorless
Crystal system	Triclinic	Triclinic
Space group	<i>P</i> -1	<i>P</i> -1
<i>a</i> (Å)	8.978(3)	8.148(3)
<i>b</i> (Å)	10.677(3)	10.726(3)
<i>c</i> (Å)	10.877(3)	13.408(4)
$\alpha$ (°)	99.677(9)	86.933(2)
$\beta$ (°)	95.437(9)	84.680(3)
$\gamma$ (°)	103.089(8)	81.508(3)
Volume (Å <sup>3</sup> )	991.50(5)	1153.10(6)
<i>Z</i>	2	2
Density (gcm <sup>-3</sup> )	1.20	1.19
$\mu$ (mm <sup>-1</sup> )	0.077	0.075
F (000)	380.0	443.9
<i>h</i> <sub>min, max</sub>	-11,11	-10,10
<i>k</i> <sub>min, max</sub>	-13,13	-13,13
<i>l</i> <sub>min, max</sub>	-13,13	-16,16
Reflections collected	21008	23543
Independent reflections	3862	4529
<i>R</i> <sub>all</sub> , <i>R</i> <sub>obs</sub>	0.1079, 0.053	0.109, 0.052

$wR_{2\_all}, wR_{2\_obs}$	0.1590, 0.1352	0.103, 0.042
$\Delta\rho_{min,max}$ ( $e \text{ \AA}^{-3}$ )	-0.175, 0.136	-0.188, 0.207
GOOF	0.994	1.059

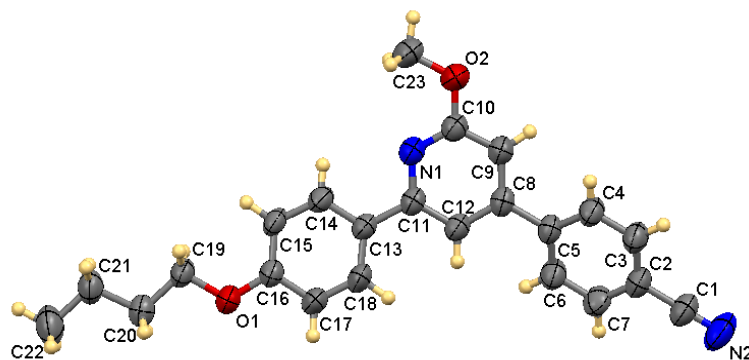


Figure 3.6 ORTEP diagram of  $LC_{14}$  with atom numbering

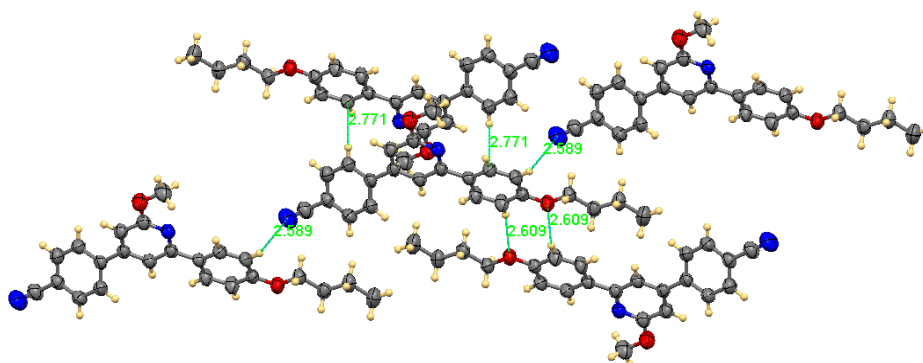


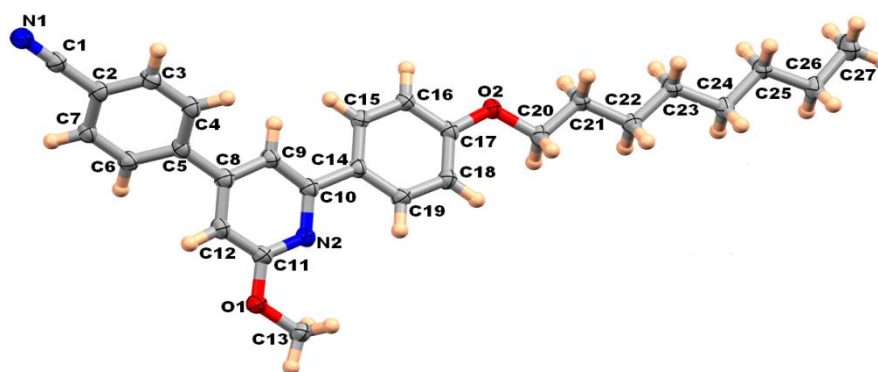
Figure 3.7 Packing diagram of  $LC_{14}$  with various kinds of short contacts

Table 3.12 Intra- and inter-molecular C-H...N interactions in the structure of  $LC_{14}$

Compound	D-H...A	D/H/Å	H...A/Å	D...A/Å	$\angle$ D-H...A/ $^\circ$	Symmetry
$LC_{14}$	C14-H14...N1	0.930	2.460	2.799(3)	101.00	x, y, z
	C15-H15...N2	0.930	2.590	3.460(3)	156.00	x+1,y-1,z

In case of compound  $LC_{16}$ , high-quality colorless block-shaped crystals were obtained by slow evaporation of solution (chloroform and methanol in 1:1 ratio). Single crystal X-ray diffraction experiment was carried out at 120 K and the obtained crystal data are presented in **Table 3.11**. Its ORTEP diagram with atom labeling is shown in **Figure 3.8**. The study revealed that crystal structure belongs to the triclinic

centrosymmetric space group  $P-1$  and cell parameters are  $a=8.148(3)$  Å,  $b=10.726(3)$  Å,  $c=13.408(4)$  Å,  $V=1153.11(6)$  Å<sup>3</sup> with  $Z=2$ . In asymmetric unit the similar molecules are held together by C-H...N interactions (**Figure 3.9**). Here, the crystalline order formed by intermolecular interactions is found to be similar to that of the columnar assembly, when the packing diagram is viewed along the  $c$  axis. In its crystal packing, molecules are arranged one above the other in an anti-parallel manner.



**Figure 3.8** ORTEP diagram of  $LC_{16}$  with atom numbering

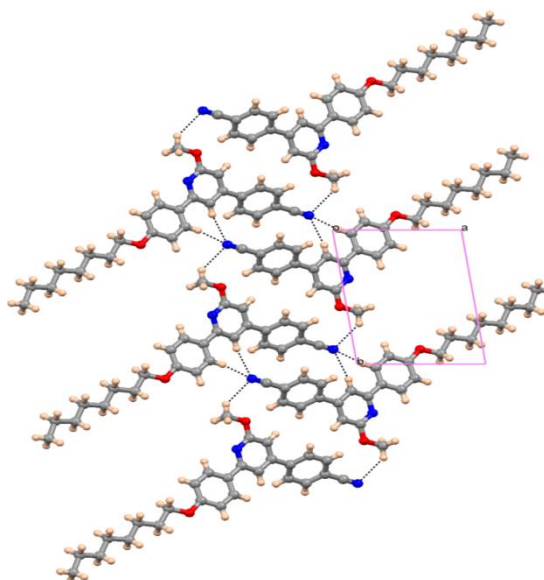


**Figure 3.9** Packing diagram of  $LC_{16}$  depicting C-H...N intermolecular interactions and column-like structure

From the crystallographic data, the compound  $LC_{16}$  is found to be non-planar and slightly more distorted than the molecular structure of  $LC_{14}$ , as evidenced by the observed large torsion angles of  $-39.9(2)^\circ$  (C6-C5-C8-C12) made by the 4-



cyanophenyl ring with the central pyridine ring and torsion angles of  $-15.1(2)^\circ$  (N2-C10-C14-C19) made by the 4-(octyloxy)phenyl ring with the central pyridine ring. The observed torsion angles of  $3.1(2)^\circ$  (C13-O2-C11-N2) around the methoxy group substituted at position-6 of pyridine are slightly different. The octyloxy chain of molecule in the crystal system is also completely staggered and almost planar with respect to the benzene ring. On the other hand, the terminal cyano group is in the same plane with respect to the benzene ring. In addition, its crystal structure exhibited several intra- and inter-molecular interactions with the six neighboring molecules. These include one kind of non-conventional C19-H19 $\cdots$ N2 intra molecular H-bond formed by the central pyridine moiety and the neighboring aromatic proton with the bond distance of 2.49 Å (**Table 3.13**). Also, two kinds of (i.e C9-H9 $\cdots$ N1 and C15-H15 $\cdots$ N1) inter-molecular hydrogen bonds, formed by nitrogen atom of terminal cyano group and the nearby aromatic protons with the bond distance of 2.54 and 2.60 Å, respectively, are present. Its structure has formed more number of short contacts (*viz.* C-H $\cdots$  $\pi$ , and C-H $\cdots$ O) with the six neighboring molecules than the number of short contacts observed in case of **LC<sub>14</sub>** (only four neighboring molecules). Thus, the number of neighboring molecules surrounded by the molecular structure mainly depends on the presence of intermolecular interactions.

**Table 3.13** Intra- and inter-molecular C-H $\cdots$ N interactions in crystal structure of **LC<sub>16</sub>**

Compound	D-H $\cdots$ A	D-H/Å	H $\cdots$ A/Å	D $\cdots$ A/Å	$\angle$ D-H $\cdots$ A/ $^\circ$	Symmetry
<b>LC<sub>16</sub></b>	C9-H9 $\cdots$ N1	0.9500	2.5400	3.471(18)	165.00	-1-x, -y, 1-z
	C15-H15 $\cdots$ N1	0.9500	2.600	3.523(18)	163.00	-1-x, -y, 1-z
	C19-H19 $\cdots$ N2	0.9500	2.4900	2.821(17)	100.00	x, y, z

*Crystal structure analysis of LC<sub>32</sub> and LC<sub>33</sub>:*

The molecular structure with atom-numbering scheme and packing of **LC<sub>32</sub>** are shown in **Figures 3.10** and **3.11**, respectively. Crystal data of **LC<sub>32</sub>** are tabulated in **Table 3.14**. The selected bond lengths and angles are given in **Table 3.15**. Single crystal X-ray study revealed that **LC<sub>32</sub>** crystallizes in triclinic space group *P*-1 with

cell parameters are  $a=7.3355$  (5) Å,  $b=9.7607$  (7) Å,  $c=19.5372$  (14) Å,  $V=4880.2$ (3) Å<sup>3</sup>,  $Z=2$ . From the X-ray analysis data, it is evident that the molecule is not exactly planar and but distorted. Interestingly, 4-pyridinyl ring substituted at position-4 of central pyridine ring makes a torsion angle  $\chi[C(26), C(3), C(4), C(27)]$  of 37.6° (4), while the 4-tetradecyloxyphenyl ring substituted at its position-6, forms a torsion angle of  $\chi[C(8), C(7), C(6), N(2)]$  of 4.2° (3), which is less than the previous one. Consequently, in **LC32**, the pyridine and tetradecyloxyphenyl ring systems become almost planar, thereby providing a greater extent of conjugation, as they have lower torsion angle. Further, the results revealed that the carbon-carbon bond lengths in the molecular skeleton are basically in-between the typical C-C single (1.54 Å) and C=C double (1.34 Å) bonds. Also, the carbon-nitrogen bond lengths are intermediate of typical C-N single (1.47 Å) and C=N double (1.27 Å) bond lengths. The length of carbon-oxygen bond directly attached to aromatic systems are also in-between the typical C-O single (1.43 Å) and C=O double (1.24 Å) bond lengths. On the basis of this observation, it can be concluded that the  $\pi$ -electrons in the molecule are highly delocalized.

**Table 3.14** Crystal data and structure refinement for **LC<sub>32</sub>** and **LC<sub>33</sub>**

Compound	LC <sub>32</sub>	LC <sub>33</sub>
Chemical formula	C <sub>31</sub> H <sub>42</sub> N <sub>2</sub> O <sub>2</sub>	C <sub>48</sub> H <sub>51</sub> N <sub>4</sub> S <sub>2</sub>
Formula mass	474.67	812.07
Crystal system	Triclinic	Orthorhombic
Space group	<i>P-1</i>	<i>Aba2</i>
<i>a</i> (Å)	7.3355 (5)	14.8343(5)
<i>b</i> (Å)	9.7607 (7)	44.690(2)
<i>c</i> (Å)	19.5372 (14)	7.3614(3)
$\alpha$ (°)	97.873 (5)	90.00
$\beta$ (°)	94.801 (4)	90.00
$\gamma$ (°)	104.460 (4)	90.00
Unit cell volume (Å <sup>3</sup> )	1331.60 (16)	4880.2 (3)
<i>Z</i>	2	4
Temperature (K)	296	100

$\rho_{\text{calc}}$ (g cm <sup>-3</sup> )	1.184	1.194
Absorption coefficient (mm <sup>-1</sup> )	0.07	0.15
$F(000)$	516.0	1753
Crystal size (mm <sup>3</sup> )	0.29 x 0.26 x 0.25	0.35 x 0.26 x 0.21
No. of reflections measured	16730	12948
No. of independent reflections	4704	4301
$R_{\text{int}}$	0.052	0.059
$\Delta\rho_{\text{min,max}}$ (e Å <sup>-3</sup> )	-0.33, 0.28	-0.47, 1.20
Final $R_I$ values ( $I > 2\sigma(I)$ )	0.0588	0.0844
Final $wR(F^2)$ value ( $I > 2\sigma(I)$ )	0.1533	0.2353
Final $R_I$ values (all data)	0.1121	0.1039
Final $wR(F^2)$ values (all data)	0.174	0.2599
GOOF	0.99	1.06
CCDC	978127	978451

**Table 3.15** The selected bond lengths (Å) and bond angles (°) for **LC<sub>32</sub>**

Bond Lengths (Å)			
O1-C10	1.378 (3)	C15-H15B	0.9700
O1-C11	1.440 (2)	C16-C17	1.525 (3)
O2-C28	1.361 (3)	C16-H16A	0.9700
O2-C29	1.436 (3)	C16-H16B	0.9700
N1-C1	1.334 (3)	C17-C18	1.525 (3)
N1-C25	1.342 (3)	C17-H17A	0.9700
N2-C28	1.329 (3)	C17-H17B	0.9700
N2-C6	1.363 (3)	C18-C19	1.525 (3)
C1-C2	1.376 (3)	C18-H18A	0.9700
C1-H1	0.9300	C18-H18B	0.9700
C2-C3	1.389 (3)	C19-C20	1.530 (3)
C2-H2	0.9300	C19-H19A	0.9700
C3-C26	1.392 (3)	C19-H19B	0.9700
C3-C4	1.472 (3)	C20-C21	1.525 (3)

Bond Angles (°)			
C10-O1-C11	116.87 (17)	C18-C17-H17A	108.9
C28-O2-C29	116.17 (18)	C16-C17-H17A	108.9
C1-N1-C25	114.8 (2)	C18-C17-H17B	108.9
C28-N2-C6	117.51 (19)	C16-C17-H17B	108.9
N1-C1-C2	124.3 (2)	H17A-C17-H17B	107.7
N1-C1-H1	117.9	C17-C18-C19	113.18 (19)
C2-C1-H1	117.9	C17-C18-H18A	108.9
C1-C2-C3	120.2 (2)	C19-C18-H18A	108.9
C1-C2-H2	119.9	C17-C18-H18B	108.9
C3-C2-H2	119.9	C19-C18-H18B	108.9
C2-C3-C26	115.8 (2)	H18A-C18-H18B	107.8
C2-C3-C4	122.1 (2)	C18-C19-C20	114.18 (19)
C26-C3-C4	122.0 (2)	C18-C19-H19A	108.7
C27-C4-C5	117.4 (2)	C20-C19-H19A	108.7

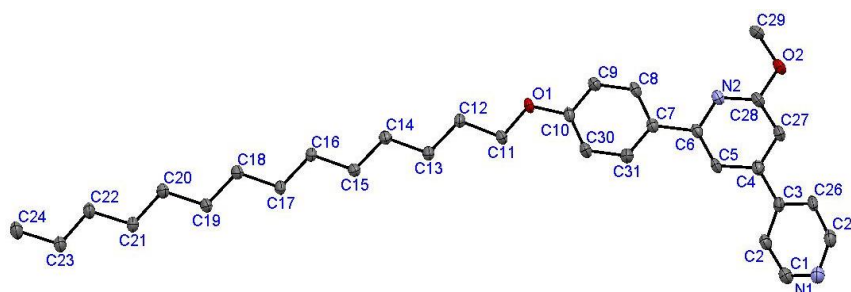


**Figure 3.10** Crystal structure of  $\text{LC}_{32}$  with atom-numbering (Hydrogen atoms are omitted for clarity)

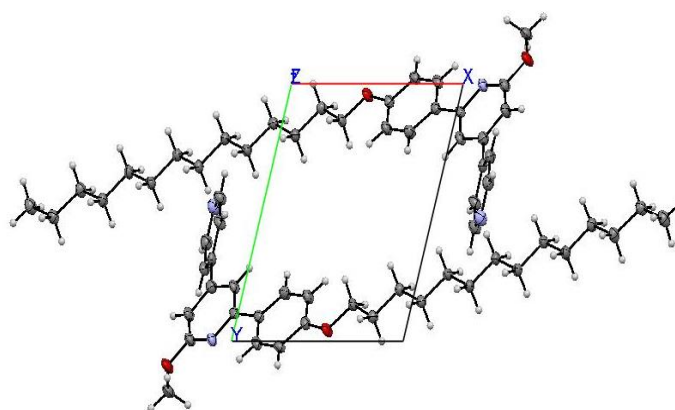


**Figure 3.11** Crystal packing pattern of  $\text{LC}_{32}$ , when viewed along c-axis

The crystal structure of **LC<sub>33</sub>** along with atom-numbering scheme and crystal packing pattern are shown in **Figures 3.12** and **3.13**, respectively. Crystal data of compound **LC<sub>33</sub>** are tabulated in **Table 3.13**. The selected bond lengths and angles are summarized in **Table 3.15**. A detailed single crystal study revealed that **LC<sub>33</sub>** crystallizes in orthorhombic space group *Aba2* with cell parameters are  $a = 14.8343(5)$  Å,  $b = 44.690(2)$  Å,  $c = 7.3614(3)$  Å,  $V = 4880.2(3)$  Å<sup>3</sup>,  $Z = 8$ . From the X-ray analysis data, it is evident that the molecule is not planar and but partly distorted. It is observed that 4-decyloxyphenylene ring substituted at position-4 of central pyridine ring forms a torsion angle  $\chi[C(27), C(8), C(3), C(16)]$  of  $-41.9^\circ$  (6), whereas the 2-thiophenyl ring substituted at its position-6, makes a torsion angle of  $\chi[C(4), C(2), C(18), C(27)]$  of  $-4.4^\circ$  (8), which is less than the earlier one. The observation indicates that the two ring systems in **LC<sub>33</sub>** are nearly planar, which provides an extended conjugated system within the molecule. Further, the results revealed that the carbon-carbon bond lengths in the molecule are basically intermediate of typical C-C single (1.54 Å) and C=C double (1.34 Å) bond lengths. The carbon-nitrogen bond lengths are also in-between the typical C-N single (1.47 Å) and C=N double (1.27 Å) bond lengths. The length of carbon-oxygen bond directly attached to aromatic systems are also intermediate of typical C-O single (1.43 Å) and C=O double (1.24 Å) bond lengths. From this observation it can be concluded that the  $\pi$ -electrons are delocalized considerably in the molecule.

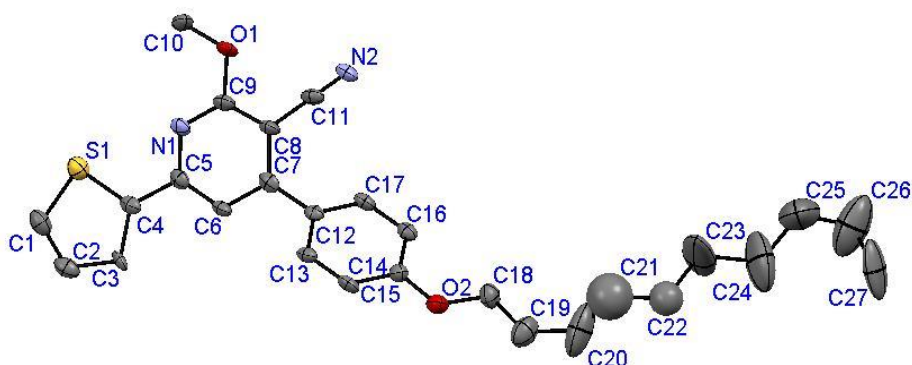


**Figure 3.12** Crystal structure of **LC<sub>33</sub>** with atom-numbering (Hydrogen atoms are omitted for clarity)

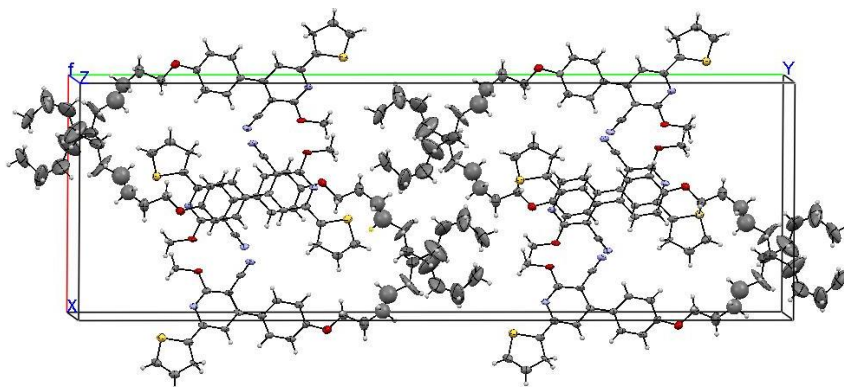


**Figure 3.13** Crystal packing of **LC<sub>33</sub>**

**Table 3.15** The selected bond lengths (Å) and bond angles (°) for compound **LC<sub>33</sub>**

Bond Lengths (Å)			
S2-C2	1.700(5)	C3-C16	1.405(7)
S2-C30	1.701(6)	N1-C23	1.141(7)
O1-C10	1.367(6)	C12-C29	1.391(7)
O1-C39	1.436(6)	C12-C14	1.396(7)
O2-C21	1.440(7)	C30-C38	1.355(9)
N4-C10	1.322(7)	C41-C42	1.245(17)
N4-C18	1.337(6)	C43-C44	1.49(4)
C8-C9	1.401(7)	C44-C45	1.65(3)
C8-C27	1.422(7)	C45-C46	1.55(4)
C2-C18	1.453(7)	C48-C47	1.61(3)
C2-C4	1.453(7)	C47-C46	1.39(4)
Bond Angles (°)			
C2-S2-C30	92.7(3)	C15-C16-C3	121.0(4)
C10-O1-C39	116.7(4)	N4-C18-C27	122.9(4)
C10-N4-C18	117.8(4)	N4-C18-C2	116.3(4)
C9-C8-C27	116.8(5)	O2-C21-C34	107.6(5)
C18-C2-S2	120.3(4)	N1-C23-C9	176.5(6)
C10-C9-C23	119.8(4)	C18-C27-C8	119.4(4)
N4-C10-O1	119.9(4)	C12-C29-C3	121.1(4)
N4-C10-C9	124.6(5)	C30-C38-C4	114.5(5)
O1-C10-C9	115.4(4)	C42-C41-C43	113.5(17)
C29-C12-C14	119.3(4)	C41-C42-C34	117.0(12)
O2-C14-C15	115.7(4)	C43-C44-C45	117(3)
O2-C14-C12	124.6(4)	C47-C46-C45	122(3)

### 3.3.2.2 Experimental procedures

The synthetic protocols for the preparation of intermediates and the target compounds **LC<sub>14-33</sub>** are explained in the following paragraphs.

*General procedure for synthesis of 4-alkoxyacetophenones 4a-f.*

The 4-alkoxyacetophenones **4a-f** were synthesized from 4-hydroxyacetophenone by treating it with the corresponding *n*-alkyl bromide using the standard procedures (Tantrawong et al. 1993) and their analytical data were found to be in agreement with the reported data.

*General procedure for synthesis of prop-2-en-1-one derivatives 6a-t.*

A mixture of respective aryl/heteroaryl ketone **4a-g** (1 equivalent) and aryl/heteroaryl aldehyde **5a-g** (1 equivalent) were dissolved in ethanol. To this 5 mL of an aqueous solution of potassium hydroxide (1.2 equivalents) was added and the reaction mixture was stirred at room temperature for 4 h. The precipitated product was filtered, washed with ethanol and finally purified by recrystallization from a chloroform and methanol mixture. Their characterization data are summarized below.

*4-(3-(4-Butoxyphenyl)-3-oxoprop-1-enyl)benzotrile (6a)*. Yield 85 %, m.p. 139-140 °C. FTIR (cm<sup>-1</sup>): 2927, 2862, 2219, 1656, 1596, 1266, 1166, 1018, 816. <sup>1</sup>H NMR (500 MHz, CDCl<sub>3</sub>) δ (ppm) 8.04 (d, *J*=9 Hz, 2H, Ar-H), 7.77 (d, *J*=15.5 Hz, 1H, Olefinic-H), 7.75-7.71 (m, 4H, Ar-H), 7.62 (d, *J*=15.5 Hz, 1H, Olefinic-H), 7.00 (d, *J*=9 Hz, 2H, Ar-H), 4.07 (t, *J*=6.5 Hz, 2H, -OCH<sub>2</sub>-), 1.84-1.80 (m, 2H, -OCH<sub>2</sub>CH<sub>2</sub>-), 1.56-1.51 (m, 2H, -CH<sub>2</sub>-), 1.02 (t, *J*=7.2 Hz, 3H, -CH<sub>3</sub>). MS (m/z): 306.1 (M+H)<sup>+</sup>. Anal. Calcd. For. C<sub>20</sub>H<sub>19</sub>NO<sub>2</sub>: C. 78.66; H. 6.27; N. 4.59; Found: C. 78.95; H. 6.24; N. 4.55.

*4-(3-(4-(Hexyloxy)phenyl)-3-oxoprop-1-enyl)benzotrile (6b)*. Yield 84 %, m.p. 115-116 °C. FTIR (cm<sup>-1</sup>): 2912, 2850, 2217, 1653, 1598, 1263, 1165, 1015, 816. <sup>1</sup>H NMR (500 MHz, CDCl<sub>3</sub>) δ (ppm) 8.04 (d, *J*=9 Hz, 2H, Ar-H), 7.77 (d, *J*=15.5 Hz, 1H, Olefinic-H), 7.75-7.71 (m, 4H, Ar-H), 7.63 (d, *J*=15.5 Hz, 1H, Olefinic-H), 7.00 (d, *J*=9 Hz, 2H, Ar-H), 4.06 (t, *J*=6.5 Hz, 2H, -OCH<sub>2</sub>-), 1.85-1.82 (m, 2H, -OCH<sub>2</sub>CH<sub>2</sub>-), 1.51-1.36 (m, 6H, -CH<sub>2</sub>-), 0.93 (t, *J*=7 Hz, 3H, -CH<sub>3</sub>). MS (m/z): 334.2 (M+H)<sup>+</sup>. Anal. Calcd. For. C<sub>22</sub>H<sub>23</sub>NO<sub>2</sub>: C. 79.25; H. 6.95; N. 4.20; Found: C. 79.46; H. 6.98; N. 4.24.

*4-(3-(4-(Octyloxy)phenyl)-3-oxoprop-1-enyl)benzotrile (6c)*. Yield 81 %, m.p. 95-97 °C. FTIR (cm<sup>-1</sup>): 2921, 2858, 2223, 1654, 1601, 1250, 1179, 987, 816. <sup>1</sup>H NMR (500

MHz, CDCl<sub>3</sub>)  $\delta$  (ppm) 8.04 (d,  $J=8.5$  Hz, 2H, Ar-H), 7.77 (d,  $J=15.5$  Hz, 1H, Olefinic-H), 7.75-7.71 (m, 4H, Ar-H), 7.63 (d,  $J=15.5$  Hz, 1H, Olefinic-H), 7.00 (d,  $J=8.5$  Hz, 2H, Ar-H), 4.06 (t,  $J=6.5$  Hz, 2H, -OCH<sub>2</sub>-), 1.87-1.81 (m, 2H, -OCH<sub>2</sub>CH<sub>2</sub>-), 1.51-1.32 (m, 10H, -CH<sub>2</sub>-), 0.91 (t,  $J=7$  Hz, 3H, -CH<sub>3</sub>). MS (m/z): 362.2 (M+H)<sup>+</sup>. Anal. Calcd. For. C<sub>24</sub>H<sub>27</sub>NO<sub>2</sub>: C. 79.74; H. 7.53; N. 3.87; Found: C. 79.97; H. 7.58; N. 3.84.

*4-(3-(4-(Decyloxy)phenyl)-3-oxoprop-1-enyl)benzotrile (6d)*. Yield 79 %, m.p. 93-94 °C. FTIR (cm<sup>-1</sup>): 2920, 2855, 2223, 1654, 1600, 1246, 1178, 985, 815. <sup>1</sup>H NMR (500 MHz, CDCl<sub>3</sub>)  $\delta$  (ppm) 8.04 (d,  $J=8.5$  Hz, 2H, Ar-H), 7.77 (d,  $J=15.5$  Hz, 1H, Olefinic-H), 7.75-7.71 (m, 4H, Ar-H), 7.63 (d,  $J=15.5$  Hz, 1H, Olefinic-H), 6.99 (d,  $J=8.5$  Hz, 2H, Ar-H), 4.06 (t,  $J=6.5$  Hz, 2H, -OCH<sub>2</sub>-), 1.86-1.81 (m, 2H, -OCH<sub>2</sub>CH<sub>2</sub>-), 1.50-1.30 (m, 14H, -CH<sub>2</sub>-), 0.90 (t,  $J=7$  Hz, 3H, -CH<sub>3</sub>). MS (m/z): 390.2 (M+H)<sup>+</sup>. Anal. Calcd. For. C<sub>26</sub>H<sub>31</sub>NO<sub>2</sub>: C. 80.17; H. 8.02; N. 3.60; Found: C. 80.43; H. 8.05; N. 3.56.

*4-(3-(4-(Dodecyloxy)phenyl)-3-oxoprop-1-enyl)benzotrile (6e)*. Yield 84 %, m.p. 95-96 °C. FTIR (cm<sup>-1</sup>): 2909, 2847, 2221, 1650, 1596, 1258, 1171, 988, 816. <sup>1</sup>H NMR (500 MHz, CDCl<sub>3</sub>)  $\delta$  (ppm) 8.04 (d,  $J=9$  Hz, 2H, Ar-H), 7.77 (d,  $J=15.5$  Hz, 1H, Olefinic-H), 7.74-7.73 (m, 4H, Ar-H), 7.63 (d,  $J=15.5$  Hz, 1H, Olefinic-H), 7.01 (d,  $J=9$  Hz, 2H, Ar-H), 4.06 (t,  $J=6.7$  Hz, 2H, -OCH<sub>2</sub>-), 1.87-1.81 (m, 2H, -OCH<sub>2</sub>CH<sub>2</sub>-), 1.51-1.29 (m, 18H, -CH<sub>2</sub>-), 0.90 (t,  $J=7$  Hz, 3H, -CH<sub>3</sub>). MS (m/z): 418.2 (M+H)<sup>+</sup>. Anal. Calcd. For. C<sub>28</sub>H<sub>35</sub>NO<sub>2</sub>: C. 80.53; H. 8.45; N. 3.35; Found: C. 80.75; H. 8.48; N. 3.37.

*4-(3-Oxo-3-(4-(tetradecyloxy)phenyl)prop-1-enyl)benzotrile (6f)*. Yield 82 %, m.p. 98-99 °C. FTIR (cm<sup>-1</sup>): 2909, 2847, 2219, 1651, 1597, 1258, 1172, 977, 816. <sup>1</sup>H NMR (500 MHz, CDCl<sub>3</sub>)  $\delta$  (ppm) 8.04 (d,  $J=9$  Hz, 2H, Ar-H), 7.77 (d,  $J=15.5$  Hz, 1H, Olefinic-H), 7.75-7.71 (m, 4H, Ar-H), 7.63 (d,  $J=15.5$  Hz, 1H, Olefinic-H), 7.00 (d,  $J=9$  Hz, 2H, Ar-H), 4.06 (t,  $J=6.7$  Hz, 2H, -OCH<sub>2</sub>-), 1.87-1.81 (m, 2H, -OCH<sub>2</sub>CH<sub>2</sub>-), 1.51-1.29 (m, 22H, -CH<sub>2</sub>-), 0.90 (t,  $J=6.7$  Hz, 3H, -CH<sub>3</sub>). MS (m/z): 446.3 (M+H)<sup>+</sup>. Anal. Calcd. For. C<sub>30</sub>H<sub>39</sub>NO<sub>2</sub>: C. 80.86; H. 8.82; N. 3.14; Found: C. 81.03; H. 8.87; N. 3.12.



*1-(4-(Decyloxy)phenyl)-3-(4-fluorophenyl)prop-2-en-1-one (6g)*. Yield 78 %, m.p. 91-92 °C. FTIR (cm<sup>-1</sup>): 2918, 2853, 1654, 1592, 1215, 1014, 817. <sup>1</sup>H NMR (500 MHz, CDCl<sub>3</sub>) δ (ppm) 8.04 (d, *J*=9 Hz, 2H, Ar-H) 7.83 (d, *J*=15.5 Hz, 1H, Olefinic-H), 7.66-7.64 (m, 2H, Ar-H), 7.49 (d, *J*=15.5 Hz, 1H, Olefinic-H), 7.12 (d, *J*=8.7 Hz, 2H, Ar-H), 6.99 (d, *J*=9 Hz, 2H, Ar-H), 4.06 (t, *J*=6.5 Hz, 2H, -OCH<sub>2</sub>-), 1.85-1.82 (m, 2H, -OCH<sub>2</sub>CH<sub>2</sub>-), 1.49-1.29 (m, 14H, -CH<sub>2</sub>-), 0.90 (t, *J*=6.5 Hz, 3H, -CH<sub>3</sub>). MS (m/z): 383.2 (M+H)<sup>+</sup>. Anal. Calcd. For. C<sub>25</sub>H<sub>31</sub>FO<sub>2</sub>: C. 78.50; H. 8.17; Found: C. 78.79; H. 8.12.

*1-(4-(Dodecyloxy)phenyl)-3-(4-fluorophenyl)prop-2-en-1-one (6h)*. Yield 81 %, m.p. 88-89 °C. FTIR (cm<sup>-1</sup>): 2913, 2848, 1655, 1596, 1250, 1015, 824. <sup>1</sup>H NMR (500 MHz, CDCl<sub>3</sub>) δ (ppm) 8.04 (d, *J*=9 Hz, 2H, Ar-H) 7.83 (d, *J*=15.5 Hz, 1H, Olefinic-H), 7.66-7.64 (m, 2H, Ar-H), 7.49 (d, *J*=15.5 Hz, 1H, Olefinic-H), 7.13 (t, *J*=8.7 Hz, 2H, Ar-H), 6.99 (d, *J*=9 Hz, 2H, Ar-H), 4.06 (t, *J*=6.5 Hz, 2H, -OCH<sub>2</sub>-), 1.85-1.82 (m, 2H, -OCH<sub>2</sub>CH<sub>2</sub>-), 1.49-1.29 (m, 18H, -CH<sub>2</sub>-), 0.90 (t, *J*=6.5 Hz, 3H, -CH<sub>3</sub>). MS (m/z): 411.3 (M+H)<sup>+</sup>. Anal. Calcd. For. C<sub>27</sub>H<sub>35</sub>FO<sub>2</sub>: C. 78.99; H. 8.59; Found: C. 78.67; H. 8.66.

*3-(4-Fluorophenyl)-1-(4-(tetradecyloxy)phenyl)prop-2-en-1-one (6i)*. Yield 74 %, m.p. 96-97.5 °C. FTIR (cm<sup>-1</sup>): 2913, 2847, 1655, 1597, 1250, 1016, 826. <sup>1</sup>H NMR (500 MHz, CDCl<sub>3</sub>) δ (ppm) 8.04 (d, *J*=9 Hz, 2H, Ar-H), 7.78 (d, *J*=15.5 Hz, 1H, Olefinic-H), 7.66-7.64 (m, 2H, Ar-H), 7.49 (d, *J*=15.5 Hz, 1H, Olefinic-H), 7.12 (t, *J*=8.5 Hz, 2H, Ar-H), 6.99 (d, *J*=8.5 Hz, 2H, Ar-H), 4.06 (t, *J*=6.5 Hz, 2H, -OCH<sub>2</sub>-), 1.86-1.81 (m, 2H, -OCH<sub>2</sub>CH<sub>2</sub>-), 1.50-1.28 (m, 22H, -CH<sub>2</sub>-), 0.90 (t, *J*=6.5 Hz, 3H, -CH<sub>3</sub>). MS (m/z): 439.3 (M+H)<sup>+</sup>. Anal. Calcd. For. C<sub>29</sub>H<sub>39</sub>FO<sub>2</sub>: C. 79.41; H. 8.96; Found: C. 79.65; H. 8.88.

*3-(4-Chlorophenyl)-1-(4-(decyloxy)phenyl)prop-2-en-1-one (6j)*. Yield 75 %, m.p. 112-113 °C. FTIR (cm<sup>-1</sup>): 2919, 2852, 1653, 1594, 1266, 1164, 1013, 812. <sup>1</sup>H NMR (500 MHz, CDCl<sub>3</sub>) δ (ppm) 8.04 (d, *J*=8.5 Hz, 2H, Ar-H), 7.76 (d, *J*=16 Hz, 1H, Olefinic-H), 7.59 (d, *J*=8.5 Hz, 2H, Ar-H), 7.53 (d, *J*=16 Hz, 1H, Olefinic-H), 7.40 (d, *J*=8.5 Hz, 2H, Ar-H), 6.99 (d, *J*=8.5 Hz, 2H, Ar-H), 4.06 (t, *J*=6.5 Hz, 2H, -OCH<sub>2</sub>-), 1.86-1.81 (m, 2H, -OCH<sub>2</sub>CH<sub>2</sub>-), 1.52-1.30 (m, 14H, -CH<sub>2</sub>-), 0.90 (t, *J*=6.5 Hz, 3H, -

$\text{CH}_3$ ). MS (m/z): 400.2 (M+H)<sup>+</sup>. Anal. Calcd. For. C<sub>25</sub>H<sub>31</sub> ClO<sub>2</sub>: C. 75.26; H. 7.83; Found: C. 75.52; H. 7.76.

*3-(4-Chlorophenyl)-1-(4-(dodecyloxy)phenyl)prop-2-en-1-one (6k)*. Yield 78 %, m.p. 116-117 °C. FTIR (cm<sup>-1</sup>): 2913, 2848, 1657, 1597, 1252, 1170, 1013, 815. <sup>1</sup>H NMR (500 MHz, CDCl<sub>3</sub>) δ (ppm) 8.04 (d, *J*=9 Hz, 2H, Ar-H), 7.76 (d, *J*=15.5 Hz, 1H, Olefinic-H), 7.59 (d, *J*=8.5 Hz, 2H, Ar-H), 7.53 (d, *J*=15.5 Hz, 1H, Olefinic-H), 7.41 (d, *J*=9 Hz, 2H, Ar-H), 6.99 (d, *J*=8.5 Hz, 2H, Ar-H), 4.06 (t, *J*=6.5 Hz, 2H, -OCH<sub>2</sub>-), 1.85-1.82 (m, 2H, -OCH<sub>2</sub>CH<sub>2</sub>-), 1.52-1.29 (m, 18H, -CH<sub>2</sub>-), 0.90 (t, *J*=6.5 Hz, 3H, -CH<sub>3</sub>). MS (m/z): 428.2 (M+H)<sup>+</sup>. Anal. Calcd. For. C<sub>27</sub>H<sub>35</sub> ClO<sub>2</sub>: C. 75.94; H. 8.26; Found: C. 75.69; H. 8.34.

*3-(4-Chlorophenyl)-1-(4-(tetradecyloxy)phenyl)prop-2-en-1-one (6l)*. Yield 72 %, m.p. 119-120 °C. FTIR (cm<sup>-1</sup>): 2912, 2846, 1654, 1597, 1251, 1170, 1014, 814. <sup>1</sup>H NMR (500 MHz, CDCl<sub>3</sub>) δ (ppm) 8.04 (d, *J*=9 Hz, 2H, Ar-H), 7.76 (d, *J*=16 Hz, 1H, Olefinic-H), 7.59 (d, *J*=9 Hz, 2H, Ar-H), 7.53 (d, *J*=16 Hz, 1H, Olefinic-H), 7.41 (d, *J*=8.5 Hz, 2H, Ar-H), 6.99 (d, *J*=8.5 Hz, 2H, Ar-H), 4.06 (t, *J*=6.5 Hz, 2H, -OCH<sub>2</sub>-), 1.86-1.81 (m, 2H, -OCH<sub>2</sub>CH<sub>2</sub>-), 1.51-1.28 (m, 22H, -CH<sub>2</sub>-), 0.90 (t, *J*=6.5 Hz, 3H, -CH<sub>3</sub>). MS (m/z): 456.2 (M+H)<sup>+</sup>. Anal. Calcd. For. C<sub>29</sub>H<sub>39</sub> ClO<sub>2</sub>: C. 76.54; H. 8.64; Found: C. 76.82; H. 8.71.

*3-(4-Bromophenyl)-1-(4-(decyloxy)phenyl)prop-2-en-1-one (6m)*. Yield 77 %, m.p. 149-150 °C. FTIR (cm<sup>-1</sup>): 2917, 2852, 1658, 1594, 1249, 1165, 1014, 814. <sup>1</sup>H NMR (400 MHz, CDCl<sub>3</sub>) δ (ppm) 8.01 (d, *J*=8 Hz, 2H, Ar-H), 7.66 (d, *J*=16 Hz, 1H, Olefinic-H), 7.54 (d, *J*=8 Hz, 2H, Ar-H), 7.47 (d, *J*=8.5 Hz, 2H, Ar-H), 7.04 (d, *J*=16 Hz, 1H, Olefinic-H), 6.96 (d, *J*=8.5 Hz, 2H, Ar-H), 4.03 (t, *J*=6.6 Hz, 2H, -OCH<sub>2</sub>-), 1.85-1.78 (m, 2H, -OCH<sub>2</sub>CH<sub>2</sub>-), 1.49-1.25 (m, 14H, -CH<sub>2</sub>-), 0.88 (t, *J*=6.6 Hz, 3H, -CH<sub>3</sub>). MS (m/z): 444.1 (M+H)<sup>+</sup>. Anal. Calcd. For. C<sub>25</sub>H<sub>31</sub> BrO<sub>2</sub>: C. 67.72; H. 7.05; Found: C. 67.97; H. 7.13.

*3-(4-Bromophenyl)-1-(4-(dodecyloxy)phenyl)prop-2-en-1-one (6n)*. Yield 68 %, m.p. 115-116 °C. FTIR (cm<sup>-1</sup>): 2911, 2857, 1658, 1598, 1249, 1165, 1014, 814. <sup>1</sup>H NMR (400 MHz, CDCl<sub>3</sub>) δ (ppm) 8.02 (d, *J*=8.5 Hz, 2H, Ar-H), 7.65 (d, *J*=16 Hz, 1H, Olefinic-H), 7.54 (d, *J*=8.5 Hz, 2H, Ar-H), 7.49 (d, *J*=8.5 Hz, 2H, Ar-H), 7.04 (d,

$J=16$  Hz, 1H, Olefinic-H), 6.96 (d,  $J=8.5$  Hz, 2H, Ar-H), 4.03 (t,  $J=6.6$  Hz, 2H, -OCH<sub>2</sub>-), 1.84-1.77 (m, 2H, -OCH<sub>2</sub>CH<sub>2</sub>-), 1.51-1.27 (m, 18H, -CH<sub>2</sub>-), 0.88 (t,  $J=6.6$  Hz, 3H, -CH<sub>3</sub>). MS (m/z): 472.1 (M+H)<sup>+</sup>. Anal. Calcd. For. C<sub>27</sub>H<sub>35</sub> BrO<sub>2</sub>: C. 68.78; H. 7.48; Found: C. 68.94; H. 7.41.

*3-(4-Bromophenyl)-1-(4-(tetradecyloxy)phenyl)prop-2-en-1-one* (**6o**). Yield 75 %, m.p. 119-120 °C. FTIR (cm<sup>-1</sup>): 2918, 2855, 1650, 1596, 1244, 1162, 1011, 814. <sup>1</sup>H NMR (400 MHz, CDCl<sub>3</sub>) δ (ppm) 8.00 (d,  $J=8.8$  Hz, 2H, Ar-H), 7.72 (d,  $J=15.6$  Hz, 1H, Olefinic-H), 7.54 (d,  $J=8.8$  Hz, 2H, Ar-H), 7.49 (d,  $J=8$  Hz, 2H, Ar-H), 7.04 (d,  $J=15.6$  Hz, 1H, Olefinic-H), 6.96 (d,  $J=8.8$  Hz, 2H, Ar-H), 4.03 (t,  $J=6.6$  Hz, 2H, -OCH<sub>2</sub>-), 1.83-1.77 (m, 2H, -OCH<sub>2</sub>CH<sub>2</sub>-), 1.50-1.26 (m, 22H, -CH<sub>2</sub>-), 0.87 (t,  $J=6.8$  Hz, 3H, -CH<sub>3</sub>). MS (m/z): 500.2 (M+H)<sup>+</sup>. Anal. Calcd. For. C<sub>29</sub>H<sub>39</sub> BrO<sub>2</sub>: C. 69.73; H. 7.87; Found: C. 69.49; H. 7.82.

*1-(4-(Decyloxy)phenyl)-3-(4-nitrophenyl)prop-2-en-1-one* (**6p**). Yield 78 %, m.p. 109-110 °C. FTIR (cm<sup>-1</sup>): 2918, 2850, 1654, 1597, 1255, 1172, 1022, 822. <sup>1</sup>H NMR (500 MHz, CDCl<sub>3</sub>) δ (ppm) 8.29 (d,  $J=9$  Hz, 2H, Ar-H), 8.05 (d,  $J=9$  Hz, 2H, Ar-H), 7.81 (d,  $J=15$  Hz, 1H, Olefinic-H), 7.79 (d,  $J=8.5$  Hz, 2H, Ar-H), 7.67 (d,  $J=15$  Hz, 1H, Olefinic-H), 7.00 (d,  $J=8.5$  Hz, 2H, Ar-H), 4.06 (t,  $J=6.5$  Hz, 2H, -OCH<sub>2</sub>-), 1.87-1.81 (m, 2H, -OCH<sub>2</sub>CH<sub>2</sub>-), 1.52-1.30 (m, 14H, -CH<sub>2</sub>-), 0.90 (t,  $J=7$  Hz, 3H, -CH<sub>3</sub>). MS (m/z): 410.2 (M+H)<sup>+</sup>. Anal. Calcd. For. C<sub>25</sub>H<sub>31</sub> NO<sub>4</sub>: C. 73.32; H. 7.63; N. 3.42; Found: C. 73.64; H. 7.59; N. 3.49.

*1-(4-(Dodecyloxy)phenyl)-3-(4-nitrophenyl)prop-2-en-1-one* (**6q**). Yield 76 %, m.p. 114-115 °C. FTIR (cm<sup>-1</sup>): 2916, 2849, 1657, 1598, 1256, 1173, 1012, 812. <sup>1</sup>H NMR (500 MHz, CDCl<sub>3</sub>) δ (ppm) 8.28 (d,  $J=9$  Hz, 2H, Ar-H), 8.05 (d,  $J=9$  Hz, 2H, Ar-H), 7.81 (d,  $J=15$  Hz, 1H, Olefinic-H), 7.79 (d,  $J=9$  Hz, 2H, Ar-H), 7.66 (d,  $J=15$  Hz, 1H, Olefinic-H), 7.00 (d,  $J=9$  Hz, 2H, Ar-H), 4.06 (t,  $J=6.5$  Hz, 2H, -OCH<sub>2</sub>-), 1.85-1.82 (m, 2H, -OCH<sub>2</sub>CH<sub>2</sub>-), 1.50-1.28 (m, 18H, -CH<sub>2</sub>-), 0.89 (t,  $J=6.7$  Hz, 3H, -CH<sub>3</sub>). MS (m/z): 438.2 (M+H)<sup>+</sup>. Anal. Calcd. For. C<sub>27</sub>H<sub>35</sub> NO<sub>4</sub>: C. 74.11; H. 8.06; N. 3.20; Found: C. 74.37; H. 8.12; N. 3.26.

*3-(4-Nitrophenyl)-1-(4-(tetradecyloxy)phenyl)prop-2-en-1-one* (**6r**). Yield 77 %, m.p. 119-120 °C. FTIR (cm<sup>-1</sup>): 2915, 2848, 1654, 1597, 1256, 1170, 1014, 814. <sup>1</sup>H NMR

(500 MHz, CDCl<sub>3</sub>)  $\delta$  (ppm) 8.29 (d,  $J=9$  Hz, 2H, Ar-H), 8.05 (d,  $J=9$  Hz, 2H, Ar-H), 7.81 (d,  $J=15$  Hz, 1H, Olefinic-H), 7.79 (d,  $J=8.5$  Hz, 2H, Ar-H), 7.66 (d,  $J=15$  Hz, 1H, Olefinic-H), 7.00 (d,  $J=9$  Hz, 2H, Ar-H), 4.06 (t,  $J=6.5$  Hz, 2H, -OCH<sub>2</sub>-), 1.85-1.82 (m, 2H, -OCH<sub>2</sub>CH<sub>2</sub>-), 1.50-1.28 (m, 22H, -CH<sub>2</sub>-), 0.89 (t,  $J=7$  Hz, 3H, -CH<sub>3</sub>). MS (m/z): 466.3 (M+H)<sup>+</sup>. Anal. Calcd. For. C<sub>29</sub>H<sub>39</sub>NO<sub>4</sub>: C. 74.81; H. 8.44; N. 3.01; Found: C. 74.57; H. 8.39; N. 3.08.

*3-(Pyridin-4-yl)-1-(4-(tetradecyloxy)phenyl)prop-2-en-1-one (6s)*. Yield 66 %, m.p. 79-80 °C. FTIR (cm<sup>-1</sup>): 2917, 2846, 1652, 1599, 1254, 1167, 1012, 814. <sup>1</sup>H NMR (400 MHz, CDCl<sub>3</sub>)  $\delta$  (ppm) 8.67 (d,  $J=6$  Hz, 2H, Pyridine-H), 8.01 (d,  $J=8.8$  Hz, 2H, Ar-H), 7.67 (s, 1H, Olefinic-H), 7.46 (d,  $J=6$  Hz, 2H, Pyridine-H), 7.26 (s, 1H, Olefinic-H), 6.98 (d,  $J=8.8$  Hz, 2H, Ar-H), 4.04 (t,  $J=6.6$  Hz, 2H, -OCH<sub>2</sub>-), 1.85-1.78 (m, 2H, -OCH<sub>2</sub>CH<sub>2</sub>-), 1.50-1.26 (m, 22H, -CH<sub>2</sub>-), 0.87 (t,  $J=6.8$  Hz, -CH<sub>3</sub>). MS (m/z): 422.3 (M+H)<sup>+</sup>. Anal. Calcd. For. C<sub>28</sub>H<sub>39</sub>NO<sub>2</sub>: C. 79.76; H. 9.32; N. 3.32; Found: C. 79.99; H. 9.25; N. 3.39.

*3-(4-(Decyloxy)phenyl)-1-(thiophen-2-yl)prop-2-en-1-one (6t)*. Yield 71 %, m.p. 102-103 °C. FTIR (cm<sup>-1</sup>): 2917, 2846, 1653, 1599, 1254, 1167, 1013, 814. <sup>1</sup>H NMR (500 MHz, CDCl<sub>3</sub>)  $\delta$  (ppm) 7.88 (d,  $J=15$  Hz, 1H, Olefinic-H), 7.71 (d,  $J=3.2$  Hz, 1H, Ar-H (Thiophene)), 7.60 (d,  $J=8.8$  Hz, 2H, Ar-H), 7.54 (d,  $J=15$  Hz, 1H, Olefinic-H), 7.49 (d,  $J=4.4$  Hz, 1H, Ar-H (Thiophene)), 7.14 (t,  $J=4.4$  Hz, 1H, Ar-H (Thiophene)), 7.02 (d,  $J=8.8$  Hz, 2H, Ar-H), 4.01 (t,  $J=6.4$  Hz, 2H, -OCH<sub>2</sub>-), 1.83-1.79 (m, 2H, -OCH<sub>2</sub>CH<sub>2</sub>-), 1.49-1.28 (m, 14H, -CH<sub>2</sub>-), 0.88 (t,  $J=6.8$  Hz, 3H, -CH<sub>3</sub>). MS (m/z): 371.2 (M+H)<sup>+</sup>. Anal. Calcd. For. C<sub>23</sub>H<sub>30</sub>O<sub>2</sub>S: C. 74.55; H. 8.16; S. 8.65; Found: C. 74.83; H. 8.10; S. 8.58.

*General procedure for synthesis of 6-alkoxyaryl/thiophenyl-4-substituted aryl-2-methoxy pyridines (LC<sub>14-33</sub>)*.

One equivalent of compound **6a-t** was added slowly to a freshly prepared solution of sodium methoxide (20 equivalents of sodium in 10 ml of methanol) while stirring. Malononitrile (1 equivalent) was then added with continuous stirring at room temperature until the precipitate separates out. The solid separated was collected by

filtration, washed with methanol and recrystallized from chloroform and methanol mixture. Their characterization data are given below.

*4-(2-(4-Butoxyphenyl)-6-methoxypyridin-4-yl)benzotrile (LC<sub>14</sub>)*. Yield 74 %. FTIR (cm<sup>-1</sup>): 2944, 2859, 2219, 1577, 1237, 1170, 1008, 823. <sup>1</sup>H NMR (500 MHz, CDCl<sub>3</sub>) δ (ppm) 8.05 (d, *J*=8 Hz, 2H, Ar-H), 7.84 (d, *J*=8 Hz, 2H, Ar-H), 7.77 (d, *J*=8.5 Hz, 2H, Ar-H), 7.46 (s, 1H, Ar-H(Pyridine)), 7.01 (d, *J*=8.5 Hz, 2H, Ar-H), 6.82 (s, 1H, Ar-H(Pyridine)), 4.22 (s, 3H, -OMe of Pyridine), 4.06 (t, *J*=7 Hz, 2H, -OCH<sub>2</sub>-), 1.86-1.81 (m, 2H, -OCH<sub>2</sub>CH<sub>2</sub>-), 1.28 (t, *J*=8.5 Hz, 2H, -CH<sub>2</sub>-), 1.01 (t, *J*=7.5 Hz, 3H, -CH<sub>3</sub>). <sup>13</sup>C NMR (100 MHz, CDCl<sub>3</sub>) δ (ppm); 164.47, 160.31, 155.57, 149.90, 143.56, 132.70, 129.19, 128.97, 118.53, 115.19, 112.05, 110.57, 106.31, 68.25, 54.67, 31.89, 19.63, 14.08. MS (m/z): 359.1 (M+H)<sup>+</sup>. Anal. Calcd. For. C<sub>23</sub>H<sub>22</sub>N<sub>2</sub>O<sub>2</sub>: C. 77.07; H. 6.19; N. 7.82; Found: C. 77.31; H. 6.14; N. 7.86.

*4-(2-(4-(Hexyloxy)phenyl)-6-methoxypyridin-4-yl)benzotrile (LC<sub>15</sub>)*. Yield 67 %. FTIR (cm<sup>-1</sup>): 2930, 2856, 2219, 1577, 1238, 1170, 1016, 825. <sup>1</sup>H NMR (500 MHz, CDCl<sub>3</sub>) δ (ppm) 8.06 (d, *J*=8 Hz, 2H, Ar-H), 7.84 (d, *J*=8 Hz, 2H, Ar-H), 7.78 (d, *J*=8.5 Hz, 2H, Ar-H), 7.47 (s, 1H, Ar-H(Pyridine)), 7.01 (d, *J*=8.5 Hz, 2H, Ar-H), 6.82 (s, 1H, Ar-H(Pyridine)), 4.19 (s, 3H, -OMe of Pyridine), 4.07 (t, *J*=6.7 Hz, 2H, -OCH<sub>2</sub>-), 1.87-1.81 (m, 2H, -OCH<sub>2</sub>CH<sub>2</sub>-), 1.57-1.36 (m, 6H, -CH<sub>2</sub>-), 0.93 (t, *J*=7 Hz, 3H, -CH<sub>3</sub>). <sup>13</sup>C NMR (100 MHz, CDCl<sub>3</sub>) δ (ppm); 164.49, 160.32, 155.58, 149.88, 143.53, 132.73, 129.19, 128.93, 127.82, 118.52, 114.88, 112.05, 110.48, 106.31, 68.29, 54.64, 31.90, 29.61, 26.03, 22.67, 14.09. MS (m/z): 387.2 (M+H)<sup>+</sup>. Anal. Calcd. For. C<sub>25</sub>H<sub>26</sub>N<sub>2</sub>O<sub>2</sub>: C. 77.69; H. 6.78; N. 7.25; Found: C. 77.99; H. 6.72; N. 7.22.

*4-(2-Methoxy-6-(4-(octyloxy)phenyl)pyridin-4-yl)benzotrile (LC<sub>16</sub>)*. Yield 62%. FTIR (cm<sup>-1</sup>): 2916, 2852, 2220, 1578, 1237, 1171, 1013, 827. <sup>1</sup>H NMR (500 MHz, CDCl<sub>3</sub>) δ (ppm) 8.05 (d, *J*=8 Hz, 2H, Ar-H), 7.84 (d, *J*=8 Hz, 2H, Ar-H), 7.78 (d, *J*=8 Hz, 2H, Ar-H), 7.46 (s, 1H, Ar-H(Pyridine)), 7.01 (d, *J*=8 Hz, 2H, Ar-H), 6.82 (s, 1H, Ar-H(Pyridine)), 4.10 (s, 3H, -OMe of Pyridine), 4.06 (t, *J*=7 Hz, 2H, -OCH<sub>2</sub>-), 1.86-1.81 (m, 2H, -OCH<sub>2</sub>CH<sub>2</sub>-), 1.59-1.27 (m, 10H, -CH<sub>2</sub>-), 0.91 (t, *J*=6.5 Hz, 3H, -CH<sub>3</sub>). <sup>13</sup>C NMR (100 MHz, CDCl<sub>3</sub>) δ (ppm); 164.50, 160.34, 155.62, 149.91, 143.55,

132.78, 129.23, 128.97, 127.82, 118.55, 114.93, 112.07, 110.50, 106.33, 68.18, 54.70, 31.94, 29.68, 29.41, 29.38, 26.07, 22.71, 14.13. MS (m/z): 415.2 (M+H)<sup>+</sup>. Anal. Calcd. For. C<sub>27</sub>H<sub>30</sub>N<sub>2</sub>O<sub>2</sub>: C. 78.23; H. 7.29; N. 6.76; Found: C. 78.47; H. 7.33; N. 6.79.

*4-(2-(4-(Decyloxy)phenyl)-6-methoxypyridin-4-yl)benzotrile (LC<sub>17</sub>)*. Yield 74 %. FTIR (cm<sup>-1</sup>): 2915, 2852, 2221, 1580, 1240, 1171, 1020, 827. <sup>1</sup>H NMR (500 MHz, CDCl<sub>3</sub>) δ (ppm) 8.05 (d, *J*=8 Hz, 2H, Ar-H), 7.84 (d, *J*=8 Hz, 2H, Ar-H), 7.78 (d, *J*=8 Hz, 2H, Ar-H), 7.46 (s, 1H, Ar-H (Pyridine)), 7.01 (d, *J*=8 Hz, 2H, Ar-H), 6.82 (s, 1H, Ar-H (Pyridine)), 4.19 (s, 3H, -OMe of Pyridine), 4.06 (t, *J*=6.5 Hz, 2H, -OCH<sub>2</sub>-), 1.86-1.81 (m, 2H, -OCH<sub>2</sub>CH<sub>2</sub>-), 1.63-1.30 (m, 14H, -CH<sub>2</sub>-), 0.91 (t, *J*=6.5 Hz, 3H, -CH<sub>3</sub>). <sup>13</sup>C NMR (100 MHz, CDCl<sub>3</sub>) δ (ppm); 164.49, 160.31, 155.59, 149.90, 143.54, 132.70, 129.19, 128.94, 127.82, 118.53, 114.89, 112.05, 110.51, 106.31, 68.28, 54.67, 31.89, 29.56, 29.40, 29.31, 29.26, 29.17, 26.04, 22.67, 14.09. MS (m/z): 443.2 (M+H)<sup>+</sup>. Anal. Calcd. For. C<sub>29</sub>H<sub>34</sub>N<sub>2</sub>O<sub>2</sub>: C. 78.70; H. 7.74; N. 6.33; Found: C. 78.95; H. 7.67; N. 6.36.

*4-(2-(4-(Dodecyloxy)phenyl)-6-methoxypyridin-4-yl)benzotrile (LC<sub>18</sub>)*. Yield 77 %. FTIR (cm<sup>-1</sup>): 2915, 2849, 2221, 1581, 1240, 1171, 1020, 827. <sup>1</sup>H NMR (500 MHz, CDCl<sub>3</sub>) δ (ppm) 8.06 (d, *J*=8 Hz, 2H, Ar-H), 7.80-7.75 (m, 4H, Ar-H), 7.46 (s, 1H, Ar-H (Pyridine)), 7.01 (d, *J*=8 Hz, 2H, Ar-H), 6.82 (s, 1H, Ar-H (Pyridine)), 4.10 (s, 3H, -OMe of Pyridine), 4.07 (t, *J*=6.7 Hz, 2H, -OCH<sub>2</sub>-), 1.86-1.81 (m, 2H, -OCH<sub>2</sub>CH<sub>2</sub>-), 1.59-1.28 (m, 18H, -CH<sub>2</sub>-), 0.91 (t, *J*=7.5 Hz, 3H, -CH<sub>3</sub>). <sup>13</sup>C NMR (100 MHz, CDCl<sub>3</sub>) δ (ppm); 164.48, 160.30, 155.57, 149.88, 143.52, 132.73, 129.17, 128.93, 127.80, 118.52, 114.87, 112.03, 110.48, 106.31, 68.29, 54.66, 31.91, 29.63, 29.58, 29.40, 29.34, 29.25, 26.03, 22.67, 14.09. MS (m/z): 471.3 (M+H)<sup>+</sup>. Anal. Calcd. For. C<sub>31</sub>H<sub>38</sub>N<sub>2</sub>O<sub>2</sub>: C. 79.11; H. 8.14; N. 5.95; Found: C. 79.33; H. 8.17; N. 5.92.

*4-(2-Methoxy-6-(4-(tetradecyloxy)phenyl)pyridin-4-yl)benzotrile (LC<sub>19</sub>)*. Yield 69 %. FTIR (cm<sup>-1</sup>): 2915, 2848, 2223, 1602, 1241, 1171, 1023, 829. <sup>1</sup>H NMR (500 MHz, CDCl<sub>3</sub>) δ (ppm) 8.05 (d, *J*=8.5 Hz, 2H, Ar-H), 7.80-7.75 (m, 4H, Ar-H), 7.46 (s, 1H, Ar-H (Pyridine)), 7.01 (d, *J*=8.5 Hz, 2H, Ar-H), 6.82 (s, 1H, Ar-H (Pyridine)), 4.10 (s,

3H, -OMe of Pyridine), 4.06 (t,  $J=7.2$  Hz, 2H, -OCH<sub>2</sub>-), 1.85-1.82 (m, 2H, -OCH<sub>2</sub>CH<sub>2</sub>-), 1.51-1.28 (m, 22H, -CH<sub>2</sub>-), 0.90 (t,  $J=7.5$  Hz, 3H, -CH<sub>3</sub>). <sup>13</sup>C NMR (100 MHz, CDCl<sub>3</sub>) δ (ppm); 164.52, 160.34, 155.61, 149.91, 143.56, 132.77, 129.21, 128.97, 127.84, 118.55, 114.91, 112.07, 110.52, 106.33, 68.19, 54.70, 31.95, 29.69, 29.62, 29.43, 29.38, 29.29, 29.20, 26.07, 22.71, 14.13. MS (m/z): 499.3 (M+H)<sup>+</sup>. Anal. Calcd. For. C<sub>33</sub>H<sub>42</sub>N<sub>2</sub>O<sub>2</sub>: C. 79.48; H. 8.49; N. 5.62; Found: C. 79.72; H. 8.53; N. 5.55.

*6-(4-(Decyloxy)phenyl)-4-(4-fluorophenyl)-2-methoxynicotinonitrile (LC<sub>20</sub>)*. Yield 68 %. FTIR (cm<sup>-1</sup>): 2914, 2851, 2218, 1588, 1231, 1170, 1016, 825. <sup>1</sup>H NMR (400 MHz, CDCl<sub>3</sub>) δ (ppm) 8.06 (d,  $J=8.4$  Hz, 2H, Ar-H), 7.66-7.62 (m, 2H, Ar-H), 7.37 (s, 1H, Pyridine-H), 7.26-7.20 (m, 2H, Ar-H), 6.99 (d,  $J=8.4$  Hz, 2H, Ar-H), 4.19 (s, 3H, -OMe of Pyridine), 4.02 (t,  $J=6$  Hz, 2H, -OCH<sub>2</sub>-), 1.83-1.80 (m, 2H, -OCH<sub>2</sub>CH<sub>2</sub>-), 1.65-1.27 (m, 14H, -CH<sub>2</sub>-), 0.87 (t,  $J=6.6$  Hz, 3H, -CH<sub>3</sub>). <sup>13</sup>C NMR (100 MHz, CDCl<sub>3</sub>) δ (ppm); 165.02, 162.48, 161.40, 157.91, 155.30, 132.56, 130.40, 129.45, 128.84, 116.18, 114.80, 112.35, 91.88, 68.24, 54.50, 31.88, 29.54, 29.37, 29.30, 29.18, 26.01, 22.66, 14.08. MS (m/z): 461.2 (M+H)<sup>+</sup>. Anal. Calcd. For. C<sub>29</sub>H<sub>33</sub>FN<sub>2</sub>O<sub>2</sub>: C. 75.62; H. 7.22; N. 6.08; Found: C. 75.91; H. 7.17; N. 6.16.

*6-(4-(Dodecyloxy)phenyl)-4-(4-fluorophenyl)-2-methoxynicotinonitrile (LC<sub>21</sub>)*. Yield 73 %. FTIR (cm<sup>-1</sup>): 2917, 2855, 2218, 1592, 1240, 1174, 1016, 827. <sup>1</sup>H NMR (400 MHz, CDCl<sub>3</sub>) δ (ppm) 8.06 (d,  $J=8.8$  Hz, 2H, Ar-H), 7.66-7.62 (m, 2H, Ar-H), 7.37 (s, 1H, Pyridine-H), 7.26-7.20 (m, 2H, Ar-H), 6.99 (d,  $J=8.8$  Hz, 2H, Ar-H), 4.19 (s, 3H, -OMe of Pyridine), 4.02 (t,  $J=6.6$  Hz, 2H, -OCH<sub>2</sub>-), 1.83-1.80 (m, 2H, -OCH<sub>2</sub>CH<sub>2</sub>-), 1.64-1.26 (m, 18H, -OCH<sub>2</sub>-), 0.87 (t,  $J=6.6$  Hz, -CH<sub>3</sub>). <sup>13</sup>C NMR (100 MHz, CDCl<sub>3</sub>) δ (ppm); 165.02, 162.48, 161.39, 157.91, 155.29, 132.56, 130.40, 129.45, 128.84, 116.18, 114.78, 112.34, 91.88, 68.24, 54.50, 31.90, 29.62, 29.57, 29.36, 29.17, 26.01, 22.67, 14.09. MS (m/z): 489.3 (M+H)<sup>+</sup>. Anal. Calcd. For. C<sub>31</sub>H<sub>37</sub>FN<sub>2</sub>O<sub>2</sub>: C. 76.20; H. 7.63; N. 5.73; Found: C. 76.45; H. 7.59; N. 5.77.

*4-(4-Fluorophenyl)-2-methoxy-6-(4-(tetradecyloxy)phenyl)nicotinonitrile (LC<sub>22</sub>)*. Yield 78 %. FTIR (cm<sup>-1</sup>): 2913, 2850, 2216, 1589, 1235, 1172, 1012, 825. <sup>1</sup>H NMR (400 MHz, CDCl<sub>3</sub>) δ (ppm) 8.06 (d,  $J=8.8$  Hz, 2H, Ar-H), 7.66-7.62 (m, 2H, Ar-H),

7.37 (s, 1H, Pyridine-H), 7.26-7.22 (m, 2H, Ar-H), 6.99 (d,  $J=8.8$  Hz, Ar-H), 4.19 (s, 3H, -OMe of Pyridine), 4.02 (t,  $J=6.6$  Hz, 2H, -OCH<sub>2</sub>-), 1.83-1.79 (m, 2H, -OCH<sub>2</sub>CH<sub>2</sub>-), 1.69-1.25 (m, 22H, -CH<sub>2</sub>-), 0.87 (t,  $J=6.6$  Hz, -CH<sub>3</sub>). <sup>13</sup>C NMR (100 MHz, CDCl<sub>3</sub>)  $\delta$  (ppm); 165.03, 162.49, 161.40, 157.91, 155.30, 132.57, 130.40, 129.46, 128.84, 116.19, 114.80, 112.35, 91.89, 68.24, 54.51, 31.91, 29.64, 29.58, 29.37, 29.18, 26.01, 22.67, 14.09. MS (m/z): 517.3 (M+H)<sup>+</sup>. Anal. Calcd. For. C<sub>33</sub>H<sub>41</sub>N<sub>2</sub>O<sub>2</sub>: C. 76.71; H. 8.00; N. 5.42; Found: C. 76.42; H. 8.06; N. 5.47.

*4-(4-Chlorophenyl)-6-(4-(decyloxy)phenyl)-2-methoxynicotinonitrile (LC<sub>23</sub>)*. Yield 68 %. FTIR (cm<sup>-1</sup>): 2911, 2849, 2216, 1583, 1237, 1173, 1020, 823. <sup>1</sup>H NMR (500 MHz, CDCl<sub>3</sub>)  $\delta$  (ppm) 8.07 (d,  $J=9$  Hz, 2H, Ar-H), 7.60 (d,  $J=8.5$  Hz, 2H, Ar-H), 7.52 (d,  $J=9$  Hz, 2H, Ar-H), 7.38 (s, 1H, Pyridine-H), 7.01 (d,  $J=9$  Hz, 2H, Ar-H), 4.21 (s, 3H, -OMe of Pyridine), 4.09-4.04 (m, 2H, -OCH<sub>2</sub>-), 1.86-1.81 (m, 2H, -OCH<sub>2</sub>CH<sub>2</sub>-), 1.52-1.27 (m, 14H, -CH<sub>2</sub>-), 0.90 (t,  $J=7$  Hz, 3H, -CH<sub>3</sub>). <sup>13</sup>C NMR (100 MHz, CDCl<sub>3</sub>)  $\delta$  (ppm); 165.06, 161.47, 158.05, 155.15, 136.25, 134.95, 129.73, 128.89, 115.63, 114.84, 112.26, 91.84, 68.17, 54.57, 31.91, 29.72, 29.58, 29.40, 29.33, 26.04, 22.69, 14.12. MS (m/z): 477.2 (M+H)<sup>+</sup>. Anal. Calcd. For. C<sub>29</sub>H<sub>33</sub>ClN<sub>2</sub>O<sub>2</sub>: C. 73.02; H. 6.97; N. 5.87; Found: C. 73.28; H. 6.93; N. 5.81.

*4-(4-Chlorophenyl)-6-(4-(dodecyloxy)phenyl)-2-methoxynicotinonitrile (LC<sub>24</sub>)*. Yield 71 %. FTIR (cm<sup>-1</sup>): 2914, 2851, 2215, 1589, 1238, 1172, 1014, 824. <sup>1</sup>H NMR (500 MHz, CDCl<sub>3</sub>)  $\delta$  (ppm) 8.07 (d,  $J=9$  Hz, 2H, Ar-H), 7.60 (d,  $J=8.5$  Hz, 2H, Ar-H), 7.52 (d,  $J=8.5$  Hz, 2H, Ar-H), 7.38 (s, 1H, Pyridine-H), 7.01 (d,  $J=9$  Hz, 2H, Ar-H), 4.21 (s, 3H, -OMe of Pyridine), 4.07-4.04 (m, 2H, -OCH<sub>2</sub>-), 1.85-1.81 (m, 2H, -OCH<sub>2</sub>CH<sub>2</sub>-), 1.51-1.29 (m, 18H, -CH<sub>2</sub>-), 0.90 (t,  $J=7$  Hz, 3H, -CH<sub>3</sub>). <sup>13</sup>C NMR (100 MHz, CDCl<sub>3</sub>)  $\delta$  (ppm); 165.02, 161.45, 158.01, 155.17, 136.22, 134.93, 129.77, 128.88, 115.62, 114.82, 112.23, 91.88, 68.15, 54.50, 31.91, 29.72, 29.58, 29.40, 29.33, 26.04, 22.69, 14.12. MS (m/z): 505.2 (M+H)<sup>+</sup>. Anal. Calcd. For. C<sub>31</sub>H<sub>37</sub>ClN<sub>2</sub>O<sub>2</sub>: C. 73.72; H. 7.38; N. 5.55; Found: C. 73.97; H. 7.44; N. 5.49.

*4-(4-Chlorophenyl)-2-methoxy-6-(4-(tetradecyloxy)phenyl)nicotinonitrile (LC<sub>25</sub>)*. Yield 75 %. FTIR (cm<sup>-1</sup>): 2919, 2850, 2224, 1588, 1242, 1175, 1016, 828. <sup>1</sup>H NMR (500 MHz, CDCl<sub>3</sub>)  $\delta$  (ppm) 8.07 (d,  $J=9$  Hz, 2H, Ar-H), 7.60 (d,  $J=8.5$  Hz, 2H, Ar-



H), 7.52 (d,  $J=8.5$  Hz, 2H, Ar-H), 7.38 (s, 1H, Pyridine-H), 7.01 (d,  $J=9$  Hz, Ar-H), 4.21 (s, 3H, -OMe of Pyridine), 4.06-4.04 (m, 2H, -OCH<sub>2</sub>-), 1.86-1.81 (m, 2H, -OCH<sub>2</sub>CH<sub>2</sub>-), 1.52-1.28 (m, 22H, -CH<sub>2</sub>-), 0.89 (t,  $J=7$  Hz, -CH<sub>3</sub>). <sup>13</sup>C NMR (100 MHz, CDCl<sub>3</sub>)  $\delta$  (ppm); 164.98, 161.40, 157.91, 155.31, 132.58, 130.41, 129.47, 128.85, 116.20, 114.81, 112.36, 91.90, 68.25, 54.51, 31.92, 29.65, 29.58, 29.37, 29.19, 26.02, 22.68, 14.10. MS (m/z): 533.3 (M+H)<sup>+</sup>. Anal. Calcd. For. C<sub>33</sub>H<sub>41</sub>ClN<sub>2</sub>O<sub>2</sub>: C. 74.34; H. 7.75; N. 5.25; Found: C. 74.59; H. 7.80; N. 5.17.

*4-(4-Bromophenyl)-2-(4-(decyloxy)phenyl)-6-methoxypyridine (LC<sub>26</sub>)*. Yield 79 %. FTIR (cm<sup>-1</sup>): 2918, 2854, 1587, 1238, 1171, 1020, 827. <sup>1</sup>H NMR (400 MHz, CDCl<sub>3</sub>)  $\delta$  (ppm) 8.03 (d,  $J=14.4$  Hz, 2H, Ar-H), 7.59 (d,  $J=10.8$  Hz, Ar-H), 7.51 (d,  $J=10.8$  Hz, 2H, Ar-H), 7.43 (s, 1H, Pyridine-H), 6.98 (d,  $J=14.4$  Hz, 2H, Ar-H), 6.78 (s, 1H, Pyridine-H), 4.07 (s, 3H, -OMe of Pyridine), 4.02 (t,  $J=6.6$  Hz, 2H, -OCH<sub>2</sub>-), 1.85-1.78 (m, 2H, -OCH<sub>2</sub>CH<sub>2</sub>-), 1.55-1.26 (m, 14 H, -CH<sub>2</sub>-), 0.89 (t,  $J=7.5$  Hz, 3H, -CH<sub>3</sub>). <sup>13</sup>C NMR (100 MHz, CDCl<sub>3</sub>)  $\delta$  (ppm); 164.45, 160.14, 155.23, 150.69, 137.90, 132.10, 131.40, 128.85, 128.06, 123.14, 114.57, 110.50, 105.87, 68.13, 53.39, 32.76, 30.04, 29.69, 29.58, 29.41, 29.32, 29.27, 29.16, 28.95, 27.41, 26.05, 22.68, 19.72, 14.10. MS (m/z): 497.2 (M+H)<sup>+</sup>. Anal. Calcd. For. C<sub>28</sub>H<sub>34</sub>BrNO<sub>2</sub>: C. 67.74; H. 6.90; N. 2.82; Found: C. 67.48; H. 6.99; N. 2.85.

*4-(4-Bromophenyl)-2-(4-(dodecyloxy)phenyl)-6-methoxypyridine (LC<sub>27</sub>)*. Yield 82 %. FTIR (cm<sup>-1</sup>): 2920, 2855, 1591, 1235, 1171, 1020, 827. <sup>1</sup>H NMR (400 MHz, CDCl<sub>3</sub>)  $\delta$  (ppm) 8.04 (d,  $J=14.4$  Hz, 2H, Ar-H), 7.58 (d,  $J=10.8$  Hz, Ar-H), 7.53 (d,  $J=10.8$  Hz, 2H, Ar-H), 7.43 (s, 1H, Pyridine-H), 6.98 (d,  $J=14.4$  Hz, 2H, Ar-H), 6.77 (s, 1H, Pyridine-H), 4.06 (s, 3H, -OMe of Pyridine), 4.02 (t,  $J=6.6$  Hz, 2H, -OCH<sub>2</sub>-), 1.85-1.78 (m, 2H, -OCH<sub>2</sub>CH<sub>2</sub>-), 1.55-1.26 (m, 18 H, -CH<sub>2</sub>-), 0.89 (t,  $J=7.5$  Hz, 3H, -CH<sub>3</sub>). <sup>13</sup>C NMR (100 MHz, CDCl<sub>3</sub>)  $\delta$  (ppm); 165.04, 161.45, 158.05, 155.05, 135.40, 132.20, 129.93, 128.87, 128.07, 124.50, 114.82, 110.53, 105.87, 68.25, 53.41, 31.91, 29.63, 29.58, 29.37, 29.32, 29.27, 29.18, 26.01, 22.68, 14.10. MS (m/z): 523.2 (M+H)<sup>+</sup>. Anal. Calcd. For. C<sub>30</sub>H<sub>38</sub>BrNO<sub>2</sub>: C. 68.69; H. 7.30; N. 2.67; Found: C. 68.92; H. 7.39; N. 2.63.

*4-(4-Bromophenyl)-2-methoxy-6-(4-(tetradecyloxy)phenyl)pyridine (LC<sub>28</sub>)*. Yield 71 %. FTIR (cm<sup>-1</sup>): 2917, 2849, 1594, 1231, 1168, 1020, 827. <sup>1</sup>H NMR (400 MHz, CDCl<sub>3</sub>) δ (ppm) 8.03 (d, *J*=12.4 Hz, 2H, Ar-H), 7.65 (d, *J*=12.8 Hz, Ar-H), 7.50 (d, *J*=12.8 Hz, 2H, Ar-H), 7.43 (s, 1H, Pyridine-H), 6.98 (d, *J*=12.4 Hz, 2H, Ar-H), 6.78 (s, 1H, Pyridine-H), 4.06 (s, 3H, -OMe of Pyridine), 4.02 (t, *J*=6.6 Hz, 2H, -OCH<sub>2</sub>-), 1.84-1.77 (m, 2H, -OCH<sub>2</sub>CH<sub>2</sub>-), 1.53-1.26 (m, 22 H, -CH<sub>2</sub>-), 0.89 (t, *J*=7.5 Hz, 3H, -CH<sub>3</sub>). <sup>13</sup>C NMR (100 MHz, CDCl<sub>3</sub>) δ (ppm); 164.47, 160.10, 155.22, 150.67, 137.88, 132.10, 131.38, 128.85, 128.06, 123.16, 114.57, 110.50, 105.83, 68.19, 53.37, 31.52, 29.69, 29.58, 29.41, 29.32, 29.27, 28.95, 27.41, 26.05, 22.68, 19.72, 14.10. MS (m/z): 553.5 (M+H)<sup>+</sup>. Anal. Calcd. For. C<sub>32</sub>H<sub>42</sub>BrNO<sub>2</sub>: C. 69.55; H. 7.66; N. 2.53; Found: C. 69.76; H. 7.62; N. 2.48.

*2-(4-(Decyloxy)phenyl)-6-methoxy-4-(4-nitrophenyl)pyridine (LC<sub>29</sub>)*. Yield 46 %. FTIR (cm<sup>-1</sup>): 2915, 2853, 1579, 1241, 1173, 1020, 829. <sup>1</sup>H NMR (500 MHz, CDCl<sub>3</sub>) δ (ppm) 8.41 (d, *J*=9 Hz, 2H, Ar-H), 8.08 (d, *J*=9 Hz, 2H, Ar-H), 7.83 (d, *J*=8.5 Hz, 2H, Ar-H), 7.60 (s, 1H, Pyridine-H), 7.10 (s, 1H, Pyridine-H), 7.02 (d, *J*=8.5 Hz, 2H, Ar-H), 4.20 (s, 3H, OMe of Pyridine), 4.07-4.04 (m, 2H, -OCH<sub>2</sub>-), 1.85-1.82 (m, 2H, -OCH<sub>2</sub>CH<sub>2</sub>-), 1.51-1.28 (m, 14H, -CH<sub>2</sub>-), 0.90 (t, *J*=7 Hz, 3H, -CH<sub>3</sub>). <sup>13</sup>C NMR (100 MHz, CDCl<sub>3</sub>) δ (ppm); 164.99, 161.70, 158.53, 148.63, 142.69, 129.54, 128.97, 124.15, 115.11, 114.91, 112.07, 68.29, 54.70, 31.91, 29.63, 29.56, 29.37, 29.34, 29.17, 26.01, 22.68, 14.10. MS (m/z): 463.3 (M+H)<sup>+</sup>. Anal. Calcd. For. C<sub>28</sub>H<sub>34</sub>N<sub>2</sub>O<sub>4</sub>: C. 72.70; H. 7.41; N. 6.06; Found: C. 72.46; H. 7.47; N. 6.09.

*2-(4-(Dodecyloxy)phenyl)-6-methoxy-4-(4-nitrophenyl)pyridine (LC<sub>30</sub>)*. Yield 48 %. FTIR (cm<sup>-1</sup>): 2913, 2850, 1576, 1238, 1171, 1018, 827. <sup>1</sup>H NMR (500 MHz, CDCl<sub>3</sub>) δ (ppm) 8.40 (d, *J*=8.5 Hz, 2H, Ar-H), 8.08 (d, *J*=8.5 Hz, 2H, Ar-H), 7.82 (d, *J*=8.5 Hz, 2H, Ar-H), 7.60 (s, 1H, Pyridine-H), 7.10 (s, 1H, Pyridine-H), 7.02 (d, *J*=8.5 Hz, 2H, Ar-H), 4.23 (s, 3H, -OMe of Pyridine), 4.05 (t, *J*=6.5 Hz, 2H, -OCH<sub>2</sub>-), 1.87-1.81 (m, 2H, -OCH<sub>2</sub>CH<sub>2</sub>-), 1.52-1.27 (m, 18H, -CH<sub>2</sub>-), 0.90 (t, *J*=7 Hz, 3H, -CH<sub>3</sub>). <sup>13</sup>C NMR (100 MHz, CDCl<sub>3</sub>) δ (ppm); 164.95, 161.72, 158.51, 148.65, 142.67, 129.51, 128.95, 124.14, 115.10, 114.94, 112.07, 68.26, 54.72, 31.91, 29.63, 29.56, 29.37, 29.34, 29.17, 26.01, 22.68, 14.10. MS (m/z): 491.3 (M+H)<sup>+</sup>. Anal. Calcd. For. C<sub>30</sub>H<sub>38</sub>N<sub>2</sub>O<sub>4</sub>: C. 73.44; H. 7.81; N. 5.71; Found: C. 73.71; H. 7.76; N. 5.66.

*2-Methoxy-4-(4-nitrophenyl)-6-(4-(tetradecyloxy)phenyl)pyridine (LC<sub>31</sub>)*. Yield 55 %. FTIR (cm<sup>-1</sup>): 2914, 2850, 1586, 1250, 1173, 1022, 828. <sup>1</sup>H NMR (500 MHz, CDCl<sub>3</sub>) δ (ppm) 8.40 (d, *J*=9 Hz, 2H, Ar-H), 8.08 (d, *J*=9 Hz, 2H, Ar-H), 7.82 (d, *J*=8.5 Hz, 2H, Ar-H), 7.71 (s, 1H, Pyridine-H), 7.30 (s, 1H, Pyridine-H), 7.02 (d, *J*=8.5 Hz, 2H, Ar-H), 4.23 (s, 3H, -OMe of Pyridine), 4.06 (t, *J*=6.5 Hz, 2H, -OCH<sub>2</sub>-), 1.85-1.82 (m, 2H, -OCH<sub>2</sub>CH<sub>2</sub>-), 1.51-1.28 (m, 22H, -CH<sub>2</sub>-), 0.89 (t, *J*=7 Hz, 3H, -CH<sub>3</sub>). <sup>13</sup>C NMR (100 MHz, CDCl<sub>3</sub>) δ (ppm); 164.97, 161.74, 158.58, 148.66, 142.64, 129.57, 128.93, 124.11, 115.15, 114.97, 112.03, 68.23, 54.72, 31.91, 29.62, 29.55, 29.37, 29.34, 29.17, 26.01, 22.68, 14.10. MS (m/z): 519.3 (M+H)<sup>+</sup>. Anal. Calcd. For. C<sub>32</sub>H<sub>42</sub>N<sub>2</sub>O<sub>4</sub>: C. 74.10; H. 8.16; N. 5.40; Found: C. 74.41; H. 8.12; N. 5.46.

*2-Methoxy-4-(pyridin-4-yl)-6-(4-(tetradecyloxy)phenyl)pyridine (LC<sub>32</sub>)*. Yield 68 %. FTIR (cm<sup>-1</sup>): 2918, 2851, 1588, 1254, 1176, 1022, 828. <sup>1</sup>H NMR (400 MHz, CDCl<sub>3</sub>) δ (ppm) 8.72 (d, *J*=6 Hz, 2H, Pyridine-H), 8.03 (d, *J*=8.8 Hz, 2H, Ar-H), 7.54 (d, *J*=6 Hz, 2H, Pyridine-H), 7.48 (s, 1H, Pyridine-H), 6.99 (d, *J*=8.8 Hz, 2H, Ar-H), 6.84 (s, 1H, Pyridine-H), 4.08 (s, 3H, -OMe of Pyridine), 4.02 (t, *J*=6.6 Hz, 2H, -OCH<sub>2</sub>-), 1.85-1.78 (m, 2H, -OCH<sub>2</sub>CH<sub>2</sub>-), 1.51-1.26 (m, 22H, -CH<sub>2</sub>-), 0.87 (t, *J*=6.8 Hz, 3H, -CH<sub>3</sub>). <sup>13</sup>C NMR (100 MHz, CDCl<sub>3</sub>) δ (ppm); 164.52, 160.30, 155.65, 150.55, 149.10, 146.37, 131.10, 129.81, 128.94, 128.10, 122.67, 121.55, 114.99, 114.64, 110.25, 106.15, 68.16, 53.51, 31.92, 29.65, 29.59, 29.40, 29.35, 29.26, 26.04, 22.68, 14.10. MS (m/z): 475.4 (M+H)<sup>+</sup>. Anal. Calcd. For. C<sub>31</sub>H<sub>42</sub>N<sub>2</sub>O<sub>2</sub>: C. 78.44; H. 8.92; N. 5.90; Found: C. 78.68; H. 8.97; N. 5.83.

*4-(4-(Decyloxy)phenyl)-2-methoxy-6-(thiophen-2-yl)nicotinonitrile (LC<sub>33</sub>)*. Yield 79 %. FTIR (cm<sup>-1</sup>): 2917, 2850, 2213, 1580, 1514, 1450, 1365, 1236, 1135, 1031, 828, 692. <sup>1</sup>H NMR (400 MHz, CDCl<sub>3</sub>) δ (ppm) 7.71 (d, *J*=3.2 Hz, 1H, Thiophene-H), 7.60 (d, *J*=8.8 Hz, 2H, Ar-H), 7.49 (d, *J*=4.8 Hz, 1H, Thiophene-H), 7.32 (s, 1H, Pyridine-H), 7.14 (t, *J*=4.8 Hz, 1H, Thiophene-H), 7.02 (d, *J*=8.8 Hz, 2H, Ar-H), 4.15 (s, 3H, -OMe of Pyridine), 4.02 (t, *J*=6.4 Hz, 2H, -OCH<sub>2</sub>-), 1.83-1.79 (m, 2H, -OCH<sub>2</sub>CH<sub>2</sub>-), 1.49-1.28 (m, 14H, -CH<sub>2</sub>-), 0.88 (t, *J*=6.8 Hz, 3H, -CH<sub>3</sub>). <sup>13</sup>C NMR (100 MHz, CDCl<sub>3</sub>) δ (ppm); 165.08, 160.78, 156.20, 152.86, 143.41, 129.77, 129.66, 128.07, 126.83, 115.92, 114.92, 111.57, 110.48, 91.97, 68.23, 54.62, 31.89, 29.56, 29.36, 29.31, 29.17, 26.01, 22.67, 14.09. MS (m/z): 449.2 (M+H)<sup>+</sup>. Anal. Calcd. For.

C<sub>27</sub>H<sub>32</sub>N<sub>2</sub>O<sub>2</sub>S: C. 72.29; H. 7.19; N. 6.24; S. 7.15; Found: C. 72.55; H. 7.24; N. 6.27; S. 7.13.

### 3.3.3 Synthesis of 2-(4,6-disubstituted aryl-3-cyanopyridyl)oxyacetohydrazones (Series-III; LC<sub>34-38</sub>)

New 2-(4,6-disubstituted aryl-3-cyanopyridyl)oxy acetohydrazones belonging to **Series-III** were synthesized and their structures were confirmed by spectroscopic techniques as well as elemental analysis. Further, their experimental results are discussed in the following section.

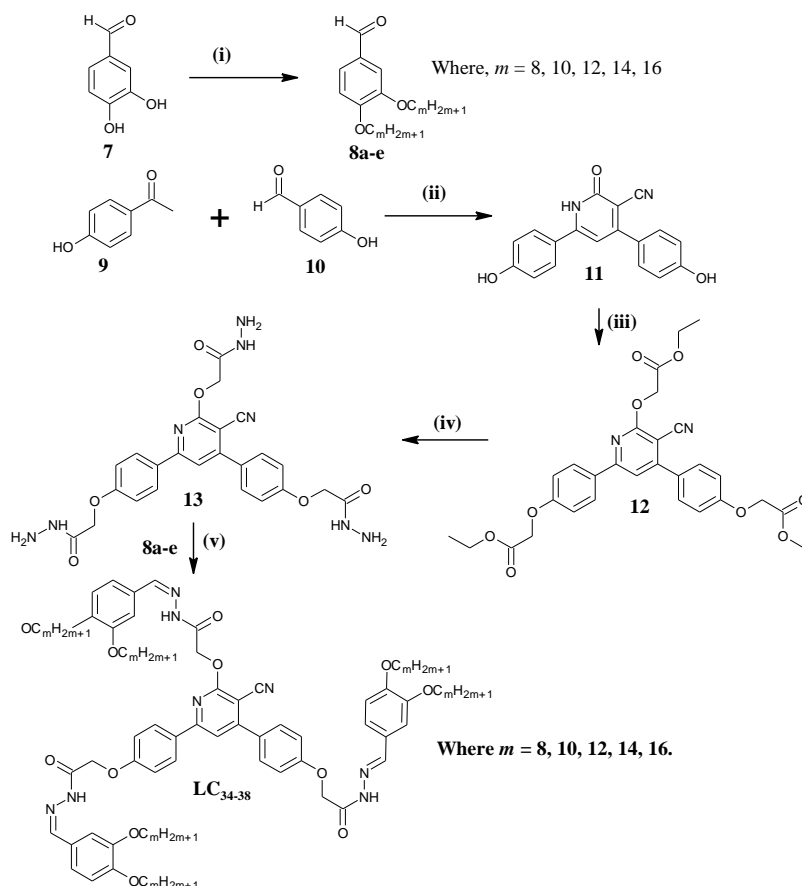
#### 3.3.3.1 Results and discussion

##### *Synthesis:*

The synthetic route for the preparation of **LC<sub>34-38</sub>** is illustrated in **Scheme 3.3**. The required 3,4-bis(alkoxy)benzaldehyde (**8a-e**) was prepared by O-alkylation of 3,4-dihydroxybenzaldehyde (**7**) with appropriate alkyl bromides (Attias et al. 2002). On the other hand, compound **11** was prepared by one pot reaction of 4-hydroxyacetophenone (**9**) and 4-hydroxybenzaldehyde (**10**) with ethyl cyanoacetate in presence of excess ammonium acetate using 1,4-dioxane as a solvent. Further, the reaction of intermediate **11** with ethyl chloroacetate and anhydrous potassium carbonate in dry DMF afforded tri-ester **12** in good yield (71 %). Furthermore, the reaction of compound **12** with hydrazine hydrate in boiling ethanol gave the trihydrazide **13**. Finally, the trihydrazide derivative **13** was condensed with substituted benzaldehyde **8a-e** in presence of glacial acetic acid as a catalyst to obtain target trihydrazone functionalized cyanopyridines **LC<sub>34-38</sub>**.

The structures of newly synthesized compounds were confirmed by FTIR, <sup>1</sup>H NMR, <sup>13</sup>C NMR spectroscopy and elemental analysis. The FTIR spectrum of **8a** showed absorption bands at about 2935, 2863 and 1662 cm<sup>-1</sup> corresponding to stretching vibrations of C-H (asym), C-H (sym) and HC=O (aldehyde) groups, respectively. Its <sup>1</sup>H NMR spectrum showed a singlet at δ 9.80 ppm due to protons of CHO group as well as signals in the region of δ 7.49-7.08 ppm due to aromatic protons. In the FTIR spectrum of cyanopyridone **11**, the observed absorption bands at 3530, 3325, 2222, 1666 and 1596 cm<sup>-1</sup> are due to stretching vibrations of O-H, N-H,

$C\equiv N$ ,  $C=O$  and  $C=N$  groups, respectively. Further, its  $^1H$  NMR spectrum showed a singlet at  $\delta$  12.40 ppm due to a N-H proton, two singlets at  $\delta$  10.15 and 10.04 ppm due to two O-H protons, and multiplets in the region of  $\delta$  7.74-6.84 ppm due to aromatic protons. The FTIR spectrum of compound **12** showed an absorption band at  $1749\text{ cm}^{-1}$ , due to stretching vibration of  $C=O$  of tri-ester groups. In  $^1H$  NMR spectrum, it displayed a singlet due to the protons of  $OCH_2CO$  group. Furthermore, FTIR spectrum of trihydrazone compound **13** showed the appearance of absorption bands at  $3442$  and  $3326\text{ cm}^{-1}$  due to  $NH_2$ ,  $NH$  functional groups, respectively, in addition to the peaks due to  $C=O$  and  $C\equiv N$  vibrations. Also, its  $^1H$  NMR spectrum displayed two peaks at  $\delta$  9.39 and 4.39 ppm which are due to protons of  $NH$  and  $NH_2$  groups, respectively.



**Scheme 3.3** Synthesis of new 2-(4,6-disubstituted aryl-3-cyanopyridyl) oxy acetohydrazone (**LC<sub>34-38</sub>**). Reagents and conditions: (i) alkyl bromides, anhydrous  $K_2CO_3$ , DMF,  $80\text{ }^\circ C$ , 12h; (ii) ethyl cyanoacetate, ammonium acetate, 1,4-dioxane, reflux, 12h; (iii) ethyl chloroacetate, anhydrous  $K_2CO_3$ , DMF,  $80\text{ }^\circ C$ , 12h; (iv)  $NH_2NH_2 \cdot H_2O$ , EtOH, reflux, 12h; (v) few drops of acetic acid, EtOH, reflux, 12h

Further, in the FTIR spectrum of **LC**<sub>34</sub>, absorption bands at 3215, 2218 and 1670 cm<sup>-1</sup> are due to stretching vibrations of NH, C≡N and C=O groups, respectively. Furthermore, its <sup>1</sup>H NMR spectrum exhibited two singlets at δ 11.51 and 7.91 ppm due to protons of NH and HC=N (azomethine) groups, respectively, confirming the formation of target compounds. In addition, the observed mass peak [M+H]<sup>+</sup> at 1554.4 for compound **LC**<sub>34</sub> is consistent with the calculated molecular weight for the formula of C<sub>93</sub>H<sub>133</sub>N<sub>8</sub>O<sub>12</sub>. **Figures 3.31-3.34** summarize the FTIR, <sup>1</sup>H NMR, <sup>13</sup>C NMR and Mass spectra of representative compound **LC**<sub>34</sub>.

### 3.3.3.2 Experimental procedures

The synthetic protocols for the preparation of intermediates as well as the new target compounds **LC**<sub>34-38</sub> are described in the following paragraphs.

#### *General procedure for the preparation of 3,4-bis(alkoxy)benzaldehydes (8a-e)*

A mixture of 3,4-dihydroxybenzaldehyde **7** (10 mmol), corresponding alkylbromide (21 mmol), anhydrous potassium carbonate (24 mmol) in dry DMF (40 ml) was heated with stirring at 80 °C for 12 h. After completion of the reaction, the reaction mixture was cooled and plunged into ice-cold water. The separated solid was filtered and recrystallized from ethanol to get pure compound **8a-e**. Their characterization data are as follows.

*3,4-Bis(octyloxy)benzaldehyde (8a)*. Yield 87 %, m.p. 59-60 °C. FTIR (cm<sup>-1</sup>): 2935, 2863, 1662, 1506, 1267, 1129, 1060, 803. <sup>1</sup>H NMR (400 MHz, DMSO-*d*<sub>6</sub>) δ (ppm) 9.80 (s, 1H, -CHO), 7.49 (d, *J*=8.4 Hz, 1H, Ar-H), 7.36 (s, 1H, Ar-H), 7.12 (d, *J*=8.4 Hz, 1H, Ar-H), 4.04 (t, *J*=6.2 Hz, 2H, -OCH<sub>2</sub>-), 3.98 (t, *J*=6.2 Hz, 2H, -OCH<sub>2</sub>-), 1.75-1.24 (m, 24H, -CH<sub>2</sub>-), 0.83 (t, *J*=6.6 Hz, 6H, -CH<sub>3</sub>). <sup>13</sup>C NMR (100 MHz, DMSO-*d*<sub>6</sub>) δ (ppm); 191.83, 154.52, 149.17, 129.98, 126.38, 112.85, 111.74, 68.87, 68.79, 31.69, 29.20, 29.19, 29.09, 28.99, 26.01, 25.98, 22.57, 14.38. MS (m/z): 363.3 (M+H)<sup>+</sup>. Anal. Calcd. For. C<sub>28</sub>H<sub>38</sub>O<sub>3</sub>: C. 76.20; H. 10.56. Found: C. 76.48; H. 10.49.

*3,4-Bis(decyloxy)benzaldehyde (8b)*. Yield 83 %, m.p. 66-68 °C. FTIR (cm<sup>-1</sup>): 2926, 2857, 1683, 1588, 1507, 1268, 1129, 803. <sup>1</sup>H NMR (400 MHz, DMSO-*d*<sub>6</sub>) δ (ppm) 9.80 (s, 1H, -CHO), 7.51 (d, *J*=8.4 Hz, 1H, Ar-H), 7.35 (s, 1H, Ar-H), 7.12 (d, *J*=8.4 Hz, 1H, Ar-H), 4.04 (t, *J*=6.6 Hz, 4H, -OCH<sub>2</sub>-), 1.61-1.23 (m, 32H, -CH<sub>2</sub>-), 0.84 (t,

$J=6.6$  Hz, 6H,  $-\text{CH}_3$ ).  $^{13}\text{C}$  NMR (100 MHz,  $\text{DMSO}-d_6$ )  $\delta$  (ppm); 191.60, 154.22, 149.20, 129.88, 126.10, 112.75, 111.64, 68.87, 68.79, 31.78, 29.54, 29.35, 29.21, 28.90, 22.56, 14.40. MS (m/z): 419.4 (M+H)<sup>+</sup>. Anal. Calcd. For.  $\text{C}_{27}\text{H}_{46}\text{O}_3$ : C. 77.46; H. 11.07. Found: C. 77.69; H. 11.18.

*3,4-Bis(dodecyloxy)benzaldehyde (8c)*. Yield 85 %, m.p. 73-74 °C. FTIR ( $\text{cm}^{-1}$ ): 2922, 2852, 1684, 1588, 1507, 1269, 1128, 803.  $^1\text{H}$  NMR (400 MHz,  $\text{DMSO}-d_6$ )  $\delta$  (ppm) 9.82 (s, 1H,  $-\text{CHO}$ ), 7.50 (s, 1H, Ar-H), 7.34 (s, 1H, Ar-H), 7.13 (s, 1H, Ar-H), 4.04 (t,  $J=6.6$  Hz, 4H,  $-\text{OCH}_2-$ ), 1.61-1.24 (m, 40H,  $-\text{CH}_2-$ ), 0.84 (s, 6H,  $-\text{CH}_3$ ).  $^{13}\text{C}$  NMR (100 MHz,  $\text{DMSO}-d_6$ )  $\delta$  (ppm); 191.73, 154.33, 149.37, 129.54, 126.38, 112.85, 111.74, 68.87, 68.79, 31.76, 29.47, 29.18, 28.88, 22.56, 14.42. MS (m/z): 475.4 (M+H)<sup>+</sup>. Anal. Calcd. For.  $\text{C}_{31}\text{H}_{54}\text{O}_3$ : C. 78.43; H. 11.46. Found: C. 78.71; H. 11.41.

*3,4-Bis(tetradecyloxy)benzaldehyde (8d)*. Yield 88 %, m.p. 77-78 °C.  $^1\text{H}$  NMR (400 MHz,  $\text{DMSO}-d_6$ )  $\delta$  (ppm) 9.78 (s, 1H,  $-\text{CHO}$ ), 7.34 (d,  $J=8$  Hz, 1H, Ar-H), 7.24 (s, 1H, Ar-H), 7.09 (d,  $J=8$  Hz, 1H, Ar-H), 4.04 (t,  $J=6.6$  Hz, 4H,  $-\text{OCH}_2-$ ), 1.61-1.23 (m, 48H,  $-\text{CH}_2-$ ), 0.84 (t,  $J=6.6$  Hz, 6H,  $-\text{CH}_3$ ).  $^{13}\text{C}$  NMR (100 MHz,  $\text{DMSO}-d_6$ )  $\delta$  (ppm); 191.86, 154.57, 149.21, 129.96, 126.31, 112.79, 111.77, 68.87, 68.79, 31.69, 29.23, 29.09, 28.99, 26.01, 22.58, 14.34. FTIR ( $\text{cm}^{-1}$ ): 2918, 2849, 1683, 1586, 1509, 1272, 1126, 803. MS (m/z): 531.4 (M+H)<sup>+</sup>. Anal. Calcd. For.  $\text{C}_{35}\text{H}_{62}\text{O}_3$ : C. 79.19; H. 11.77. Found: C. 79.45; H. 11.73.

*3,4-Bis(hexadecyloxy)benzaldehyde (8e)*. Yield 82%, m.p. 85-87 °C. FTIR ( $\text{cm}^{-1}$ ): 2915, 2847, 1681, 1589, 1509, 1270, 1131, 805.  $^1\text{H}$  NMR (400 MHz,  $\text{DMSO}-d_6$ )  $\delta$  (ppm) 9.74 (s, 1H,  $-\text{CHO}$ ), 7.35 (d,  $J=8$  Hz, 1H, Ar-H), 7.25 (s, 1H, Ar-H), 7.08 (d,  $J=8$  Hz, 1H, Ar-H), 4.04 (t,  $J=6.6$  Hz, 4H,  $-\text{OCH}_2-$ ), 1.61-1.23 (m, 56H,  $-\text{CH}_2-$ ), 0.84 (t,  $J=6.6$  Hz, 6H,  $-\text{CH}_3$ ).  $^{13}\text{C}$  NMR (100 MHz,  $\text{DMSO}-d_6$ )  $\delta$  (ppm); 191.81, 154.52, 149.14, 129.98, 126.38, 112.85, 111.79, 68.87, 68.73, 31.75, 29.48, 29.16, 22.55, 14.42. MS (m/z): 587.5 (M+H)<sup>+</sup>. Anal. Calcd. For.  $\text{C}_{39}\text{H}_{70}\text{O}_3$ : C. 79.80; H. 12.02. Found: C. 80.06; H. 12.07.

*Procedure for the preparation of 4,6-bis(4-hydroxyphenyl)-2-oxo-1,2-dihydropyridine-3-carbonitrile (11)*

An equimolar mixture of 4-hydroxyacetophenone **9**, 4-hydroxybenzaldehyde **10**, ethyl cyanoacetate and ammonium acetate (excess) in 1,4-dioxane (40 ml) was refluxed for 12 h. The obtained precipitate was filtered off, washed successively with 1,4-dioxane followed by ethyl acetate. Pure product was obtained by recrystallization from ethanol/DMF. Yield 62 %, m.p. >349 °C. FTIR (cm<sup>-1</sup>): 3530, 3325, 2222, 1666, 1596, 1514, 1435, 1340, 1283, 1225, 1176, 820. <sup>1</sup>H NMR (400 M Hz, DMSO-*d*<sub>6</sub>) δ (ppm) 12.40 (s, 1H, NH (pyridine)), 10.15 (s, 1H, Ar-OH), 10.04 (s, 1H, Ar-OH), 7.74 (d, *J*=8.4 Hz, 2H, Ar-H), 7.61-7.57 (m, 2H, Ar-H), 6.92-6.84 (m, 4H, Ar-H), 6.62 (s, 1H, Ar-H (pyridine)). <sup>13</sup>C NMR (100 MHz, DMSO-*d*<sub>6</sub>) δ (ppm); 162.78, 160.85, 160.14, 130.51, 129.93, 127.10, 117.16, 116.19, 115.97. MS (m/z): 305.1 (M+H)<sup>+</sup>. Anal. Calcd. For. C<sub>18</sub>H<sub>12</sub>N<sub>2</sub>O<sub>3</sub>: C. 71.05; H. 3.97; 9.21. Found: C. 71.29; H. 3.88; N. 9.31.

*Procedure for the preparation of cyanopyridine based triester (12)*

A mixture of cyanopyridone **11** (10 mmol), ethyl chloroacetate (32 mmol), anhydrous potassium carbonate (34 mmol) in dry DMF (40 ml) was heated with stirring at 80 °C for 12 h. The reaction mixture was cooled and the mixture was added to cold water. The precipitated solid was filtered off and recrystallized from ethanol to get pure cyanopyridine based triester **12**. Yield 71 %, m.p. 124.4-125.0 °C. FTIR (cm<sup>-1</sup>): 2986, 2213, 1749, 1582, 1510, 1378, 1183, 1058, 825. <sup>1</sup>H NMR (400 M Hz, DMSO-*d*<sub>6</sub>) δ (ppm) 7.97 (d, *J*=7.2 Hz, 2H, Ar-H), 7.63 (d, *J*=12 Hz, 2H, Ar-H), 7.42 (s, 1H, Ar-H (pyridine)), 7.05 (d, *J*=7.2 Hz, 2H, Ar-H), 6.98 (d, *J*=12 Hz, 2H, Ar-H), 5.05 (s, 2H, -OCH<sub>2</sub>CO-), 4.68 (s, 4H, -OCH<sub>2</sub>CO-) 4.31 (t, *J*=8 Hz, 6H, -COOCH<sub>2</sub>CH<sub>3</sub>), 1.34-1.24 (m, 9H, -COOCH<sub>2</sub>CH<sub>3</sub>). <sup>13</sup>C NMR (100 MHz, CDCl<sub>3</sub>) δ (ppm); 167.48, 167.45, 167.41, 162.51, 158.82, 158.31, 155.81, 155.20, 129.37, 128.97, 128.51, 127.84, 114.36, 114.12, 113.88, 112.24, 91.06, 64.37, 64.30, 62.70, 60.56, 60.26, 13.23, 13.16. MS (m/z): 563.2 (M+H)<sup>+</sup>. Anal. Calcd. For. C<sub>30</sub>H<sub>30</sub>N<sub>2</sub>O<sub>9</sub>: C. 64.05; H. 5.38; N. 4.98. Found: C. 64.25; H. 5.31; N. 4.88.



*Procedure for the preparation of trihydrazide (13)*

A solution of cyanopyridine based triester **12** (10 mmol) in ethanol (50 ml) and hydrazine hydrate (32 mmol) was refluxed for 12 h. The separated solid after cooling was then filtered and washed with ethanol. Pure product was obtained by recrystallization from ethanol solvent. Yield 48 %, m.p. 117-119 °C. FTIR (cm<sup>-1</sup>): 3442, 3326, 2986, 2215, 1746, 1585, 1513, 1376, 1184, 1058, 825. <sup>1</sup>H NMR (400 MHz, DMSO-*d*<sub>6</sub>) δ (ppm) 9.39-9.37 (s, 3H, 3 × -CONH-), 8.23-8.15 (m, 2H, Ar-H), 7.76-7.61 (m, 2H, Ar-H), 7.23 (s, 1H, Ar-H (pyridine)), 7.17-7.04 (m, 4H, Ar-H), 4.97 (s, 2H, -OCH<sub>2</sub>CO-), 4.57 (s, 4H, -OCH<sub>2</sub>CO-) 4.39 (bs, 6H, -CONHNH<sub>2</sub>). <sup>13</sup>C NMR (100 MHz, DMSO-*d*<sub>6</sub>) δ (ppm); 166.92, 166.89, 161.41, 160.01, 159.41, 157.76, 154.98, 131.08, 130.65, 130.14, 129.47, 117.18, 115.31, 108.97, 85.89, 66.75. MS (m/z): 521.2 (M+H)<sup>+</sup>. Anal. Calcd. For. C<sub>24</sub>H<sub>24</sub>N<sub>8</sub>O<sub>6</sub>: C. 55.38; H. 4.65; N. 21.53. Found: C. 55.64; H. 4.57; N. 21.61.

*General procedure for the preparation of 2-(4,6-disubstituted aryl-3-cyanopyridyl) oxy acetohydrazones LC<sub>34-38</sub>*

A mixture of cyanopyridine based trihydrazide **13** (10 mmol) and 3,4-bis(alkyloxy)benzaldehyde **8a-e** (31 mmol) and few drops of acetic acid in ethanol (50 mL) was refluxed for 12 h. The obtained precipitate after cooling was filtered and washed with ethanol. Pure product was obtained by recrystallization from chloroform/methanol mixture. Their characterization data are as follows.

**LC<sub>34</sub>**: Yield 72 %. FTIR (cm<sup>-1</sup>): 3215, 3073, 2916, 2850, 2218, 1670, 1590, 1508, 1437, 1376, 1231, 1179, 1138, 1082, 824. <sup>1</sup>H NMR (400 MHz, DMSO-*d*<sub>6</sub>) δ (ppm) 11.51 (s, 3H, -CONH-), 8.22-8.12 (m, 2H, Ar-H), 7.91 (s, 3H, -CH=N), 7.76-7.71 (m, 2H, Ar-H), 7.50 (s, 1H, Ar-H (pyridine)), 7.36 (s, 2H, Ar-H), 7.30-7.27 (m, 2H, Ar-H), 7.19-7.11 (m, 3 H, Ar-H), 7.05-7.04 (m, 3H, Ar-H), 6.99-6.96 (m, 3H, Ar-H), 5.12 (s, 2H, -OCH<sub>2</sub>CO-), 4.76 (s, 4H, -OCH<sub>2</sub>CO-), 3.97 (t, *J*=6.5 Hz, 12H, -OCH<sub>2</sub>-), 1.80-1.68 (s, 12H, -OCH<sub>2</sub>CH<sub>2</sub>-), 1.50-1.17 (m, 60H, -CH<sub>2</sub>-) 0.83 (t, *J*=6.8 Hz, 18H, -CH<sub>3</sub>). <sup>13</sup>C NMR (100 MHz, DMSO-*d*<sub>6</sub>) δ (ppm); 166.30, 152.37, 136.72, 134.83, 118.18, 74.26, 66.75, 48.86, 37.15, 32.93, 25.22, 22.18, 21.22, 19.90, 13.99. MS

(m/z): 1554.4 (M+H)<sup>+</sup>. Anal. Calcd. For. C<sub>93</sub>H<sub>132</sub>N<sub>8</sub>O<sub>12</sub>: C. 71.87; H. 8.56; N. 7.21. Found: C. 72.09; H. 8.63; N. 7.26.

**LC<sub>35</sub>**: Yield 64 %. FTIR (cm<sup>-1</sup>): 3215, 3074, 2918, 2852, 2219, 1670, 1590, 1507, 1436, 1376, 1228, 1177, 1137, 1081, 823. <sup>1</sup>H NMR (400 MHz, DMSO-*d*<sub>6</sub>) δ (ppm) 11.51 (s, 3H, -CONH-), 8.22-8.12 (m, 2H, Ar-H), 7.91 (s, 3H, -CH=N), 7.76-7.71 (m, 2H, Ar-H), 7.50 (s, 1H, Ar-H (pyridine)), 7.36 (s, 2H, Ar-H), 7.30-7.27 (m, 2H, Ar-H), 7.19-7.11 (m, 3 H, Ar-H), 7.05-7.04 (m, 3H, Ar-H), 6.99-6.96 (m, 3H, Ar-H), 5.12 (s, 2H, -OCH<sub>2</sub>CO-), 4.76 (s, 4H, -OCH<sub>2</sub>CO-), 3.97 (t, *J*=6.5 Hz, 12H, -OCH<sub>2</sub>-), 1.80-1.68 (s, 12H, -OCH<sub>2</sub>CH<sub>2</sub>-), 1.50-1.17 (m, 84H, -CH<sub>2</sub>-) 0.83 (t, *J*=6.8 Hz, 18H, -CH<sub>3</sub>). <sup>13</sup>C NMR (100 MHz, DMSO-*d*<sub>6</sub>) δ (ppm); 166.37, 152.31, 136.65, 134.81, 118.14, 74.28, 66.72, 48.86, 37.15, 32.97, 25.22, 22.18, 21.24, 19.96, 13.99. MS (m/z): 1722.2 (M+H)<sup>+</sup>. Anal. Calcd. For. C<sub>105</sub>H<sub>156</sub>N<sub>8</sub>O<sub>12</sub>: C. 73.22; H. 9.13; N. 6.51. Found: C. 73.47; H. 9.06; N. 6.45.

**LC<sub>36</sub>**: Yield 69 %. FTIR (cm<sup>-1</sup>): 3215, 3074, 2917, 2850, 2221, 1673, 1590, 1508, 1437, 1378, 1230, 1177, 1136, 1081, 820. <sup>1</sup>H NMR (400 MHz, DMSO-*d*<sub>6</sub>) δ (ppm) 11.50 (s, 3H, -CONH-), 8.22-8.12 (m, 2H, Ar-H), 7.91 (s, 3H, -CH=N), 7.76-7.71 (m, 2H, Ar-H), 7.50 (s, 1H, Ar-H (pyridine)), 7.36 (s, 2H, Ar-H), 7.30-7.27 (m, 2H, Ar-H), 7.19-7.11 (m, 3 H, Ar-H), 7.05-7.04 (m, 3H, Ar-H), 6.99-6.96 (m, 3H, Ar-H), 5.12 (s, 2H, -OCH<sub>2</sub>CO-), 4.76 (s, 4H, -OCH<sub>2</sub>CO-), 3.97 (t, *J*=6.6 Hz, 12H, -OCH<sub>2</sub>-), 1.80-1.68 (s, 12H, -OCH<sub>2</sub>CH<sub>2</sub>-), 1.50-1.17 (m, 108H, -CH<sub>2</sub>-) 0.83 (t, *J*=6.8 Hz, 18H, -CH<sub>3</sub>). <sup>13</sup>C NMR (100 MHz, DMSO-*d*<sub>6</sub>) δ (ppm); 166.34, 152.35, 136.76, 134.83, 118.14, 74.26, 66.78, 48.86, 37.12, 32.93, 25.26, 22.18, 21.27, 19.96, 13.99. MS (m/z): 1890.4 (M+H)<sup>+</sup>. Anal. Calcd. For. C<sub>117</sub>H<sub>180</sub>N<sub>8</sub>O<sub>12</sub>: C. 74.32; H. 9.60; N. 5.93. Found: C. 74.61; H. 9.56; N. 5.95.

**LC<sub>37</sub>**: Yield 73 %. FTIR (cm<sup>-1</sup>): 3215, 3073, 2916, 2850, 2218, 1670, 1590, 1508, 1437, 1376, 1231, 1179, 1138, 1082, 824. <sup>1</sup>H NMR (400 MHz, DMSO-*d*<sub>6</sub>) δ (ppm) 11.51 (s, 3H, -CONH-), 8.22 -8.09 (m, 2H, Ar-H), 7.91 (s, 3H, -CH=N), 7.76-7.72 (m, 2H, Ar-H), 7.50 (s, 1H, Ar-H (pyridine)), 7.35 (s, 2H, Ar-H), 7.30-7.27 (m, 2H, Ar-H), 7.20-7.11 (m, 3 H, Ar-H), 7.06-7.04 (m, 3H, Ar-H), 6.99-6.89 (m, 3H, Ar-H), 5.12 (s, 2H, -OCH<sub>2</sub>CO-), 4.78 (s, 4H, -OCH<sub>2</sub>CO-), 3.96 (t, *J*=6.5 Hz, 12H, -OCH<sub>2</sub>-),

1.69-1.68 (s, 12H, -OCH<sub>2</sub>CH<sub>2</sub>-), 1.40-1.19 (m, 132H, -CH<sub>2</sub>-) 0.83 (s, 18H, -CH<sub>3</sub>). <sup>13</sup>C NMR (100 MHz, CDCl<sub>3</sub>) δ (ppm); 163.56, 149.41, 130.35, 129.92, 126.51, 123.05, 115.23, 112.46, 111.81, 111.07, 110.81, 77.36, 77.00, 76.63, 69.39, 69.17, 31.24, 29.02, 28.66, 25.56, 22.03, 13.86. MS (m/z): 2058.6 (M+H)<sup>+</sup>. Anal. Calcd. For. C<sub>129</sub>H<sub>204</sub>N<sub>8</sub>O<sub>12</sub>: C. 75.25; H. 9.99; N. 5.44. Found: C. 75.52; H. 9.93; N. 5.50.

**LC<sub>38</sub>**: Yield 61 %. FTIR (cm<sup>-1</sup>): 3216, 3075, 2915, 2848, 2219, 1674, 1590, 1508, 1437, 1379, 1231, 1177, 1136, 1077, 818. <sup>1</sup>H NMR (400 MHz, DMSO-*d*<sub>6</sub>) δ (ppm) 9.60-9.29 (m, 2H, -CONH-), 9.11-8.92 (m, 1H, -NH), 8.22-8.12 (m, 2H, Ar-H), 7.91 (s, 3H, -CH=N), 7.76-7.71 (m, 2H, Ar-H), 7.50 (s, 1H, Ar-H (pyridine)), 7.39 (s, 2H, Ar-H), 7.30-7.27 (m, 2H, Ar-H), 7.19-7.11 (m, 3 H, Ar-H), 7.05-7.04 (m, 3H, Ar-H), 6.99-6.96 (m, 3H, Ar-H), 5.04 (s, 2H, -OCH<sub>2</sub>CO-), 4.80 (s, 4H, -OCH<sub>2</sub>CO-), 4.05 (t, *J*=6.6 Hz, 12H, -OCH<sub>2</sub>-), 1.87-1.81 (s, 12H, -OCH<sub>2</sub>CH<sub>2</sub>-), 1.47-1.25 (m, 156H, -CH<sub>2</sub>-) 0.87 (t, *J*=6.4 Hz, 18H, -CH<sub>3</sub>). <sup>13</sup>C NMR (100 MHz, CDCl<sub>3</sub>) δ (ppm); 163.46, 149.47, 130.29, 129.90, 126.55, 123.05, 115.21, 112.46, 111.81, 111.07, 110.81, 77.32, 77.00, 76.68, 69.33, 69.14, 63.71, 31.92, 29.70, 29.36, 29.16, 29.08, 28.99, 26.01, 22.68, 14.09. MS (m/z): 2226.8 (M+H)<sup>+</sup>. Anal. Calcd. For. C<sub>141</sub>H<sub>228</sub>N<sub>8</sub>O<sub>12</sub>: C. 76.03; H. 10.32; N. 5.03. Found: C. 76.28; H. 10.38; N. 5.07.

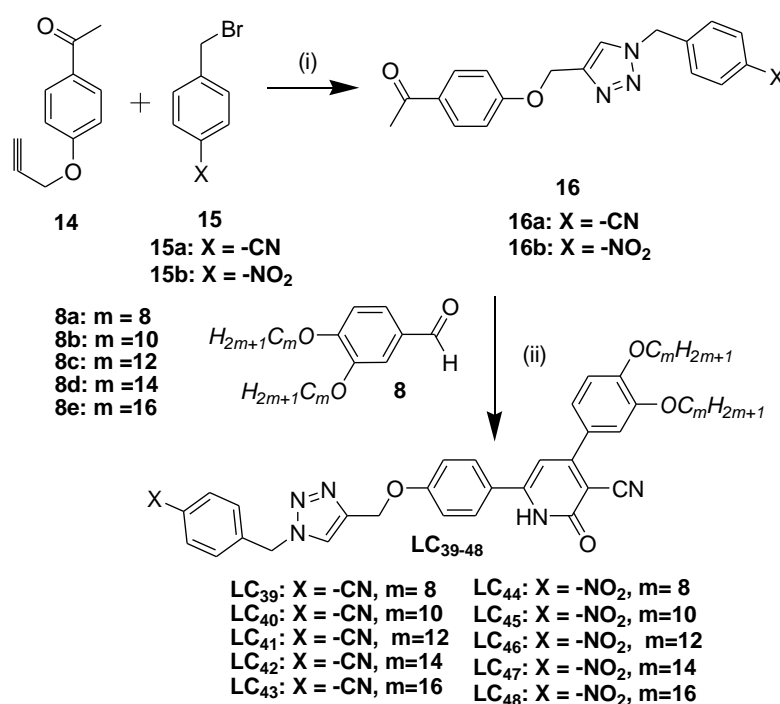
### 3.3.4 Synthesis of 4,6-disubstituted aryl-3-cyanopyridones (Series-IV; LC<sub>39-48</sub>)

The synthesis of title compounds involves two important steps as shown in **Scheme 3.4**; the first step consist of one pot synthesis of acetyl functionalized 1,4-disubstituted 1,2,3-triazole intermediate **16** via slightly modified click reaction. Whereas second step comprises one pot synthesis of title compounds by heating a mixture of acetyl functionalized 1,4-disubstituted 1,2,3-triazole intermediate **16**, 3,4-bis(alkyloxy)benzaldehyde **8**, ethyl cyanoacetate and ammonium acetate. The progress of the reactions was monitored by thin layer chromatography, and the structures of new compounds were confirmed by spectral methods as well as elemental analysis. The synthesis of intermediate **8a-e** is given in the **Scheme 3.3**. The experimental results are discussed in the following section.

## 3.3.4.1 Results and discussion

*Synthesis:*

The synthetic route for the preparation of target compounds **LC**<sub>39-48</sub> is shown in **Scheme 3.4**. The intermediate acetyl functionalized 1,4-disubstituted 1,2,3-triazole compound **16** was prepared from one pot reaction between 4-propargyloxyacetophenone **14** and 4-substituted benzylbromide **15** via a little modified click reaction using ethanol (50%) as a solvent. Another intermediate 3,4-bis(alkoxy)benzaldehyde **8** was prepared by reacting 3,4-dihydroxybenzaldehyde with various alkylbromides using Williamson method (Attias et al. 2002). Finally, cyanopyridone derivatives **LC**<sub>39-48</sub> were prepared by one pot reaction of acetyl functionalized 1,2,3-triazole **16** and 3,4-bis(alkoxy)benzaldehyde **8** with ethyl cyanoacetate in presence of ammonium acetate in 1,4-dioxane medium.



**Scheme 3.4** Synthetic route for the preparation of target compounds **LC**<sub>39-48</sub>.

Reagents and conditions: (i) NaN<sub>3</sub>, CuI (10 mol%), ethanol (50%) 80 °C, 12h; (ii) ethyl cyanoacetate, ammonium acetate, 1,4-dioxane, reflux, 12h

The structures of newly synthesized compounds were confirmed by FTIR, <sup>1</sup>H NMR, <sup>13</sup>C NMR spectroscopy and elemental analysis. In the <sup>1</sup>H NMR spectrum of

**16a**, aromatic protons appeared as doublet in the region of  $\delta$  8.20-7.00 ppm and a proton of triazole ring appeared as singlet in the range of  $\delta$  7.80-7.64 ppm. The two singlets at  $\delta$  5.60 ppm and  $\delta$  5.26 ppm are due to the protons of  $-\text{OCH}_2-$  and  $-\text{CH}_2-$  groups, respectively. Also, three protons of  $-\text{COCH}_3$  group resonated at  $\delta$  2.55 ppm as singlet, which confirms the chemical structure of **16a**. In the  $^1\text{H}$  NMR spectrum of **LC**<sub>43</sub>, peaks due to aromatic protons appeared in the range of  $\delta$  7.96-7.00 ppm. Two singlet peaks at  $\delta$  7.80 and  $\delta$  7.61 ppm were due to the proton of triazole and cyanopyridone, respectively. Further, the appearance of two singlets at  $\delta$  5.65 ppm and  $\delta$  5.28 ppm was attributed to the protons of  $-\text{OCH}_2-$  and  $\text{Ar-CH}_2-$  groups respectively in it. Also, the peaks for primary and secondary protons of alkoxy chains appeared in the region of  $\delta$  1.70-0.84 ppm, which confirms the formation of **LC**<sub>43</sub>. Furthermore, the mass spectrum observed for **LC**<sub>43</sub>, showed the mass peak  $[\text{M}+\text{H}]^+$  at 965.6, which is consistent with a calculated molecular weight for the formula of  $\text{C}_{61}\text{H}_{85}\text{N}_6\text{O}_4$ . **Figures 3.35-3.38** show FTIR,  $^1\text{H}$  NMR,  $^{13}\text{C}$  NMR and Mass spectra of representative compound **LC**<sub>44</sub>, respectively.

#### Crystal structure analysis of **16a**:

Superior quality crystals of **16a** were grown by slow evaporation of chloroform/methanol solution for the determination of X-ray single crystal structure and the crystal data are presented in **Table 3.16**. The compound **16a** crystallizes in monoclinic crystal system with  $P 21/c$  space group and cell parameters are  $a=20.3809(14)$  Å,  $b=5.5940(4)$  Å,  $c=15.3584(11)$  Å,  $V=1683.91\text{Å}^3$  with  $Z=4$ . The crystal structure of molecule **16a** with atom labeling is shown in **Figure 3.14**.

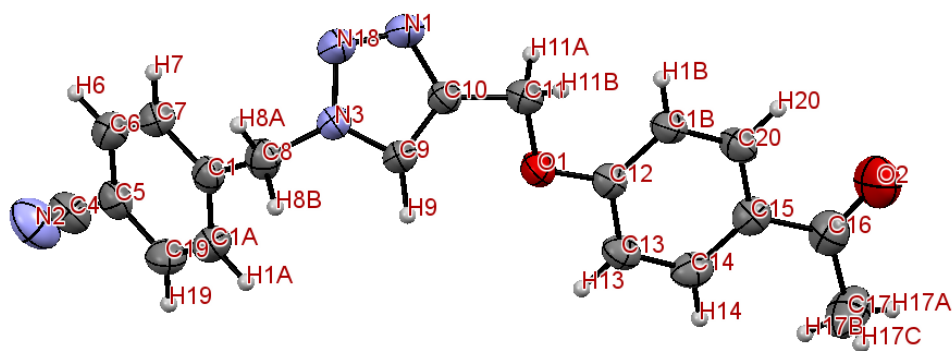


**Figure 3.14** ORTEP diagram of **16a** with atom numbering. ORTEP diagram is drawn with 50% probability ellipsoids at 296 K

**Table 3.16** Crystal data and structure refinement for **16a**

Compound	16a
Formula	C <sub>19</sub> H <sub>16</sub> N <sub>4</sub> O <sub>2</sub>
Formula weight	332.36
CCDC number	966496
Temperature (K)	296
Crystal form	Block
Color	Colorless
Crystal system	Monoclinic
Space group	<i>P 21/c</i>
<i>a</i> (Å)	20.3809(14)
<i>b</i> (Å)	5.5940(4)
<i>c</i> (Å)	15.3584(11)
$\alpha$ (°)	90
$\beta$ (°)	105.915(4)
$\gamma$ (°)	90
Volume (Å <sup>3</sup> )	1683.91
<i>Z</i>	4
Density (gcm <sup>-3</sup> )	1.311
$\mu$ (mm <sup>-1</sup> )	0.09
F (000)	696.0
<i>h</i> <sub>min, max</sub>	-23,25
<i>k</i> <sub>min, max</sub>	-5,6
<i>l</i> <sub>min, max</sub>	-18,16
Reflections collected	11617
Independent reflections	3240
<i>R</i> <sub>all</sub> , <i>R</i> <sub>obs</sub>	0.1022,0.0526
<i>wR</i> <sub>2_all</sub> , <i>wR</i> <sub>2_obs</sub>	0.1587,0.1373
$\Delta\rho$ <sub>min,max</sub> (e Å <sup>-3</sup> )	-0.23, 0.26
GOOF	0.92

The molecular structure of **16a** is found to be non-planar as evidenced by the observed large torsion angles of  $-91.3(3)^\circ$  (C9-N3-C8-C1) made by methylbenzonitrile ring with 1,2,3-triazole ring, while a torsion angle of  $31.5(3)^\circ$  (C9-C10-C11-O1) made by 4-((4-acetylphenoxy)methyl) ring with 1,2,3-triazole ring. Further, the crystal structure of **16a** involves various kinds of non-conventional hydrogen bonds, *viz.* C-H $\cdots$ N and C-H $\cdots$ O interactions (**Figure 3.15**). The two kinds of C-H $\cdots$ N interactions are observed, in which one kind of C-H $\cdots$ N interaction is formed between the H9 atom of 1,2,3-triazole ring and the neighboring molecule carrying N1 atom of 1,2,3-triazole ring with the bond distance of 2.409 Å (C9-H9 $\cdots$ N1). Similarly, second kind of C-H $\cdots$ N interaction is formed by nitrogen atom of terminal cyano group and the nearby aromatic protons, with the bond distance of 2.622 Å (N2 $\cdots$ H6-C6). In addition to C-H $\cdots$ N interactions, one kind of C-H $\cdots$ O hydrogen bond is identified between the oxygen atom of acetyl group and the nearby aromatic protons, with the bond distance of 2.628 Å (C19-H19 $\cdots$ O2). Thus, these interactions are responsible to hold the molecules together resulting in its crystal assembly.

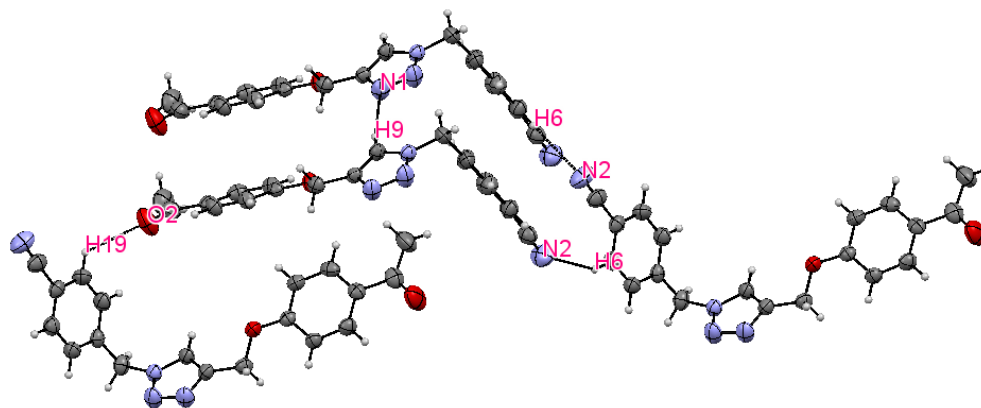


**Figure 3.15** Packing pattern of **16a** showing non-conventional hydrogen bonds

#### 3.3.4.2 Experimental Procedures

The experimental procedures employed for the synthesis of new target molecules **LC**<sub>39-48</sub> are given below.

##### *General procedure for the preparation of compounds (16a, b)*

A mixture of 1-(4-(prop-2-ynyloxy)phenyl)ethanone **14** (1.0 mmol), 4-(bromomethyl)benzonitrile **15a** or 1-(bromomethyl)-4-nitrobenzene **15b** (1.1 mmol),

sodium azide (1.2 mmol) in presence of copper iodide (10 mol%) was heated at 80 °C with stirring in ethanol and water mixture (5 mL) for 12 h. After cooling, water was added to reaction mixture and stirred for 30 min at room temperature. The obtained solid was filtered and washed with ethanol. Finally, the pure product was obtained by recrystallization from chloroform/methanol mixture. Their characterization data are as follows.

*4-((4-((4-Acetylphenoxy)methyl)-1H-1,2,3-triazol-1-yl)methyl)benzotrile* (**16a**).

Yield 69 %, m.p. 126-128 °C. FTIR (cm<sup>-1</sup>): 2919, 2869, 2232, 1676, 1607, 1359, 1258, 1180, 1050, 812. <sup>1</sup>H NMR (400 MHz, CDCl<sub>3</sub>) δ (ppm) 7.92 (d, *J*=8.8 Hz, 2H, Ar-H), 7.80 (s, 1H, Ar-H(Triazole)), 7.66 (d, *J*=8 Hz, 2H, Ar-H), 7.35 (d, *J*=8 Hz, 2H, Ar-H), 7.00 (d, *J*=8.8 Hz, 2H, Ar-H), 5.60 (s, 2H, -OCH<sub>2</sub>-), 5.26 (s, 2H, Ar-CH<sub>2</sub>-), 2.55 (s, 3H, -COCH<sub>3</sub>). <sup>13</sup>C NMR (100 MHz, CDCl<sub>3</sub>) δ (ppm); 196.65, 161.87, 144.38, 139.59, 134.90, 131.65, 130.92, 128.45, 122.90, 118.04, 114.42, 112.95, 77.00, 53.50, 51.91, 26.33. MS (m/z): 333.1 (M+H)<sup>+</sup>. Anal. Calcd. For. C<sub>19</sub>H<sub>16</sub>N<sub>4</sub>O<sub>2</sub>: C. 68.66; H. 4.85; N. 16.86. Found: C. 68.88; H. 4.93; N. 16.91.

*1-(4-((1-(4-Nitrobenzyl)-1H-1,2,3-triazol-4-yl)methoxy)phenyl)ethanone* (**16b**).

Yield 76 %, m.p. 131-133 °C. FTIR (cm<sup>-1</sup>): 2923, 2851, 1664, 1602, 1513, 1421, 1348, 1254, 1172, 1050, 804. <sup>1</sup>H NMR (400 MHz, CDCl<sub>3</sub>) δ (ppm) 8.20 (d, *J*=8.8 Hz, 2H, Ar-H), 7.91 (d, *J*=8.8 Hz, 2H, Ar-H), 7.64 (s, 1H, Ar-H(Triazole)), 7.41 (d, *J*=8 Hz, 2H, Ar-H), 7.00 (d, *J*=8.8 Hz, 2H, Ar-H), 5.65 (s, 2H, -OCH<sub>2</sub>-), 5.26 (s, 2H, Ar-CH<sub>2</sub>-), 2.53 (s, 3H, -COCH<sub>3</sub>). <sup>13</sup>C NMR (100 MHz, CDCl<sub>3</sub>) δ (ppm); 196.67, 161.86, 144.44, 141.34, 130.92, 128.63, 128.25, 124.33, 122.97, 114.42, 114.01, 77.32, 61.99, 53.22, 26.31. MS (m/z): 353.1 (M+H)<sup>+</sup>. Anal. Calcd. For. C<sub>18</sub>H<sub>16</sub>N<sub>4</sub>O<sub>4</sub>: C. 61.36; H. 4.58; N. 15.90. Found: C. 61.63; H. 4.61; N. 15.86.

*General procedure for the synthesis of 4,6-disubstituted aryl-3-cyanopyridones (LC<sub>39-48</sub>)*

A mixture of compound **16** (1.0 mmol), compound **8** (1.0 mmol), ethyl cyanoacetate (1.1 mmol) ammonium acetate (8.0 mmol) in 1,4-dioxane (5 ml) was refluxed for 12 h. The obtained precipitate was filtered, washed successively with 1,4-



dioxane, followed by ethyl acetate and finally recrystallized from ethanol/DMF to afford the pure product (**LC<sub>39-48</sub>**). Their characterization data are as follows.

*4-(3,4-Bis(octyloxy)phenyl)-6-(4-((1-(4-cyanobenzyl)-1H-1,2,3-triazol-4-yl)methoxy)phenyl)-2-oxo-1,2-dihydropyridine-3-carbonitrile (**LC<sub>39</sub>**)*. Yield 72 %. FTIR (cm<sup>-1</sup>): 2918, 2847, 2217, 1723, 1580, 1508, 1465, 1440, 1264, 1181, 1017, 801. <sup>1</sup>H NMR (400 MHz, CDCl<sub>3</sub>) δ (ppm) 8.12 (s, 1H, N-H), 7.92 (d, *J*=8.8 Hz, 2H, Ar-H), 7.80 (s, 1H, Ar-H(Triazole)), 7.73 (s, 1H, Ar-H), 7.66 (d, *J*=8 Hz, 2H, Ar-H), 7.61 (s, 1H, Ar-H(Pyridone)), 7.35 (d, *J*=8 Hz, 2H, Ar-H), 7.12 (d, *J*=8.4 Hz, 2H, Ar-H), 7.00 (d, *J*=8.8 Hz, 2H, Ar-H), 5.60 (s, 2H, -OCH<sub>2</sub>-), 5.26 (s, 2H, Ar-CH<sub>2</sub>-), 4.04 (t, *J*=6.2 Hz, 4H, -OCH<sub>2</sub>-), 1.75-1.24 (m, 24H, -CH<sub>2</sub>-), 0.83 (t, *J*=6.6 Hz, 6H, -CH<sub>3</sub>). <sup>13</sup>C NMR (100 MHz, CDCl<sub>3</sub>) δ (ppm); 154.88, 127.55, 113.94, 77.30, 77.00, 76.68, 69.26, 69.12, 31.91, 29.60, 29.34, 29.05, 28.96, 26.00, 22.68, 14.22, 14.09. MS (m/z): 741.4 (M+H)<sup>+</sup>. Anal. Calcd. For. C<sub>45</sub>H<sub>52</sub>N<sub>6</sub>O<sub>4</sub>: C. 72.95; H. 7.07; N. 11.34. Found: C. 73.19; H. 7.01; N. 11.43.

*4-(3,4-Bis(decyloxy)phenyl)-6-(4-((1-(4-cyanobenzyl)-1H-1,2,3-triazol-4-yl)methoxy)phenyl)-2-oxo-1,2-dihydropyridine-3-carbonitrile (**LC<sub>40</sub>**)*. Yield 77 %. FTIR (cm<sup>-1</sup>): 2917, 2849, 2217, 1723, 1580, 1508, 1467, 1440, 1264, 1180, 1017, 801. <sup>1</sup>H NMR (400 MHz, CDCl<sub>3</sub>) δ (ppm) 8.12 (s, 1H, N-H), 7.92 (d, *J*=8.8 Hz, 2H, Ar-H), 7.80 (s, 1H, Ar-H(Triazole)), 7.73 (s, 1H, Ar-H), 7.66 (d, *J*=8 Hz, 2H, Ar-H), 7.61 (s, 1H, Ar-H(Pyridone)), 7.35 (d, *J*=8 Hz, 2H, Ar-H), 7.12 (d, *J*=8.4 Hz, 2H, Ar-H), 7.00 (d, *J*=8.8 Hz, 2H, Ar-H), 5.60 (s, 2H, -OCH<sub>2</sub>-), 5.26 (s, 2H, Ar-CH<sub>2</sub>-), 4.04 (t, *J*=6.6 Hz, 4H, -OCH<sub>2</sub>-), 1.61-1.23 (m, 32H, -CH<sub>2</sub>-), 0.84 (t, *J*=6.6 Hz, 6H, -CH<sub>3</sub>). <sup>13</sup>C NMR (100 MHz, CDCl<sub>3</sub>) δ (ppm); 154.85, 127.57, 113.94, 77.32, 77.00, 76.68, 69.26, 69.12, 31.91, 29.60, 29.34, 29.05, 28.96, 26.00, 22.68, 14.22, 14.09. MS (m/z): 797.5 (M+H)<sup>+</sup>. Anal. Calcd. For. C<sub>49</sub>H<sub>60</sub>N<sub>6</sub>O<sub>4</sub>: C. 73.84; H. 7.59; N. 10.54. Found: C. 74.12; H. 7.67; N. 10.63.

*4-(3,4-Bis(dodecyloxy)phenyl)-6-(4-((1-(4-cyanobenzyl)-1H-1,2,3-triazol-4-yl)methoxy)phenyl)-2-oxo-1,2-dihydropyridine-3-carbonitrile (**LC<sub>41</sub>**)*. Yield 81 %. FTIR (cm<sup>-1</sup>): 2919, 2852, 2218, 1723, 1580, 1508, 1467, 1440, 1264, 1180, 1017, 804. <sup>1</sup>H NMR (400 MHz, CDCl<sub>3</sub>) δ (ppm) 8.12 (s, 1H, N-H), 7.92 (d, *J*=8.8 Hz, 2H, Ar-H),

7.80 (s, 1H, Ar-H(Triazole)), 7.73 (s, 1H, Ar-H), 7.66 (d,  $J=8$  Hz, 2H, Ar-H), 7.61 (s, 1H, Ar-H(Pyridone)), 7.35 (d,  $J=8$  Hz, 2H, Ar-H), 7.12 (d,  $J=8.4$  Hz, 2H, Ar-H), 7.00 (d,  $J=8.8$  Hz, 2H, Ar-H), 5.60 (s, 2H, -OCH<sub>2</sub>-), 5.26 (s, 2H, Ar-CH<sub>2</sub>-), 4.04 (t,  $J=6.6$  Hz, 4H, -OCH<sub>2</sub>-), 1.61-1.24 (m, 40H, -CH<sub>2</sub>-), 0.84 (s, 6H, -CH<sub>3</sub>). <sup>13</sup>C NMR (100 MHz, CDCl<sub>3</sub>)  $\delta$  (ppm); 154.87, 127.55, 124.34, 113.94, 112.34, 77.31, 77.00, 76.68, 69.26, 69.12, 62.36, 31.93, 29.63, 29.60, 29.40, 29.36, 29.06, 28.96, 26.01, 25.94, 22.69, 14.22, 14.10. MS (m/z): 853.5 (M+H)<sup>+</sup>. Anal. Calcd. For. C<sub>53</sub>H<sub>68</sub>N<sub>6</sub>O<sub>4</sub>: C. 74.61; H. 8.03; N. 9.85. Found: C. 74.88; H. 8.10; N. 9.89.

*4-(3,4-Bis(tetradecyloxy)phenyl)-6-(4-((1-(4-cyanobenzyl)-1H-1,2,3-triazol-4-yl)methoxy)phenyl)-2-oxo-1,2-dihydropyridine-3-carbonitrile (LC<sub>42</sub>)*. Yield 68 %. FTIR (cm<sup>-1</sup>): 2919, 2849, 2217, 1725, 1580, 1508, 1467, 1440, 1264, 1182, 1017, 806. <sup>1</sup>H NMR (400 MHz, CDCl<sub>3</sub>)  $\delta$  (ppm) 8.12 (s, 1H, N-H), 7.92 (d,  $J=8.8$  Hz, 2H, Ar-H), 7.80 (s, 1H, Ar-H(Triazole)), 7.73 (s, 1H, Ar-H), 7.66 (d,  $J=8$  Hz, 2H, Ar-H), 7.61 (s, 1H, Ar-H(Pyridone)), 7.35 (d,  $J=8$  Hz, 2H, Ar-H), 7.12 (d,  $J=8.4$  Hz, 2H, Ar-H), 7.00 (d,  $J=8.8$  Hz, 2H, Ar-H), 5.60 (s, 2H, -OCH<sub>2</sub>-), 5.26 (s, 2H, Ar-CH<sub>2</sub>-), 4.04 (t,  $J=6.6$  Hz, 4H, -OCH<sub>2</sub>-), 1.61-1.23 (m, 48H, -CH<sub>2</sub>-), 0.84 (t,  $J=6.6$  Hz, 6H, -CH<sub>3</sub>). <sup>13</sup>C NMR (100 MHz, CDCl<sub>3</sub>)  $\delta$  (ppm); 154.84, 127.58, 124.37, 113.94, 112.31, 77.32, 77.00, 76.68, 69.26, 69.12, 62.36, 31.93, 29.63, 29.60, 29.40, 29.36, 29.06, 28.96, 26.01, 25.94, 22.69, 14.22, 14.10. MS (m/z): 909.6 (M+H)<sup>+</sup>. Anal. Calcd. For. C<sub>57</sub>H<sub>76</sub>N<sub>6</sub>O<sub>4</sub>: C. 75.29; H. 8.42; N. 9.24. Found: C. 75.59; H. 8.49; N. 9.30.

*4-(3,4-Bis(hexadecyloxy)phenyl)-6-(4-((1-(4-cyanobenzyl)-1H-1,2,3-triazol-4-yl)methoxy)phenyl)-2-oxo-1,2-dihydropyridine-3-carbonitrile (LC<sub>43</sub>)*. Yield 83 %. FTIR (cm<sup>-1</sup>): 2917, 2849, 2217, 1723, 1580, 1508, 1469, 1440, 1264, 1180, 1017, 804. <sup>1</sup>H NMR (400 MHz, CDCl<sub>3</sub>)  $\delta$  (ppm) 8.12 (s, 1H, N-H), 7.92 (d,  $J=8.8$  Hz, 2H, Ar-H), 7.80 (s, 1H, Ar-H(Triazole)), 7.73 (s, 1H, Ar-H), 7.66 (d,  $J=8$  Hz, 2H, Ar-H), 7.61 (s, 1H, Ar-H(Pyridone)), 7.35 (d,  $J=8$  Hz, 2H, Ar-H), 7.12 (d,  $J=8.4$  Hz, 2H, Ar-H), 7.00 (d,  $J=8.8$  Hz, 2H, Ar-H), 5.65 (s, 2H, -OCH<sub>2</sub>-), 5.28 (s, 2H, Ar-CH<sub>2</sub>-), 4.06 (t,  $J=6.4$  Hz, 4H, -OCH<sub>2</sub>-), 1.61-1.23 (m, 56H, -CH<sub>2</sub>-), 0.84 (t,  $J=6.6$  Hz, 6H, -CH<sub>3</sub>). <sup>13</sup>C NMR (100 MHz, CDCl<sub>3</sub>)  $\delta$  (ppm); 154.86, 127.58, 124.33, 113.94, 112.34, 77.32, 77.00, 76.68, 69.26, 69.12, 62.36, 31.93, 29.63, 29.60, 29.40, 29.36, 29.06, 28.96, 26.01,

25.94, 22.69, 14.22, 14.10. MS (m/z): 965.6 (M+H)<sup>+</sup>. Anal. Calcd. For. C<sub>61</sub>H<sub>84</sub>N<sub>6</sub>O<sub>4</sub>: C. 75.89; H. 8.77; N. 8.71. Found: C. 76.16; H. 8.88; N. 8.66.

*4-(3,4-Bis(octyloxy)phenyl)-6-(4-((1-(4-nitrobenzyl)-1H-1,2,3-triazol-4-yl)methoxy)phenyl)-2-oxo-1,2-dihydropyridine-3-carbonitrile (LC<sub>44</sub>)*. Yield 75 %. FTIR (cm<sup>-1</sup>): 2919, 2850, 2216, 1723, 1580, 1508, 1440, 1263, 1180, 1018, 801. <sup>1</sup>H NMR (400 MHz, CDCl<sub>3</sub>) δ (ppm) 8.23 (d, *J*=8.4 Hz, 2H, Ar-H), 8.12 (s, 1H, N-H), 7.93 (d, *J*=8.8 Hz, 2H, Ar-H), 7.73 (s, 1H, Ar-H(Triazole)), 7.62 (s, 1H, Ar-H), 7.45 (s, 1H, Ar-H(Pyridone)), 7.41 (d, *J*=8.4 Hz, 2H, Ar-H), 7.00 (d, *J*=8.8 Hz, 2H, Ar-H), 6.91 (d, *J*=8.4 Hz, 2H, Ar-H), 5.60 (s, 2H, -OCH<sub>2</sub>-), 5.26 (s, 2H, Ar-CH<sub>2</sub>-), 4.04 (t, *J*=6.2 Hz, 2H, -OCH<sub>2</sub>-), 1.75-1.24 (m, 24H, -CH<sub>2</sub>-), 0.83 (t, *J*=6.6 Hz, 6H, -CH<sub>3</sub>). <sup>13</sup>C NMR (100 MHz, CDCl<sub>3</sub>) δ (ppm); 163.26, 154.84, 153.98, 149.13, 127.59, 124.32, 116.41, 113.88, 112.31, 77.32, 77.00, 76.68, 69.24, 69.11, 62.35, 31.54, 31.49, 29.69, 29.00, 28.91, 25.66, 25.59, 22.57, 14.21, 13.98. MS (m/z): 761.4 (M+H)<sup>+</sup>. Anal. Calcd. For. C<sub>44</sub>H<sub>52</sub>N<sub>6</sub>O<sub>6</sub>: C. 69.45; H. 6.89; N. 11.04. Found: C. 69.72; H. 6.97; N. 11.13.

*4-(3,4-Bis(decyloxy)phenyl)-6-(4-((1-(4-nitrobenzyl)-1H-1,2,3-triazol-4-yl)methoxy)phenyl)-2-oxo-1,2-dihydropyridine-3-carbonitrile (LC<sub>45</sub>)*. Yield 78 %. FTIR (cm<sup>-1</sup>): 2916, 2852, 2219, 1725, 1580, 1508, 1442, 1263, 1180, 1018, 801. <sup>1</sup>H NMR (400 MHz, CDCl<sub>3</sub>) δ (ppm) 8.23 (d, *J*=8.4 Hz, 2H, Ar-H), 8.12 (s, 1H, N-H), 7.93 (d, *J*=8.8 Hz, 2H, Ar-H), 7.73 (s, 1H, Ar-H(Triazole)), 7.62 (s, 1H, Ar-H), 7.45 (s, 1H, Ar-H(Pyridone)), 7.41 (d, *J*=8.4 Hz, 2H, Ar-H), 7.00 (d, *J*=8.8 Hz, 2H, Ar-H), 6.91 (d, *J*=8.4 Hz, 2H, Ar-H), 5.60 (s, 2H, -OCH<sub>2</sub>-), 5.26 (s, 2H, Ar-CH<sub>2</sub>-), 4.04 (t, *J*=6.2 Hz, 2H, -OCH<sub>2</sub>-), 1.61-1.23 (m, 32H, -CH<sub>2</sub>-), 0.84 (t, *J*=6.6 Hz, 6H, -CH<sub>3</sub>). <sup>13</sup>C NMR (100 MHz, CDCl<sub>3</sub>) δ (ppm); 163.28, 154.84, 153.96, 149.13, 127.54, 116.41, 113.88, 112.31, 77.32, 77.00, 76.68, 69.24, 69.11, 62.35, 31.54, 31.49, 29.69, 29.00, 28.91, 25.66, 25.59, 22.57, 14.21, 13.98. MS (m/z): 817.5 (M+H)<sup>+</sup>. Anal. Calcd. For. C<sub>48</sub>H<sub>60</sub>N<sub>6</sub>O<sub>6</sub>: C. 70.56; H. 7.40; N. 10.29. Found: C. 70.79; H. 7.47; N. 10.23.

*4-(3,4-Bis(dodecyloxy)phenyl)-6-(4-((1-(4-nitrobenzyl)-1H-1,2,3-triazol-4-yl)methoxy)phenyl)-2-oxo-1,2-dihydropyridine-3-carbonitrile (LC<sub>46</sub>)*. Yield 64 %. FTIR (cm<sup>-1</sup>): 2913, 2851, 2218, 1723, 1580, 1509, 1440, 1263, 1182, 1018, 801. <sup>1</sup>H NMR (400 MHz, CDCl<sub>3</sub>) δ (ppm) 8.23 (d, *J*=8.4 Hz, 2H, Ar-H), 8.12 (s, 1H, N-H), 7.93 (d,

$J=8.8$  Hz, 2H, Ar-H), 7.73 (s, 1H, Ar-H(Triazole)), 7.62 (s, 1H, Ar-H), 7.45 (s, 1H, Ar-H(Pyridone)), 7.41 (d,  $J=8.4$  Hz, 2H, Ar-H), 7.00 (d,  $J=8.8$  Hz, 2H, Ar-H), 6.91 (d,  $J=8.4$  Hz, 2H, Ar-H), 5.60 (s, 2H, -OCH<sub>2</sub>-), 5.26 (s, 2H, Ar-CH<sub>2</sub>-), 4.04 (t,  $J=6.2$  Hz, 2H, -OCH<sub>2</sub>-), 1.61-1.24 (m, 40H, -CH<sub>2</sub>-), 0.84 (s, 6H, -CH<sub>3</sub>). <sup>13</sup>C NMR (100 MHz, CDCl<sub>3</sub>)  $\delta$  (ppm); 163.24, 154.84, 153.94, 149.13, 127.55, 124.32, 116.41, 113.88, 112.34, 77.32, 77.00, 76.68, 69.24, 62.35, 31.54, 29.69, 29.00, 28.91, 25.66, 25.59, 22.57, 14.21, 13.98. MS (m/z): 873.5 (M+H)<sup>+</sup>. Anal. Calcd. For. C<sub>52</sub>H<sub>68</sub>N<sub>6</sub>O<sub>6</sub>: C. 71.53; H. 7.85; N. 9.63. Found: C. 71.82; H. 7.79; N. 9.70.

*4-(3,4-Bis(tetradecyloxy)phenyl)-6-(4-((1-(4-nitrobenzyl)-1H-1,2,3-triazol-4-yl)methoxy)phenyl)-2-oxo-1,2-dihydropyridine-3-carbonitrile (LC<sub>47</sub>)*. Yield 73 %. FTIR (cm<sup>-1</sup>): 2914, 2850, 2218, 1723, 1580, 1508, 1440, 1265, 1180, 1019, 806. <sup>1</sup>H NMR (400 MHz, CDCl<sub>3</sub>)  $\delta$  (ppm) 8.23 (d,  $J=8.4$  Hz, 2H, Ar-H), 8.12 (s, 1H, N-H), 7.93 (d,  $J=8.8$  Hz, 2H, Ar-H), 7.73 (s, 1H, Ar-H(Triazole)), 7.62 (s, 1H, Ar-H), 7.45 (s, 1H, Ar-H(Pyridone)), 7.41 (d,  $J=8.4$  Hz, 2H, Ar-H), 7.00 (d,  $J=8.8$  Hz, 2H, Ar-H), 6.91 (d,  $J=8.4$  Hz, 2H, Ar-H), 5.60 (s, 2H, -OCH<sub>2</sub>-), 5.26 (s, 2H, Ar-CH<sub>2</sub>-), 4.04 (t,  $J=6.2$  Hz, 2H, -OCH<sub>2</sub>-), 1.61-1.23 (m, 48H, -CH<sub>2</sub>-), 0.84 (t,  $J=6.6$  Hz, 6H, -CH<sub>3</sub>). <sup>13</sup>C NMR (100 MHz, CDCl<sub>3</sub>)  $\delta$  (ppm); 163.27, 154.84, 153.94, 149.13, 127.56, 124.32, 116.41, 113.88, 112.31, 77.32, 76.68, 69.11, 62.35, 31.54, 31.49, 29.00, 28.91, 25.66, 25.59, 22.57, 14.21, 13.98. MS (m/z): 929.6 (M+H)<sup>+</sup>. Anal. Calcd. For. C<sub>56</sub>H<sub>76</sub>N<sub>6</sub>O<sub>6</sub>: C. 72.38; H. 8.24; N. 9.04. Found: C. 72.68; H. 8.29; N. 9.12.

*4-(3,4-Bis(hexadecyloxy)phenyl)-6-(4-((1-(4-nitrobenzyl)-1H-1,2,3-triazol-4-yl)methoxy)phenyl)-2-oxo-1,2-dihydropyridine-3-carbonitrile (LC<sub>48</sub>)*. Yield 67 %. FTIR (cm<sup>-1</sup>): 2919, 2850, 2218, 1725, 1580, 1508, 1442, 1263, 1180, 1019, 801. <sup>1</sup>H NMR (400 MHz, CDCl<sub>3</sub>)  $\delta$  (ppm) 8.23 (d,  $J=8.4$  Hz, 2H, Ar-H), 8.12 (s, 1H, N-H), 7.93 (d,  $J=8.8$  Hz, 2H, Ar-H), 7.73 (s, 1H, Ar-H(Triazole)), 7.62 (s, 1H, Ar-H), 7.45 (s, 1H, Ar-H(Pyridone)), 7.41 (d,  $J=8.4$  Hz, 2H, Ar-H), 7.00 (d,  $J=8.8$  Hz, 2H, Ar-H), 6.91 (d,  $J=8.4$  Hz, 2H, Ar-H), 5.60 (s, 2H, -OCH<sub>2</sub>-), 5.26 (s, 2H, Ar-CH<sub>2</sub>-), 4.04 (t,  $J=6.2$  Hz, 2H, -OCH<sub>2</sub>-), 1.61-1.23 (m, 56H, -CH<sub>2</sub>-), 0.84 (t,  $J=6.6$  Hz, 6H, -CH<sub>3</sub>). <sup>13</sup>C NMR (100 MHz, CDCl<sub>3</sub>)  $\delta$  (ppm); 163.29, 154.84, 153.93, 149.13, 127.59, 124.32, 116.44, 113.88, 112.31, 77.32, 77.00, 76.68, 69.24, 62.35, 31.54, 31.49, 29.69, 29.00, 28.91,

25.66, 25.59, 22.57, 14.21, 13.98. MS (m/z): 985.6 (M+H)<sup>+</sup>. Anal. Calcd. For. C<sub>60</sub>H<sub>84</sub>N<sub>6</sub>O<sub>6</sub>: C. 73.14; H. 8.59; N. 8.53. Found: C. 73.39; H. 8.66; N. 8.45.

### Spectrograms of selected target compounds

FTIR, <sup>1</sup>H NMR, <sup>13</sup>C NMR and Mass spectra of representative title compounds have been given below.

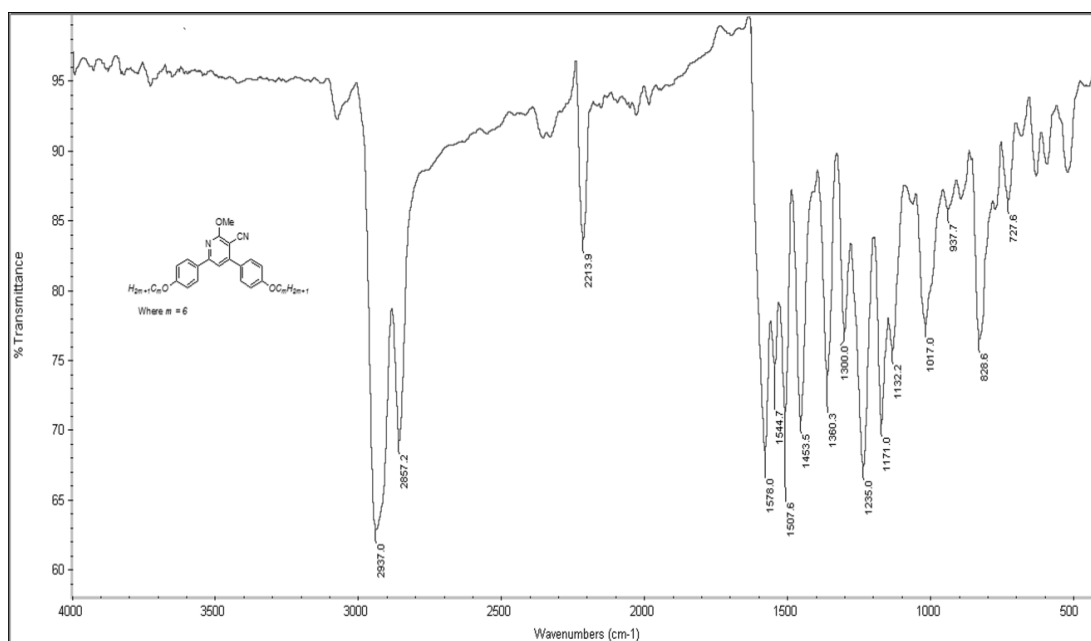


Figure 3.16 FTIR spectrum of LC<sub>2</sub>

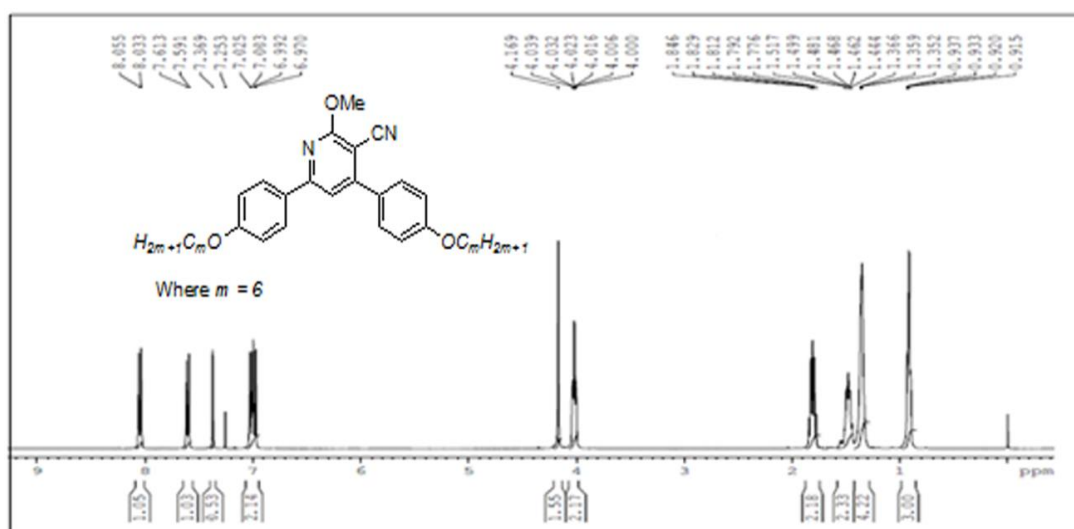
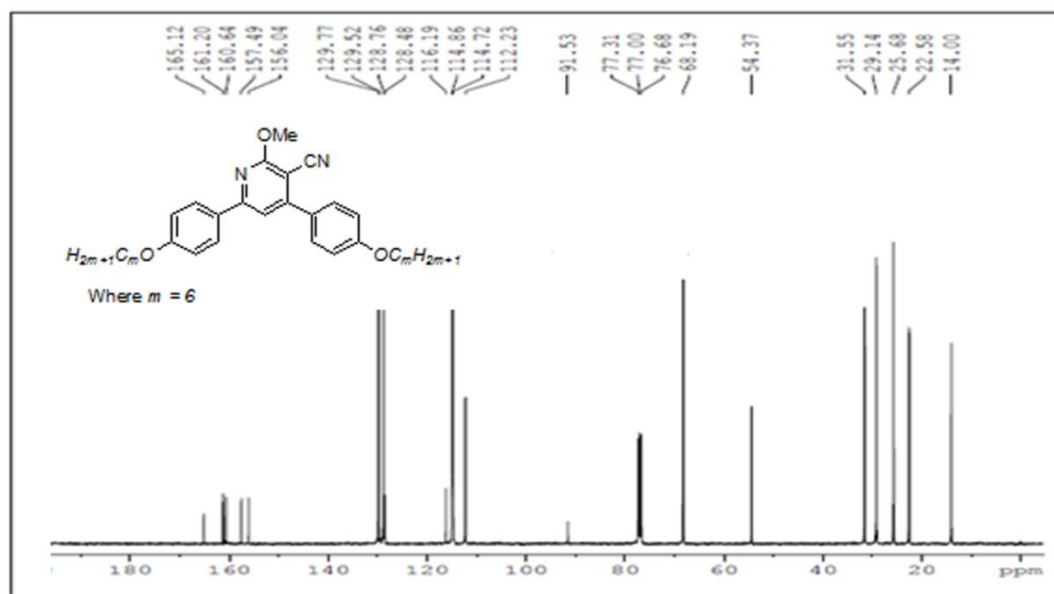
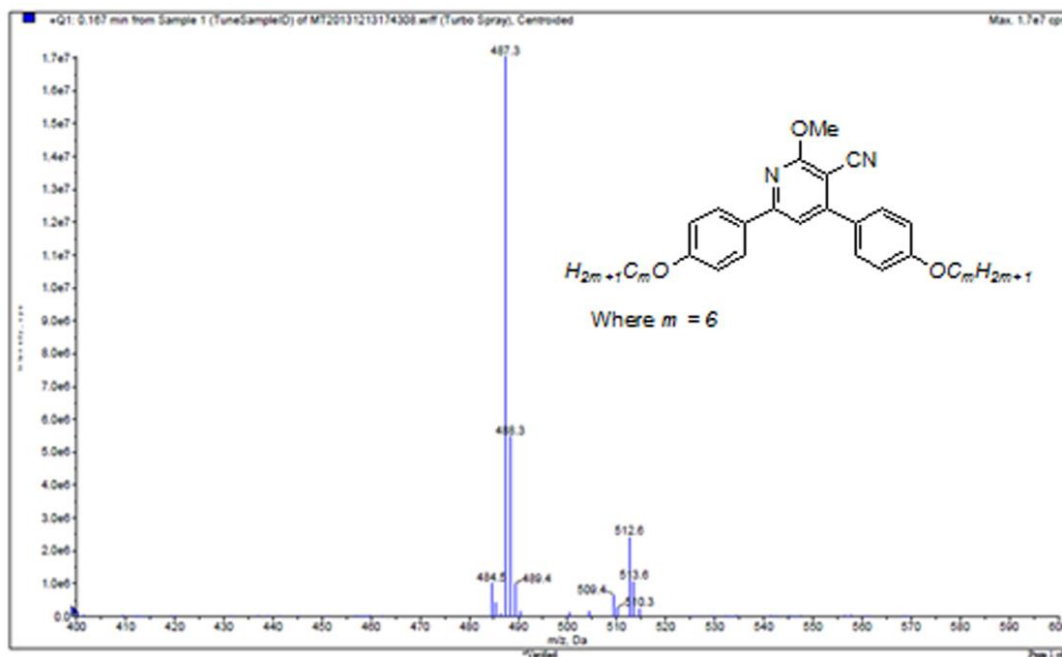
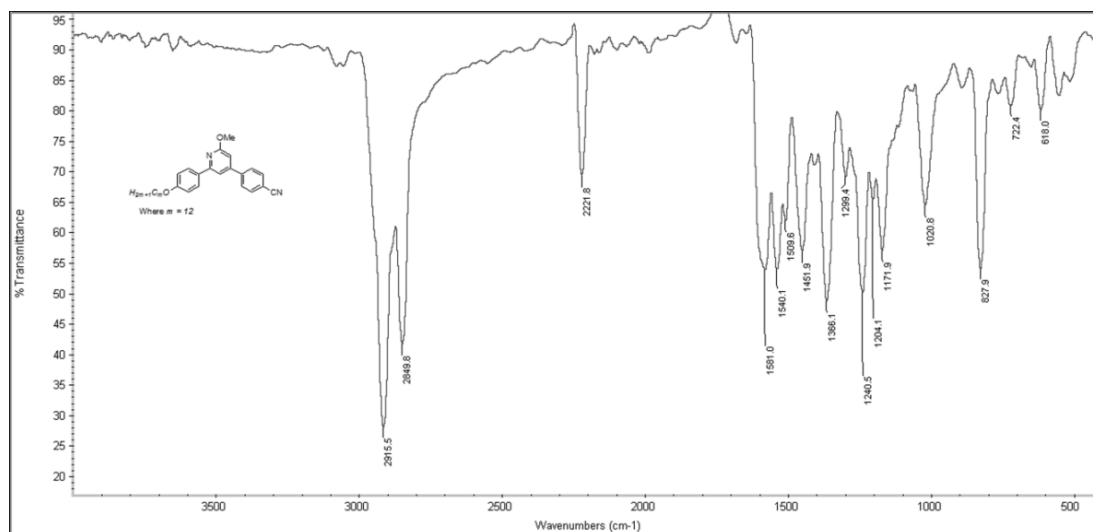
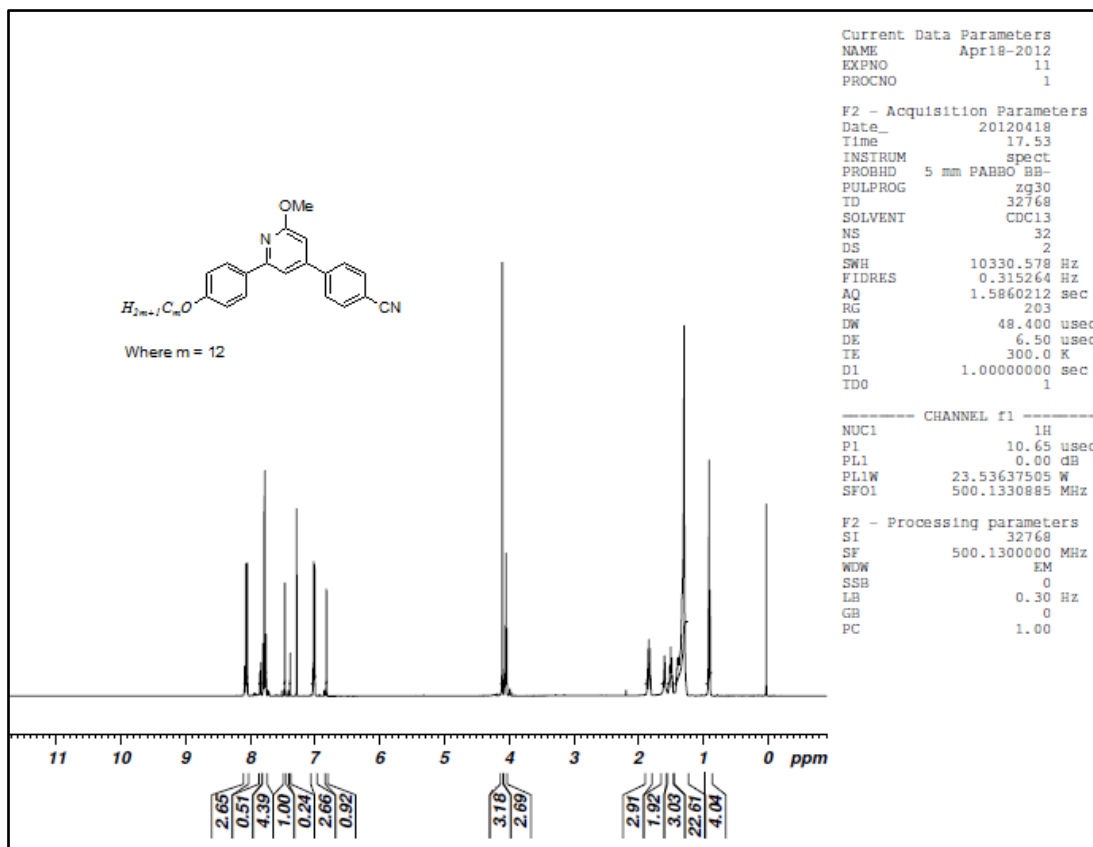
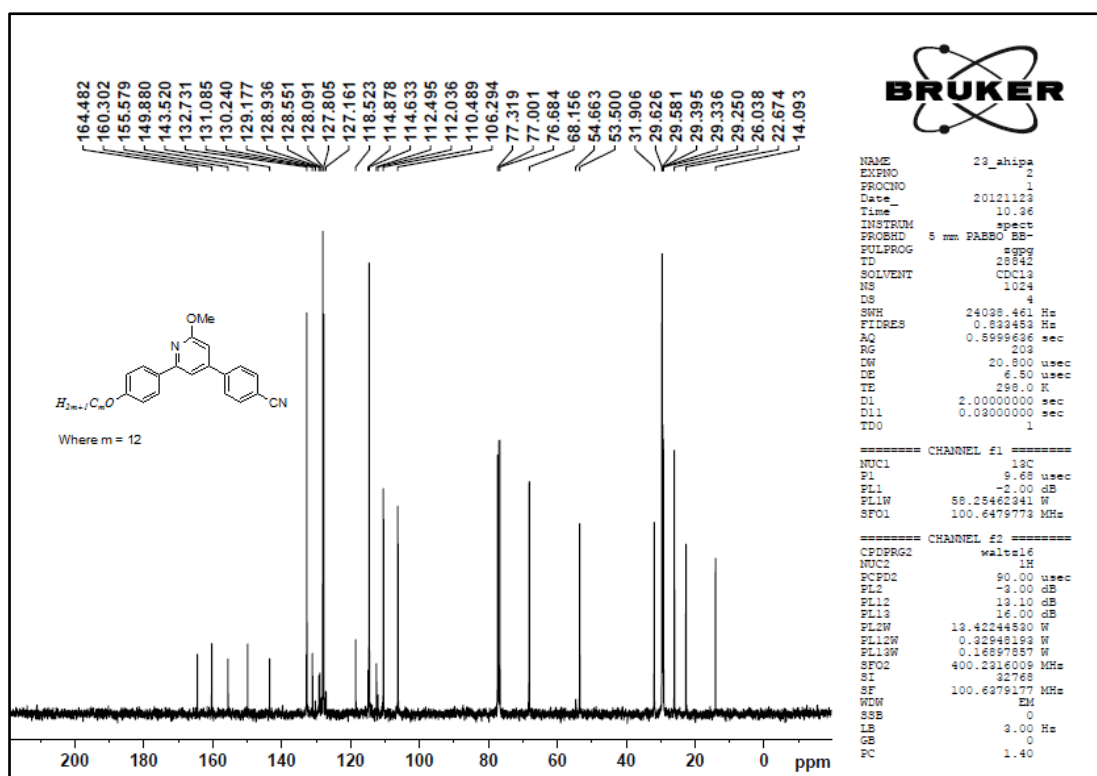
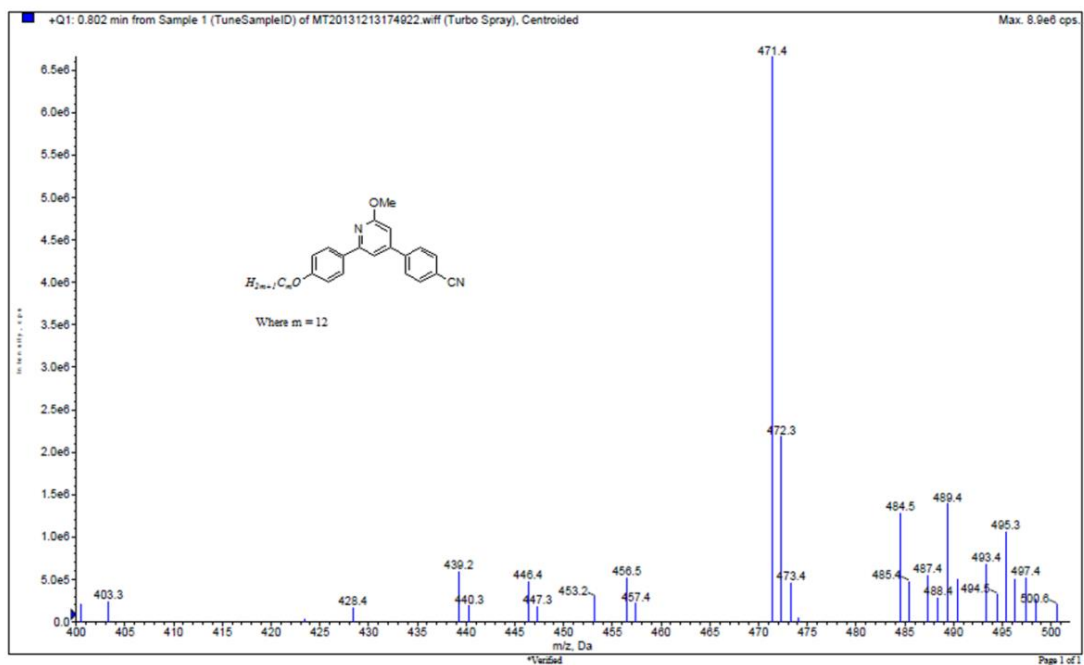


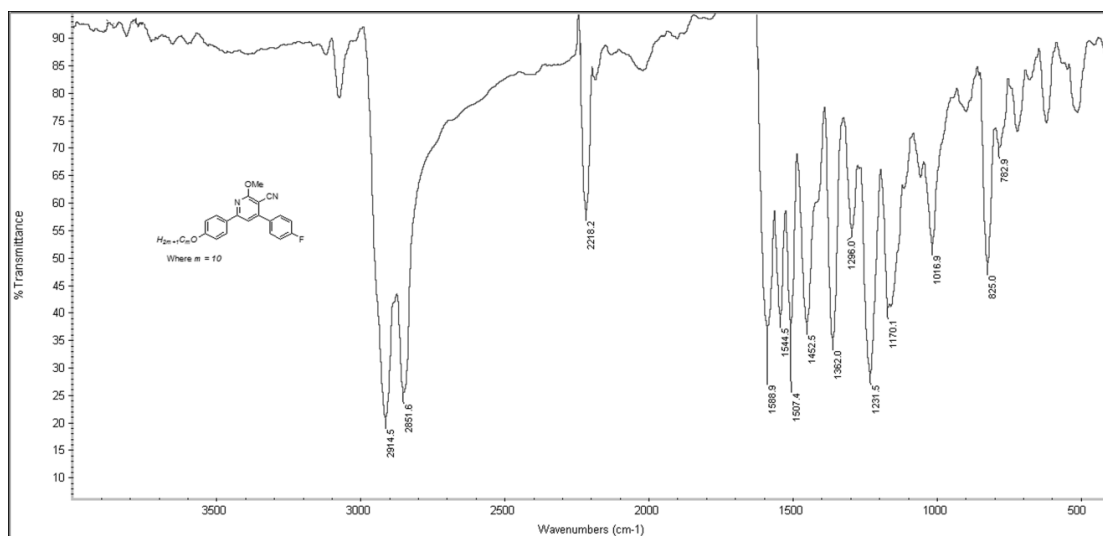
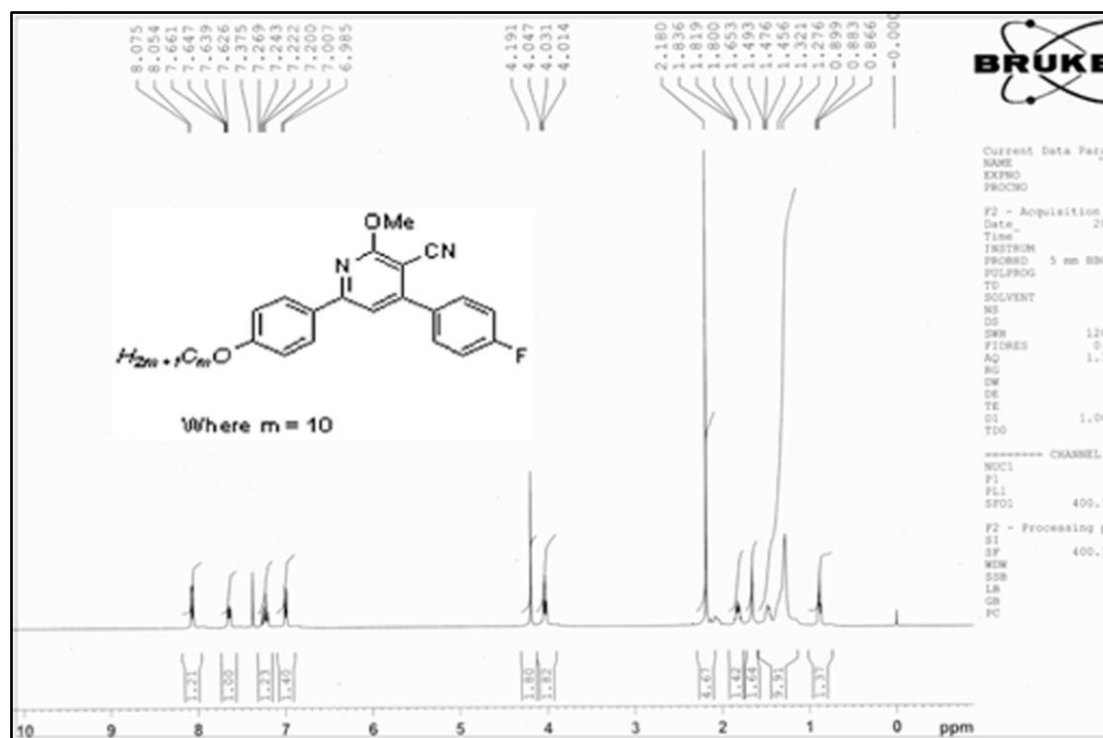
Figure 3.17 <sup>1</sup>H NMR spectrum of LC<sub>2</sub>

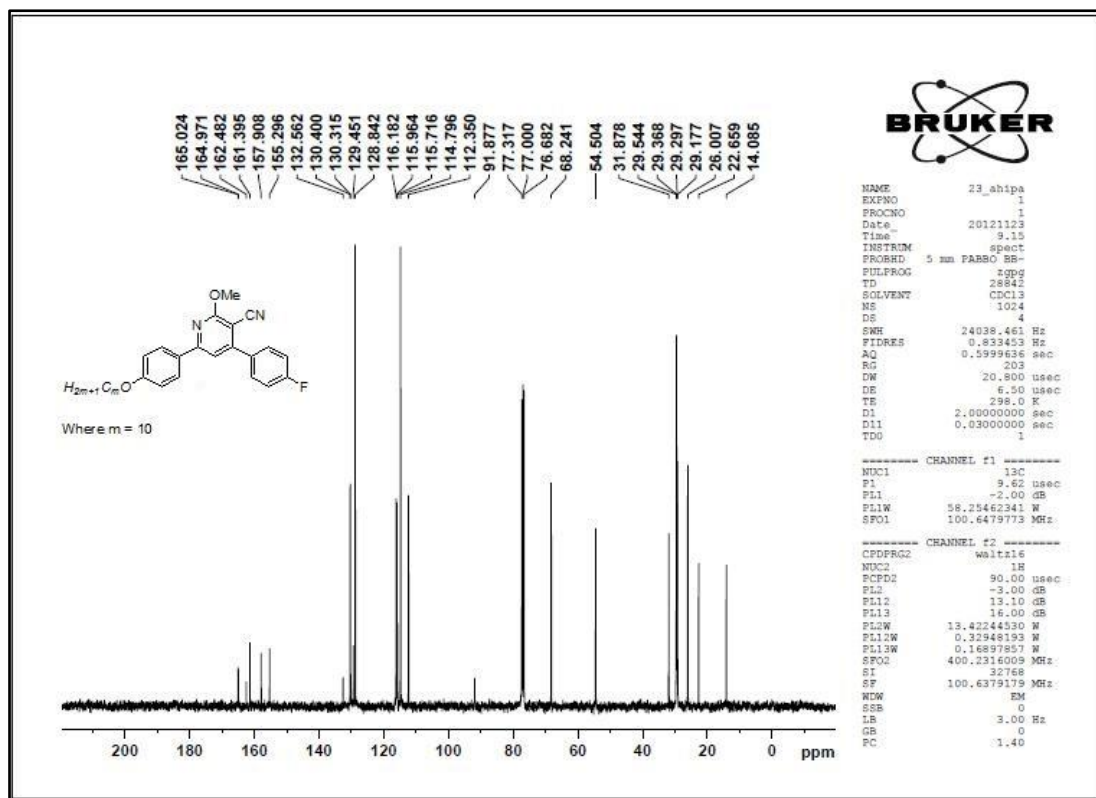
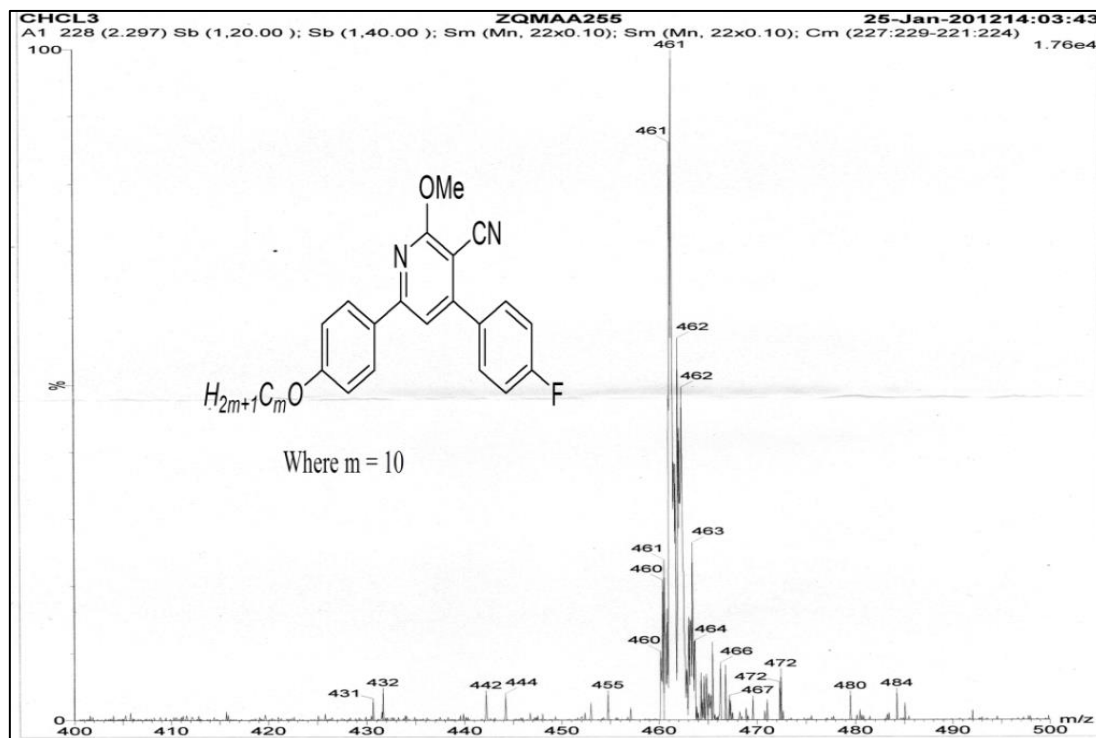
Figure 3.18  $^{13}\text{C}$  NMR spectrum of  $\text{LC}_2$ Figure 3.19 Mass spectrum of  $\text{LC}_2$

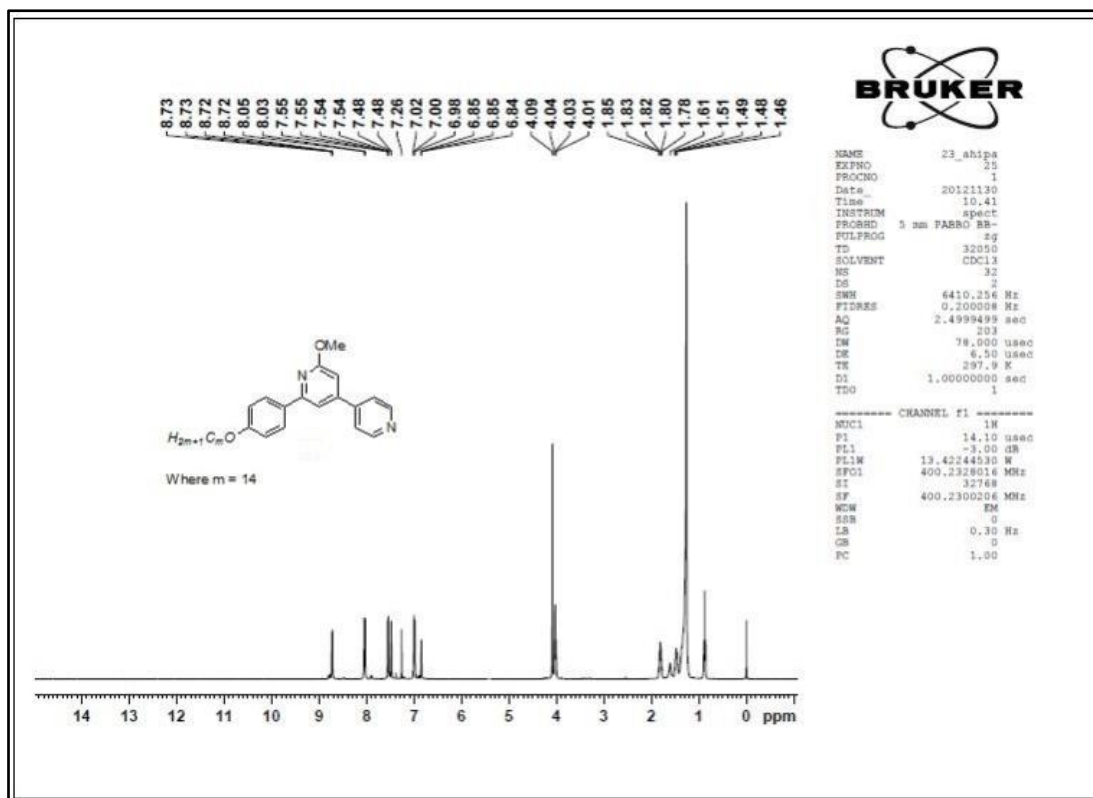
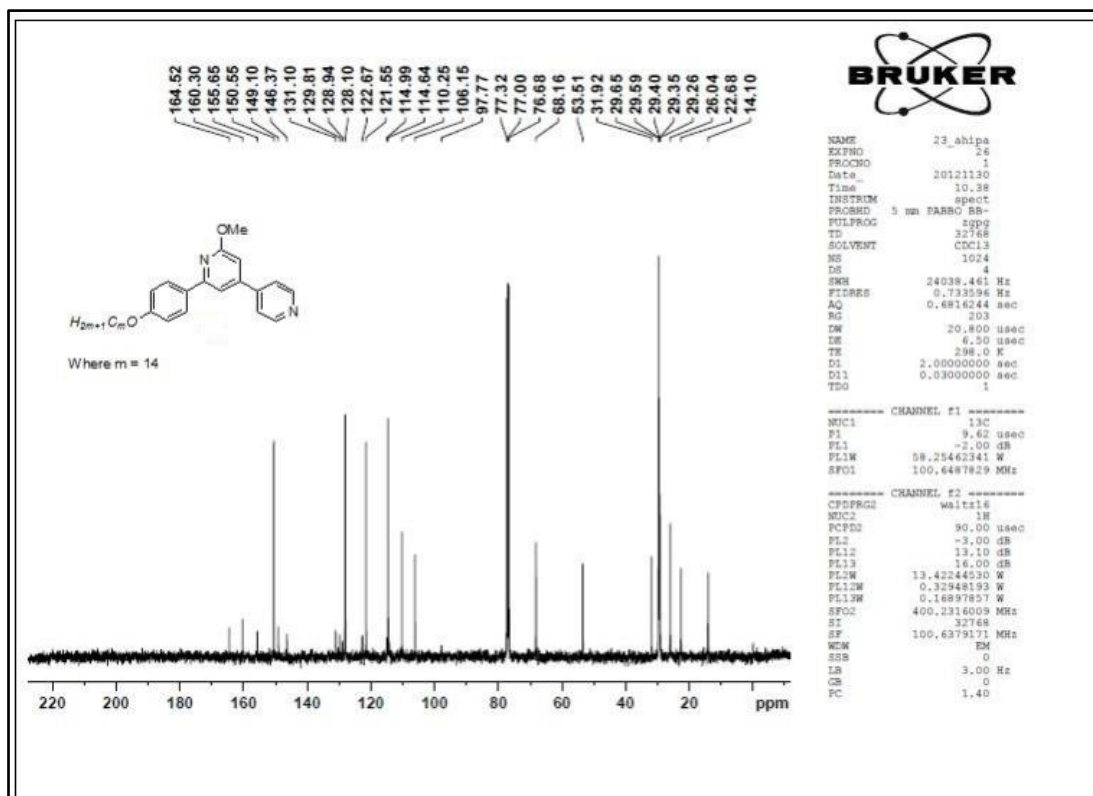
Figure 3.20 FTIR spectrum of LC<sub>18</sub>Figure 3.21 <sup>1</sup>H NMR spectrum of LC<sub>18</sub>

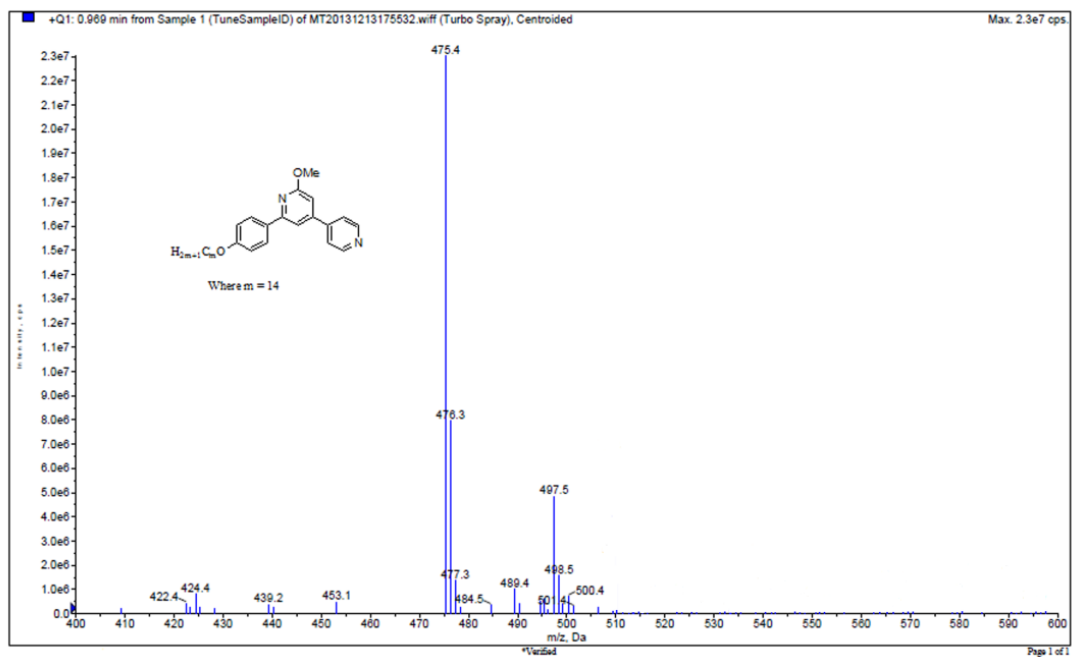
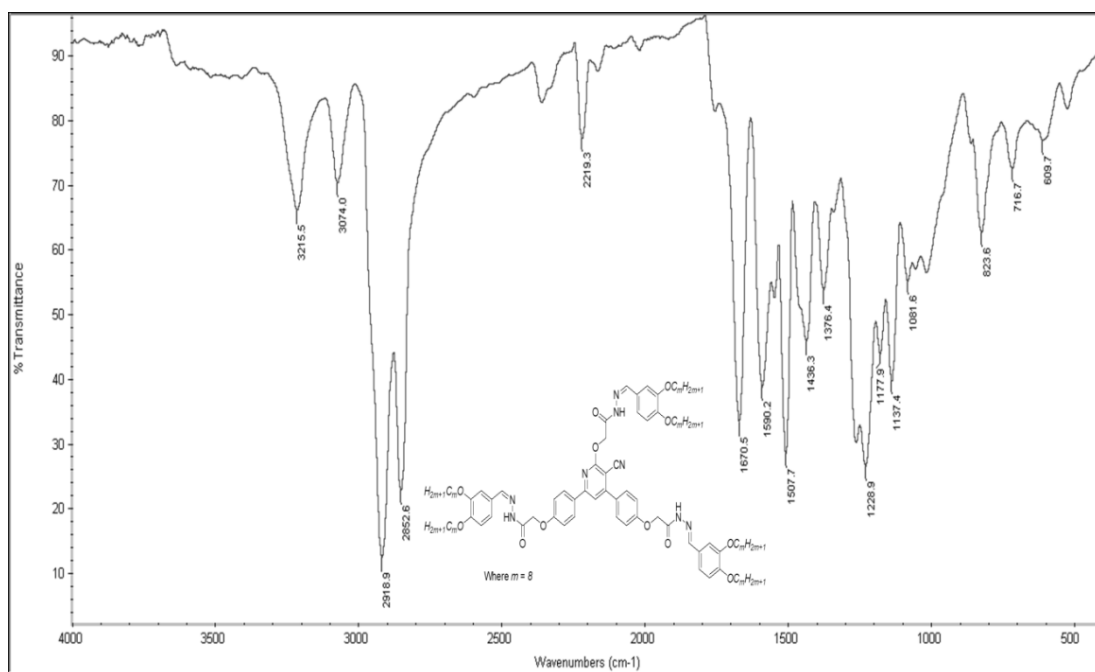
Figure 3.22  $^{13}\text{C}$  NMR spectrum of  $\text{LC}_{18}$ Figure 3.23 Mass spectrum of  $\text{LC}_{18}$

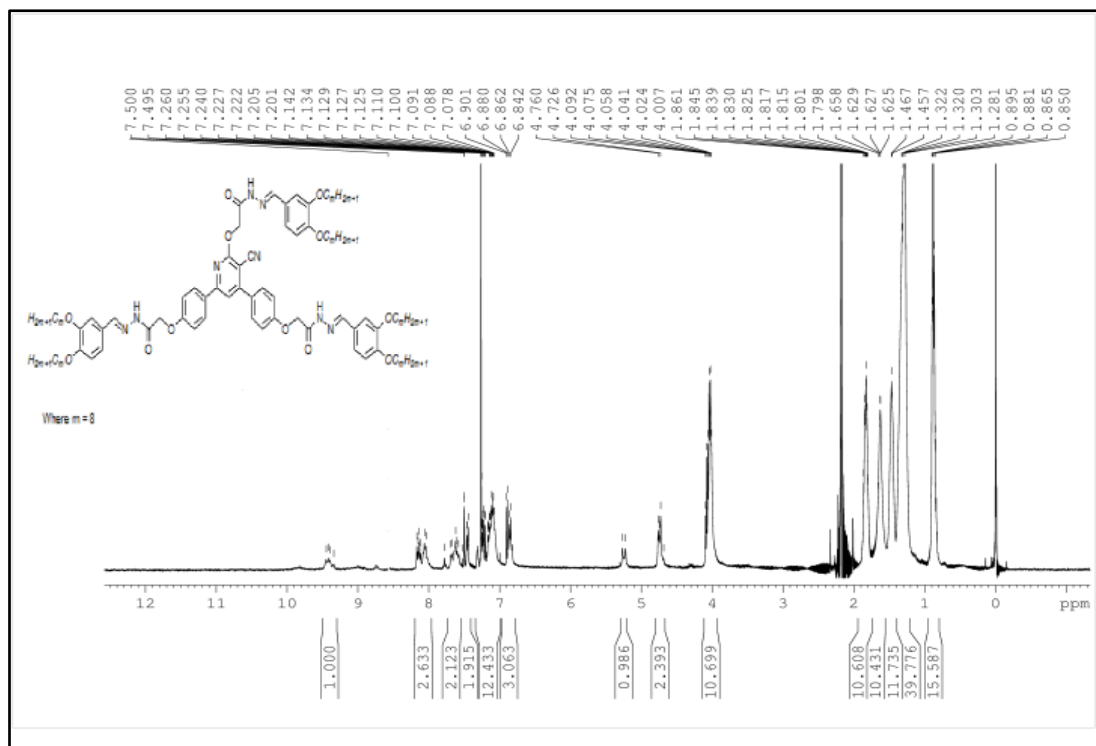
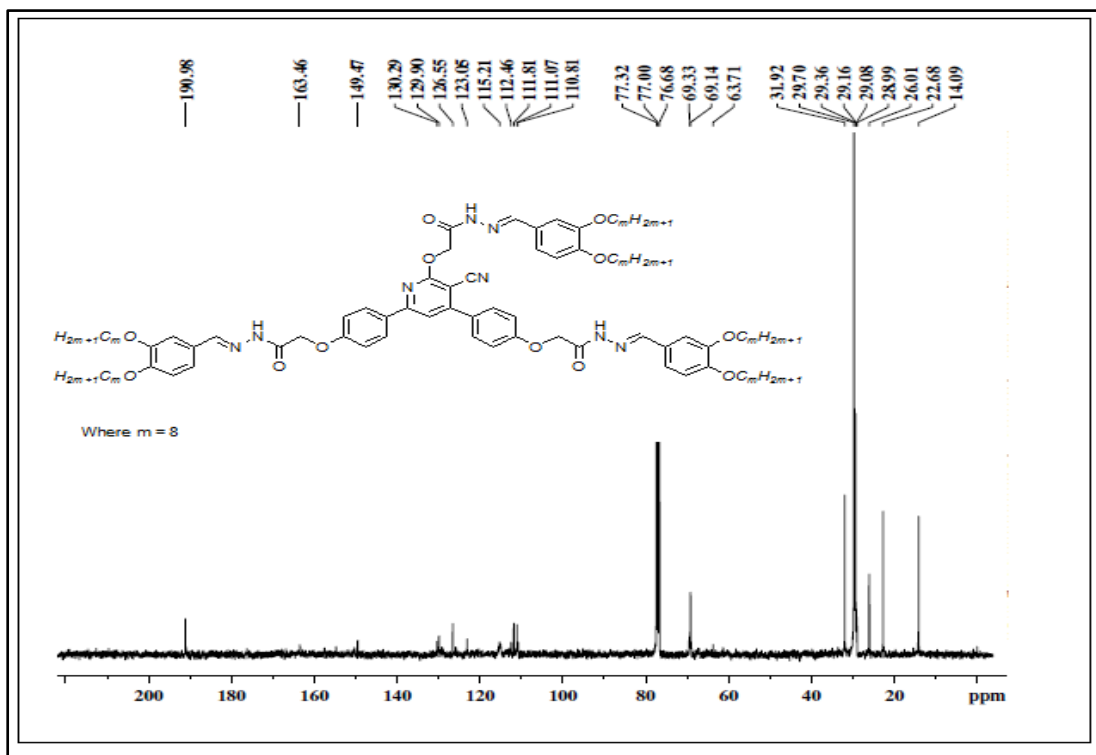


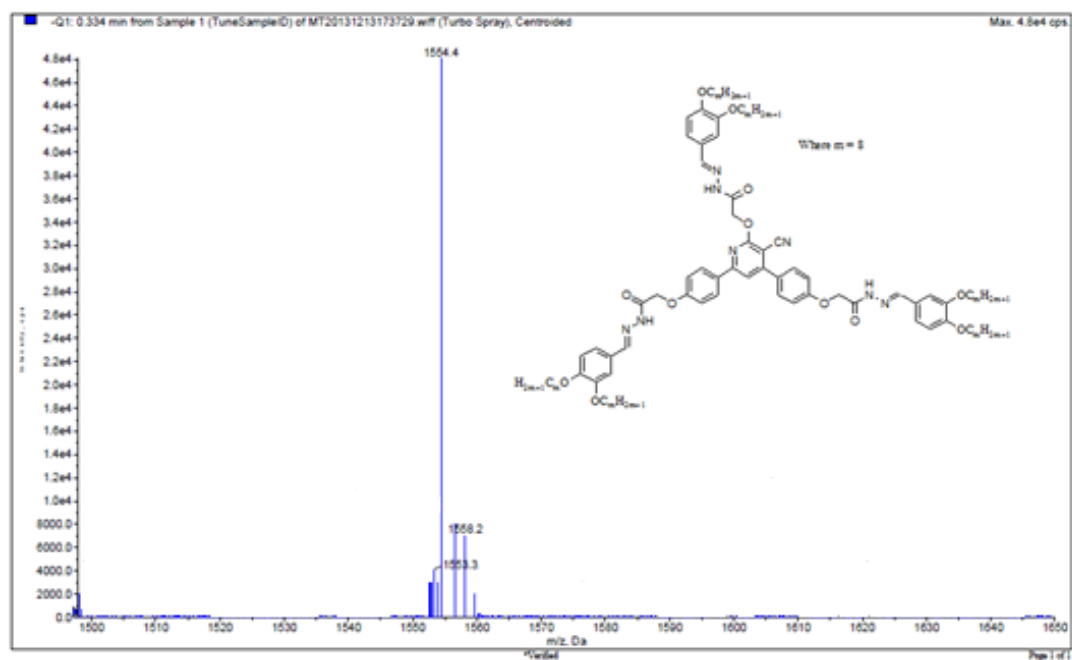
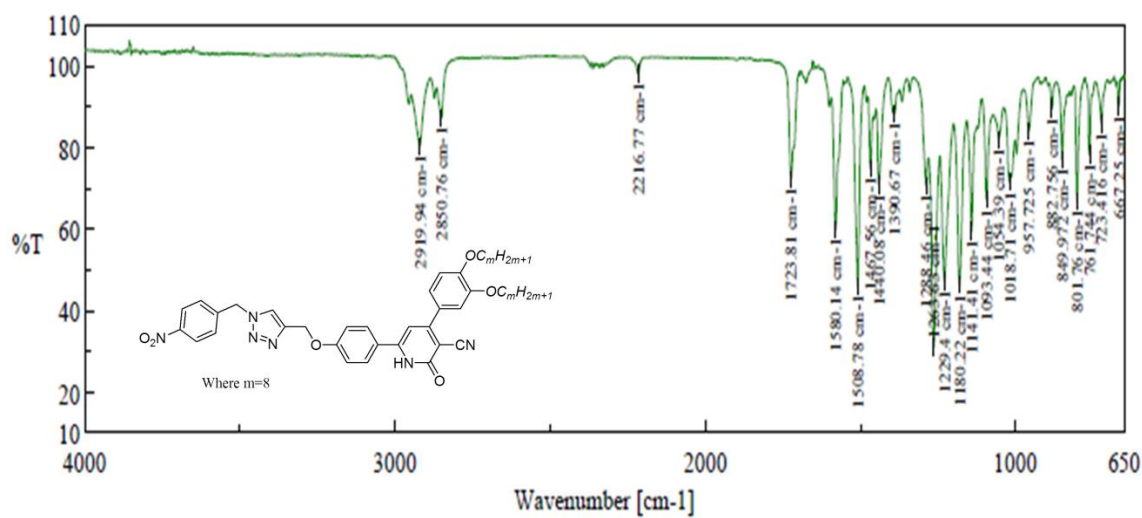
Figure 3.24 FTIR spectrum of LC<sub>20</sub>Figure 3.25 <sup>1</sup>H NMR spectrum of LC<sub>20</sub>

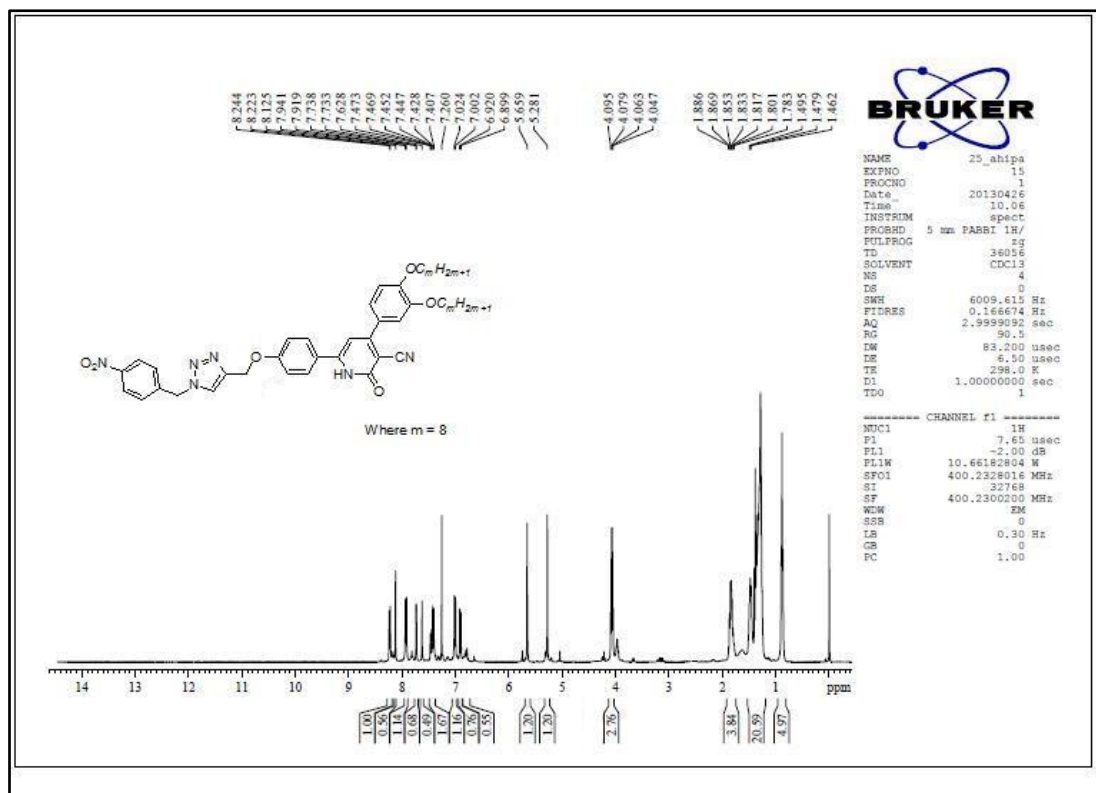
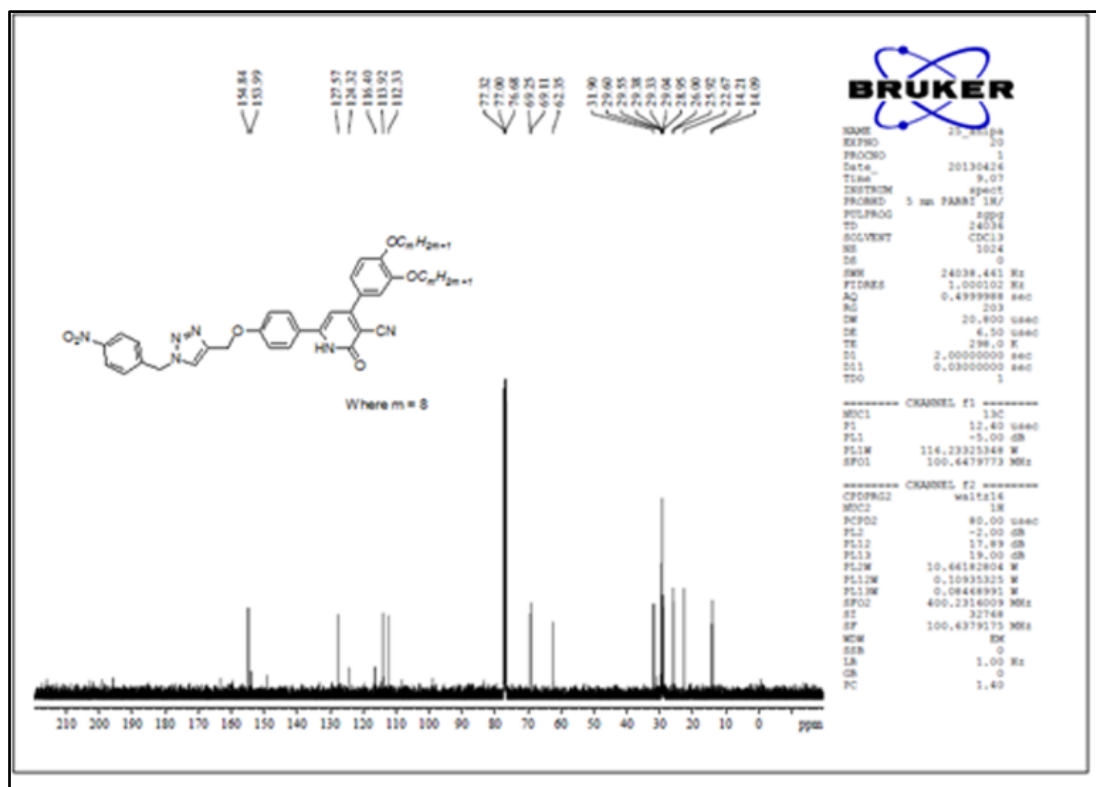
Figure 3.26 <sup>13</sup>C NMR spectrum of LC<sub>20</sub>Figure 3.27 Mass spectrum of LC<sub>20</sub>

Figure 3.28 <sup>1</sup>H NMR spectrum of LC<sub>32</sub>Figure 3.29 <sup>13</sup>C NMR spectrum of LC<sub>32</sub>

Figure 3.30 Mass spectrum of LC<sub>32</sub>Figure 3.31 FTIR spectrum of LC<sub>34</sub>

Figure 3.32 <sup>1</sup>H NMR spectrum of LC<sub>34</sub>Figure 3.33 <sup>13</sup>C NMR spectrum of LC<sub>34</sub>

Figure 3.34 Mass spectrum of LC<sub>34</sub>Figure 3.35 FTIR spectrum of LC<sub>44</sub>

Figure 3.36  $^1\text{H}$  NMR spectrum of LC<sub>44</sub>Figure 3.37  $^{13}\text{C}$  NMR spectrum of LC<sub>44</sub>

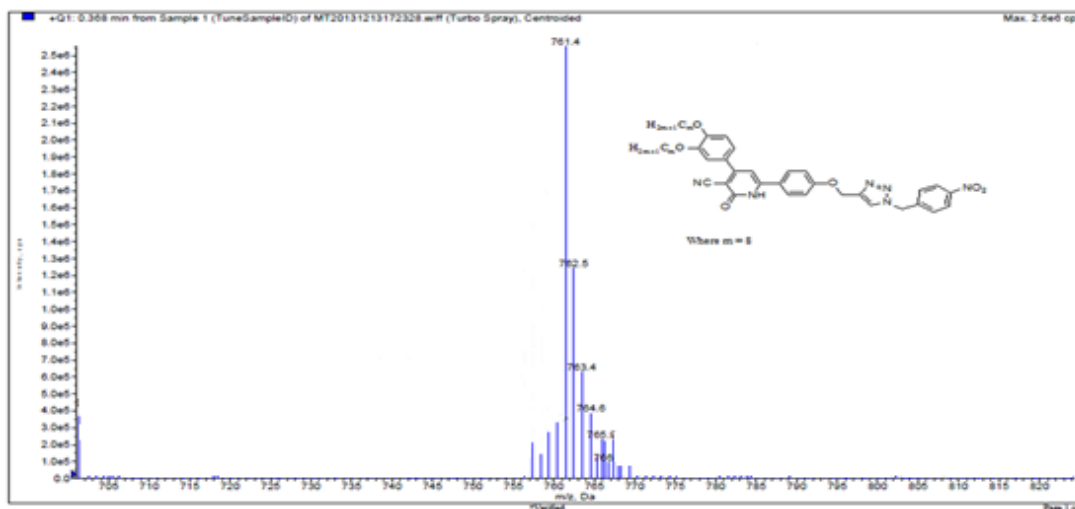


Figure 3.38 Mass spectrum of LC<sub>44</sub>

### 3.4 CONCLUSIONS

In conclusion, forty eight newly designed pyridine based compounds (LC<sub>1-48</sub>) carrying various alkoxy chain lengths, linking groups and polar substituents were successfully synthesized, following appropriate synthetic routes, as per the **Schemes 3.1-3.4**. The synthetic methods have been optimized with respect to solvent, yield, and other reaction conditions. The purification techniques for all the new compounds were established. Further, the structures of new intermediates as well as final compounds were confirmed by techniques such as FTIR, <sup>1</sup>H NMR, <sup>13</sup>C NMR and Mass spectrometry followed by elemental analysis methods. Finally three dimensional crystal structures of certain selected intermediate and final compounds were established using SCXRD technique. Also, nature of short contacts, planarity of molecule and other crystallographic information were explored.



**CHAPTER 4**

**INVESTIGATION OF MESOGENIC, OPTICAL AND  
OPTOELECTRONIC PROPERTIES OF NEW PYRIDINE  
DERIVATIVES**

### *Abstract*

*This chapter describes investigation of liquid crystalline property of newly synthesized pyridine derivatives with the aid of POM, DSC, XRD techniques. Further, it covers a description on effect of their structure on observed liquid crystalline property. Also, it involves study of their photophysical properties using UV-visible and fluorescence spectroscopic techniques to explore their linear optical behaviour. In the end, investigation of optoelectronic properties of a selected compound has been included.*

## **4.1 INTRODUCTION**

In the previous chapter, synthesis and characterization of four new series of pyridine derivatives comprising forty eight compounds (**LC<sub>1-48</sub>**) have been discussed in detail. The present chapter describes the investigation of liquid crystalline and photophysical properties of newly synthesized pyridine derivatives.

## **4.2 INVESTIGATION OF LIQUID CRYSTALLINE BEHAVIOUR OF NEW PYRIDINE DERIVATIVES**

The experimental procedures followed for investigation of liquid crystalline property of title compounds are given in the following section.

### **4.2.1 Experimental procedures**

#### *Instruments and methods*

In the present work, the sequence of phases and phase transition temperatures of samples were identified by observing the textures and textural changes under the polarizing optical microscope (POM). Polarized light microscopic study was carried out using a Leitz Ortholux II Pol-BK microscope equipped with a Mettler FP82HT hot stage, which was used for temperature control (temperature stabilization within  $\pm 0.1$  K). The phase transition temperatures were determined using a SHIMADZU DSC-60 differential scanning calorimeter with a heating rate of  $10\text{ }^{\circ}\text{C min}^{-1}$  (the apparatus was calibrated with indium,  $156.6\text{ }^{\circ}\text{C}$ ). About 3 mg of sample was hermetically sealed in an aluminium pan and placed in a nitrogen atmosphere. X-Ray diffraction (XRD) studies were carried out on powder samples filled in Lindemann capillaries with  $\text{CuK}_{\alpha}$  radiation using an Image Plate Detector (MAC Science, Japan) equipped with double mirror focusing optics.

## 4.2.2 Results and discussion

The experimental results of LC study pertaining to new pyridine derivatives along with their structure-property relationship were discussed in the following section.

### 4.2.2.1 Mesomorphic behavior of 4,6-dialkoxyaryl-2-methoxy nicotinonitriles (Series-I; LC<sub>1-13</sub>)

The polarizing optical microscopic (POM) observations and differential scanning calorimetry (DSC) data were obtained for compounds LC<sub>1-13</sub> (Series-I). Their results are tabulated in **Table 4.1**. **Figure 4.1** shows the POM textures showing Cr-N and N-I transitions for LC<sub>1</sub> under the first heating cycle. It displayed nematic liquid crystal phase transition while heating. The results reveal that the molecule exhibit Schlieren texture with four brushed disclinations typically observed for nematic phases. In compound LC<sub>1</sub>, the nematic phase was observed above 78 °C and it was seen up to a clearing temperature of 112 °C under POM. Further, its DSC data indicates that it exhibits a melting transition at around 78 °C with an enthalpy change of -24.5 kJ mol<sup>-1</sup> and N-I transitions at 112.6 °C with an enthalpy change of -0.8 kJ mol<sup>-1</sup>, on heating. As seen earlier, the molecular structure of LC<sub>1</sub> possesses a bent conformation, wherein two 4-butoxy phenyl groups are substituted at position-4 and -6 of 2-methoxy-3-cyanopyridine. Since it possesses terminal lower alkoxy chains (*i.e.* butoxy) and highly polarizable lateral cyano group on pyridine, LC<sub>1</sub> exhibits positional less ordered nematic phase.

As can be seen from the results, the compounds LC<sub>2-13</sub> showed the formation of enantiotropic stable columnar phase (Col) at room temperature. Some of the selected columnar textures of compounds LC<sub>5</sub> and LC<sub>7</sub> are depicted in **Figure 4.2**. The obtained POM observations for the phase transitions of these compounds at a particular temperature are in good compliance with that of their DSC thermograms. Thus, the DSC thermogram of one of the representative compounds, *i.e.* LC<sub>3</sub> is shown in **Figure 4.3**. Notably, the compounds LC<sub>2-13</sub> possess poor tendency towards crystallization upon cooling to room temperature and results in transparent films which remain stable for couple of weeks without any crystallization. Even at room

temperature, these compounds exhibited columnar phase as mesophase. The observed texture obtained by POM was confirmed by using PXRD studies. PXRD studies were carried out on representative compounds, *i.e.* **LC<sub>4</sub>** and **LC<sub>7</sub>** at room temperature. The X-ray diffraction pattern of compound **LC<sub>4</sub>** is shown in **Figure 4.4**. The observed PXRD pattern of **LC<sub>4</sub>** is indicative of the formation of a highly ordered rectangular columnar (Col<sub>r</sub>) structure. The pattern consists of three peaks at  $d=16.01$  Å,  $d=11.66$  Å and  $d=8.06$  Å in the small angle region that correspond to (200), (110) and (400) reflections, respectively, indicating a rectangular lattice of the columns with lattice parameters of  $a=32.02$  Å and  $b=12.51$  Å. Similarly, the PXRD pattern of **LC<sub>7</sub>** also exhibits three peaks at  $d=20.19$  Å,  $d=15.34$  Å and  $d=7.80$  Å in the low angle region that correspond to (200), (110) and (510) reflections, respectively, with lattice parameters of  $a=40.38$  Å and  $b=16.58$  Å. The observed diffraction peaks could be indexed to rectangular lattices of the columnar phase and their results are tabulated in **Table 4.2**. The caption of **Table 4.2** shows the details of necessary calculations. In both the X-ray patterns, only reflections with  $h+k=2n$  have been observed in the small angle region and the reflections can be assigned to a centred rectangular lattice ( $c2mm$ ). The powder X-ray diffractograms of compounds **LC<sub>4</sub>** and **LC<sub>7</sub>**, of Col<sub>r</sub> phase show a broad diffused scattering band, centred on 4.4-4.9 Å at wide angle region. This confirms the presence of liquid like order of the peripheral tails in Col<sub>r</sub> phase. Thus, the compounds **LC<sub>2-13</sub>** exhibit well stabilized Col<sub>r</sub> phase over a wide thermal range at and above room temperature.

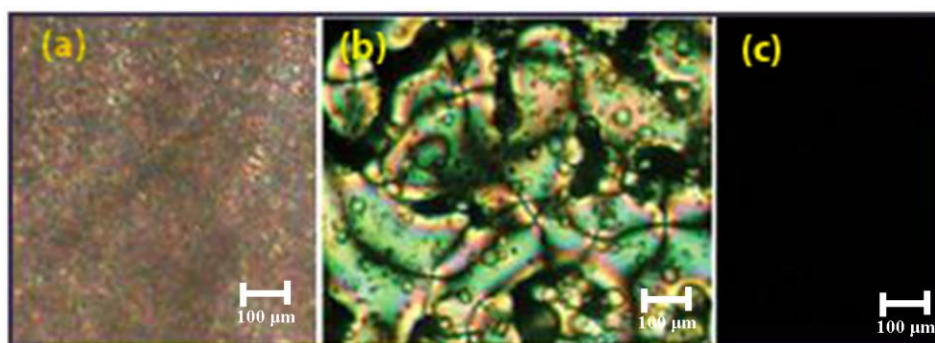


**Figure 4.1** Optical textures for (a) the crystalline phase at 30 °C (b) the nematic Schlieren texture at 105 °C and (c) the isotropic phase at 118 °C of **LC<sub>1</sub>** (first heating cycle)

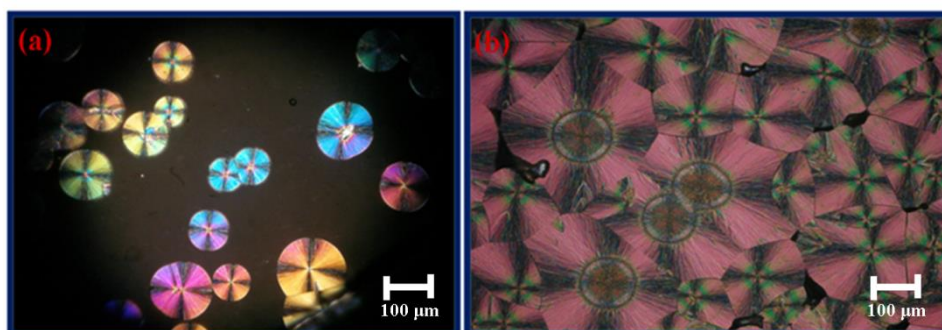


**Figure 4.2** Optical texture of Col<sub>r</sub> phase in compounds (a) LC<sub>5</sub> and (b) LC<sub>7</sub>

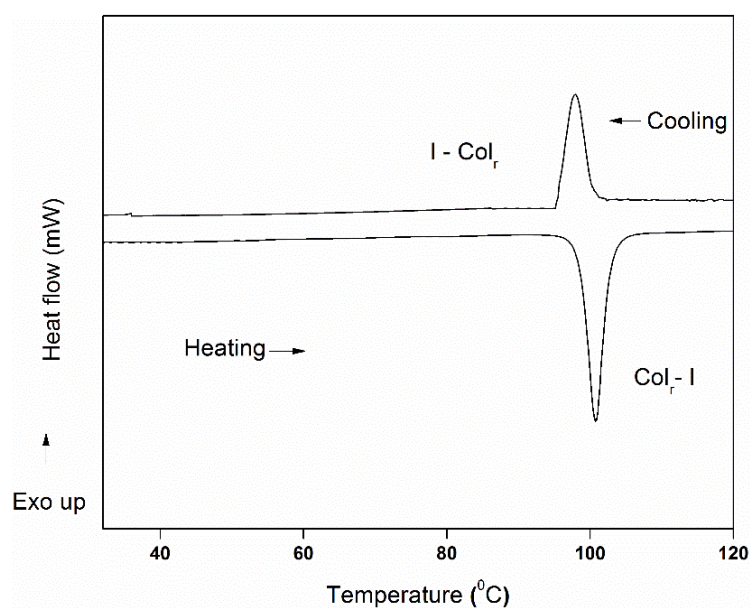


**Figure 4.3** DSC thermogram of LC<sub>3</sub> on heating and cooling cycles

**Table 4.1** Thermal behavior of LC<sub>1-13</sub> (first heating cycle)

Compound	X	m	Transition	T (°C)	ΔH (kJ mol <sup>-1</sup> )
LC <sub>1</sub>	-H	4	Cr - N	78.1	24.5
			N - I	112.6	0.8
LC <sub>2</sub>	-H	6	Col <sub>r</sub> - I	81.0	5.4
LC <sub>3</sub>	-OMe	6	Col <sub>r</sub> - I	100.1	6.1
LC <sub>4</sub>	-OEt	6	Col <sub>r</sub> - I	95.5	5.7
LC <sub>5</sub>	-H	8	Col <sub>r</sub> - I	93.7	5.9
LC <sub>6</sub>	-OMe	8	Col <sub>r</sub> - I	85.9	6.3
LC <sub>7</sub>	-OEt	8	Col <sub>r</sub> - I	95.4	6.5
LC <sub>8</sub>	-H	10	Col <sub>r</sub> - I	62.0	4.7

LC <sub>9</sub>	-OMe	10	Col <sub>r</sub> - I	78.9	6.8
LC <sub>10</sub>	-OEt	10	Col <sub>r</sub> - I	73.7	4.1
LC <sub>11</sub>	-H	12	Col <sub>r</sub> - I	64.7	5.4
LC <sub>12</sub>	-OMe	12	Col <sub>r</sub> - I	72.4	4.0
LC <sub>13</sub>	-OEt	12	Col <sub>r</sub> - I	80.4	5.3

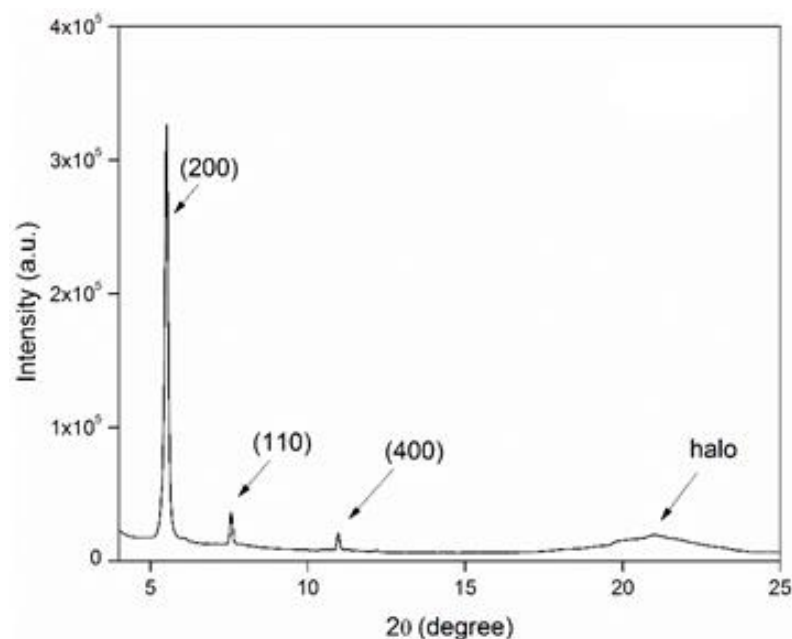


**Figure 4.4** PXRD pattern of LC<sub>4</sub> at room temperature

**Table 4.2** PXRD data of LC<sub>4</sub> and LC<sub>7</sub> at room temperature

Compound	<i>T</i> (°C)	<i>d</i> <sub>obs</sub> (Å)	Phase symmetry	Miller indices ( <i>hkl</i> )	<i>d</i> <sub>cal</sub> (Å)	Lattice parameters
LC <sub>4</sub>	25	16.01	Col <sub>r</sub>	200	16.00	<i>a</i> = 32.02 Å
		11.66		<i>c2mm</i>	110	11.65
		8.06		400	8.05	<i>S</i> = 400.57 Å <sup>2</sup>
		4.89		halo		<i>V</i> <sub>m</sub> = 881.26 Å <sup>3</sup> <i>S</i> <sub>col</sub> = 200.28 Å <sup>2</sup>
LC <sub>7</sub>	25	20.19	Col <sub>r</sub>	200	20.18	<i>a</i> = 40.38 Å
		15.34		<i>c2mm</i>	110	15.32
		7.80		510	7.80	<i>S</i> = 669.50 Å <sup>2</sup>
		4.57		halo		<i>V</i> <sub>m</sub> = 974.42 Å <sup>3</sup> <i>S</i> <sub>col</sub> = 334.75 Å <sup>2</sup>

*Details of calculation:* The data *d*<sub>obs</sub> and *d*<sub>cal</sub> are the measured and theoretical diffraction spacings; *d*<sub>cal</sub> is deduced from the following mathematical expression:  $1/d_{hk} = \sqrt{(h^2/a^2 + k^2/b^2)}$ ; *hk* are the indexations of the reflections corresponding to the

rectangular symmetry, and  $a$  and  $b$  are the lattice parameters of the  $Col_r$  phase ( $a=2d_{20}$ ). For the  $Col_r$ ,  $S=a \times b$  where  $S$  is the lattice area and  $S_{col}=S/2$  where,  $S_{col}$  is the columnar cross-section. Molecular volume  $V_m$  is calculated using the formula  $V_m=M / \lambda \delta N_A$  where  $M$  is the molecular weight of the compound,  $N_A$  is the Avogadro number,  $\delta$  is the volume mass density ( $\approx 1 \text{ g cm}^{-3}$ ), and  $\lambda(T)$  is a temperature correction coefficient at the temperature of the experiment ( $T$ ),  $\lambda=V_{CH_2}(T_0)/V_{CH_2}(T)$ , where  $T_0=25 \text{ }^\circ\text{C}$ ,  $V_{CH_2}(T)=26.5616+0.02023T$ .

By combining the data of powder X-ray and single crystal pattern (discussed in **Chapter 3**), it is possible to create a schematic diagram for  $LC_2$  and  $LC_3$  as shown in **Figures 4.5** and **4.6**, respectively. These diagrams represent the shape of individual molecule and type of molecular interactions substantially influenced for molecular self-organization into column. The self-organized columns of  $LC_2$  exhibit certain molecular interactions like C-H $\cdots$ N hydrogen bonds, C-H $\cdots$  $\pi$  interactions and C-H $\cdots$ H-C intermolecular contacts between the terminal alkoxy chains as evidenced by SCXRD results. Similarly, the self-organized columns of  $LC_3$  also exhibit similar kind of molecular interactions that are observed in columns of  $LC_2$ . In addition to these interactions, one more type of interaction, *viz.* C-H $\cdots$ O bonding is noticed in the columns of  $LC_3$ , offered by the additional methoxy group. Similar molecular interactions are also expected in rest of the compounds, *viz.*  $LC_{4-13}$ . Also, the other phases are most probably of the same type, because of the structural similarity of textures. Therefore, it can be confirmed that the compounds  $LC_{2-13}$  exhibit rectangular columnar mesophase.

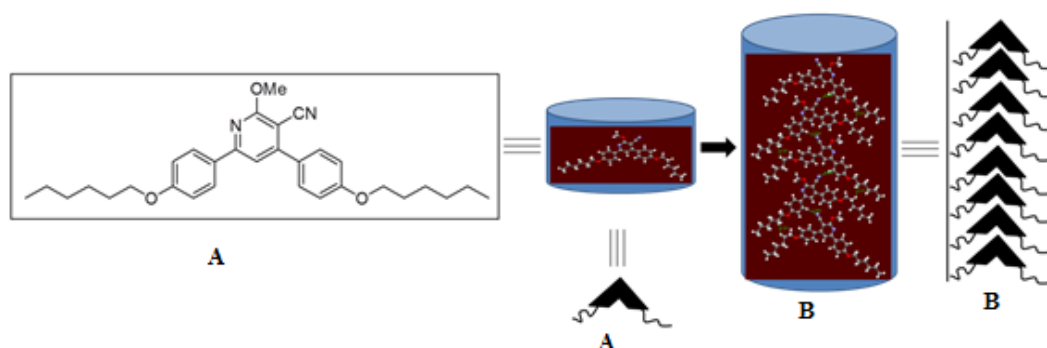


**Figure 4.5** Generation of columnar structure by  $LC_2$ . A: shape of the individual molecule; B: self-organized molecules in column

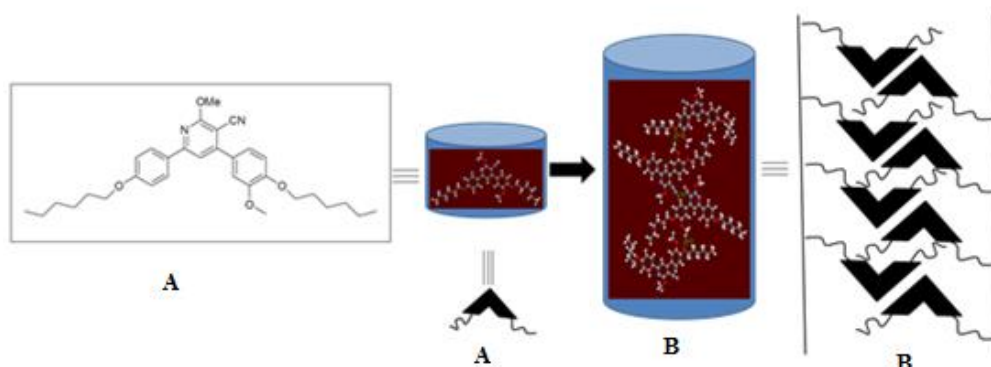


**Figure 4.6** Generation of columnar structure by LC<sub>3</sub>. A: shape of the individual molecule; B: self-organized molecules in column

To summarize, the thirteen newly synthesized pyridine derivatives of the **Series-I** were shown to exhibit nematic or Col<sub>r</sub> phase. The compounds containing lower alkoxy chain (butoxy) exhibit nematic phase at higher temperature while compounds containing higher alkoxy chains display Col<sub>r</sub> phase at ambient temperature. The observed nematic phase in the compounds is largely driven by the presence of highly polar cyano group in the molecule as lateral substituent. On the other hand, the observed Col<sub>r</sub> phase in the compounds is mainly attributed to the presence of higher alkoxy chains in the molecule as terminal substituents. Finally, the existence of mesophase was confirmed by PXRD studies.

#### 4.2.2.2 Mesomorphic behavior of 6-alkoxyaryl/thiophenyl-4-substituted aryl-2-methoxy pyridines (Series-II; LC<sub>14-33</sub>)

The transition temperatures and phase assignments of LC<sub>14-33</sub> were investigated by POM and DSC studies. The compounds LC<sub>14-19</sub> exhibited liquid crystalline phase, particularly nematic or orthorhombic columnar phase. Their results are summarized in **Table 4.3**. In particular, the compound LC<sub>14</sub> (*i.e.* m=4) with shorter alkoxy terminal group [*i.e.* m=4] showed enantiotropic nematic phase as shown in **Figure 4.7(a)**. On the other hand, compounds LC<sub>15-19</sub> [m=6-14 (only even)] with longer alkoxy terminal groups displayed a columnar phase with orthorhombic symmetry behavior as confirmed by temperature dependent PXRD study. **Figure**



**4.7(b)** represents the plastic orthorhombic columnar phase observed under POM for **LC<sub>18</sub>** and **Figure 4.8** represents the DSC trace of **LC<sub>19</sub>**.

**Table 4.3** Phase transitions and enthalpy changes of **LC<sub>14-19</sub>** (first heating cycle)

Compound	m	Transition	Temperature (°C)	$\Delta H$ (kJ mol <sup>-1</sup> )
<b>LC<sub>14</sub></b>	4	Cr-N	127.1	10.6
		N-I	142.8	0.8
<b>LC<sub>15</sub></b>	6	Cr-Col <sub>ortho</sub>	105.5	14.8
		Col <sub>ortho</sub> -I	125.2	2.3
<b>LC<sub>16</sub></b>	8	Cr-Col <sub>ortho</sub>	105.1	5.9
		Col <sub>ortho</sub> -I	121.4	1.4
<b>LC<sub>17</sub></b>	10	Cr-Col <sub>ortho</sub>	102.6	21.2
		Col <sub>ortho</sub> -I	120.5	4.3
<b>LC<sub>18</sub></b>	12	Cr-Col <sub>ortho</sub>	101.6	13.2
		Col <sub>ortho</sub> -I	118.2	1.4
<b>LC<sub>19</sub></b>	14	Cr-Col <sub>ortho</sub>	99.3	26.1
		Col <sub>ortho</sub> -I	113.3	3.7

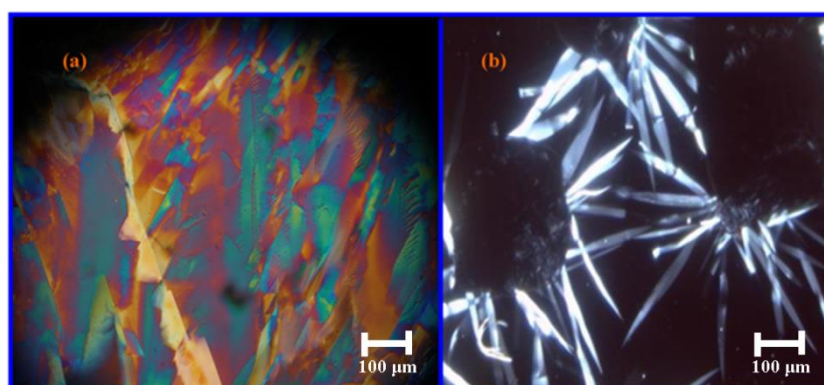


**Figure 4.7** Optical texture of (a) marble textured nematic phase in **LC<sub>14</sub>** at 137 °C;  
(b) plastic orthorhombic columnar phase in **LC<sub>18</sub>** at 102 °C

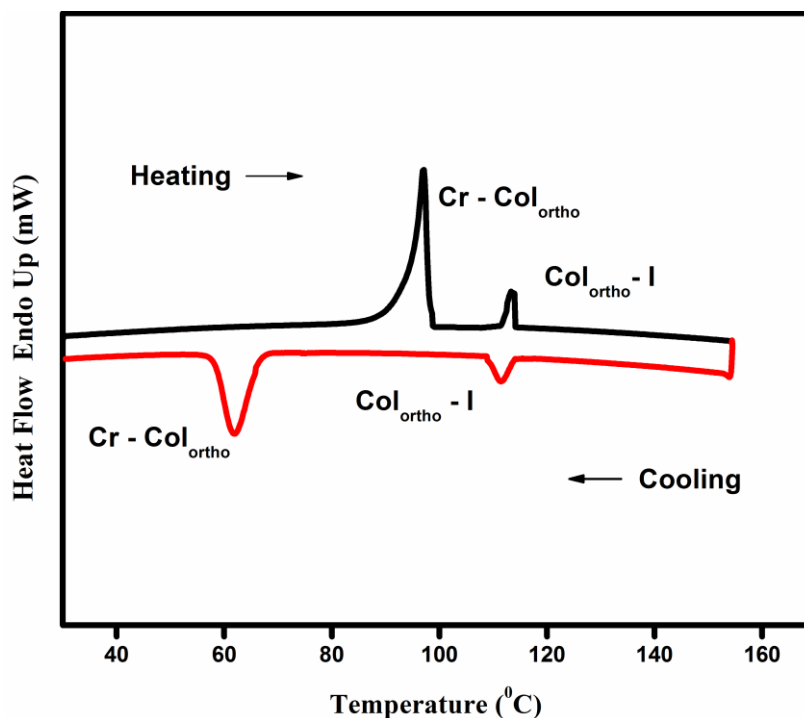


Figure 4.8 DSC trace of LC<sub>19</sub>

The compound LC<sub>14</sub> displays characteristic nematic phase sequence under POM observation. On slow cooling, the compound LC<sub>14</sub> exhibits a marble texture, which is typically observed for nematic phases. In addition, compounds LC<sub>15-19</sub> on cooling from isotropic phase, exhibit a more ordered phase with birefringent texture. Further, characterization using X-ray diffraction measurement of LC<sub>18</sub> confirms the columnar nature of the underlying structure of these intermediate phases, the results of which are summarized in Table 4.4. Raw X-ray profiles obtained in the mesophase for a representative compound, LC<sub>18</sub>, is shown in Figure 4.9. X-ray diffraction pattern of LC<sub>18</sub> at 104 °C, exhibits a number of sharp peaks in both small and wide angle regions. The obtained pattern, when subjected to peak fitting and indexing analysis, confirms that the observed mesophase has a columnar structure characterized by an orthorhombic symmetry with lattice parameters  $a=43.44\text{\AA}$ ,  $b=14.47\text{\AA}$ ,  $c=4.49\text{\AA}$ ,  $\alpha=\beta=\gamma=90^\circ$ , as shown in Figure 4.9 (obtained after background subtraction). Additionally, a diffused halo peak at  $\sim 4.3\text{\AA}$  was still observed in the wide angle regions, ruling out the phase to be a truly crystalline one. Thus, the proposed phase is to be a plastic columnar phase, *i.e.* a phase which has positional ordering in all the three dimensions, while still retaining certain orientational degrees

of freedom. The fact that the spacing of the first reflection is lower than the length of the molecule obtained from molecular modeling (29.2 Å), and being indexed to (200) plane, has suggested that the in-plane rectangular lattice consists of two molecules, perhaps held together by the non-conventional intermolecular hydrogen-bonding.

The molecular architecture of LC<sub>14-19</sub> possesses bent conformation. The compound LC<sub>14</sub> containing terminal polar cyano group and lower alkoxy chain (butoxy) exhibit positional less ordered nematic phase, while, compounds LC<sub>15-19</sub> containing terminal polar cyano group and higher alkoxy chains exhibit plastic orthorhombic columnar phase.

**Table 4.4** PXRD analysis data of LC<sub>18</sub>

Phase symmetry	$d_{obs}$ (Å)	$d_{cal}$ (Å)	Miller indices ( $hkl$ )	Lattice parameters
Col <sub>ortho</sub>	21.96	21.58	2 0 0	a = 43.43 Å
<i>P</i> 222	12.11	12.10	2 1 1	b = 14.47 Å
	10.28	10.25	3 1 0	c = 4.49 Å
	7.48	7.43	5 1 0	V = 2824 Å <sup>3</sup>
	7.26	7.30	0 2 0	
	6.49	6.51	3 2 0	
	6.04	6.05	4 2 0	
	5.13	5.13	6 2 0	
	4.72	4.71	7 2 0	
	4.50	4.48	0 0 1	
	4.35	4.34	8 2 0	
	4.23	4.24	5 3 0	
	4.09	4.10	3 1 1	
	3.93	3.93	11 0 0	
	3.78	3.79	11 1 0	
	3.68	3.68	6 1 1	
	3.42	3.42	9 3 0	
	3.22	3.21	3 3 1	

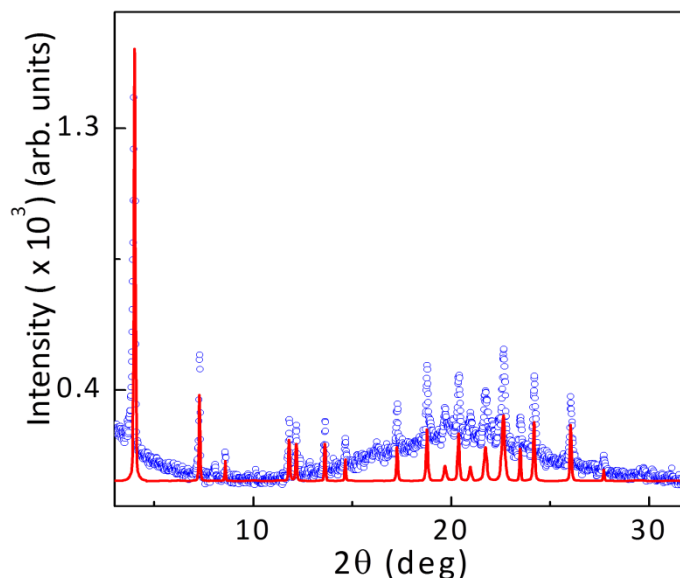


**Figure 4.9** PXR D pattern of **LC<sub>18</sub>** at 104 °C. The blue circles indicate measured data and the red line shows the profile fitting after background correction

Further, the transition temperature and phase assignment of **LC<sub>20-33</sub>** were investigated by POM and DSC studies and their results are summarized in **Table 4.5**. Among **LC<sub>20-33</sub>**, compounds **LC<sub>20-32</sub>** were shown to display liquid crystal to isotropic transition and the compound **LC<sub>33</sub>** was shown to possess only crystalline to isotropic transition. Interestingly, the compounds bearing 2-methoxy-3-cyanopyridine as central core show nematic phase except **LC<sub>33</sub>**, while compounds carrying 2-methoxypyridine as a central core exhibit columnar phase. In structure of **LC<sub>20-22</sub>**, the appearance of nematic phase (**Figure 4.10(a)**) is mainly attributed to the presence of polar 4-fluorophenyl at position-4 and alkoxyphenyl ( $m=10, 12$  and  $14$ ) at position-6 of 2-methoxy-3-cyanopyridine core. Similarly, the compounds **LC<sub>23-25</sub>** carrying terminal  $-Cl$  substituents exhibit same effect in inducing liquid crystalline phase as that of the compounds **LC<sub>20-22</sub>** carrying  $-F$  substituent. In compounds **LC<sub>23-25</sub>**, the existence of nematic phase is due to the presence of polar 4-chlorophenyl at position-4 and alkoxyphenyl ( $m=10, 12$  and  $14$ ) at position-6 of 2-methoxy-3-cyanopyridine core. In both the cases, the presence of lateral highly polar  $-CN$  group and terminal  $-F$  or  $-Cl$  group in their motifs is responsible for exhibiting positional less ordered nematic phase.

The liquid crystalline phases of compounds **LC**<sub>26-32</sub> show well defined fan-shaped texture appeared as rectangular columnar phase ( $\text{Col}_r$ ). The rectangular columnar phase of **LC**<sub>27</sub>, **LC**<sub>28</sub> and **LC**<sub>32</sub> are shown in **Figure 4.10(b-d)**, respectively. In case of compounds **LC**<sub>26-28</sub>, the appearance of  $\text{Col}_r$  is mainly attributed to presence of 4-bromophenyl group at position-4 and alkoxyphenyl ( $m=10, 12$  and  $14$ ) group at position-6 of 2-methoxypyridine core. Here, this structural feature facilitates to form dipole-dipole interaction between the molecules, which may be one of the reasons for the formation of  $\text{Col}_r$  phase. Further, these compounds show wide range of  $\text{Col}_r$  phase from ambient temperature to  $114\text{ }^\circ\text{C}$  both at the heating and the cooling cycle. To confirm this, the non-aligned sample **LC**<sub>28</sub> was subjected to PXRD measurements at  $35\text{ }^\circ\text{C}$ . The obtained pattern was subjected to peak indexing analysis and the peaks are being indexed to a  $\text{Col}_r$  phase (**Figure 4.11**) with symmetry  $P2/a$  (lattice constants:  $a=38.76\text{ \AA}$ ,  $b=26.66\text{ \AA}$  (**Table 4.6**). In the small angle region, the observed d-spacing values  $21.97$ ,  $19.38$  and  $15.67$  can be indexed to  $(110)$ ,  $(200)$  and  $(210)$  planes, respectively. A small as well as a broad peak corresponding to the stacking periodicity of a columnar structure (ca.  $3.63\text{ \AA}$ ) was seen. This observation is indicative of disordering of the molecular stacking.

Results clearly indicate that, the compounds **LC**<sub>29-31</sub> also exhibit  $\text{Col}_r$  phase at higher temperature ranging from  $100$  to  $140\text{ }^\circ\text{C}$ . The  $\text{Col}_r$  phase in these compounds can be attributed to dimerization of molecules caused by the presence of terminal 4-nitrophenyl group at position-4 of 2-methoxypyridine unit as well as variation of other terminal 4-alkoxyphenyl group at position-6. Notably,  $\text{Col}_r$  mesophase range in these compounds is nearly  $10\text{-}20\text{ }^\circ\text{C}$  even though it carries highly polarizable nitro functionality. Generally, it is expected that nitro functionality provides a wide range of mesophase, but the obtained mesophase range is very much less than that of **LC**<sub>27-29</sub>. This observation is due to the presence of terminal large planar nitro group that is believed to promote crystallization. Because of enhanced crystallization, compounds **LC**<sub>29-31</sub> exhibit  $\text{col}_r$  phase at high melting temperature with decreased mesophase.

Also, the compound **LC**<sub>32</sub> exhibits  $\text{Col}_r$  phase from ambient to  $94\text{ }^\circ\text{C}$ . Here, the appearance of  $\text{Col}_r$  phase is due to the presence of 4-pyridyl group at position-4

and 4-tetradecyloxyphenyl group at position-6 of 2-methoxypyridine core. In addition, PXRD measurements of the non-aligned sample **LC**<sub>32</sub> at 35 °C gave a pattern that is characteristic of a Col<sub>r</sub> phase with symmetry C2mm (lattice constants: a=31.04 Å, b=25.08 Å; **Table 4.6**). In the small angle region, the observed d-spacing values 19.51, 15.52 and 9.51 Å can be indexed to (110), (200) and (220) planes, respectively. Also, only reflections  $h+k=2n$  have been observed in the small angle region and thus, these reflections can be assigned to a centered rectangular lattice (C2mm). A small and broad peak corresponding to the stacking periodicity of a columnar structure (ca. 3.63 Å) has been seen. This observation is indicative of disordering of the molecular stacking. But, the compound **LC**<sub>33</sub>, was unable to exhibit any kind of liquid crystal transitions even though it possesses 2-thiophenyl group at position-6 as well as 4-decyloxyphenyl group at position-4 of 2-methoxy-3-cyanopyridine core, probably due to lack of structural anisotropy.

**Table 4.5** Phase transition data of **LC**<sub>20-33</sub> (first heating cycle)

Compound	m	Terminal substituent	Transition	Temperature (°C)	ΔH (kJ mol <sup>-1</sup> )
<b>LC</b> <sub>20</sub>	10	-F	Cr-N	115.7	21.0
			N-I	128.3	0.8
<b>LC</b> <sub>21</sub>	12	-F	Cr-N	109.6	20.0
			N-I	128.7	1.3
<b>LC</b> <sub>22</sub>	14	-F	Cr-N	101.4	18.9
			N-I	125.3	1.4
<b>LC</b> <sub>23</sub>	10	-Cl	Cr-N	117.9	22.0
			N-I	133.7	0.6
<b>LC</b> <sub>24</sub>	12	-Cl	Cr-N	109	20.9
			N-I	128.2	1.1
<b>LC</b> <sub>25</sub>	14	-Cl	Cr-N	122.2	24.1
			N-I	138.8	1.4
<b>LC</b> <sub>26</sub>	10	-Br	Col <sub>r</sub> -I	107.2	4.8
<b>LC</b> <sub>27</sub>	12	-Br	Col <sub>r</sub> -I	113.6	5.1
<b>LC</b> <sub>28</sub>	14	-Br	Col <sub>r</sub> -I	90.84	6.4
<b>LC</b> <sub>29</sub>	10	-NO <sub>2</sub>	Cr-Col <sub>r</sub>	100.9	8.6
			Col <sub>r</sub> -I	114.9	3.7
<b>LC</b> <sub>30</sub>	12	-NO <sub>2</sub>	Cr-Col <sub>r</sub>	129.2	15.1
			Col <sub>r</sub> -I	137.8	3.6
<b>LC</b> <sub>31</sub>	14	-NO <sub>2</sub>	Cr-Col <sub>r</sub>	104.7	14.8
			Col <sub>r</sub> -I	117.9	4.7
<b>LC</b> <sub>32</sub>	14	4-pyridinyl	Col <sub>r</sub> -I	93.7	8.8
<b>LC</b> <sub>33</sub>	10	-----	Cr-I	98.6	28.6

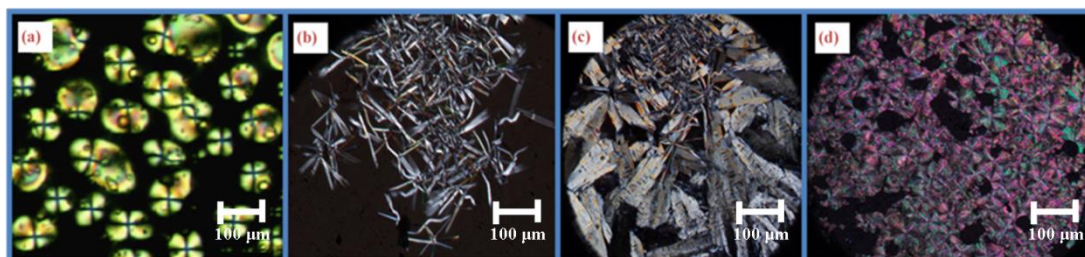


**Figure 4.10** Optical texture of (a) nematic phase in  $LC_{22}$  at  $105\text{ }^{\circ}\text{C}$ ; (b) columnar phase in  $LC_{27}$  at  $110\text{ }^{\circ}\text{C}$  (c) columnar phase in  $LC_{28}$  at  $88\text{ }^{\circ}\text{C}$ ; (d) columnar phase in  $LC_{32}$  at  $35\text{ }^{\circ}\text{C}$ .

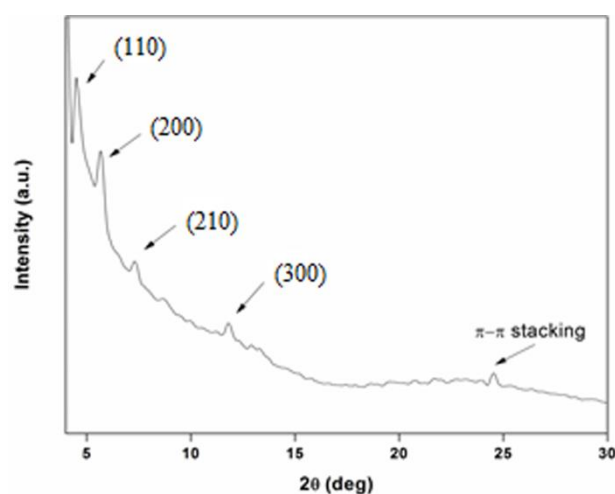


**Figure 4.11** PXRD pattern of  $LC_{28}$  at  $35\text{ }^{\circ}\text{C}$

**Table 4.6** PXRD results of  $LC_{28}$  and  $LC_{32}$  in their columnar phase

Compound	$d_{\text{obs}}$ ( $\text{\AA}$ )	Phase Symmetry	Miller indices ( $hkl$ )	$d_{\text{cal}}$ ( $\text{\AA}$ )	Lattice parameters
$LC_{28}$	21.97	$Col_r$	110	21.97	$T = 35\text{ }^{\circ}\text{C}$
	19.38	$P2/a$	200	19.38	$a = 38.76\text{ \AA}$
	15.67		210	15.67	$b = 26.66\text{ \AA}$
	12.62		300	12.92	$S = 1033.34\text{ \AA}^2$
	4.26		halo (h)		$V_m = 924.41\text{ \AA}^3$
	3.63		$\pi$ - $\pi$ stacking		$S_{\text{col}} = 516.67\text{ \AA}^2$
$LC_{33}$	19.51	$Col_r$	110	19.51	$T = 35\text{ }^{\circ}\text{C}$
	15.52	$C2mm$	200	15.52	$a = 31.04\text{ \AA}$
	9.51		220	9.70	$b = 25.08\text{ \AA}$
	4.50		halo (h)		$S = 778.48\text{ \AA}^2$
	3.75		$\pi$ - $\pi$ stacking		$V_m = 794.10\text{ \AA}^3$ $S_{\text{col}} = 395.53\text{ \AA}^2$

*Details of calculation: The data  $d_{\text{obs}}$  and  $d_{\text{cal}}$  are the measured and theoretical diffraction spacings;  $d_{\text{cal}}$  is deduced from the following mathematical expression:  $1/d_{hk} = \sqrt{(h^2/a^2 + k^2/b^2)}$ ;  $hk$  are the indexations of the reflections corresponding to the*

rectangular symmetry, and  $a$  and  $b$  are the lattice parameters of the  $Col_r$  phase ( $a=2d_{20}$ ). For the  $Col_r$ ,  $S=a \times b$  where  $S$  is the lattice area and  $S_{col}=S/2$  where,  $S_{col}$  is the columnar cross-section. Molecular volume  $V_m$  is calculated using the formula  $V_m=M / \lambda \delta N_A$ , where  $M$  is the molecular weight of the compound,  $N_A$  is the Avogadro number,  $\delta$  is the volume mass density ( $\approx 1 \text{ g cm}^{-3}$ ), and  $\lambda(T)$  is a temperature correction coefficient at the temperature of the experiment ( $T$ ),  $\lambda=V_{CH_2}(T_0)/V_{CH_2}(T)$ , where  $T_0=25 \text{ }^\circ\text{C}$ ,  $V_{CH_2}(T)=26.5616+0.02023T$ .

To sum up, **LC**<sub>14-33</sub> were shown to display either nematic,  $Col_{ortho}$  or  $Col_r$  phase. It is observed that the compounds containing lower alkoxy chain (butoxy) exhibit nematic phase. While, the compounds containing higher alkoxy chains and terminal substituents like -F, -Cl groups show nematic phase. Further, compounds containing higher alkoxy chains and terminal substituents like -CN, -NO<sub>2</sub>, -Br, 4-pyridinyl groups exhibit either  $Col_{ortho}$  or  $Col_r$  phase. The observed nematic phase in the compounds is largely driven by the presence of groups like -CN, -F, -Cl either as lateral or terminal substituents, whereas the observed  $col_{ortho}$  and  $Col_r$  phase in the compounds are largely attributed to the presence of groups like -CN, -NO<sub>2</sub>, -Br, 4-pyridinyl and higher alkoxy chains (greater than butoxy chains) as terminal substituents. The observed mesophases were confirmed by PXRD study.

#### 4.2.2.3 Mesomorphic behavior of 2-(4,6-disubstituted aryl-3-cyanopyridyl) oxy acetohydrazones (Series-III; **LC**<sub>34-38</sub>)

The mesophase behavior of **LC**<sub>34-38</sub> ( $m=8, 10, 12, 14, 16$ ) was studied by POM and DSC techniques and their results are summarized in **Table 4.7**. Newly synthesized **LC**<sub>34-38</sub> carrying different alkoxy chain lengths as terminal groups exhibited liquid crystalline phase over a wide range of temperature from ambient temperature to 110  $^\circ\text{C}$ . The observed optical texture under POM confirms the existence of hexagonal columnar phase in **LC**<sub>34-38</sub>. The polarizing optical micrograph of a representative compound **LC**<sub>38</sub> shows hexagonal columnar phase (**Figure 4.12**). **Figure 4.13** depicts the DSC trace obtained for **LC**<sub>34</sub> which indicates  $Col_h$  to isotropic transition. The FTIR spectrum has shown peaks due to N-H stretching vibrations at 3215  $\text{cm}^{-1}$  and C=O stretching at 1673  $\text{cm}^{-1}$ . This observation clearly confirms the presence of inter molecular hydrogen bonding through  $\text{N-H}\cdots\text{O}=\text{C}$  along the columns (Shen et al. 2006; Zhang and Li 2008). Also, the observed peaks at 2916 and 2850



$\text{cm}^{-1}$  due to asymmetric and symmetric stretching vibrations indicate the disordered state of alkoxy chains. Thus, FTIR data confirms that formation of columnar mesophases is mainly due to intermolecular hydrogen bond exerted by the individual trihydrazone functionalized cyanopyridine on each other. Generally, for any device application, stability of the mesophase over a wide range of use temperature is an important requirement. Since the compounds  $\text{LC}_{34-38}$  possess good mesogenic stability from ambient temperature to  $110\text{ }^{\circ}\text{C}$ , they can act as good charge carrier candidates for their applications in OLED devices.

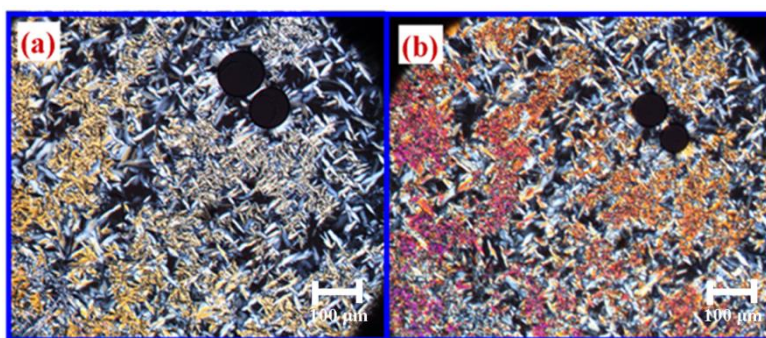


**Figure 4.12** Optical texture of hexagonal columnar phase in  $\text{LC}_{38}$  (a) at  $30\text{ }^{\circ}\text{C}$ ;  
(b) at  $75\text{ }^{\circ}\text{C}$

**Table 4.7** Phase transition temperatures and enthalpy changes for  $\text{LC}_{34-38}$  (first heating cycle)

Compound	m	Transition	Temperature ( $^{\circ}\text{C}$ )	$\Delta H$ ( $\text{kJ mol}^{-1}$ )
$\text{LC}_{34}$	8	$\text{Col}_h\text{-I}$	110	4.5
$\text{LC}_{35}$	10	$\text{Col}_h\text{-I}$	87.2	5.3
$\text{LC}_{36}$	12	$\text{Col}_h\text{-I}$	71.6	5.6
$\text{LC}_{37}$	14	$\text{Col}_h\text{-I}$	74.3	4.8
$\text{LC}_{38}$	16	$\text{Col}_h\text{-I}$	81.3	6.1

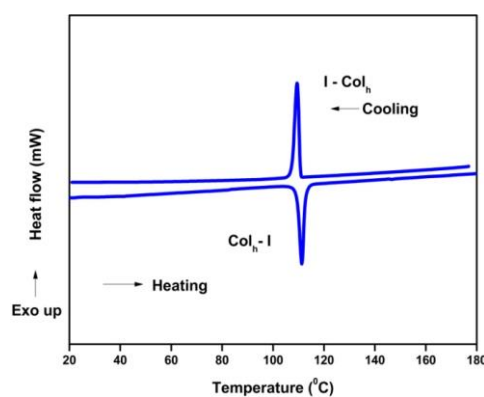


**Figure 4.13** DSC trace of  $\text{LC}_{34}$  (at a rate of  $10\text{ }^{\circ}\text{C}/\text{min}$ )

PXRD study has been performed for the compounds **LC<sub>34</sub>** and **LC<sub>38</sub>** at room temperature to confirm their mesophase behavior and the obtained results are summarized in **Table 4.8**. Characteristic patterns of hexagonal columnar phase (Col<sub>h</sub>) with sharp peaks at lower angle region and a broad halo at higher angle region (about 20°) were observed, as shown in **Figure 4.14**. The obtained diffraction pattern of **LC<sub>34</sub>** at 30 °C in the columnar phase shows six sharp peaks corresponding to the *d* spacings of 25.95, 15.05, 13.02, 8.69, 6.50, and 5.20 Å, which are indexed in sequence as (100), (110), (200), (300), (400), and (500) of a Col<sub>h</sub> lattice, respectively. In the wide-angle region, there are four diffused peaks, a broad one at  $2\theta \approx 20^\circ$  and other three relatively sharp peaks appeared at higher angles. The broad peak with a *d* spacing of  $\approx 4.20$  Å is corresponding to liquid-like packing of the aliphatic chains. The appearance of other three sharp peaks corresponding to the *d* spacings of 3.24, 3.20, and 3.03 Å is due to core-to-core (intra-columnar) separation. The core-core separation observed in the hexagonal columnar phase of **LC<sub>34</sub>** is 3.24, 3.20, 3.03 Å, which are found to be very close to the shortest core-core separations reported in the literature (Gearba et al. 2003).

In the PXRD pattern of **LC<sub>38</sub>**, only one strong reflection peak was observed in the small angle region with a *d* spacing of 38.6 Å and it was indexed as (100) plane of Col<sub>h</sub> lattice. In addition, one broad halo peak and three relatively sharp peaks for the presence of liquid-like packing of aliphatic chains and for intra-columnar core-to-core separations, respectively. From the data, it is clear that the columnar arrangements in compounds **LC<sub>34-38</sub>** are due to the presence of strong hydrogen bond and  $\pi$ - $\pi$  interactions between the cores in their molecular architecture. **Figure 4.15** shows the proposed molecular packing of **LC<sub>34-38</sub>** in the hexagonal columnar liquid crystalline phase. The PXRD results of **LC<sub>34</sub>** clearly suggests that the number of molecules inside a disk of each column is approximately one molecule ( $Z=1$ ), if the assumed density is almost  $1.0 \text{ g cm}^{-3}$  (**Table 4.8**). Here, the presence of strong hydrogen bond and  $\pi$ - $\pi$  interactions between the disks are responsible for their regular arrangements in column. Further, each column is separated by a distance of 25.95 Å in its Col<sub>h</sub> lattice.

In case of **LC<sub>38</sub>**, the number of molecules inside a disk of each column is approximately two ( $Z=2$ ) and each column is separated by a distance of 38.60 Å in its  $\text{Col}_h$  lattice. Since **LC<sub>38</sub>** molecules are much more planar and possessing elongated terminal alkoxy chains, the disc of the column retains two molecules. Further, in the DSC study, enthalpy changes of **LC<sub>34</sub>**, **LC<sub>35</sub>**, and **LC<sub>36</sub>** for the liquid crystalline to isotropic transitions were found to be 4.5-5.6 kJ/mol, and that of **LC<sub>37</sub>** was found to be 4.8 kJ/mol. But, the transition enthalpy of **LC<sub>38</sub>** was found to be 6.1 kJ/mol, which is the largest among **LC<sub>34-38</sub>**. Thus, the increase in enthalpy clearly indicates the tightness in packing of the columns.

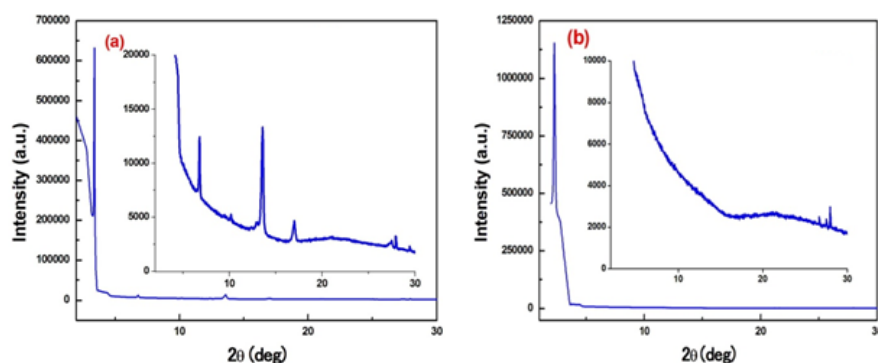


**Figure 4.14** PXRD pattern for (a) **LC<sub>34</sub>** and (b) **LC<sub>38</sub>** at 30 °C (inset shows the enlarged part of the wide angle region)

**Table 4.8** PXRD results of **LC<sub>34</sub>** and **LC<sub>38</sub>** in their hexagonal columnar phase

Compound	$d_{\text{exp}}$ (Å)	Miller indices ( $hkl$ )	Intensity (I)	$d_{\text{theo}}$ (Å)	Lattice parameters
<b>LC<sub>34</sub></b>	25.95	100	VS (sh)	25.95	T=30 °C
	15.05	110	S (sh)	14.98	a= 30.03Å
	13.02	200	S (sh)	13.00	S=777.58Å <sup>2</sup>
	8.69	300	M (sh)	8.65	V <sub>cell</sub> =3297Å <sup>3</sup>
	6.50	400	S (sh)	6.50	V <sub>mol</sub> =2591Å <sup>3</sup>
	5.20	500	M (sh)	5.20	Z = 1.27
	4.24	halo ( $h$ )	VW (br)		
	3.24	$\pi$ - $\pi$ stacking	M (sh)		
	3.20	$\pi$ - $\pi$ stacking	M (sh)		
	3.03	$\pi$ - $\pi$ stacking	M (sh)		
<b>LC<sub>38</sub></b>	38.60	100	VS (sh)	38.60	T=30 °C
	4.20	halo ( $h$ )	VW (br)		a= 44.57Å
	3.34	$\pi$ - $\pi$ stacking	M (sh)		S=1720Å <sup>2</sup>

3.24	$\pi$ - $\pi$ stacking	M (sh)	$V_{cell}=7224\text{\AA}^3$
3.20	$\pi$ - $\pi$ stacking	M (sh)	$V_{mol}=3713\text{\AA}^3$
			$Z = 1.95$

*Details of calculation: The notations  $d_{exp}$  and  $d_{theo}$  are experimental and theoretical diffraction spacings, respectively.  $d_{theo}$  is deduced from the lattice parameter  $a$  ( $Col_h$ ) from the following mathematical expression:  $d_{theo}=[2/(\sqrt{3}N_{hk})].[\sum_{hk}d_{hk}\sqrt{(h^2+k^2+hk)}]$ , where  $N_{hk}$  is the number of  $hk$  reflections observed for the  $Col_h$  phase.  $S$  is the lattice area, given by:  $S=(a^2\sqrt{3})/2$  Cell volume,  $V_{cell}=h.S$  (where  $h$  is the thickness of hexagonal stratum). The molecular volume is defined as  $V_{mol}=M/(\delta\times 0.6022)$ , where,  $M$  is molecular weight;  $V_{CH_2}(T)=26.5616+0.02023T$  ( $T$  in  $^{\circ}C$ ,  $T_0=25^{\circ}C$ ); density  $\delta=V_{CH_2}(T_0)/V_{CH_2}(T)$ ; the aggregation number or the number of molecular equivalents per stratum of column  $Z=V_{cell}/V_{mol}$ .  $I$  represents the intensity of reflections (VS: very strong, S: strong, M: medium, VW: very weak, br: broad);  $hk$  are the indexations of the reflections corresponding to the  $Col_h$  phase.*

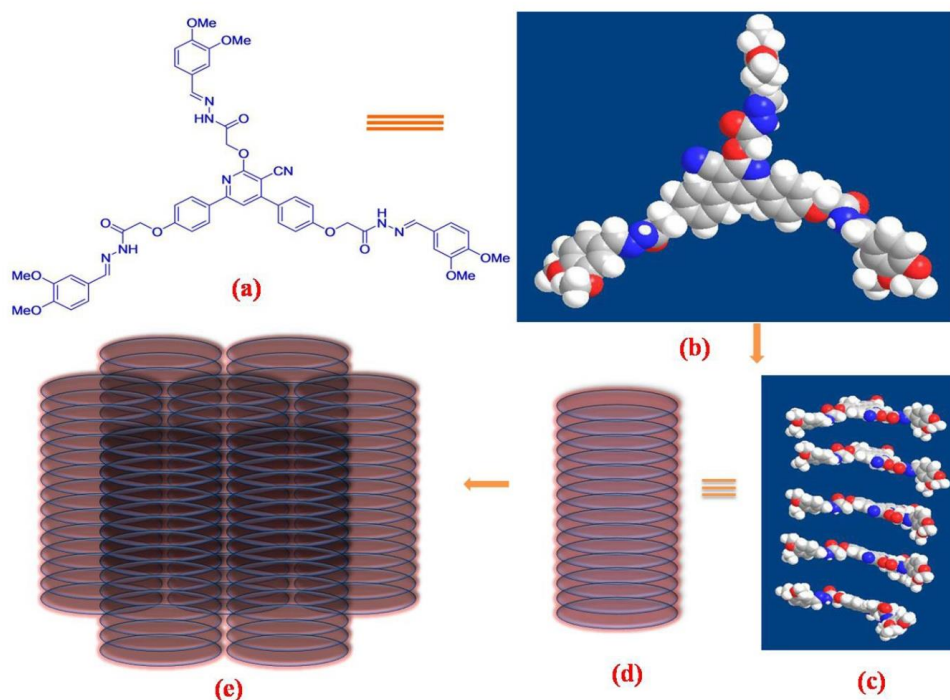


**Figure 4.15** Schematic representation of self-assembled structure of  $LC_{34-38}$  in columnar liquid crystalline phase. (a) molecular structure (terminal chains represented as methoxy group for clarity); (b) space filling model; (c) stacking in column; (d) each disk representing molecules; (e) arrangements of molecules in the hexagonal columnar mesophase

To summarize, five new pyridine compounds **LC<sub>34-38</sub>** were shown to exhibit  $\text{Col}_h$  phase with a wide mesophase range starting from room temperature to 110 °C. Their mesophase formation is due to the presence of intermolecular hydrogen bonding and core-to-core interaction caused by the trihydrazone functionalized cyanopyridine motifs. The presence of intermolecular interactions was confirmed by PXRD study.

#### 4.2.2.4 Mesomorphic behavior of 4,6-disubstituted aryl-3-cyanopyridones (Series-IV; **LC<sub>39-48</sub>**)

The LC behavior of **LC<sub>39-48</sub>** was investigated by POM and DSC techniques. The result of POM and DSC studies involving phase transition temperatures and values of enthalpy change are summarized in **Table 4.9**. Analysis of POM data of compounds **LC<sub>39-48</sub>** confirms the presence of a non-crystalline soft anisotropic phase at ambient temperature that remains highly viscous until they move into their isotropic liquid state. The well-defined fan-shaped texture characteristic of the hexagonal columnar mesophases ( $\text{Col}_h$ ) is observed upon heating as well as cooling processes. The stability of mesophase varies with the terminal alkoxy chain lengths as well as nature of polar substituent's (-CN or -NO<sub>2</sub>).

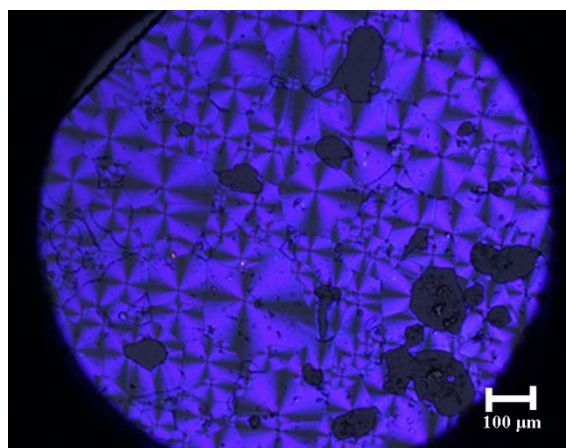


**Figure 4.16** Optical texture of  $\text{Col}_h$  phase in **LC<sub>40</sub>** at 30 °C

In addition, DSC thermograms display first-order transitions at the phase transition temperatures. The first member **LC<sub>39</sub>** with cyano and two octyloxy chains as terminal substituents was found to exhibit enantiotropic mesomorphism, wherein, on heating  $\text{Col}_h$ -I transition is observed at 68.9 °C, while upon cooling the phase transition reverts. Similar phase transitions are seen in compounds **LC<sub>40-43</sub>**. But, their

clearing temperature has enhanced from 68.9 °C (**LC**<sub>39</sub>; *m*=8) to 94.1 °C (**LC**<sub>43</sub>; *m*=16) indicating the improved stability of Col<sub>h</sub> mesophase with the increase in chain lengths. Further, identical DSC thermograms and mesophase stability are perceived in the case of compounds **LC**<sub>44-48</sub> with -NO<sub>2</sub> as one of the terminal polar substituents. Thus, it clearly suggests that the variation of chain lengths in the molecular architecture helps for improving the mesophase stability. **Figure 4.16** depicts the fan-shaped columnar texture of compound **LC**<sub>40</sub> while **Figure 4.17** shows its DSC trace.

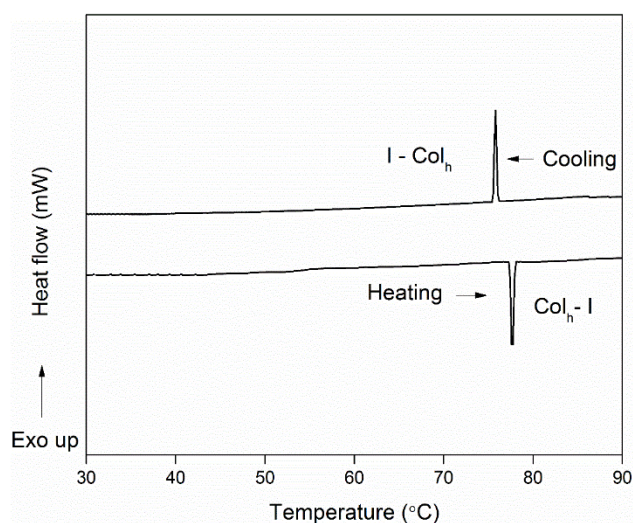


**Figure 4.17** DSC trace of **LC**<sub>40</sub>

**Table 4.9** Phase transition temperatures and enthalpy changes for **LC**<sub>39-48</sub> (first heating cycle)

Compound	<i>m</i>	X	Transition	Temperature (°C)	ΔH (kJ mol <sup>-1</sup> )
<b>LC</b> <sub>39</sub>	8		Col <sub>h</sub> -I	68.9	4.5
<b>LC</b> <sub>40</sub>	10		Col <sub>h</sub> -I	77.7	3.8
<b>LC</b> <sub>41</sub>	12	-CN	Col <sub>h</sub> -I	80.7	6.1
<b>LC</b> <sub>42</sub>	14		Col <sub>h</sub> -I	89.8	5.2
<b>LC</b> <sub>43</sub>	16		Col <sub>h</sub> -I	94.1	6.9
<b>LC</b> <sub>44</sub>	8		Col <sub>h</sub> -I	61.4	5.4
<b>LC</b> <sub>45</sub>	10		Col <sub>h</sub> -I	84.1	8.0
<b>LC</b> <sub>46</sub>	12	-NO <sub>2</sub>	Col <sub>h</sub> -I	76.3	6.3
<b>LC</b> <sub>47</sub>	14		Col <sub>h</sub> -I	82.7	4.0
<b>LC</b> <sub>48</sub>	16		Col <sub>h</sub> -I	86.9	4.9

In order to explore the molecular-packing in their liquid crystalline phase, the PXRD measurements were performed for the selected compounds **LC<sub>40</sub>** and **LC<sub>44</sub>**. Their results are summarized in **Table 4.10**. The powder X-ray diffractogram (**Figure 4.18**) obtained for the compound **LC<sub>40</sub>** in liquid crystalline state shows a sharp diffraction peak in the small angle region, which can be indexed to (100) plane of hexagonal lattice of columnar phase. Also, in the wide angle region, a broad diffuse scattering centered at 4.11 Å appears; that can be attributed to the liquid like order of the terminal two decyloxy chain lengths. The calculated molecular length of **LC<sub>40</sub>** is found to be 27.6 Å, as obtained by **MM2** method. The experimentally obtained diameter (48 Å) of the Col<sub>h</sub> phase is reasonable to the calculated molecular length, only when cyano terminal substituted compound **LC<sub>40</sub>** is involved in dimer formation, as shown in **Figure 4.18**. This kind of dimerization has been also observed in the crystal packing of intermediate compound **16a** and it has been shown in **Figure 3.15 (Chapter 3)**.

Further, the number of molecules arranged side by side in a single stratum of column is found to be eight ( $Z=8$ ). There are two main reasons for holding eight molecules in a stratum; firstly because of the dimer formation between the cyano functional groups and secondly, the formation of intermolecular hydrogen bond between the cyanopyridone moieties. Further, PXRD diffractogram pattern of compound **LC<sub>44</sub>** in its liquid crystalline phase shows a diffraction peak in the small angle region corresponding to  $d$ -spacing of 37.96 Å, which is indexed to (100) plane of hexagonal lattice of columnar phase. Further, in the wide angle region, the observed halo peak at 4.31 Å is due to the liquid like order exerted by the presence of terminal two octyloxy chain lengths in its structure. Its calculated molecular length, diameter and number of molecules per stratum are found to be 25.38 Å, 44 Å and six ( $Z=6$ ), respectively for the Col<sub>h</sub> phase of **LC<sub>44</sub>**. Here, the established molecular assembly is predominantly due to the dimerization of the molecule and the presence of hydrogen bond as in **LC<sub>40</sub>**.

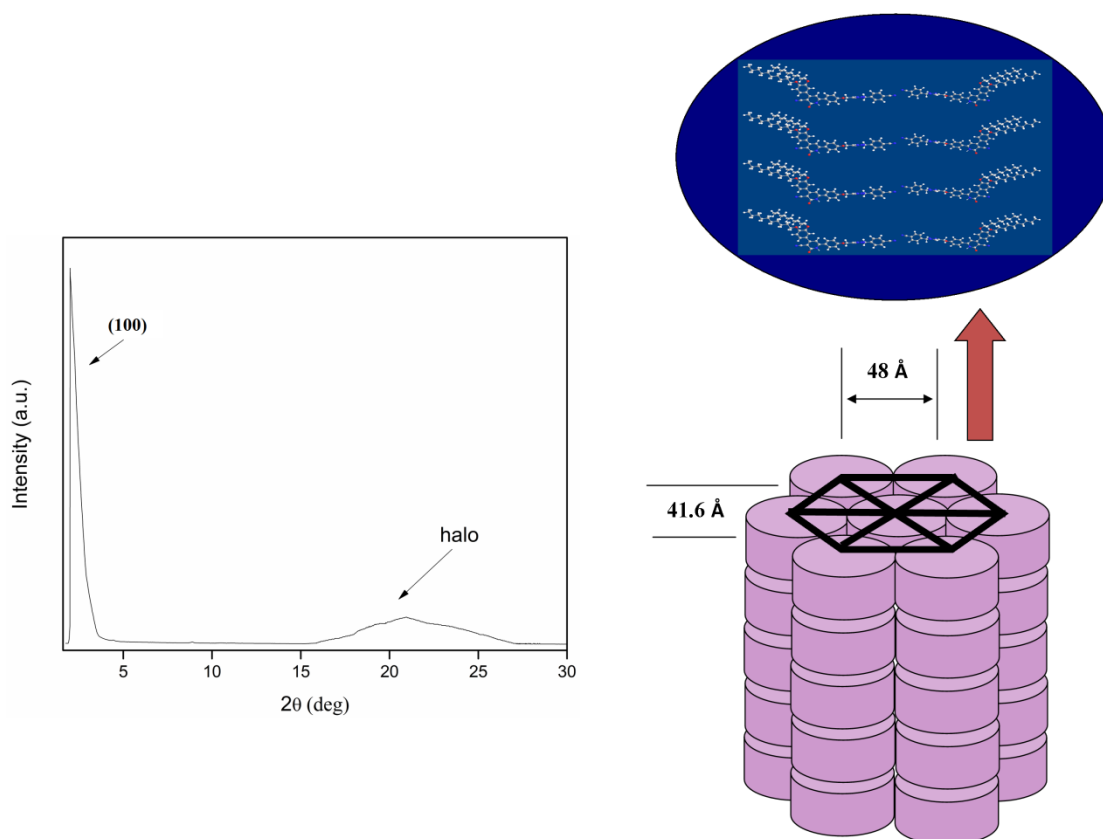


**Figure 4.18** PXRD pattern and packing model of **LC<sub>40</sub>**

**Table 4.10** PXRD results of **LC<sub>40</sub>** and **LC<sub>44</sub>** in their hexagonal columnar phase

Compound	$d_{\text{exp}}$ (Å)	Miller indices ( $hkl$ )	$d_{\text{theo}}$ (Å)	Lattice parameters
<b>LC<sub>40</sub></b>	41.61	100	41.61	T= 30 °C
	4.11	halo ( $h$ )		a= 48.10 Å S= 2675 Å <sup>2</sup> $V_{\text{cell}}$ = 10995 Å <sup>3</sup> $V_{\text{mol}}$ = 1329 Å <sup>3</sup> Z = 8
<b>LC<sub>44</sub></b>	37.96	100	37.96	T= 30 °C
	4.31	halo ( $h$ )		a= 44 Å S= 1666 Å <sup>2</sup> $V_{\text{cell}}$ = 7180 Å <sup>3</sup> $V_{\text{mol}}$ = 1267 Å <sup>3</sup> Z = 6

*Details of calculation: The notations  $d_{\text{exp}}$  and  $d_{\text{theo}}$  are experimental and theoretical diffraction spacings, respectively.  $d_{\text{theo}}$  is deduced from the lattice parameter  $a$  ( $\text{Col}_h$ ) from the following mathematical expression:  $d_{\text{theo}} = [2/(\sqrt{3}N_{hk})] \cdot [\sum_{hk} d_{hk} \sqrt{(h^2 + k^2 + hk)}]$ , where  $N_{hk}$  is the number of  $hk$  reflections observed for the  $\text{Col}_h$  phase.  $S$  is the lattice area, given by:  $S = (a^2\sqrt{3})/2$  Cell volume,  $V_{\text{cell}} = h \cdot S$  (where  $h$  is the thickness of hexagonal stratum). The molecular volume is defined as  $V_{\text{mol}} = M/(\delta \times 0.6022)$ , where*



$M$  is molecular weight;  $V_{CH_2}(T) = 26.5616 + 0.02023T$  ( $T$  in  $^{\circ}C$ ,  $T_0 = 25^{\circ}C$ ); density  $\delta = V_{CH_2}(T_0) / V_{CH_2}(T)$ ; the aggregation number or the number of molecular equivalents per stratum of column  $Z = V_{cell} / V_{mol}$ .  $I$  represents the intensity of reflections (VS: very strong, S: strong, M: medium, VW: very weak, br: broad);  $hk$  are the indexations of the reflections corresponding to the  $Col_h$  phase.

In conclusion, ten new pyridine compounds were shown to exhibit  $Col_h$  phase with a wide mesophase range starting from room temperature to  $94^{\circ}C$ . Their mesophase formation is due to the presence of terminal substituents, *viz.* polar groups ( $-CN$  or  $-NO_2$ ), variable alkoxy chain lengths and introduction of two highly electron deficient motifs, *viz.* cyanopyridone and 1,2,3-triazole. It is observed that as the terminal alkoxy chain length increases, the clearing temperature as well as thermal range of the columnar phase also increases considerably. PXRD measurements combined with textural observations evidence the hexagonal symmetry of the columnar phase formed by the compounds. The columnar assembly is due to the presence of hydrogen bonds as well as the participation of cyano functional group to form dimer. The dimerization and hydrogen bond formation have been confirmed by the SCXRD analysis of compound **16a**.

#### *Mesogenic behavior of LC<sub>1-48</sub>:*

In brief, amongst the forty eight compounds, almost all the compounds exhibit LC phase. **Table 4.11** summarizes the type of mesophase and its temperature range, shown by **LC<sub>1-48</sub>**. Only eight compounds, *viz.* **LC<sub>1</sub>**, **LC<sub>14</sub>** and **LC<sub>20-25</sub>** display nematic phase. The observed nematic phase in compounds **LC<sub>1</sub>** and **LC<sub>14</sub>** is due to the presence of polar cyano group and lower alkoxy chains (butoxy) in their structure; while compounds **LC<sub>20-25</sub>** display nematic phase because of the presence of lateral cyano group as well as  $-F$  or  $-Cl$  group and variable alkoxy chains as terminal substituents in them. 4-Cyano-4'-pentylbiphenyl (**5CB**) is a commonly used nematic liquid crystal in devices. Also, it exhibits liquid crystal phases near room temperature with the specific intention of using them in liquid crystal displays (Gray et al. 1973). In particular, liquid crystal **5CB** undergoes a phase transition from a crystalline state to a nematic state at  $18^{\circ}C$  and it goes from a nematic to an isotropic state at  $35^{\circ}C$ . However, the newly synthesized compounds **LC<sub>1</sub>**, **LC<sub>14</sub>** and **LC<sub>20-25</sub>** exhibit nematic phase at slightly higher temperature compared to compound **5CB**.

The compounds **LC<sub>2-13</sub>** and **LC<sub>26-33</sub>** show rectangular columnar phase. Appearance of ambient temperature rectangular columnar phase in compounds **LC<sub>2-13</sub>**, is attributed to the strong intermolecular interactions and the effect of higher alkoxy chains in them, while presence of elevated temperature rectangular columnar phase in compounds **LC<sub>26-33</sub>** is mainly due to the effect of -NO<sub>2</sub>, -Br, or 4-pyridinyl group and variable alkoxy chains as terminal substituents.

The compounds **LC<sub>15-19</sub>** exhibit orthorhombic columnar phase at an elevated temperature range (99-125 °C) owing to the presence of polar cyano group and higher alkoxy chains.

The compounds **LC<sub>34-38</sub>** and **LC<sub>39-48</sub>** show hexagonal columnar phase at ambient temperature. The formation of mesophase in compounds **LC<sub>34-38</sub>** is due to the existence of intermolecular hydrogen bonds and  $\pi$ - $\pi$  interactions exerted by the cyanopyridine core as well as variable alkoxy chain lengths. While, the observed mesophase in compounds **LC<sub>39-48</sub>** can be attributed to the presence of terminal polar substituents -CN or -NO<sub>2</sub> and variable alkoxy chain lengths. Also, the presence of hydrogen bond that holds cyanopyridone moiety together with planar 1,2,3-triazole unit contributes significantly in the formation of the observed mesophase.

Generally, the typical columnar liquid-crystalline molecules have a  $\pi$ -electron-rich aromatic core attached by flexible alkyl chains. This structure is attracting particular attention for potential molecular electronics in which aromatic parts transport electrons or holes and alkyl chains act as insulating parts. The advantages of liquid-crystalline conductors are their anisotropy, processibility, and self-healing characteristics for structural defects. However, Shen et al. (2009) prepared various oligophenylethynyl conjugates bearing long-chain pyridine-2,6-dicarboxamides and achieved columnar phase at above 117 °C in them. But, in the present study, the compounds exhibited columnar phase even from ambient to elevated temperature. Thus, these compounds are suitable candidates for electronic devices such as photovoltaic cells, field effect transistors and organic light emitting devices (OLEDs).

**Table 4.11** Observed mesophase for LC<sub>1-48</sub> and their temperature range

<b>Nematic Phase</b>					
<b>Compd.</b>	<b>Temp. range</b>	<b>Compd.</b>	<b>Temp. range</b>	<b>Compd.</b>	<b>Temp. range</b>
LC <sub>1</sub>	78.1 - 112.6	LC <sub>21</sub>	109.6 - 128.7	LC <sub>24</sub>	109 - 128.2
LC <sub>14</sub>	127.1 - 142.8	LC <sub>22</sub>	101.4 - 125.3	LC <sub>25</sub>	122.2 - 138.8
LC <sub>20</sub>	115.7 - 128.3	LC <sub>23</sub>	117.9 - 133.7		
<b>Rectangular Columnar Phase</b>					
<b>Compd.</b>	<b>Temp. range</b>	<b>Compd.</b>	<b>Temp. range</b>	<b>Compd.</b>	<b>Temp. range</b>
LC <sub>2</sub>	rt - 81.0	LC <sub>9</sub>	rt - 78.9	LC <sub>28</sub>	90.84 - 88.58
LC <sub>3</sub>	rt - 100.1	LC <sub>10</sub>	rt - 73.7	LC <sub>29</sub>	100.9 - 114.9
LC <sub>4</sub>	rt - 95.5	LC <sub>11</sub>	rt - 64.7	LC <sub>30</sub>	129.2 - 137.8
LC <sub>5</sub>	rt - 93.7	LC <sub>12</sub>	rt - 72.4	LC <sub>31</sub>	104.7 - 117.9
LC <sub>6</sub>	rt - 85.9	LC <sub>13</sub>	rt - 80.4	LC <sub>32</sub>	rt - 93.7
LC <sub>7</sub>	rt - 95.4	LC <sub>26</sub>	107.2 - 104.8		
LC <sub>8</sub>	rt - 62.0	LC <sub>27</sub>	113.6 - 111.3		
<b>Orthorhombic Columnar Phase</b>					
<b>Compd.</b>	<b>Temp. range</b>	<b>Compd.</b>	<b>Temp. range</b>	<b>Compd.</b>	<b>Temp. range</b>
LC <sub>15</sub>	105.5 - 125.2	LC <sub>17</sub>	102.6 - 120.5	LC <sub>19</sub>	99.3 - 113.3
LC <sub>16</sub>	105.1 - 121.4	LC <sub>18</sub>	101.6 - 118.2		
<b>Hexagonal Columnar Phase</b>					
<b>Compd.</b>	<b>Temp. range</b>	<b>Compd.</b>	<b>Temp. range</b>	<b>Compd.</b>	<b>Temp. range</b>
LC <sub>34</sub>	rt - 110	LC <sub>39</sub>	rt - 68.9	LC <sub>44</sub>	rt - 61.4
LC <sub>35</sub>	rt - 87.2	LC <sub>40</sub>	rt - 77.7	LC <sub>45</sub>	rt - 84.1
LC <sub>36</sub>	rt - 71.6	LC <sub>41</sub>	rt - 80.7	LC <sub>46</sub>	rt - 76.3
LC <sub>37</sub>	rt - 74.3	LC <sub>42</sub>	rt - 89.8	LC <sub>47</sub>	rt - 82.7
LC <sub>38</sub>	rt - 81.3	LC <sub>43</sub>	rt - 94.1	LC <sub>48</sub>	rt - 86.9

### 4.3 INVESTIGATION OF OPTICAL PROPERTIES OF NEW PYRIDINE DERIVATIVES

Optical techniques involve the study of interaction of electromagnetic radiation with the sample. Among various optical techniques, UV-visible absorption and fluorescence emission spectral studies are important, as they provide valuable information regarding the material property. It is well-established that study of interaction between LC material and light is essential for their optical characterization. The absorption spectroscopy deals with electronic transitions from ground state to the excited state while the fluorescence spectroscopy involves the electronic transitions from the excited state to the ground state. The results of linear optical studies are useful to evaluate the important parameters like optical band gap and fluorescent quantum yield of the LC materials. These are valuable parameters that

are taken into account for selecting such LCs for optoelectronic device applications. Therefore, the target compounds **LC<sub>1-48</sub>** were subjected to UV-visible and fluorescence spectral studies.

### 4.3.1 Experimental procedures

The UV-visible and photoluminescence spectra of the compounds **LC<sub>1-48</sub>** were recorded using GBC Cintra 101 and Perkin Elmer LS55 fluorescence spectrophotometers at concentrations of  $10^{-5}$  and  $10^{-6}$  M, respectively.

### 4.3.2 Results and discussion

The experimental data of optical measurements are summarized in **Tables 4.12-4.17** and are discussed in detail in the following section.

#### 4.3.2.1 Optical properties of 4,6- dialkoxyaryl-2-methoxy nicotinonitriles (Series-I; **LC<sub>1-13</sub>**)

The solution phase UV-visible absorption and fluorescence emission spectra of newly synthesized compound **LC<sub>1</sub>** were run at room temperature in dilute solutions ( $10^{-5}$ M) with different organic solvents like, hexane, chloroform, tetrahydrofuran (THF), acetone, methanol (MeOH), dimethylformamide (DMF) and dimethyl sulfoxide (DMSO), in order to explore its optical property and interaction with different organic solvents. These solvents are selected on the basis of increasing order of their dielectric constant values. The absorption and fluorescence spectral data along with the dielectric constants of solvents are tabulated in **Table 4.12**. **Figure 4.19** shows the UV-visible absorption and **Figure 4.20** shows the fluorescence emission spectra of **LC<sub>1</sub>** in different solvents, respectively.

Generally, solvatochromism is caused by differential solvation of the ground and the first excited state of the light absorbing molecule. If the ground state of the molecule is better stabilized by solvation with the solvent molecules of increased polarity than the excited state, then it leads to negative solvatochromism (blue shift). On the other hand, if the first excited state is more stabilized by solvation with the solvent molecules of increased polarity than the ground state, then it shows positive solvatochromism (red shift). In all the solvents, compound **LC<sub>1</sub>** showed one intense band in UV region, the position of the energy bands lies between 328 and 338 nm.

These energy bands were due to a  $\pi \rightarrow \pi^*$  electronic transition occurring in the conjugated 4,6-diaryloxycyanopyridine unit. **Table 4.12** shows that the absorption maxima of the compound **LC<sub>1</sub>** have shifted to longer wavelength with the increase in solvent polarity except acetone. This anomalous behaviour of acetone suggests that the position of the absorption maxima does not strictly correlate with the dielectric properties of the solvent, indicating weak interactions between solvent and the chromophore. However, the absorption band of the compound **LC<sub>1</sub>** in acetone was blue shifted when compared to other solvents.

In its fluorescence spectra (**Table 4.12**), upon excitation of the absorption maxima, an intense emission band with their peak lying between 374 nm (hexane) and 408 nm (DMSO) have been observed. When compared with the absorption spectra, its fluorescence spectral behaviour shows significantly larger solvatochromism. There was no appreciable change in absorption band with the variation of solvent systems from non-polar (hexane) to highly polar (DMSO) solvent. However, there was a considerable red shifting of emission bands in its fluorescence spectrum. This is attributed to the enhanced interaction between the molecule and solvent of high polarity.

**Table 4.12** Dielectric constant, absorption and fluorescence spectral data of **LC<sub>1</sub>** in different solvents

Solvent	Dielectric constant (D)	$\lambda_{\text{abs}}$ (nm)	$\lambda_{\text{em}}$ (nm)
Hexane	1.87	328	374
Chloroform	4.80	333	393
THF	7.58	333	392
Acetone	20.70	328	400
MeOH	32.70	335	405
DMF	36.71	337	404
DMSO	46.68	338	408

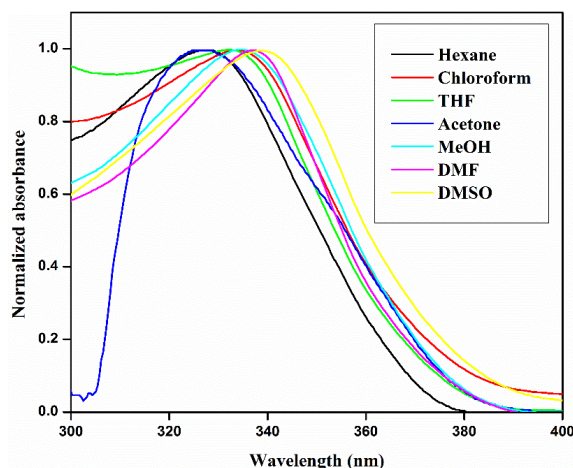


**Figure 4.19** UV-visible spectra of compound  $LC_1$  in different solvents ( $10^{-5}$  M)

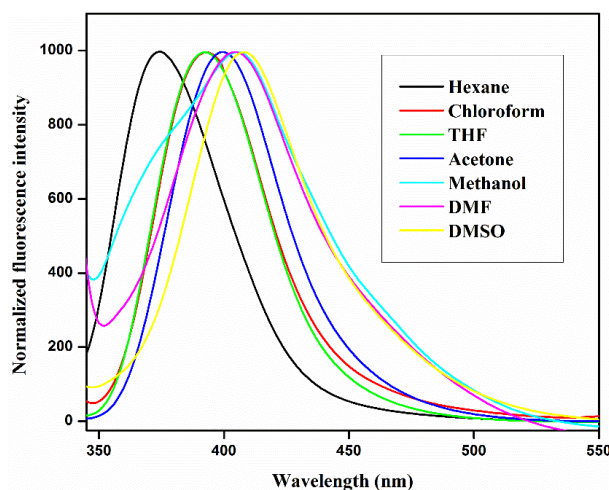


**Figure 4.20** Fluorescence spectra of  $LC_1$  in different solvents ( $10^{-6}$  M)

On the similar lines, in order to examine the luminescent nature of remaining compounds of the series *i.e.*  $LC_{2-13}$ , the UV-visible spectra were recorded in chloroform solutions at concentrations of  $10^{-5}$  M and fluorescence spectra were recorded in chloroform solutions at concentrations of  $10^{-6}$  M as well as in thin films. The thin films were prepared by dissolving the compounds in chloroform and the resultant solutions were fabricated over the glass substrate by using spin coating technique. Also, the morphology of these films was noticed as columnar mesophase. The results of optical characterization are summarized in **Table 4.13**. The spectra of all the compounds are almost identical to each other and hence only representative spectra of  $LC_2$  are shown in **Figure 4.21**. The compounds display nearly same intensity absorption band ( $\lambda_{\text{abs}}$ ) in the range of 337 to 339 nm. The appearance of this

absorption band is assigned to the  $\pi \cdots \pi^*$  electronic transitions of the conjugated 4, 6-diaryloxycyanopyridine system.

Fluorescence spectra of **LC**<sub>2-13</sub> in chloroform solution and in film state were recorded using excitation wavelength ( $\lambda_{\text{exc}}$ ) at 330 nm. A strong blue emission band ( $\lambda_{\text{em}}$ ) was observed in the range of 398-415 nm for **LC**<sub>2-13</sub> in their solution state. Thus, these bands slightly red shifted by 6-12 nm in case of dried films. Fluorescence spectra observed for compound **LC**<sub>2</sub> both in solution and in film state are also shown in **Figure 4.21**. Further, the emission quantum yields ( $\Phi_f$ ) of **LC**<sub>2-13</sub> in solution state were determined using quinine sulphate in degassed 0.1M sulphuric acid as reference standard ( $\Phi_f=54\%$ ) (Crosby and Demas 1971). Accordingly, the compounds exhibit good quantum yield of 28-49 % in solution state and a quite considerable quantum yields ( $\Phi_f=10-22\%$ ) in film state too (Kawamura et al. 2004).

**Table 4.13** Optical properties of **LC**<sub>2-13</sub>

Compound	$\lambda_{\text{abs}}$ (nm)	$\lambda_{\text{em}}$ (nm)	$\Phi_f$ (%)	$\lambda_{\text{em}}$ (nm)	$\Phi_f$ (%)
	solution	solution	solution	film	film
<b>LC</b> <sub>2</sub>	337	398	28	411	19
<b>LC</b> <sub>3</sub>	339	409	37	416	11
<b>LC</b> <sub>4</sub>	339	412	43	416	13
<b>LC</b> <sub>5</sub>	339	409	39	421	14
<b>LC</b> <sub>6</sub>	339	413	49	418	11
<b>LC</b> <sub>7</sub>	339	415	43	418	10
<b>LC</b> <sub>8</sub>	333	396	29	416	15
<b>LC</b> <sub>9</sub>	338	411	41	419	22
<b>LC</b> <sub>10</sub>	338	415	42	417	19
<b>LC</b> <sub>11</sub>	338	412	26	418	17
<b>LC</b> <sub>12</sub>	338	413	41	421	21
<b>LC</b> <sub>13</sub>	338	414	43	418	18

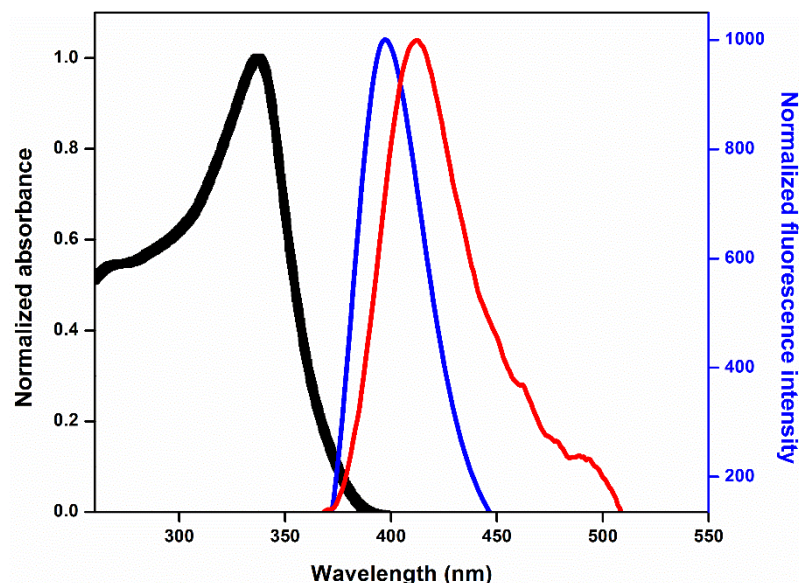


**Figure 4.21** UV-visible (black line), and fluorescence emission (blue line) spectra of  $LC_2$  in chloroform solution and film state (red line) at room temperature

#### 4.3.2.2 Optical properties of 6-alkoxyaryl/thiophenyl- 4-substituted aryl-2-methoxy pyridines (Series-II; $LC_{14-33}$ )

The UV-visible absorption and fluorescence emission spectra of compounds  $LC_{14-19}$  were recorded over the range of wavelength ( $\lambda$ ) using chloroform as a solvent at the concentration of  $10^{-5}$  M and  $10^{-6}$  M, respectively. The results are summarized in **Table 4.14**. The UV-visible absorption and fluorescence emission spectra of compounds  $LC_{14}$  are shown in **Figure 4.22**. In the absorption spectra of  $LC_{14-19}$ , a strong absorption band ( $\lambda_{abs}$ ) was observed in the range of 335 to 345 nm and found to be similar in shape because of their structural similarities. The fluorescence emission spectra of compounds ( $LC_{14-19}$ ) were recorded in chloroform solution ( $10^{-6}$  M) at  $\lambda_{exc}=330$  nm. Interestingly, all of them were found to be luminescent and showed a broad blue light emission band ( $\lambda_{em}$ ) in the visible region (415-425 nm). This observed blue light emission may be attributed to extended conjugation of cyano group in association with the mesogenic core. Further, their fluorescence quantum yields ( $\Phi_f$ ) in solution state were determined using the method reported by Demas and Crosby, with quinine sulphate in degassed 0.1M sulphuric acid as reference standard ( $\Phi_f=54$  %). Accordingly, the compounds exhibited good quantum yield in the range of 42-50 %. In addition, they exhibited strong blue fluorescence emission band in the



range of 434-460 nm in solid state too with quite considerable quantum yields ( $\Phi_f=5-13\%$ ). Thus, the compounds **LC**<sub>14-19</sub> have emerged as good blue fluorescent materials and can be used as an emissive dopant in an electroluminescent device.

**Table 4.14** Optical characteristics of **LC**<sub>14-19</sub>

Compound	$\lambda_{\text{abs}}$ (nm)	$\lambda_{\text{em}}$ (nm)	$\Phi_f$ (%)	$\lambda_{\text{em}}$ (nm)	$\Phi_f$ (%)
	solution	solution	solution	solid	solid
<b>LC</b> <sub>14</sub>	345	421	43	460	5.01
<b>LC</b> <sub>15</sub>	340	416	50	448	7.40
<b>LC</b> <sub>16</sub>	340	418	48	452	5.60
<b>LC</b> <sub>17</sub>	339	418	49	444	6.82
<b>LC</b> <sub>18</sub>	336	418	42	453	5.88
<b>LC</b> <sub>19</sub>	336	417	45	434	12.15

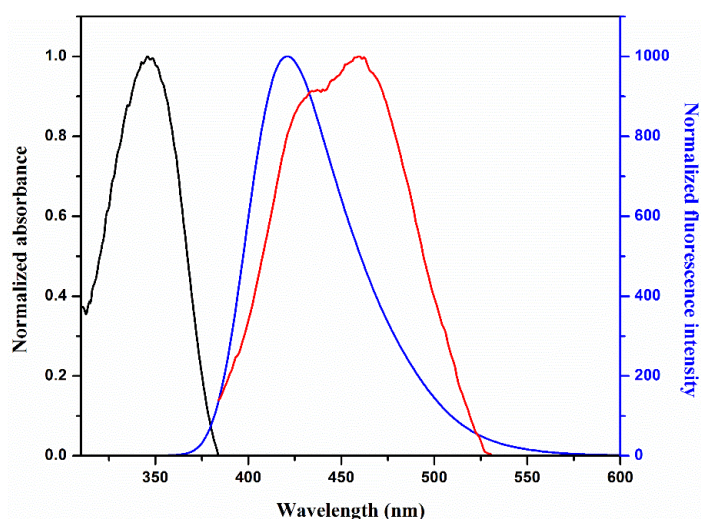


**Figure 4.22** UV-visible (black line) and fluorescence spectra (blue line) of **LC**<sub>14</sub> in chloroform solution and solid state (red line) at room temperature

The UV-visible absorption and fluorescence emission spectra of compounds **LC**<sub>20-33</sub> were recorded using chloroform as a solvent in the concentration of  $10^{-5}$  M and  $10^{-6}$  M, respectively. Their results are tabulated in **Table 4.15**. The UV-visible absorption spectra of compounds **LC**<sub>20</sub>, **LC**<sub>23</sub>, **LC**<sub>26</sub>, **LC**<sub>29</sub>, **LC**<sub>32</sub>, and **LC**<sub>33</sub> are shown in **Figure 4.23**. Their absorption spectral data revealed that the compounds show a strong absorption band ( $\lambda_{\text{abs}}$ ) in the range of 330-350 nm which was assigned to  $\pi-\pi^*$  electronic transition focusing on the conjugated cyanopyridine unit. Also, these absorption bands depend on the presence of terminal electron donating alkoxy

substituents and electron withdrawing substituents like  $-\text{NO}_2$ ,  $-\text{CN}$ ,  $-\text{Cl}$  and  $-\text{F}$  on the molecular architecture, which attributed to the increased electron drift from electron-donating group to the electron-withdrawing group through  $\pi$ -conjugated system. As well, the compound **LC<sub>33</sub>**, with the molecular structure consisting of decyloxyphenyl ring as one terminal substituent and un-substituted electron donating thiophene ring as another substituent at position-4 and -6 of central cyanopyridine core, respectively, showed a strong absorption band at 344 nm confirming the development of donor-acceptor-donor (D-A-D) system.

The fluorescence emission spectra of **LC<sub>20-33</sub>** were recorded over the range of wavelength between 300 to 700 nm in chloroform solution at room temperature (**Figure 4.23**). All the compounds emit blue light with an emission band ( $\lambda_{\text{em}}$ ) in the range of 397-418 nm and wide Stokes shift values of 55-85 nm. The spectral data, summarized in **Table 4.15**, clearly reveal that as the strength of polar substituent increases on the molecular architecture, it leads to red shift. Hence, the compound with highly polar substituent like  $-\text{NO}_2$ ,  $-\text{CN}$  showed 15-20 nm red shifts in emission maximum when compared to the compound with low polar substituent (*i.e.*  $-\text{Cl}$ ,  $-\text{F}$ ).

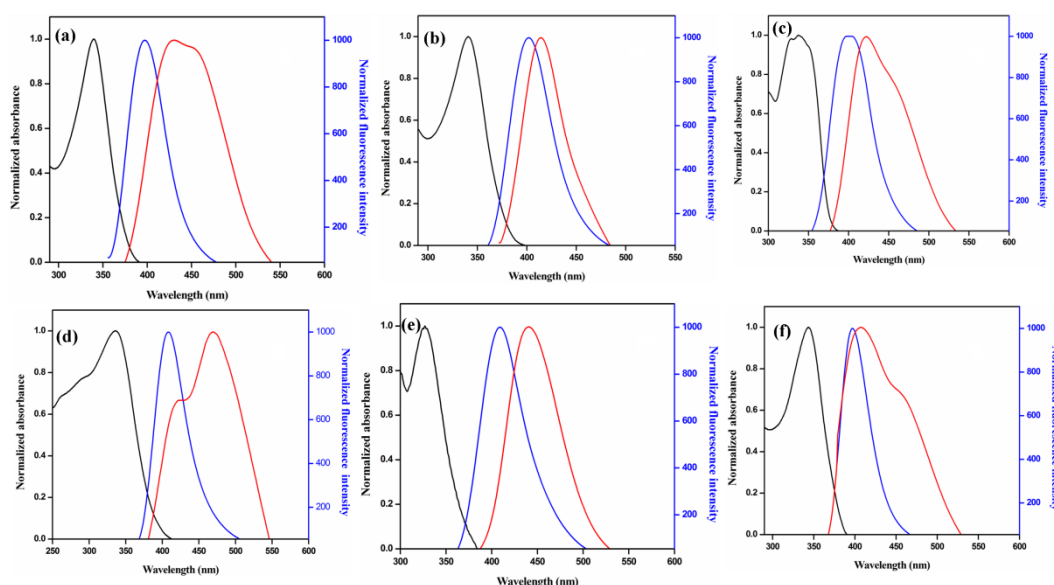


**Figure 4.23** Photophysical properties of compounds (a) **LC<sub>20</sub>**, (b) **LC<sub>23</sub>**, (c) **LC<sub>26</sub>**, (d) **LC<sub>29</sub>**, (e) **LC<sub>32</sub>**, and (f) **LC<sub>33</sub>**. Where, black line-absorption band in solution; blue and red line- emission bands in solution and film states, respectively

**Table 4.15** Optical characteristics of LC<sub>20-33</sub> in chloroform

Compound	$\lambda_{\text{abs}}$ (nm)	$\lambda_{\text{em}}$ (nm)	Stokes shift (nm)
LC <sub>20</sub>	339	397	58
LC <sub>21</sub>	339	398	59
LC <sub>22</sub>	340	397	57
LC <sub>23</sub>	340	402	62
LC <sub>24</sub>	341	402	61
LC <sub>25</sub>	341	402	61
LC <sub>26</sub>	338	404	66
LC <sub>27</sub>	343	402	59
LC <sub>28</sub>	340	402	62
LC <sub>29</sub>	337	408	71
LC <sub>30</sub>	348	415	67
LC <sub>31</sub>	337	411	74
LC <sub>32</sub>	327	409	82
LC <sub>33</sub>	344	397	53

#### 4.3.2.3 Optical properties of 2-(4,6-disubstituted aryl-3-cyanopyridyl)oxy acetohydrazones (Series-III; LC<sub>34-38</sub>)

The UV-visible absorption ( $10^{-5}$  M) and fluorescence ( $10^{-6}$  M) spectra of compounds LC<sub>34-38</sub> recorded in chloroform solution at room temperature. Optical data of compounds LC<sub>34-38</sub> in chloroform are summarized in **Table 4.16**. In absorption spectra of LC<sub>34-38</sub>, an intense broad band was observed at around 320 nm, which are similar in shape because of their structural similarities. Thus, the UV-visible spectrum of the representative compound LC<sub>34</sub> is presented in **Figure 4.24**. The fluorescence spectra of compounds LC<sub>34-38</sub> were recorded in chloroform under the excitation wavelength of 330 nm. They exhibit strong blue emission fluorescence with maxima at around 389 nm. Further, it is noticed that the variation of terminal alkoxy chain lengths does not affect their photophysical properties. Also, the emission quantum yields ( $\Phi_f$ ) of LC<sub>34-38</sub> in solution state were determined using quinine sulphate in degassed 0.1M sulphuric acid as reference standard ( $\Phi_f=54$  %). Accordingly, the compounds exhibit good quantum yield of 36-38 % in solution state.

Further, the compounds LC<sub>34-38</sub> were subjected to fluorescence emission study in their liquid crystalline state at room temperature. Thin films of compounds at their liquid crystalline state were prepared over the glass substrate. The required films are

obtained by heating the samples to isotropic phase followed by slow cooling to room temperature. The results of emission studies of these films reveal that compounds exhibit blue fluorescence emission maxima at around 454 nm with an absolute quantum yields of 7-10 %. The emission spectrum of the compound **LC<sub>34</sub>** in liquid crystalline state is shown in **Figure 4.24**. The emission spectrum of **LC<sub>34</sub>** in liquid crystalline state shows a broader emission band and the maxima is found to be red shifted when compared to its emission band in solution state. Thus, the observed broad emission band along with significant red shift in emission maxima of **LC<sub>34-38</sub>** films are indicative of the emission arising from the aggregated state of these molecules in the liquid crystalline phase. In conclusion, the optical study reveals that the title compounds are blue fluorescence emitters both in solution state and in liquid crystalline phase and hence they are potential candidates for OLED applications.

**Table 4.16** Optical properties of **LC<sub>34-38</sub>** in chloroform

Compound	$\lambda_{\text{abs}}$ (nm)	$\lambda_{\text{em}}$ (nm)	$\Phi_f$ (%)	Stokes shift (nm)
<b>LC<sub>34</sub></b>	320	389	38.63	69
<b>LC<sub>35</sub></b>	321	390	36.85	69
<b>LC<sub>36</sub></b>	321	389	37.11	68
<b>LC<sub>37</sub></b>	324	390	37.06	66
<b>LC<sub>38</sub></b>	320	389	36.83	69

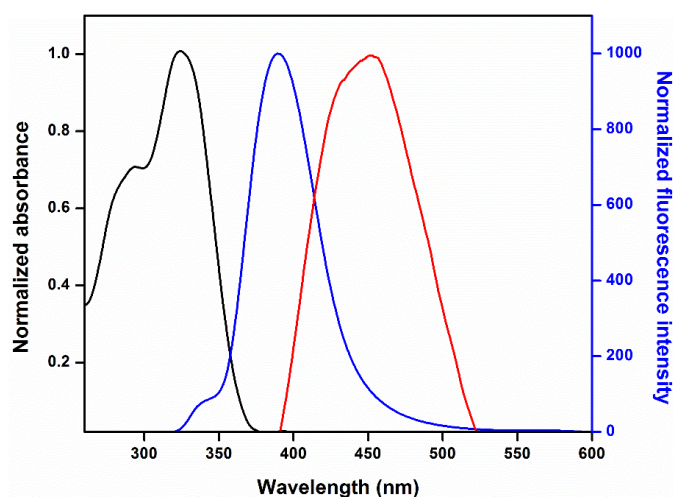


**Figure 4.24** UV-visible (black line) and fluorescence (blue line) spectra of **LC<sub>34</sub>** in chloroform; red line represents the fluorescence emission spectrum of **LC<sub>34</sub>** in liquid crystalline state.

#### 4.3.2.4 Optical properties of 4,6-disubstituted aryl-3-cyanopyridones (Series-IV; LC<sub>39-48</sub>)

The UV-visible absorption spectra of LC<sub>39-48</sub> were recorded in chloroform solution at the concentration of  $10^{-5}$  M and the spectral data are summarized in **Table 4.17**. The solution absorption spectra of LC<sub>39-48</sub> have nearly identical absorption band ( $\lambda_{\text{abs}}$ ) at  $\sim 370$  nm. Indeed, no considerable change in absorption properties were observed even with the variation of terminal alkoxy chain lengths and the introduction of polar groups such as -CN and -NO<sub>2</sub>. Here, the absorption band can be attributed to  $\pi$ - $\pi^*$  transitions from their molecular architecture.

The fluorescence emission spectra were recorded in chloroform solution at the concentration of  $10^{-6}$  M and the values are summarized in **Table 4.17**. The compounds emit a strong blue fluorescence emission band ( $\lambda_{\text{em}}$ ) at  $\sim 466$  nm with large Stokes shifts ranging from 94 to 99 nm. The fluorescence quantum yield ( $\Phi_f$ ) in solution state was determined using the method described by Demas and Crosby, with quinine sulphate in degassed 0.1M sulphuric acid as reference standard ( $\Phi_f=54$  %). All the compounds exhibited good quantum yield in the range of 60-62 %. In addition, the emission properties of the compounds were investigated in their liquid crystalline state, as they show liquid crystalline phase at room temperature. The liquid crystalline films were prepared over a glass slide by heating the compound to isotropic phase and followed by slow cooling to liquid crystalline phase. These films exhibited strong blue fluorescence emission band in the range of 472-478 nm. Also, in film state, bathochromic shift of about 10 nm in the emission band was observed when compared to its solution state. The observed bathochromic shift can be attributed to intimate overlap of molecular cores in the hexagonal columnar phase via hydrogen bonds that brings the energy levels closer in the film state. The UV-visible spectral data of LC<sub>39-48</sub> are almost identical and similar observations were made for their emission spectra also. **Figure 4.25** shows the UV-visible and fluorescence spectra of LC<sub>39</sub>.

**Table 4.17** Optical characteristics of LC<sub>39-48</sub>

Compound	$\lambda_{\text{abs}}$ (nm) solution	$\lambda_{\text{em}}$ (nm) solution	$\Phi_f$ (%) solution	Stokes shift (nm)	$\lambda_{\text{em}}$ (nm) film
LC <sub>39</sub>	369	468	62	99	474
LC <sub>40</sub>	370	466	62	96	477
LC <sub>41</sub>	368	462	61	94	473
LC <sub>42</sub>	370	466	62	96	479
LC <sub>43</sub>	369	468	62	99	478
LC <sub>44</sub>	369	467	61	98	475
LC <sub>45</sub>	371	465	62	94	471
LC <sub>46</sub>	371	468	61	97	476
LC <sub>47</sub>	371	466	62	95	478
LC <sub>48</sub>	371	468	62	97	477

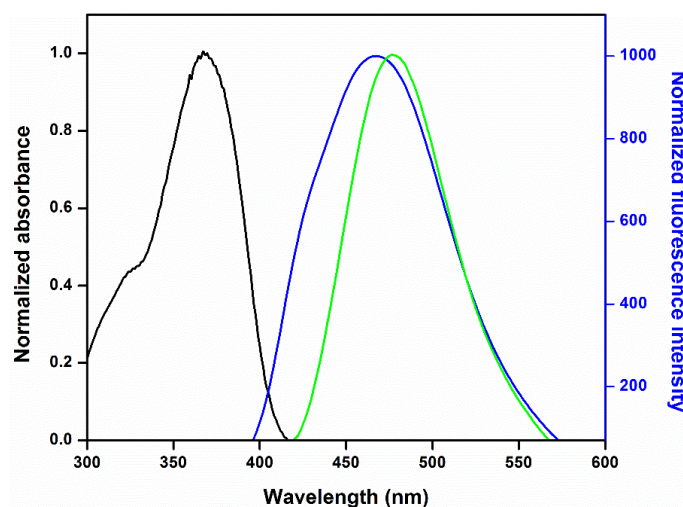


**Figure 4.25** Spectra of LC<sub>39</sub>; black line represents UV-visible absorption spectrum, blue line and green line represents fluorescence spectra in solution and film state, respectively

In conclusion, UV-visible absorption and fluorescence emission spectra of all the forty eight compounds, LC<sub>1-48</sub> show a strong absorption band in the range of 320-370 nm and a strong blue emission band in the range of 380-470 nm, which is mainly due to the occurrence of  $\pi$ - $\pi^*$  electronic transition in them. The solvent dependent fluorescence emission study of LC<sub>1</sub> reveals that the blue emission bands shift to

higher wavelength (positive solvatochromism) with the variation of organic solvents (non-polar to polar). Fluorescence spectra of **LC**<sub>2-13</sub> in solution state show blue emission band in the range of 398-415 nm and these bands are slightly red shifted by 6-12 nm in the liquid crystalline film state. Also, the compounds exhibit good quantum yield of 28-49 % in solution state and a quite considerable quantum yields ( $\Phi_f=10-22$  %) in film state too. The fluorescence emission spectra of compounds (**LC**<sub>14-19</sub>; **LC**<sub>34-38</sub> and **LC**<sub>39-48</sub>) display emission band in the visible region in the range of 380-466 nm ( $\Phi_f=42-60$  %) in solution state and emission band in the range of 434-480 nm in their film state.

It is clear from the photophysical studies that the compounds **LC**<sub>2-13</sub> and **LC**<sub>34-48</sub> exhibit good blue emission behavior in liquid crystalline film state at room temperature. Also, their liquid crystalline study reveals that these compounds exhibit columnar phase at ambient temperature. Here the observed columnar arrangement is due to the presence of strong attractive  $\pi-\pi$  interactions offered by the core. Consequently, the well-stacked columnar assembly possesses very high charge carrier mobility and hence it acts as a good charge transporting material too. Thus, these compounds are found to be ideal candidates for the optoelectronic device fabrication. In the following section a brief account of optoelectronic and device fabrication studies of compound **LC**<sub>38</sub> was discussed.

#### **4.4 INVESTIGATION OF OPTOELECTRONIC PROPERTIES OF **LC**<sub>38</sub>**

Finally, a representative compound **LC**<sub>38</sub> was studied to evaluate its optoelectronic properties in order to explore its suitability in device application. The chemical structure of **LC**<sub>38</sub> is given in **Figure 4.26**. The selection was based on its ambient temperature mesogenic (Col<sub>h</sub>) as well as blue emissive characteristics.

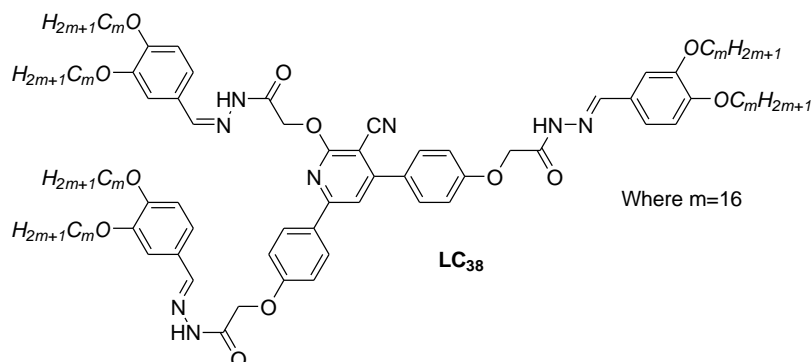


**Figure 4.26** Chemical structure of LC<sub>38</sub>

Electrochemical behavior of LC<sub>38</sub> was investigated by cyclic voltammetry (CV) in order to determine its redox behavior as well as highest occupied molecular orbital (HOMO) and lowest unoccupied molecular orbital (LUMO) energy levels. CV measurement was carried out at 25 °C in dry acetonitrile solution containing 0.1 M tetrabutylammonium perchlorate (Bu<sub>4</sub>NPCl<sub>4</sub>) as supporting electrolyte, glassy carbon as working electrode, Pt wire as counter electrode and Ag/AgCl as reference electrode with a scan rate of 50 mV/s. Also, the instrument was calibrated using ferrocene as internal standard. The obtained cyclic voltammogram of LC<sub>38</sub> is shown in **Figure 4.27**. It represents two single electron onset oxidation potentials at +0.41 and +0.95 V during anodic cycle as well as onset reduction potentials at -1.18 V during cathodic cycle. The first onset oxidation and reduction potential values have been used for the calculation of HOMO and LUMO energy levels by using equations,  $E_{HOMO} = -[E_{onset}^{oxd} + 4.4eV]$  and  $E_{LUMO} = -[E_{onset}^{red} + 4.4eV]$ , where  $E_{onset}^{oxd}$  and  $E_{onset}^{red}$  are the observed onset oxidation and onset reduction potentials versus standard calomel electrode. It's HOMO and LUMO energy levels were found to be -4.81 and -3.22 eV, respectively. Thus, the electrochemical band gap was calculated to be 1.60 eV. The obtained HOMO and LUMO energy levels for LC<sub>38</sub> are comparable to that of the ITO (4.5-5.0 eV) and LiF:Al (3.6-3.8 eV) work functions. Therefore, a single layer device with device structure ITO/LC<sub>38</sub>/LiF(10 nm)/Al(110 nm) was fabricated.



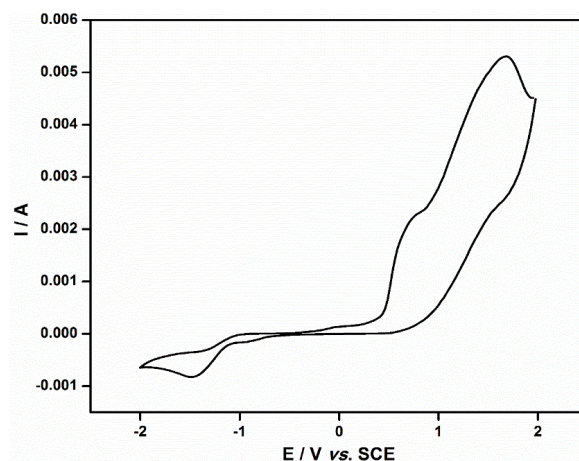


**Figure 4.27** Cyclic voltammogram of  $LC_{38}$

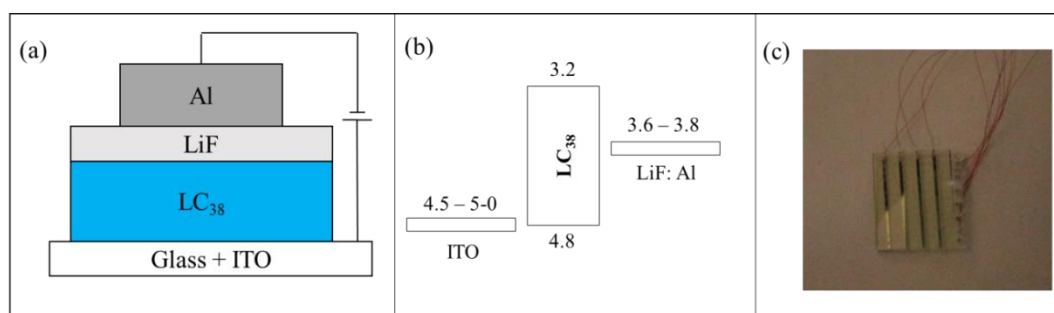


**Figure 4.28** (a) Schematic diagram of the fabricated device, (b) energy level and (c) actual device

#### 4.4.1 Device fabrication and characterization

The schematic diagram of the fabricated device, energy level and the actual device are shown in **Figure 4.28**. Commercially patterned indium tin oxide (ITO) coated glass with sheet resistance of  $15 \Omega/\square$  (Xin Yan Technology Ltd., Hong Kong) was used as anode. The size of the substrate is 1"×1" having ITO strips of width 0.8 mm. Aluminum (99.999% wire, Sigma-Aldrich) was used as electron injecting contact (cathode). ITO shows a work-function of 4.5-5.0 eV in dependence of the surface treatment prior to deposition of the organic layers. Al has a work-function of approximately 4.2 eV which reduces to 3.6-3.8 eV when used in combination with a thin layer of lithium-fluoride (LiF).

To begin with, ITO substrates were cleaned with detergent. Then they were ultrasonicated in detergent (to remove oil), distilled water (to remove detergent), acetone (to remove most of the chemical contaminant), IPA and finally with distilled

water sequentially for 10 min each. The substrates were degreased with acetone and they were cleaned using cotton swab. Finally, the substrates were UV-ozone treated for 15 minutes.

About 10 mg of the sample was dissolved in 6 ml of chloroform. The sample was coated onto the pre-cleaned ITO substrate by dip-coating. The substrate was dipped 5 times into the solution and each time the film was dried using a hot air blower. The ITO substrate coated with **LC<sub>38</sub>** was loaded into a physical vapour deposition (PVD) system equipped with a turbo-molecular pump and multi-stage roots pump. Lithium fluoride (LiF) was placed in molybdenum boat and aluminum (Al) wire was placed in a tungsten helical fixed to the electrodes. The sample chamber was evacuated to a base pressure below  $5 \times 10^{-6}$  mbar. The materials to be deposited are electrically heated and evaporated sequentially. When the evaporated materials cool down, they condense onto the surface of the sample. The current flow through the system was controlled manually to obtain a thickness of 10 nm of LiF and 110 nm of Al electrode in such a way that the evaporation rates are 0.1 Å/sec and 6-10 Å/sec, respectively. The deposition rate and the thickness were controlled by using quartz crystal monitor and both the layers were coated without breaking vacuum. After the deposition of LiF, a mask was placed on the substrate in order to coat Al through the mask. The mask has 0.8 mm openings separated by 4mm from the next opening. The effective device area is  $\sim 6.4 \text{ cm}^2$ .

After the fabrication, the device was taken out from the deposition system and wire contacts were made using indium. The electrical measurements were performed for the fabricated device under dark, UV lamp (8 W) and metal halide (MH) lamp (150 W, 6500 K) using Keithley 2400 source-meter. The J-V characteristics obtained for single layer **LC<sub>38</sub>** device and its data are given in **Figure 4.29** and **Table 4.18**, respectively. From the results, it is evident that the device with **LC<sub>38</sub>** is exhibiting good photo-response nature both in forward and reverse bias voltage under UV- and MH- lamp illumination. Also, to get a clear insight on the existence of emission wavelengths and their intensities present in UV- and MH-lamps, the spectra were recorded using a computer controlled Horiba Jobin Yvon iHR320 Spectrometer and the obtained spectra is depicted in **Figure 4.30**. Thus, **LC<sub>38</sub>** material is found to be a

potential candidate for photo-detector/photovoltaic devices as active material and electron transporting material in OLEDs.

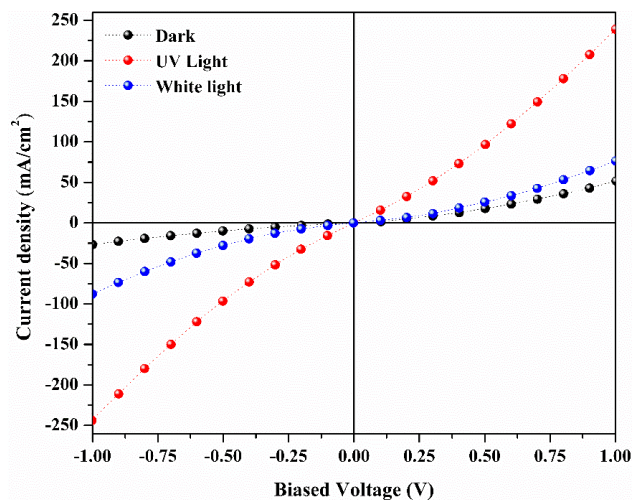


**Figure 4.29** J-V characteristics for single layer  $LC_{38}$  device under dark, UV- and MH- lamp illuminations

**Table 4.18** J-V data for single layer  $LC_{38}$  device

Bias Voltage		Current density ( $\text{mA}/\text{cm}^2$ )		
		Dark	MH- lamp	UV- lamp
Reverse	-1	-27	-87	-243
	-5	-389	-1281	-2976
Forward	+1	51	76	239
	+5	890	1712	1948

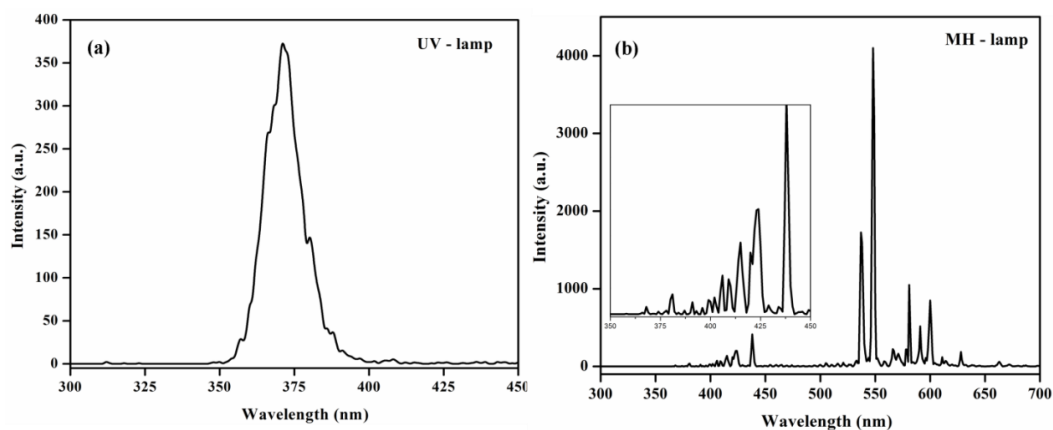


**Figure 4.30** The spectra: (a) UV-lamp source; (b) MH-lamp source (inset shows the enlarged spectrum of 350-450 nm regions)

#### **4.5 CONCLUSIONS**

The newly synthesized pyridine derivatives (**LC<sub>1-48</sub>**) were subjected to POM, DSC and PXRD studies to explore their LC behavior. The study reveals that almost all compounds exhibit either nematic, rectangular columnar, orthorhombic columnar or hexagonal columnar phase with a wide mesophase range. Further, their photophysical properties were investigated by UV-visible and fluorescence spectrophotometric techniques to determine their linear optical behavior. The UV-visible spectral study reveals that the compounds exhibit absorption band in the range of 320-370 nm, while fluorescence spectral study reveals that the compounds show blue emission in the range of 380-470 nm. From the result it is observed that the compounds possess both liquid crystalline property and luminescent behavior. The device fabrication study reveals that the compounds are suitable candidates for optoelectronic device applications.

## **CHAPTER 5**

### **SUMMARY AND CONCLUSIONS**

*Abstract*

*This chapter contains summary and the important conclusions drawn from present research work.*

**5.1 SUMMARY AND CONCLUSIONS**

The quest for new LCs has undergone a very rapid development in recent years. One of the growing areas in LCs is a design and development of new heterocyclic mesogens with good photophysical properties. It is well established that heterocyclic systems bring about excellent charge carrying ability and impart anisotropic behavior with polarized light emission property. Also, they are well known for controlling intensity of polarized emission/absorption and direction by the application of an electric field. Thus, use of heterocyclic LC materials make it possible to have brighter and cheaper displays, as such devices would require the use of only one polarizer instead of two, being used in currently produced displays.

In this context, the present research work has mainly focused on the design and synthesis of new pyridine derivatives as LC materials with good photophysical properties. It is also aimed at investigation of their liquid crystalline and optical properties in detail.

Further, based on a detailed literature survey, four new series of pyridine derivatives were designed as mesogens. The various groups such as cyano, nitro, halo, alkoxy, hydrazone etc. were incorporated in the new molecular architecture carrying pyridine ring as a core. The newly designed pyridine-based compounds are as follows:

- (i) 4,6-Dialkoxyaryl-2-methoxynicotinonitriles (**Series-I; LC<sub>1-13</sub>**)
- (ii) 6-Alkoxyaryl/thiophenyl-4-substituted aryl-2-methoxy pyridines (**Series-II; LC<sub>14-33</sub>**)
- (iii) 2-(4,6-Disubstitutedaryl-3-cyanopyridyl)oxy acetohydrazones (**Series-III; LC<sub>34-38</sub>**)
- (iv) 4,6-Disubstituted aryl-3-cyanopyridones (**Series-IV; LC<sub>39-48</sub>**)

The newly designed compounds **LC<sub>1-48</sub>** were synthesised following standard synthetic protocols. Their synthetic methods have been established and their reaction conditions were optimized to get maximum yield. Purification techniques were developed for the new compounds. The structures of new intermediates and final compounds were confirmed by various spectral and elemental analyses. Further, single crystal X-ray crystallographic study was carried out for few compounds in order to elucidate their final structure, molecular shape, hydrogen bonds and nature of short contacts. Their mesogenic properties were investigated in detail using POM, DSC, and PXRD techniques. Further, their photophysical properties were studied using UV-visible and fluorescence spectrometry.

Following important conclusions have been drawn from the present research work:

- New unsymmetrical pyridine derivatives **LC<sub>1-48</sub>** were successfully synthesized.
- The SCXRD study on **LC<sub>1</sub>**, **LC<sub>2</sub>**, **LC<sub>3</sub>**, **LC<sub>14</sub>**, **LC<sub>16</sub>**, **LC<sub>32</sub>**, and **LC<sub>33</sub>** revealed that the 3-dimensional molecular architecture of pyridine possesses non-planar structure and various kinds of intermolecular interactions.
- The SCXRD study confirmed the effective formation of **LC<sub>1</sub>**, **LC<sub>2</sub>**, **LC<sub>3</sub>** and **LC<sub>33</sub>** carrying 2-methoxy-3-cyanopyridine as a core, via cyclization, whereas the effective formation of **LC<sub>14</sub>**, **LC<sub>16</sub>**, and **LC<sub>32</sub>** carrying 2-methoxypyridine as a core, via cyclization.
- The liquid crystal study on compounds **LC<sub>1-48</sub>** showed either nematic, Col<sub>i</sub>, Col<sub>ortho</sub> or Col<sub>h</sub> phase depending on the nature of substituents and intermolecular interactions.
- **LC<sub>1</sub>**, **LC<sub>14</sub>**, **LC<sub>20-25</sub>** exhibited nematic phase at high temperature. Also, the **LC<sub>1</sub>** showed a wide nematic phase at temperature range, 78-112 °C, when compared to **LC<sub>14</sub>**, **LC<sub>20-25</sub>**.
- **LC<sub>2-13</sub>**, **LC<sub>26-32</sub>** displayed a wide range of rectangular columnar phase. **LC<sub>2-13</sub>**, **LC<sub>32</sub>** exhibited ambient temperature rectangular columnar phase, while **LC<sub>26-31</sub>** showed elevated temperature rectangular columnar phase. **LC<sub>3</sub>** possesses a wide rectangular columnar phase from room temperature to 100.1 °C.

- **LC<sub>15-19</sub>** exhibited orthorhombic columnar phase at higher temperature (99.3-125.2 °C).
- **LC<sub>34-48</sub>** showed room temperature hexagonal columnar phase, whereas **LC<sub>34</sub>** exhibited a wide hexagonal columnar phase range (rt-110 °C).
- The UV-visible absorption study on **LC<sub>1-48</sub>** revealed that the compounds exhibit absorption band in the range of 320-370 nm, while fluorescence spectral study indicated that the compounds show blue emission in the range of 380-470 nm with quantum yield of 10-60 % in solution/film/liquid crystalline states.
- Optoelectronic device study revealed that **LC<sub>38</sub>** is a potential candidate for photo-detector/ photovoltaic and OLED devices.

The present research work revealed that compounds carrying methoxypyridine, 2-methoxy-3-cyanopyridine and 3-cyanopyridone systems as a core, and groups like fluoro, chloro, bromo, nitro, cyano, or 4-pyridinyl and variable alkoxy chains as terminal substituents exhibit good mesogenic behavior as well as luminescent property. Thus, these materials can be subjected to further device performance study in order to reveal their suitability for electro-optical devices.



---

**REFERENCES**

- Al-Arab, M.M. (1989). "A facile synthesis of 6-alkoxy-2,4-diaryl-5-cyanopyridine." *J. Heterocyclic Chem.*, 26 (6), 1665–1673.
- Aldred, M.P., Eastwood, A.J., Kitney, S.P., Richards, G.J., Vlachos, P., Kelly, S.M. and O'Neill, M. (2005). "Synthesis and mesomorphic behaviour of novel light-emitting liquid crystals." *Liq. Cryst.*, 32 (10), 1251–1264.
- Aoyama, Y., Endo, K., Anzai, T., Yamaguchi, Y., Sawaki, T., Kobayashi, K., Kanehisa, N., Hashimoto, H., Kai, Y. and Masuda, H. (1996). "Crystal Engineering of Stacked Aromatic Columns. Three-Dimensional Control of the Alignment of Orthogonal Aromatic Triads and Guest Quinones via Self-Assembly of Hydrogen-Bonded Networks." *J. Am. Chem. Soc.*, 118 (24), 5562–5571.
- Asano, T., Uenoyama, M., Moriya, K., Yano, S., Takatani, S. and Kagabu, S. (1997). "Polymesomorphism in a homologous series of 2-(4-alkoxyphenyl)-5-(4-methylphenyl)pyridines." *Liq. Cryst.*, 23 (3), 365–369.
- Ashton, P.R., Joachimi, D., Spencer, N., Stoddart, J.F., Tschierske, C., White, A.J.P., Williams, D.J. and Zab, K. (1994). "Neuartigemakrocyclische Flüssigkristalle." *Angew. Chem. Int. Ed.*, 106 (14), 1563-1566.
- Attias, A.-J., Cavalli, C., Bloch, B., Guillou, N. and Noël, C. (1999). "New liquid crystalline conjugated derivatives of 3,3'-bipyridine as components for optoelectronic materials." *Chem. Mater.*, 11 (8), 2057–2068.
- Attias, A.-J., Cavalli, C., Donnio, B., Guillon, D., Hapiot, P. and Malthête, J. (2002). "Columnar mesophase from a new disc like mesogen based on a 3,5-dicyano-2,4,6-tristyrylpyridine core." *Chem. Mater.*, 14 (1), 375–384.
- Aziz, N., Kelly, S.M., Duffy, W. and Goulding, M. (2009). "Rod-shaped dopants for flexoelectric nematic mixtures." *Liq. Cryst.*, 36 (5), 503–520.

- Bagley, M.C., Lin, Z. and Pope, S.J.A. (2009). "Rapid synthesis of 3-cyanopyridine-derived chromophores with two-dimensional tunability and solvatochromic photophysical properties." *Chem. Commun.*, (34), 5165–5167.
- Bahadur, B. (1990). "Liquid Crystals: Applications and uses." World scientific, London.
- Beltrán, E., Serrano, J.L., Sierra, T. and Giménez, R. (2010). "Tris(triazolyl)triazine via Click-chemistry: a C<sub>3</sub> electron-deficient core with liquid crystalline and luminescent properties." *Org. Lett.*, 12 (7), 1404–1407.
- Binnemans, K. (2009). "Luminescence of metallomesogens in the liquid crystal state." *J. Mater. Chem.*, 19 (4), 448–453.
- Bohlmann, F. and Rahtz, D. (1957). "Über eine neue Pyridinsynthese." *Eur. J. Inorg. Chem.*, 90 (10), 2265-2272.
- Bönnemann, H. (1985). "Organocobalt compounds in the synthesis of pyridines—an example of structure-effectivity relationships in homogeneous catalysis." *Angew. Chem. Int. Ed.*, 24 (4), 248–262.
- Breemen, A.J.J.M. van, Herwig, P.T., Chlon, C.H.T., Sweelssen, J., Schoo, H.F.M., Setayesh, S., Hardeman, W.M., Martin, C.A., Leeuw, D.M. de, Valetton, J.J.P., Bastiaansen, C.W.M., Broer, D.J., Popa-Merticaru, A.R. and Meskers, S.C.J. (2006). "Large area liquid crystal monodomain field-effect transistors." *J. Am. Chem. Soc.*, 128 (7), 2336–2345.
- Buchecker, D.R., Germann, A., Kelly, D.S. and Schadt, D.M. (1991). "Liquid-crystalline pyridine derivatives. (Hoffmann-La-Roche), EP 242.716 (1987/04/09).
- Chang, T-H., Wu, B-Ru, Chiang, M.Y., Liao, S-C., Ong, C.W., Hsu, H-F. and Lin, S.-Y.(2005). "Synthesis and mesomorphic behavior of a donor–acceptor-type hexaazatriphenylene." *Org. Lett.*, 7, 4075-4078.

- Chia, W.-L., Li, C.-L. and Lin, C.-H. (2009). "Synthesis and mesomorphic studies on the series of 2-(4-alkoxyphenyl)-5-phenylpyridines and 2-(6-alkoxynaphthalen-2-yl)-5-phenylpyridines." *Liq. Cryst.*, 37 (1), 23–30.
- Chia, W.-L. and Lin, C.-W. (2013). "Synthesis and thermotropic studies of a novel series of nematogenic liquid crystals 2-(6-alkoxynaphthalen-2-yl)-5-cyanopyridines." *Liq. Cryst.*, 40 (7), 922–931.
- Crosby, G.A. and Demas, J.N. (1971). "Measurement of photoluminescence quantum yields. Review." *J. Phys. Chem.*, 75 (8), 991–1024.
- Czupryński, K., Przedmojski, J. and Baran, J.W. (1995). "A new smectic phase in 4,4'-dialkylbiphenyl." *Mol. Cryst. Liq. Cryst.*, 260 (1), 435–442.
- Demus, D., Hauser, A., (1990). "Selected Topics in Liquid Crystal Research." Ed.: H.-D. Koswig, Akademie-Verlag, Berlin, 19.
- Desiraju, G.R. (1996). "The C–H···O Hydrogen Bond: Structural Implications and Supramolecular Design." *Acc. Chem. Res.*, 29 (9), 441–449.
- Dikundwar, A.G., Dutta, G.K., Guru Row, T.N. and Patil, S. (2011). "Polymorphism in Opto-electronic materials with a benzothiazole-fluorene core: A consequence of high conformational flexibility of  $\pi$ -conjugated backbone and alkyl side chains." *Cryst. Growth Des.*, 11 (5), 1615–1622.
- Echeverría, J., Aullón, G., Danovich, D., Shaik, S. and Alvarez, S. (2011). "Dihydrogen contacts in alkanes are subtle but not faint." *Nat. Chem.*, 3 (4), 323–330.
- El-Ghayoury, A., Douce, L., Ziessel, R. and Skoulios, A. (2000). "Thermotropic liquid crystals from a monosubstituted 2,2'-bipyridine." *Liq. Cryst.*, 27 (12), 1653–1662.
- Frank, R.L. and Seven, R.P. (1949). "Pyridines. IV. A study of the chichibabin synthesis." *J. Am. Chem. Soc.*, 71 (08), 2629–2635.

- Gallardo, H., Bortoluzzi, A.J. and Santos D.M.P.O. (2008). Synthesis, crystalline structure and mesomorphic properties of new liquid crystalline 1,2,3-triazole derivatives. *Liq. Cryst.*, 35, 719–725.
- Gattermann, L. and Skita, A. (1916). "Eine synthese von pyridin-derivaten." *Ber. Dtsch. Chem. Ges.*, 49 (01), 494-501.
- Gearba, R.I., Lehmann, M., Levin, J., Ivanov, D.A., Koch, M.H.J., Barbera, J., Debije, M.G., Piris, J. and Geerts, Y.H. (2003). "Tailoring discotic mesophases: Columnar order enforced with hydrogen bonds." *Adv. Mater.*, 15, 1614-1618.
- Getmanenko, Y.A., Twieg, R.J. and Ellman, B.D. (2006). "2,5-Dibromopyridine as a key building block in the synthesis of 2,5-disubstituted pyridine-based liquid crystals." *Liq. Cryst.*, 33 (3), 267–288.
- Ghodbane, S., Oweimreen, G.A. and Martire, D.E. (1991). "Thermodynamics of solution of non-mesomorphic solutes at infinite dilution in the smectic-A, nematic and isotropic phases of *p-n*-octyl-*p'*-cyanobiphenyl: A gas—liquid chromatographic study." *J. Chromatogr. A*, 556 (1–2), 317–330.
- Goda, F.E., Abdel-Aziz, A.A.-M. and Attef, O.A. (2004). "Synthesis, antimicrobial activity and conformational analysis of novel substituted pyridines: BF<sub>3</sub>-promoted reaction of hydrazine with 2-alkoxy pyridines." *Bioorg. Med. Chem.*, 12 (8), 1845–1852.
- Gray, G.W., Harrison, K.J. and Nash, J.A. (1973). "New family of nematic liquid crystals for displays." *Electron. Lett.*, 9 (6), 130-131.
- Gray, G.W. and Lacey, D. (1983). "Synthesis and properties of some 2- n-alkyl-6-(4'-cyanophenyl)-naphthalenes -3,4-dihydronaphthalenes, and -1, 2, 3, 4-tetrahydronaphthalenes." *Mol. Cryst. Liq. Cryst.*, 99 (1), 123–138.
- Gregg, B.A., Fox, M.A. and Bard, A.J. (1990). "Photovoltaic effect in symmetrical cells of a liquid crystal porphyrin." *J. Phys. Chem.* 94, 1586-1598.

- Ha, S.-T., Koh, T.-M., Lee, S.-L., Yeap, G.-Y., Lin, H.-C. and Ong, S.-T. (2010). "Synthesis of new schiff base ester liquid crystals with a benzothiazole core." *Liq. Cryst.*, 37 (5), 547–554.
- Halls, J.J.M., Walsh, C.A., Greenham, N.C., Marseglia, E.A., Friend, R.H., Moratti, S.C. and Holmes, A.B. (1995). "Efficient photodiodes from interpenetrating polymer networks." *Nature*, 376 (6540), 498–500.
- Hamdy, N.A. and Gamal-Eldeen, A.M. (2009). "New pyridone, thioxopyridine, pyrazolopyridine and pyridine derivatives that modulate inflammatory mediators in stimulated RAW 264.7 murine macrophage." *Eur. J. of Med. Chem.*, 44 (11), 4547–4556.
- Han, J., Geng, Q., Chen, W., Zhu, L., Wu, Q. and Wang, Q. (2012). "Self-assembled liquid crystals formed by hydrogen bonding between non-mesogenic 1,3,4-oxadiazole-based pyridines and substituted benzoic acids." *Supramol. Chem.*, 24 (3), 157–164.
- Hantzsch, A. (1881). "Condensationsprodukte aus aldehydammoniak und ketonartigen verbindungen." *Ber. Dtsch. Chem. Ges.*, 14 (02), 1637-1638.
- Heinemann, S., Kresse, H., Saito, S. and Demus, D. (1996). "Dielectric studies of a series of liquid crystalline pyridine derivatives." *Z. Naturforsch.*, 51a, 1019-1026.
- Hide, F., Díaz-García, M.A., Schwartz, B.J., Andersson, M.R., Pei, Q. and Heeger, A.J. (1996). "Semiconducting polymers: A new class of solid-state laser materials." *Science*, 273 (5283), 1833–1836.
- Iino, H., Hanna, J. and Haarer, D. (2005). "Electronic and ionic carrier transports in discotic liquid crystalline photoconductors." *Phys. Rev. B*, 72, 193203.
- Inoue, H., Inukai, T., Ohno, K., Saito, S. and Miyazawa, K., (1987). "2-(Alkyloxycarbonyloxyphenyl)-5-alkylpyridine and composition containing same." (Chisso), *EP 239.403 (26/03/1987)*.

- Jokisaari, J. and Hiltunen, Y. (1983). "Solute molecular structure determination by N.M.R." *Mol. Phys.*, 50 (5), 1013–1023.
- Jones, R.L. and Rees, C.W. (1969). "Mechanism of heterocyclic ring expansions. Part III. Reaction of pyrroles with dichlorocarbene." *J. Chem. Soc. C.*, 18, 2249-2251.
- Kawamura, Y., Sasabe, H. and Adachi, C. (2004). "Simple accurate system for measuring absolute photoluminescence quantum efficiency in organic solid-state thin films." *Jpn. J. Appl. Phys.*, 43 (11A), 7729–7730.
- Kelly, S.M. and Fünfschilling, J. (1993). "Liquid-crystal transition temperatures and physical properties of some new alkenyl-substituted phenylpyrimidine and phenylpyridineesters." *J. Mater. Chem.*, 3 (9), 953–963.
- Kelly, S.M. and Fünfschilling, J. (1996). "An investigation of the dependence on the position and type of dipoles and chain configuration on the smectic mesomorphism of a model biphenyl/phenylpyridine/phenylpyrimidine system." *Ferroelectrics*, 180 (1), 269–289.
- Kelly, S.M. and Fünfschilling, J. (1996). "Novel 2-(4-octylphenyl)pyridin-5-yl alkanoates and alkenoates: Influence of dipoles and chain conformation on smectic C formation." *Liq. Cryst.*, 20 (1), 77–93.
- Kelly, S.M., Fünfschilling, J. and Villiger, A. (1993a). "Smectic C phenylpyridines with an alkenyloxy chain." *Liq. Cryst.*, 14 (4), 1169–1180.
- Kestemont, G., de Halleux, V., Lehmann, M., Ivanov, D.A., Watson, M. and Geerts, Y.H. (2001). "Discotic mesogens with potential electron carrier properties". *Chem. Commun.*, 2074-2075.
- Kohlmeier, A. and Janietz, D. (2007). "Hydrogen-bonded block mesogens derived from semiperfluorinated benzoic acids and the non-mesogenic 1,2-bis(4-pyridyl)ethylene." *Liq. Cryst.*, 34 (1), 65–71.

- Kohmoto, S., Hara, Y. and Kishikawa, K. (2010). "Hydrogen-bonded ionic liquid crystals: pyridinylmethylimidazolium as a versatile building block." *Tetrahedron Lett.*, 51 (11), 1508–1511.
- Kouji, O., Shinichi, S. and Hiromichi, I. (1989). (Chisso), *EP 306.195* (1988/08/22).
- Kozhevnikov, V.N., Cowling, S.J., Karadakov, P.B. and Bruce, D.W. (2008). "Mesomorphic 1,2,4-triazine-4-oxides in the synthesis of new heterocyclic liquid crystals." *J. Mater. Chem.*, 18 (14), 1703–1710.
- Kozhevnikov, V.N., Donnio, B. and Bruce, D.W. (2008). "Phosphorescent, terdentate, liquid-crystalline complexes of platinum(II): stimulus-dependent emission." *Angew. Chem. Int. Ed.*, 47 (33), 6286–6289.
- Kubo, K., Sutoh, T., Mori, A. and Ujiie, S. (2002). "Synthesis, structure, and mesomorphic properties of liquid crystals with a bitropone core." *Bull. Chem. Soc. Jpn.*, 75 (6), 1353–1358.
- Kumar, S. (2006). "Self-organization of disc-like molecules: chemical aspects". *Chem. Soc. Rev.*, 35, 83-109.
- Lee, J., Jin, J., Achard, M.F. and Hardouin, F. (2003). "Cholesterol-based hydrogen-bonded liquid crystals." *Liq. Cryst.*, 30 (10), 1193–1199.
- Lee, J.H., Han, M.-J., Hwang, S.H., Jang, I., Lee, S.J., Yoo, S.H., Jho, J.Y. and Park, S.-Y. (2005). "Self-assembled discotic liquid crystals formed by hydrogen bonding of alkoxy stilbazoles." *Tetrahedron Lett.*, 46 (42), 7143–7146.
- Lehn, J.-M. (1995). "Supramolecular chemistry: concepts and perspectives." VCH: Weinheim.
- Liu, C., Fechtenkötter, A., Watson, M.D., Müllen, K. and Bard, A.J. (2003). "Room temperature discotic liquid crystalline thin films of hexa-peri-hexabenzocoronene: Synthesis and optoelectronic properties." *Chem. Mater.*, 15, 124-130.
- Longa, L., de Jeu, W. H. (1982). "Microscopic one-particle description of reentrant behavior in nematic liquid crystals." *Phys. Rev., Ser. A.*, 26(3), 1632-1647.

- Mallia, V.A., Antharjanam, P.K.S. and Das, S. (2003). "Synthesis and studies of some 4-substituted phenyl-4'-azopyridine-containing hydrogen-bonded supramolecular mesogens." *Liq. Cryst.*, 30 (2), 135–141.
- Matsui, M., Oji, A., Hiramatsu, K., Shibata, K. and Muramatsu, H. (1992). "Synthesis and characterization of fluorescent 4,6-disubstituted-3-cyano-2-methylpyridines." *J. Chem. Soc., Perkin Trans. 2* (2), 201–206.
- Meyer, R.B., Liebert, L., Strzelecki, L. and Keller, P. (1975). "Ferroelectric liquid crystals." *J. Phys. Lett.-Paris*, 36 (3), 69–71.
- Mieczkowski, J., Gomola, K., Koseska, J., Pocięcha, D., Szydłowska, J. and Gorecka, E. (2003). "Liquid crystal phases formed by asymmetric bent-shaped molecules." *J. Mater. Chem.*, 13 (9), 2132–2137.
- Misaki, M., Ueda, Y., Nagamatsu, S., Yoshida, Y., Tanigaki, N. and Yase, K. (2004). "Formation of single-crystal-like poly(9,9-dioctylfluorene) thin film by the friction-transfer technique with subsequent thermal treatments." *Macromolecules*, 37 (18), 6926–6931.
- Moriya, K., Harada, F., Yano, S. and Kagabu, S. (2000). "The synthesis and liquid crystalline behaviour of 2-(4-n-alkoxyphenyl)-5-methylpyridines." *Liq. Cryst.*, 27 (12), 1647–1651.
- Murashiro, K., Okabe, E., Tanabe, M., Fukushima, M., Takeda, H., Shiomi, M., Kaneko, T., Matsuki, M. and Koden, M. (1995) (Chisso; Sharp) *EP 632.116 (1994/06/30)*.
- Osman, M.A. (1985). "Substituted terminal alkyl groups and their prospects in liquid crystal chemistry." *Mol. Cryst. Liq. Cryst.*, 131 (3-4), 353–360.
- Osman, M.A. and Huynh-Ba, T. (1983). "Nematogens for matrix-addressed twisted nematic displays.II." *ZeitschriftFür Naturforschung. Teil B, Anorganische Chemie, Organische Chemie*, 38 (10), 1221–1226.



- Oswald, P. and Pieranski, P. (2005). "Nematic and Cholesteric Liquid Crystals: Concepts and Physical Properties Illustrated by Experiments." CRC Press,
- Pavluchenko, A.I., Petrov, V.F. and Smirnova, N.I. (1995). "Liquid crystalline 2,5-disubstituted pyridine derivatives." *Liq. Cryst.*, 19 (6), 811–821.
- Pavluchenko, A.I., Titov, V.V. and Smirnova, N.I. (1980). *Adv. Liq. Cryst. Res. Appl.* (Ed. Bata, L.), 1007-1013.
- Sagara, Y. and Kato, T. (2008). "Stimuli-responsive luminescent liquid crystals: change of photoluminescent colors triggered by a shear-induced phase transition." *Angew. Chem. Int. Ed.*, 47 (28), 5175–5178.
- Saravanan, C., Ambili, V. and Kannan, P. (2010). "Hydrogen-bond induced side-chain liquid crystalline polymers based on nicotinic acid derivatives." *React. Funct. Polym.*, 70 (4), 217–222.
- Schubert, H., (1970). *Wiss.Z. Univ. Halle, Math.-Nat. R.*, 19 (5), 1.
- Shanker, G., Prehm, M., Yelamaggad, C.V. and Tschierske, C. (2011). "Benzylidenehydrazine based room temperature columnar liquid crystals." *J. Mater. Chem.*, 21 (14), 5307–5311.
- Shen, H., Jeong, K.-U., Xiong, H., Graham, M.J., Leng, S., Zheng, J.X., Huang, H., Guo, M., Harris, F.W. and Cheng, S.Z.D. (2006). "Phase behaviors and supramolecular structures of a series of symmetrically tapered bisamides." *Soft Matter*, 2 (3), 232–242.
- Shen, Y.-T., Li, C.-H., Chang, K.-C., Chin, S.-Y., Lin, H.-A., Liu, Y.-M., Hung, C.-Y., Hsu, H.-F. and Sun, S.-S. (2009). "Synthesis, optical, and mesomorphic properties of self-assembled organogels featuring phenylethynyl framework with elaborated long-chain pyridine-2,6-dicarboxamides." *Langmuir*, 25 (15), 8714–8722.
- Sirringhaus, H., Tessler, N. and Friend, R.H. (1998). "Integrated optoelectronic devices based on conjugated polymers." *Science*, 280 (5370), 1741–1744.

- Sung, H.-H. and Lin, H.-C. (2005). "Synthesis and characterization of poly(fluorene)-based copolymers containing various 1,3,4-oxadiazole pendants." *J. Polym. Sci. A Polym. Chem.*, 43 (13), 2700–2711.
- Swanson, B.D. and Sorensen, L.B. (1995). "What forces bind liquid crystals." *Phys. Rev. Lett.*, 75 (18), 3293–3296.
- Tang, J., Huang, R., Gao, H., Cheng, X., Prehm, M. and Tschierske, C. (2012). "Columnar mesophases of luminescent polycatenar liquid crystals incorporating a 1,3-substituted benzene ring interconnecting two 1,3,4-oxadiazoles." *RSC Adv.*, 2 (7), 2842–2847.
- Tantrawong, S., Styring, P. and Goodby, J.W. (1993). "Discotic mesomorphism in oxovanadium(IV) complexes possessing four alkyl substituents." *J. Mater. Chem.*, 3 (12), 1209–1216.
- Torralba, M.C., Huck, D.M., Nguyen, H.L., Horton, P.N., Donnio, B., Hursthouse, M.B. and Bruce, D.W. (2006). "Mesomorphism of complexed 2,6-disubstituted pyridine ligands: crystal and molecular structure of two bent-core pyridines." *Liq. Cryst.*, 33 (4), 399–407.
- Vasconcelos, U.B., Dalmolin, E. and Merlo, A.A. (2005). "Synthesis and thermal behavior of new *N*-heterotolan liquid crystals." *Org. Lett.*, 7 (6), 1027–1030.
- Veber, M. and Berruyer, G. (2000). "Ionic liquid crystals: synthesis and mesomorphic properties of dimeric 2,4,6-triarylpyrylium tetrafluoroborates." *Liq. Cryst.*, 27 (5), 671–676.
- Vishnumurthy, K.A., Sunitha, M.S., Safakath, K., Philip, R. and Adhikari, A.V. (2011). "Synthesis, electrochemical and optical studies of new cyanopyridine based conjugated polymers as potential fluorescent materials." *Polymer*, 52 (19), 4174–4183.
- Wang, H., Gen, T., Fu, R., Zhu, J., Wei, X., Li, H. and Liu, J. (1992). "Gas chromatographic separation of polycyclic aromatic hydrocarbons on a mesomorphic copolysiloxane stationary phase." *J. Chromatogr. A*, 609 (1–2), 414–418.

Yelamaggad, C.V. and Achalkumar, A.S. (2006). "Tris( *N*-salicylideneanilines) [TSANs] exhibiting a room temperature columnar mesophase: synthesis and characterization." *Tetrahedron. Lett.* 47, 7071-7075.

Yelamaggad, C.V., Bonde, N.L., Achalkumar, A.S., Shankar Rao, D.S., Prasad, S.K. and Prajapati, A.K. (2007). "Frustrated Liquid Crystals: Synthesis and Mesomorphic Behavior of Unsymmetrical Dimers Possessing Chiral and Fluorescent Entities." *Chem. Mater.*, 19 (10), 2463–2472.

Yelamaggad, C.V., Prabhu, R., Rao, D.S.S. and Prasad, S.K. (2010). "The first examples of supramolecular discotic  $C_{3h}$  tris(*N*-salicylideneamine)s featuring inter- and intra-molecular H-bonding: synthesis and characterization." *Tetrahedron Lett.*, 51 (34), 4579–4583.

You, J., Lai, S., Liu, W., Ng, T., Wang, P. and Lee, S. (2012). "Bipolar cyano-substituted pyridine derivatives for applications in organic light-emitting devices." *J. Mater. Chem.*, 22, 8922-8929.

Zhang, X. and Li, M. (2008). "Synthesis and self-assembly of novel hydrazide derivatives containing multi-alkoxy chains with different lengths." *J. Mol. Struct.*, 892 (1–3), 490–494.

Zhao, B., Liu, B., Png, R.Q., Zhang, K., Lim, K.A., Luo, J., Shao, J., Ho, P.K.H., Chi, C. and Wu, J. (2010). "New discotic mesogens based on triphenylene-fused triazatruxenes: synthesis, physical properties, and self-assembly." *Chem. Mater.*, 22, 435-449.

Zhao, X.-L. and Mak, T.C.W. (2004). "Silver cages with encapsulated acetylenediide as building blocks for hydrothermal synthesis of supramolecular complexes with *n*-cyanopyridine and pyridine-*n*-carboxamide ( $n=3, 4$ )." *Dalton Trans.*, 20, 3212–3217.

## List of publications

### Papers published in international journals

1. T.N. Ahipa, Vijith Kumar and Airody V. Adhikari (2012). "Synthesis, structural analysis and solvatochromic behaviour of 4,6-bis(4-butoxyphenyl)-2-methoxynicotinonitrile mesogen." *Liquid Crystals*, 40, 31-38.
2. T.N. Ahipa and AirodyVasudevaAdhikari, (2012). "Synthesis and mesomorphism of new 2-methoxy-3-cyanopyridine mesogens." *Proc. SPIE 8279, Emerging Liquid Crystal Technologies VII*, 827915.
3. T.N. Ahipa and AirodyVasudevaAdhikari (2014). "Trihydrazone functionalized cyanopyridinediscoids: synthesis, mesogenic and optical properties". *Tetrahedron Letters*, 55 (2), 495-500.
4. T.N. Ahipa, Vijith Kumar and Airody Vasudeva Adhikari (2014). "New columnar liquid crystal materials based on luminescent 2-methoxy-3-cyanopyridines". *Structural Chemistry*, 25, 1165-1174.
5. T.N. Ahipa, Vijith Kumar, Doddamane S. Shankar Rao, Subbarao Krishna Prasad and Airody Vasudeva Adhikari (2014). "New 4-(2-(4-alkoxyphenyl)-6-methoxypyridin-4-yl)benzonnitriles: Synthesis, liquid crystalline behavior and photophysical properties". *Crystal Engineering Communications*, 16, 5573-5582.
6. T.N. Ahipa and Airody Vasudeva Adhikari (2014). "New cyanopyridone based luminescent liquid crystalline materials: Synthesis and characterization". *Photochemical & Photobiological Sciences*, DOI: 10.1039/C4PP00031E.
7. T.N. Ahipa and Airody Vasudeva Adhikari (2014). "2-Methoxypyridine derivatives: synthesis, liquid crystalline and photo-physical properties". *New Journal of Chemistry*, 38 (10), 5018-5029.

### Research papers presented in international conferences

1. T.N. Ahipa and Airody Vasudeva Adhikari, "Synthesis, characterization and mesomorphic properties of 2-methoxy-3-cyanopyridine core." International Conference on Synthetic and Structural Chemistry (ICSSC-2011), Mangalore University Mangalore, December 8-10, 2011.

2. T.N. Ahipa and Airody Vasudeva Adhikari, "Synthesis and mesomorphism of new 2-methoxy-3-cyanopyridine mesogens." Emerging Liquid Crystal Technologies VII (SPIE OPTO), San Francisco, California, United States, January 21-26, 2012.
3. T.N. Ahipa, Vijith Kumar, Doddamane S. Shankar Rao, Subbarao Krishna Prasad and Airody Vasudeva Adhikari. "Synthesis, characterization and liquid crystalline behavior of new methoxy pyridines carrying terminal alkoxy pendent and polar nitrile group." International Conference on Recent Advances in Material Science and Technology - 2013 (ICRAMST - 13), National Institute of Technology Karnataka, Surathkal, January 17-19, 2013.

\*\*\*\*\*

---

## CURRICULUM VITAE

### Present address

Ahipa T.N.  
Research Scholar  
Department of Chemistry  
NITK-Surathkal  
Srinivasnagar, Mangalore  
Karnataka, India-575 025  
Email: [ahipatn@gmail.com](mailto:ahipatn@gmail.com)  
Phone: +919480170854

### Permanent Address

Ahipa T.N.  
S/o Nagaraja Bhat T.S.  
M.K. Street  
Sringeri Taluk  
Chickmagalur District  
Karnataka, India-577 139  
Email: [ahipatn@gmail.com](mailto:ahipatn@gmail.com)  
Phone: +919481651046

---

### Research Experience:

Dec 2010-Present: **Research Scholar**  
Department of Chemistry  
National Institute of Technology Karnataka, India  
Research: Synthesis and luminescent liquid crystalline studies  
of new pyridine derivatives

Oct/2009-Dec/2010: **Research Associate**  
Indian Plywood Industries Research and Training Institute  
Bangalore, Karnataka.  
Project Area: Synthesis, extraction and characterization of  
furfural based various resin

### Education:

Dec 2010-Present: **Ph.D.**  
Department of Chemistry  
National Institute of Technology Karnataka, India  
Title: 'Synthesis, characterization and mesomorphic behavior  
of some new pyridine derivatives'  
Supervisor: Prof A. Vasudeva Adhikari

July/2004-June/2009: Integrated **M.Sc.** (Hons) in Applied Chemistry  
Sahyadri Science College  
Shimoga,  
Karnataka, India

### List of Publications

1. T.N. Ahipa, Vijith Kumar and Airody V. Adhikari (2012). "Synthesis, structural analysis and solvatochromic behaviour of 4,6-bis(4-butoxyphenyl)-2-methoxynicotinonitrile mesogen." *Liquid Crystals*, 40, 31-38.

- 
2. T.N. Ahipa and Airody Vasudeva Adhikari, (2012). "Synthesis and mesomorphism of new 2-methoxy-3-cyanopyridine mesogens." *Proc. SPIE 8279, Emerging Liquid Crystal Technologies VII*, 827915.
  3. T.N. Ahipa and Airody Vasudeva Adhikari (2014). "Trihydrazone functionalized cyanopyridine discoids: synthesis, mesogenic and optical properties". *Tetrahedron Letters*, 55, 2, 495-500.
  4. T.N. Ahipa., Vijith Kumar and Airody Vasudeva Adhikari, "New columnar liquid crystal materials based on luminescent 2-methoxy-3-cyanopyridines". *Structural Chemistry*, 25, 1165-1174.
  5. T.N. Ahipa, Pooja R. Kamath, Vijith Kumar and Airody Vasudeva Adhikari (2014). "New luminescent 2-methoxy-6-(4-methoxy-phenyl)-4-p-tolyl-nicotinonitrile: synthesis, crystal structure, DFT and photophysical studies". *Spectrochimica Acta Part A: Molecular and Biomolecular Spectroscopy*, 124, 230-236.
  6. T.N. Ahipa, Vijith Kumar, Doddamane S. Shankar Rao, Subbarao Krishna Prasad and Airody Vasudeva Adhikari (2014). "New 4-(2-(4-alkoxyphenyl)-6-methoxypyridin-4-yl)benzonnitriles: Synthesis, liquid crystalline behavior and photophysical properties". *Crystal Engineering Communications*, 16, 5573-5582.
  7. T.N. Ahipa and Airody Vasudeva Adhikari (2014). "New cyanopyridone based luminescent liquid crystalline materials: Synthesis and characterization". *Photochemical & Photobiological Sciences*, DOI: 10.1039/C4PP00031E.
  8. T.N. Ahipa and Airody Vasudeva Adhikari (2014). "2-Methoxypyridine derivatives: synthesis, liquid crystalline and photo-physical properties". *New Journal of Chemistry*, 38 (10), 5018-5029.

#### **List of conference papers presented**

1. T.N. Ahipa and Airody Vasudeva Adhikari, "Synthesis, characterization and mesomorphic properties of 2-methoxy-3-cyanopyridine core." International Conference on Synthetic and Structural Chemistry (ICSSC-2011), Mangalore University Mangalore, December 8-10, 2011.
2. T.N. Ahipa and Airody Vasudeva Adhikari, "Synthesis and mesomorphism of new 2-methoxy-3-cyanopyridine mesogens." Emerging Liquid Crystal

---

Technologies VII (SPIE OPTO), San Francisco, California, United States, January 21-26, 2012.

3. T.N. Ahipa, Vijith Kumar, Doddamane S. Shankar Rao, Subbarao Krishna Prasad and Airody Vasudeva Adhikari. "Synthesis, characterization and liquid crystalline behavior of new methoxy pyridines carrying terminal alkoxy pendent and polar nitrile group." International Conference on Recent Advances in Material Science and Technology - 2013 (ICRAMST – 13), National Institute of Technology Karnataka, Surathkal, January 17-19, 2013.

\*\*\*\*\*